ValorNatural – Valorização de Recursos Naturais através da Extração de Ingredientes de Elevado Valor Acrescentado para Aplicações na Indústria Alimentar.

Entregável nº 3.1.6

Versão do Documento: 1

Data de Submissão: 11/07/2019

Responsável: IPB-CIMO

Nome do Documento: Publicação dos ingredientes com maior capacidade corante e sem toxicidade

Histórico de Revisão

Revisão	Data	Parceiros Envolvidos	Descrição

Lista de Autores

Isabel Ferreira

Cristina Caleja

Maria Inês Dias

Eliana Pereira

Sumário

Publicações relativas aos ingredientes com maior capacidade corante e que não apresentam toxicidade.

Índice

Cofinanciado por:

1. Identificação

Deliverable	3.1.6
Tipo de *deliverable*	Publicação
Nível de disseminação	Público
PPS	3

2. Informação

As publicações relativas aos ingredientes com maior capacidade corante e sem toxicidade são:

Stability of a cyanidin-3-*O*-glucoside extract obtained from *Arbutus unedo* L. and incorporation into wafers for colouring purposes
Lopez C. J., Caleja C., Prieto M. A., Sokovic M., Calhelha R. C., Barros L., Ferreira I. C. F. R.
Food Chemistry, 275, 426-438, 2019

Incorporation of natural colorants obtained from edible flowers in yogurts
Pires T. C. S. P., Dias M. I., Barros L., Barreira J. C. M., Santos-Buelga C., Ferreira I. C. F. R.
LWT-Food Science and Technology, 97, 668-675, 2018

Gomphrena globosa L. as a novel source of food-grade betacyanins: Incorporation in ice-cream and comparison with beet-root extracts and comercial betalains.
Roriz C. L., Barreira J. C. M., Morales P., Barros L., Ferreira I. C. F. R.
LWT, 92, 101-107, 2018

Optimization of heat- and ultrasound-assisted extraction of anthocyanins from *Hibiscus sabdariffa* calyces for natural food colorants
Pinela J., Prieto M. A., Pereira E., Jabeur I., Barreiro M. F., Barros L., Ferreira I. C. F. R.
Food Chemistry, 275, 309-321,2019

Optimization of the Extraction Process to Obtain a Colorant Ingredient from Leaves of *Ocimum basilicum* var. *purpurascens*
Fernandes F., Pereira E., Prieto M. A., Calhelha R. C., ´Ciric A., Sokovi´c M., Simal-Gandara J., Barros L., Ferreira I. C. F. R.
Molecules, 24, 686, 2019

Recovery og bioactive anthocyanin pigments from *Ficus carica* L. peel by heat, microwave, and ultrasound based extraction techniques
Backes E., Pereira C., Barros L., Prieto M. A., Genena A. K., Barreiros M. F., Ferreira I. C. F. R.
Food Research International, 113, 197-209, 2018

Ultrasound as a Rapid and Low-Cost Extraction Procedure to Obtain Anthocyanin-Based Colorants from *Prunus spinosa* L. Fruit Epicarp: Comparative Study with Conventional Heat-Based Extraction
Leichtweis M. G., Pereira C., Prieto M.A., Barreiro M. F., Braldi I. J., Barros L., Ferreira I. C. F. R.
Molecules, 24, 573, 2019

3. Anexos

Stability of a cyanidin-3-*O*-glucoside extract obtained from *Arbutus unedo* L. and incorporation into wafers for colouring purposes

Cecilia Jiménez López[a], Cristina Caleja[a,b], M.A. Prieto[a,c], Marina Sokovic[d], Ricardo C. Calhelha[a], Lillian Barros[a,*], Isabel C.F.R. Ferreira[a,*]

[a] *Centro de Investigação de Montanha (CIMO), Instituto Politécnico de Bragança, Campus de Santa Apolónia, 5300-253 Bragança, Portugal*
[b] *Laboratoire of Separation and Reaction Engineering (LSRE), Associate Laboratory LSRE/LCM, IPB, Campus de Santa Apolónia, 1134, 5301-857 Bragança, Portugal*
[c] *Nutrition and Bromatology Group, Faculty of Food Science and Technology, University of Vigo, Ourense Campus, E32004 Ourense, Spain*
[d] *University of Belgrade, Department of Plant Physiology, Institute for Biological Research "Siniša Stanković", Bulevar Despota Stefana 142, 11000 Belgrade, Serbia*

ABSTRACT

An extract from *Arbutus unedo* fruits, rich in anthocyanins, was studied as a natural colorant with bioactive properties (antioxidant, antimicrobial and cytotoxic). The aqueous stability of the extract was monitored using the anthocyanins' content as response (determined by HPLC-DAD) in function of time, temperature and pH. Aided by mechanistic/phenomenological models, the conditions that favours the stabilization of the extract were provided, highlighting the suitability of the colorant for pastry/bakery products. As a case study, the extract was incorporated into wafers and the changes on the nutritional profile, free sugars, fatty acids and antioxidant properties were monitored during 6 days of storage. The results provide information for: i) potential application of the rich extract in anthocyanins for producing a natural colorant with bioactive properties; and ii) shelf-life predictions. The extract incorporation did not cause changes in the nutritional components of wafers but added colorant and antioxidant properties.

1. Introduction

Anthocyanins are secondary metabolites of plants belonging to the group of phenolic compounds, colouring from fruits and flowers, to roots and seeds (Cavalcanti, Santos, & Meireles, 2011). Besides that, their beneficial effects to human health are well known: thanks to the presence of phenolic hydroxyl groups, they show antioxidant properties, preventing pathologies such as cardiovascular diseases, cancer and diabetes (Ge & Ma, 2013; Prior & Wu, 2006). Several studies also attribute to these compounds chemopreventive and chemotherapeutic capacity, due to their ability to inhibit tumour cells' growth (Ding et al., 2006). However, their stability also deserves a special mention due to a chemical structure very susceptible to degradation by several factors, as temperature, pH, presence of oxygen and even light (Cevallos-Casals & Cisneros-Zevallos, 2004; Garzón, 2008).

Although artificial colours began to dominate the market for paints and textiles, in the nineteenth century these pigments started to be highly used in food industry to improve the appearance of certain foods. Initially, these colorants began to be applied in wine, pasta and butter (Ibañez, Torre, & Irigoyen, 2003), but their use was not fully regulated. The use of artificial colorants by the industry raised the concern of

consumers, due to some reports on health problems (hyperactivity and allergic reactions) (Esatbeyoglu, Wagner, Schini-Kerth, & Rimbach, 2015). Nowadays, it is a subject very well regulated, both at continental and world level, through various committees created by WHO, FAO and European Communities' Commission (EFSA). The extensive use of artificial colorants to make food more attractive for consumers (Ibañez et al., 2003) has been related to harmful effects, which increased the interest for labels as "natural" or "without artificial additives" (Carocho, Barreiro, Morales, & Ferreira, 2014; Martins, Roriz, Morales, Barros, & Ferreira, 2016).

Following the legal and commercial requirements that are emerging, there is a trend of the food industry for natural ingredients (Esatbeyoglu et al., 2015). In the case of colorants, anthocyanins represent an attractive and natural alternative to the artificial ones. Anthocyanins stability is essential to ensure the quality and delivery of these bioactive components. However, natural extracts rich in anthocyanins are susceptible to degradation by several factors and the stability of these compounds during its application is a crucial step. The main identified factors affecting the stability are time (*t*), temperature (*T*) and pH (Komatsu et al., 2014; Zhu et al., 2002). Nonetheless, other factors such as light exposure, moisture content, metal ions content,

---

etc., have also been pointed out as relatively important (Li, Taylor, & Mauer, 2011).

Arbutus unedo L. is a shrub belonging to the subfamily *Vaccionioideae* (or *Arbutoideae,* according to the different authors) of the *Ericaceae* family (Miguel, Faleiro, Guerreiro, & Antunes, 2014). The edible fruits are grown in this shrub and are popularly recognized for their beneficial properties, particularly in the treatment of some symptomatology's (Ziyyat et al., 2002). The antimicrobial and antioxidant properties of the fruits are described in the literature and are associated, according to some authors, with the presence of phenolic compounds (Guimarães et al., 2013; Miguel et al., 2014).

Therefore, the aims of this study were to evaluate: 1) the bioactive properties (antioxidant, antimicrobial and cytotoxic) of the colorant extract produced; and 2) the stability of the extract considering the main affecting variables of *t*, *T* and *pH* in aqueous solution, by analysing the anthocyanins content by HPLC-DAD. Once the extract was stabilized, it was incorporated into wafers as a case study of the potential application in pastry products. Nutritional profile, free sugars, fatty acids and antioxidant activity were monitored after the wafers were baked, and after 3 and 6 days of storage.

2. Material and methods

2.1. Preparation of an anthocyanins rich extract from A. unedo fruits

2.1.1. Source material

The fruits of *A. unedo* L. (strawberry tree) were provided by a local producer of Torre de Moncorvo, Portugal. The fruits (1 kg) were lyophilized (FreeZone 4.5, Labconco, Kansas City, MO, USA) and reduced to powder ($\sim$20 mesh). The obtained powder was then mixed to guarantee the homogeneity of the samples, which were stored in a freezer (average $-20\,°C$), and protected from light, until further analysis.

2.1.2. Heat assisted extraction

The extract rich in cyanidin-3-*O*-glucoside was obtained from *A. unedo* L. following the optimized process previously reported by Jiménez et al. (2018). Briefly, the samples (600 mg) were placed in a beaker with 80% of acidified ethanol (acidified with 0.05% of hydrochloric acid) in order to obtain the desired solid/liquid ratio (10 g/L). The beaker was placed in a thermostatic water bath under continuous electro-magnetic stirring using a CIMAREC i Magnetic Stirrer (Thermo Scientific, San Jose, CA, USA) with a fixed agitation speed (500 rpm) for 5 min at 90 °C. Then, the extract solution was filtered through Whatman n° 4 paper and evaporated at 35 °C to remove the ethanol, frozen and lyophilized, to obtain a dry extract. As reported by Jiménez et al. (2018), following this procedure, it was obtained a residual extract of $\sim$60% of the total fruit dw, with a total anthocyanins content of $\sim$500 μg/g of fruit dw ($\sim$800 μg/g of extracted material).

2.2. Evaluation of the bioactive properties of the anthocyanins rich extract

A brief summary of the work performed is presented in Fig. 1. Next, each step performed will be described in detail.

2.2.1. General

The extract rich in anthocyanins (125 g) was dissolved in acidified distilled water (500 mL, 0.05% HCl). Dry extracts were further diluted to different concentrations to be submitted to the in vitro bioassays: i) final concentration 20 mg/mL in 80% of ethanol (0.05% HCl) and further diluted to working solutions of 5–0.156 mg/mL, for antioxidant activity; ii) stock concentration of 8 mg/mL, re-dissolved in water (0.05% HCl) and further diluted to 400–1.5 μg/mL working solutions for cytotoxic evaluation; and iii) the extracts were diluted in appropriate media according to bacteria requirements and the pH was adjusted with 0.05% HCl and successive dilutions were carried out in the

wells (1–0.1 mg/mL of final concentration).

2.2.1.1. Evaluation of antioxidant properties. DPPH radical-scavenging activity and reducing power were evaluated using ELX800 microplate Reader (Bio-Tek Instruments, Inc., Winooski, VT, USA) at 515 and 690 nm, respectively. β-Carotene bleaching inhibition and lipid peroxidation inhibition, using the thiobarbituric acid reactive substances – TBARS, were evaluated spectrophotometrically at 470 and 532 nm, respectively. The complete protocols were previously described by the authors (Sarmento, Barros, Fernandes, Carvalho, and Ferreira, 2015).

2.2.1.2. Evaluation of cytotoxicity properties. The extract was re-dissolved in water at a concentration of 8 mg/mL. According with Guimarães et al. (2013), four human tumour cell lines were used: MCF-7 (breast adenocarcinoma), NCI-H460 (non-small cell lung cancer), HeLa (cervical carcinoma) and HepG2 (hepatocellular carcinoma). The cell growth inhibition was measured using sulforhodamine B assay, where the amount of pigmented cells is directly proportional to the total protein mass and, therefore, to the number of bounded cells.

For hepatotoxicity evaluation, a cell culture was prepared from a freshly harvested porcine liver which was acquired from certified slaughterhouses and was used in order to obtain the cell culture, designated as PLP2. A phase-contrast microscope was used to monitor the growth of the cell cultures. They were sub-cultured and plated in 96 well plates (density of 1.0×10^4 cells/well). Dulbecco's modified eagle's medium (DMEM) was used, with 10% of Fetal bovine serum (FBS), 100 U/mL of penicillin and 100 μg/mL of streptomycin. The growth inhibition was evaluated using the sulphorhodamine B (SRB) assay, as previously described (Guimarães et al., 2013).

2.2.1.3. Evaluation of antimicrobial properties. Following the procedure previously described by Soković, Glamočlija, Marin, Brkić, and van Griensven (2010), the antibacterial activity was evaluated against four Gram-negative bacteria: *Escherichia coli* (ATCC 35210), *Pseudomonas aeruginosa* (ATCC 27853), *Salmonella typhimurium* (ATCC 13311), *Salmonella enteritidis* (ATCC 13076), and four Gram-positive bacteria: *Staphylococcus aureus* (ATCC 6538), *Bacillus cereus* (clinical isolate), *Micrococcus flavus* (ATCC 10240), and *Listeria monocytogenes* (NCTC 7973).

Following the procedure previously described by Soković & van Griensven (2006), the antifungal activity was evaluated against eight fungi: *Aspergillus fumigatus* (ATCC 1022), *Aspergillus ochraceus* (ATCC 12066), *Aspergillus versicolor* (ATCC 11730), *Penicillium funiculosum* (ATCC 36839), *Penicillium ochrochloron* (ATCC 9112), *Candida crusei* (clinical isolate) and *Penicillium verrucosum* (food isolate).

2.2.2. Response evaluation and statistical analysis

Antioxidant responses were evaluated by the EC_{50} values (sample concentration providing 50% of antioxidant activity or 0.5 of absorbance in the reducing power assay) and expressed in μg/mL. Trolox was used as positive control in all the assays.

Cytotoxicity responses were determined by the GI_{50} values (sample concentration providing 50% of cytotoxic activity) and the results were expressed in μg/mL. Ellipticine was used as a positive control.

Antimicrobial responses were evaluated by the minimum inhibitory (*MIC*) and minimum bactericidal or fungicidal (*MBC* or *MFC*) concentrations and results were expressed in μg/mL. Streptomycin and ampicillin were used as positive controls for bacteria growth, while bifonazole and ketokonazole were used as controls for fungi growth.

In all cases the assays were carried out in triplicate. The results were expressed as mean values and standard deviation (SD).
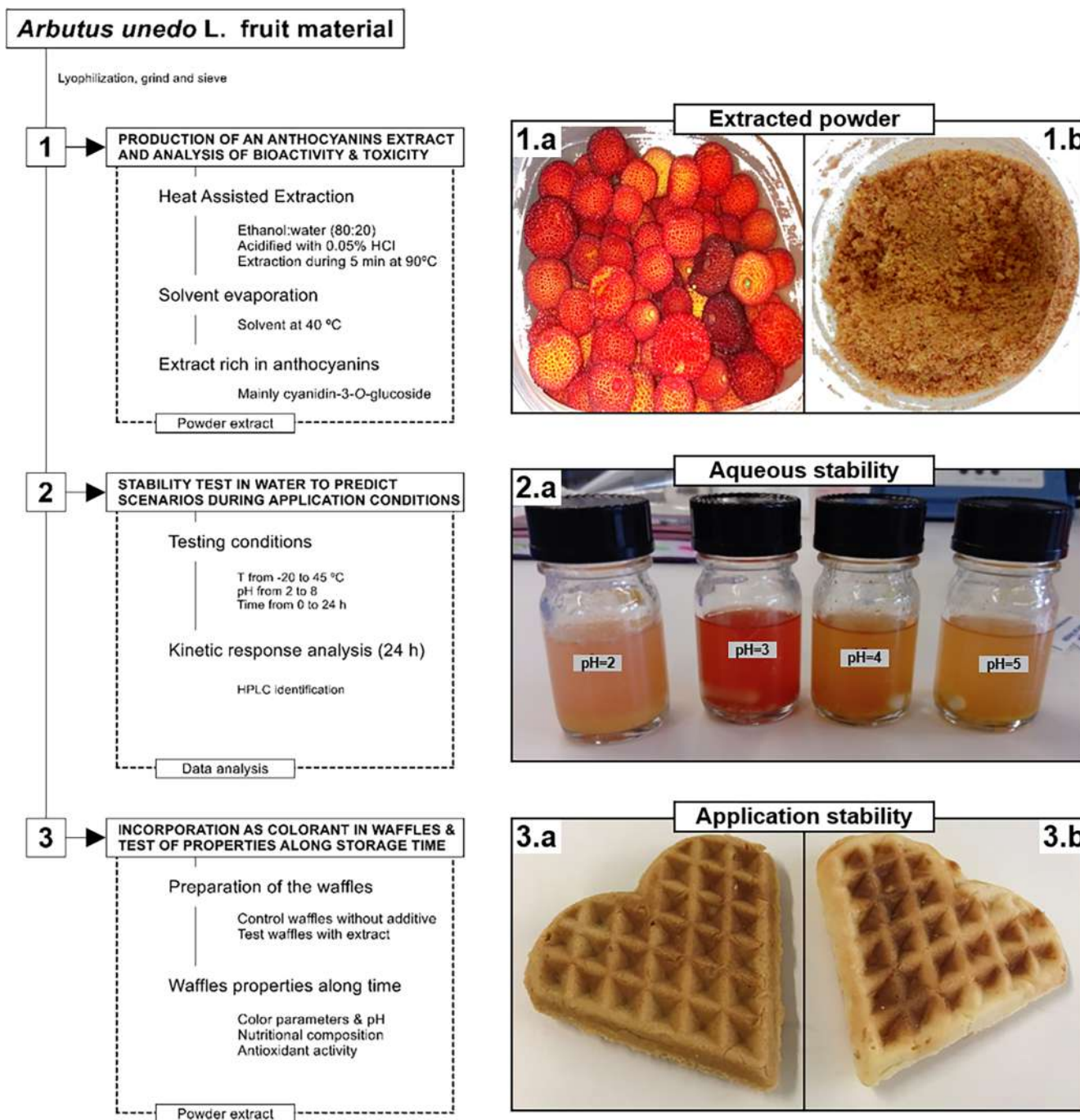
Fig. 1. Summarized diagram describing work performed: Section 1 shows the extraction process of anthocyanin compounds, Fig. 1.a and b presents the *A. unedo* fruit and extract, respectively; Section 2 shows the stability in aqueous solution systems considering its potential application in food matrices (Fig. 2.a shows the differences caused by the *pH* variable); and Section 3 shows the visual results of *A. unedo* extract rich in cyanidin-3-*O*-glucoside incorporated into wafers (Fig. 3.a shows wafer with *A. unedo* extract and 3.b control wafer).

2.3. Stability of the of the anthocyanins rich extract in aqueous solution systems

A brief summary of the work performed is presented in Fig. 1. Next, each step performed will be described in detail.

2.3.1. General procedure

The extract rich in anthocyanins (125 g) was dissolved in acidified distilled water (500 mL, 0.05% HCl). This solution was divided in 5 different flasks with 100 mL and adjusted with the addition of HCl (1 M) or NaOH (3%) to different *pH* values (2, 3.5, 5, 6.5 and 8). Then, the samples were subdivided in amber vials containing 2 mL (50 vials per *pH* tested) and the samples were stored at different temperatures of 4, 25, 40, 55 and 70 °C for monitoring of the anthocyanin stability along the time (*t*). Samples were collected at different *t* values of the storage period depending on the *T* applied, for example at all *pH* values, at 4 °C only 3 *t* values were used (0, 72 and 140 h), meanwhile at 70 °C 12 *t* values were used (0, 2, 4, 8, 12, 20, 48, 72, 96, 140, 164, 190 h). A total of 250 individual experimental points were collected to understand the patterns behind the stability of the extract in aqueous solution. As response criteria, the anthocyanins content was determined through HPLC-DAD, at each period of time. All independent measures were

obtained in triplicate (n = 3).

2.3.2. Identification and quantification of anthocyanins by HPLC-DAD

Each individual experimental point was filtered through a 0.22 μm disposable LC filter disk before chromatographic analysis, which was performed with a HPLC-DAD-ESI/MSn (Dionex Ultimate 3000 UPLC, Thermo Scientific, San Jose, CA, USA) system. The separation was achieved on a Waters Spherisorb S3 ODS-2 C18 (3 μm, 4.6 mm × 150 mm, Waters, Milford, MA, USA) operating at 35 °C. The solvents used were: (A) 0.1% TFA in water, and (B) 100% acetonitrile. The gradient elution followed these parameters: 10% B for 3 min, from 10 to 15% B for 12 min, 15% B for 5 min, from 15 to 18% B for 5 min, from 18 to 30% B for 20 min, from 30 to 35% B for 5 min, and from 35 to 10% B for 10 min. The resulting total run time was 60 min, followed by column reconditioning of 10 min, using a flow rate of 0.5 mL/min. Detection was carried out by DAD, using 520 nm as the preferred wavelength. Data acquisition was carried out with Xcalibur® data system (Thermo Finnigan, San Jose, CA, USA). A total of three anthocyanin compounds (Fig. A1, Supplementary material) were found and identified: delphinidin-3-*O*-glucoside (C1), cyanidin-3-*O*-glucoside (C2) and cyanidin-3-*O*-pentoside (C3), as previously described by Jiménez et al. (2018). For quantitative analysis, a 5-level calibration curve was obtained by injection of known concentrations (50–0.25 μg/mL) of cyanidin-3-*O*-glucoside ($y = 243287x – 1000000$; $R^2 = 0.9953$).

2.3.3. Responses evaluation and statistical analysis

The anthocyanins content was studied as function of mechanistic and phenomenological equations typically applied in similar processes.

2.3.3.1. Individual model for the analysis of the stability variable effects. *Effect of the time on the stability response*

For the *t* effect, a typical exponential function was applied:

$$e(t) = k \exp(-rt) \quad (1)$$

where *k* represents the starting point and *r* is the decay degradation rate of the reaction.

Effect of the temperature on the stability response

The Arrhenius equation establishes that the rate constant of a chemical reaction is a function of the absolute *T* according to the following relation:

$$e(T) = A \exp\left(-\frac{Ea}{RT}\right) \quad (2)$$

where the pre-exponential factor *A* represents the frequency of collisions among reacting molecules, *Ea* is the activation energy (kJ) and *R* the constant of gases (8.31 kJ/mol.K). In context, *A* and *Ea* can be considered as fitting parameters.

Effect of the pH on the stability response

The characteristic solution for the description of the *pH* effect is the exponential function, similar to the one used for *t* effect, that is usually found in many biological system responses (Komatsu et al., 2014; Prieto, Vázquez, & Murado, 2012b) and can be expressed as follows:

$$e(pH) = s \exp(-bpH) \quad (3)$$

where *s* represents the starting point and *b* is the degradation rate of the reaction.

2.3.3.2. Multivariable analysis.

To be able to develop a multivariable analysis of these three variables, the logical approach is to insert the equations that take control of pH and *T* into Eq. (1) that governs the time variable by modifying its parameters, the starting value (*k*) and the degradation rate (*r*). Even if the three variables are fully independent, any event that may occur in the surrounding environment of a reaction must be always referred to the time variable. Therefore, a global possible description of the stability at the molecular level could be described by the following approach:

$$e(t, pH, T) = k \cdot \exp(-r \cdot t) \quad \text{where} \quad \begin{array}{l} k(pH, T) = k \times e(T) \times e(pH) \\ r(pH, T) = r \times e(T) \times e(pH) \end{array}$$

$$(4)$$

where *k* represents the starting point and *r* is the degradation rate of the reaction caused by the effect of time as described Eq. (1) but modified by the governing equations of the effect of *T* (Eq. (2)) and *pH* (Eq. (3)).

2.3.3.3. Numerical methods and statistical analysis.

Fitting procedures, coefficient estimates and statistical calculations were performed as previously described (Pinela et al., 2016). In brief, a) the coefficient measurement was performed using the nonlinear least-square (quasi-Newton) method provided by the macro "Solver" in Microsoft Excel, which allows minimizing the sum of the quadratic differences between the observed and model-predicted values; b) the coefficient significance was evaluated using the 'SolverAid' to determine the parametric confidence intervals. Not statistically significant terms (*p*-value > 0.05) were dropped to simplify the model; and c) the model reliability was verified using the following criteria: i) the Fisher *F*-test (α = 0.05) was used to determine whether the constructed models were adequate to describe the observed data; ii) the 'SolverStat' macro was used for the assessment of parameter and model prediction uncertainties; iii) the R^2 was interpreted as the proportion of variability of the dependent variable explained by the model.

2.4. Incorporation of the anthocyanins rich extract in wafers as natural colorant additives. Evaluation of colour, nutritional composition and antioxidant activity along storage time

A brief summary of the work performed is presented in Fig. 1. Next, each step performed will be described in detail.

2.4.1. Preparation of the wafers samples

A traditional formulation was followed to prepare the wafers: 165 g of wheat flour was thoroughly mixed with 100 g of sugar and 1 g of baking powder. Then, 130 g of butter were sequentially added to the mixture while mixing vigorously with a hand mixer at 450 W during 5 min and after 2 eggs and 20 mL of lemon juice were added. Two lots of wafers (18 per lot, 6 wafers for each storage time) were prepared: i) control wafers – without the addition of any substance; and ii) wafers with the *A. unedo* extract rich in cyanidin-3-*O*-glucoside (5.50 g). The wafers were baked in a wafers machine for 10 min. All samples were lyophilized, finely crushed and analysed, in triplicate, immediately after preparation and after three and six days of storage (at room temperature and packed in a sealed plastic bags covered with aluminium paper).

2.4.2. Evaluation of colour parameters and pH of the wafers along storage time

The colour of the samples was measured using a colorimeter (model CR-400, Konica Minolta Sensing Inc., Tokyo, Japan). The illuminate C was used and a diaphragm aperture of 8 mm and previously calibrated against a standard white tile. The CIE L^* (lightness), a^* (greenness/redness), b^* (blueness/yellowness) colour space values were registered using a data software "Spectra Magic Nx" (version CM-S100W 2.03.0006) (Caleja et al., 2016). The samples' pH was measured by inserting the pH-meter (HI 99161, Hanna Instruments, Woonsocket, Rhode Island, USA) in the waffle sample. The determinations were performed in triplicate for each sample.

2.4.3. Evaluation of the proximate composition, free sugars, fatty acids and antioxidant activity of the wafers along storage time

- The contents of protein, fat, carbohydrates and ash, were determined following the AOAC methods (AOAC International, 2016). Total energy was calculated following the equation: Energy

Table 1
Antioxidant, cytotoxic and antimicrobial activities of *Arbutus unedo* L. extract (mean ± SD).

Antioxidant activity			*A. unedo* extract EC_{50} (µg/mL)	Control (Trolox) EC_{50} (µg/mL)
DPPH scavenging activity			295 ± 13	41 ± 1
Reducing power			447 ± 4	41.7 ± 0.3
β-carotene bleaching inhibition			901 ± 41	18 ± 1
Thiobarbituric acid reactive substances (TBARS)			257 ± 4	23 ± 1
Cytotoxicity in tumour cell lines			*A. unedo* extract GI_{50} (µg/mL)	Control (Ellipticine) GI_{50} (µg/mL)
NCI-H460 (non-small cell lung carcinoma)			> 400	1.0 ± 0.1
HeLa (cervical carcinoma)			350 ± 10	1.91 ± 0.06
HepG2 (hepatocellular carcinoma)			> 400	1.1 ± 0.2
MCF-7 (breast carcinoma)			338 ± 14	0.91 ± 0.04
Cytotoxicity in non-tumour cells			*A. unedo* extract GI_{50} (µg/mL)	Control (Ellipticine) GI_{50} (µg/mL)
PLP 2 (porcine liver primary cells)			> 400	3.2 ± 0.7

Antibacterial activity	*A. unedo* extract		Control (Ampicillin)	
	MIC (µg/mL)	MBC (µg/mL)	MIC (µg/mL)	MBC (µg/mL)
Gram negative bacteria				
Escherichia coli	> 1000	> 1000	400	500
Salmonella enteritidis	150	300	300	600
Salmonella typhimurium	200	300	400	750
Enterobacter cloacae	> 1000	> 1000	250	500
Gram positive bacteria				
Staphylococcus aureus	300	600	250	450
Bacillus cereus	150	450	250	400
Micrococcus flavus	300	600	250	400
Listeria monocytogenes	300	600	400	500

Antifungal activity	*A. unedo* extract		Control (Ketoconazole)	
	MIC (µg/mL)	MFC (µg/mL)	MIC	MFC
Aspergillus fumigatus	150	450	250	500
Aspergillus ochraceus	200	450	1500	2000
Aspergillus versicolor	300	600	200	500
Penicillium funiculosum	450	600	200	500
Penicillium ochrochloron	300	600	2500	3500
Candida crusei	300	600	075	150
Penicillium verrucosum	450	600	200	300

EC_{50} values correspond to the sample concentration achieving 50% of antioxidant activity or 0.5 of absorbance in the reducing power assay. GI_{50} values correspond to the sample concentration achieving 50% of growth inhibition in human tumour cell lines or in liver primary culture PLP2. *MIC* values correspond to the minimal sample concentration that inhibited the bacterial growth; *MBC* or *MFC* correspond to the minimum bactericidal or fungicidal concentrations, respectively.

(kcal) = 4 × (g proteins + g carbohydrates) + 9 × (g lipids). Total protein content (N × 5.70) was calculated as nitrogen content by the Kjeldahl method, while crude fat relied on the extraction of dried samples with petroleum ether using a Soxhlet apparatus. Finally, the ash content was determined by incineration at 550 ± 15 °C (Barros et al., 2013).

- For free sugars analysis, 1.0 g of dried sample powder was spiked with melezitose as internal standard (IS, 5 mg/mL), and extracted with 40 mL of 80% aqueous ethanol at 80 °C for 30 min. The resulting suspension was centrifuged (Centurion K24OR refrigerated centrifuge, West Sussex, UK) at 15,000g for 10 min. The supernatant was concentrated at 60 °C under reduced pressure and defatted three times with 10 mL of ethyl ether, successively. After concentration at 40 °C, the solid residues were dissolved in water to a final volume of 5 mL and filtered through 0.2 µm Whatman nylon filters. Free sugars were determined in defatted samples by HPLC coupled to a refraction index (RI) detector following a procedure previously described (Caleja et al., 2016). The free sugars were identified by comparison with standards and further quantified considering the internal standard (melezitose) (g/100 g of wafers).

- The fat obtained after the Soxhlet extraction was subjected to a methylation process with 5 mL of methanol: sulfuric acid: toluene 2: 1: 1 (v: v: v), for 12 h in a water bath at 50 °C and 160 rpm; then 3 mL of deionized water was added to obtain phase separation; FAME was recovered by adding 3 mL of diethyl ether, stirring on a Vortex shaker and passing the upper phase through a micro-column of anhydrous sodium sulfate, in order to eliminate the water. The sample was collected in a vial with Teflon and filtered with a 0.2 µm Whatman nylon filter before injection. The fatty acids were determined, by gas chromatography coupled to flame ionization detector (GC-FID), identified by comparison with standards (standard 47885, Sigma-Aldrich, St. Louis, Missouri, USA) and expressed as relative percentages of each fatty acid (Caleja et al., 2016).

- For evaluation of the antioxidant activity, the samples were submitted to DPPH and reducing power assays, described in a previous section (results expressed in EC_{50} values mg/mL).

2.4.4. Response evaluation and statistical analysis

The results were analysed using a Students *t*-student test in order to determine the significant difference between less than three different samples, with $p = 0.05$, and this treatment was carried out using the SPSS v. 23.0 program.

3. Results and discussion

3.1. Bioactive properties of the anthocyanins rich extract

Our research group has previously developed some works using fruits of *A. unedo* due to their traditional uses in the northeast of Portugal. The studies described the antioxidant properties of those fruits as well as the presence of important antioxidant molecules such as tocopherols and carotenoids (Barros, Carvalho, Morais, & Ferreira, 2010; Guimaraes, Barros, Carvalho, & Ferreira, 2010). Later, Guimarães et al. (2013) carried out an extensive characterization of the phenolic compounds present in *A. unedo* fruits and compared the bioactive properties of two different extracts rich in non-anthocyanin phenolic compounds and anthocyanins, respectively (Guimarães et al., 2014). Furthermore, an extraction optimization from these fruits was performed in order to obtain a rich extract in cyanidin-3-*O*-glucoside (Jiménez et al., 2018). The extract obtained under the optimal point was evaluated in the present study regarding bioactive and colorant simultaneous capacities, as also the conditions that most favoured its stability.

3.1.1. Antioxidant properties

There are several techniques that can be used to evaluate the antioxidant activity of pure compounds or complex mixtures (as in the case of plant extracts). In our study, to evaluate the antioxidant activity of *A. unedo* extract, four complementary *in vitro* assays were selected: DPPH free radicals scavenging, reducing power, β-carotene bleaching inhibition and TBARS formation inhibition. The results are expressed in EC_{50} values (µg/mL) and summarized in Table 1. The anthocyanins extract obtained from *A. unedo* fruits showed high antioxidant activity in the

different assays, mainly in the ability to inhibit TBARS formation with the lowest EC_{50} value. In a recent study, an extract from *A. unedo* rich in catechin was prepared and a high antioxidant activity was also described (Takwa et al., 2018). The reducing power assay was the only method performed that gave a higher antioxidant activity result (EC_{50} value = 328 ± 2 µg/mL), in comparison with this study; for the remaining assays the present extract revealed a greater antioxidant activity.

3.1.2. Cytotoxic properties

The potential effects of natural phenolic compounds as anticancer agents *in vitro* as well as *in vivo* has been described in different studies (Carocho & Ferreira, 2013). Thus, the effects of the extracts on the growth of the four human tumour cell lines (MCF-7, NCI-H460, HeLa, and HepG2) were determined and the values of the GI_{50} (concentrations that caused 50% of the cell growth inhibition) are detailed in Table 1. The *A. unedo* extract rich in cyanidin-3-*O*-glucoside did not show positive results for NCI-H460, nor HepG2 cell lines ($GI_{50} > 400$ µg/mL), showing to be able to inhibit the growth of HeLa (cervical carcinoma) and MCF7 (breast carcinoma) cell lines in a moderate way. This extract did not demonstrate cytotoxicity in PLP2 cell lines ($GI_{50} > 400$ µg/ mL). These results are in agreement with the work presented by Ziani et al. (2015), which studied the bioactive properties of infusions prepared from *A. unedo* flowers and leaves (rich in phenolic compounds, such as flavonoids, especially flavonols and phenolic acid esters), describing the absence of cytotoxic effects.

3.1.3. Antimicrobial properties

The antimicrobial activity was also studied against a panel of eight bacteria and eight fungi chosen due to their importance in public health. The results obtained for this activity are presented in Table 1 and were divided into antibacterial and antifungal activities. Results are expressed as *MIC* and *MBC* or *MFC* values (µg/mL). The results showed that *A. unedo* extract rich in cyanidin-3-*O*-glucoside, besides its high antioxidant activity, it also has a high antimicrobial activity. This activity was particularly high against *Salmonella enteritidis* and *Bacillus cereus*. Otherwise, the high antifungal activity of the extract was also confirmed, being *Aspergillus fumigatus* and *A. ochraceus* the most sensitive fungi, with the lowest *MIC* and *MFC* values. The antioxidant and antimicrobial capacities demonstrated by the *A. unedo* extract may be explained by the presence of significant levels of phenolic compounds, such as anthocyanins, as previously demonstrated by Mak, Chuah, Ahmad, and Bhat (2013).

3.2. Stability of the extracts in aqueous solution systems

The *A. unedo* extract rich in anthocyanins (mainly cyanidin-3-*O*-glucoside, Fig. A1) presents a total optimized content of ~500 µg/g of fruit dw or ~800 µg/g of R extract residue (knowing that the residual extract was ~60% of the total fruit dw). Such values can be located within the intermediate values described by other authors in similar plant-based samples. The anthocyanins content varies widely in similar fruit samples, from ~20 µg/g of fruit dw (plum) (Timberlake and Henry, 1988) to ~15000 µg/g of fruit dw (elderberry) (Clifford, 2000). The achieved results are within the same values as those well-known fruits with high content of anthocyanins such as *Nitraria tangutorum* Bobr. (~650 µg/g of fruit dw) (Sang, Sang, Ma, Hou, & Li, 2017) and *Aristotelia chilensis* L. (400 at 1500 µg/g of fruit dw) (Gironés-Vilaplana et al., 2014). Non-controllable variables such as soil properties, sun exposition, harvest time, etc., and controllable variables such as the extraction conditions (time, solvent, temperature, etc.) and techniques (ultrasound, maceration, microwave, etc.), may affect compounds concentration and could increase/decrease the yield efficiencies. However, the higher efficiencies in anthocyanins extraction from *A. unedo* fruits, in comparison with other sources emphasizes the need to perform more detailed evaluations of the stability of the compounds

obtained. From the stability point of view, the main factors includes *t* (Komatsu et al., 2014), *pH* (Su, Leung, Huang, & Chen, 2003), *T* (Demeule et al., 2002), oxygen level (Labbé, Têtu, Trudel, & Bazinet, 2008) and concentration of other compounds such as antioxidants level, metal ions and other compositional ingredients (Zhu, Zhang, Tsang, Huang, & Chen, 1997). Although all of these parameters are relevant, most of the authors agree that the essential ones are *t*, *pH* and *T* (Komatsu et al., 2014; Li, Taylor, Ferruzzi, & Mauer, 2012; Li et al., 2011). Therefore, the stability of anthocyanins content was studied regarding the functions *t*, *pH* and *T* in an aqueous solution system. For all these responses, the stability of the compounds was monitored by HPLC-DAD.

The mathematical analysis of the stability of anthocyanin compounds is first performed from an invariable perspective, fitting each set of conditions of *T* and *pH* to the time-dependent model of Eq. (1). Afterwards, the effects caused by the affecting variables *T* and *pH* over the time-dependent parametric values of Eq. (1) are depicted and stablished in mathematical terms by auxiliary functions. Then, the mathematical analysis is presented with a global performing fitting analysis from a multivariable perspective. Mathematical analysis using an invariable or multivariable perspective allowed to summarize the response behaviour into parametric information, which helps to perform easier comparisons and predictions. However, the development of models from a multivariable perspective facilitates the possibility of combining the effects of all variables simultaneously into a single master curve that is able to fit all the experimental data (Prieto, Vázquez, & Murado, 2012a). Such a solution allows to control most factors that affect the system, helping to reduce the over fitted resolutions that perturbs the comprehension of the real effects caused by the variables and therefore, the final parametric values are more reproducible.

3.2.1. Individual time analysis of each of the conditions of temperature and pH

The individual time-dependent graphical analysis of the stability of the anthocyanin content in aqueous solution as function of the *pH* and *T* are presented in Section A of Figs. 2 and 3. Fig. 2 shows the stability results for the total anthocyanin content, meanwhile Fig. 3 shows the stability of the individual content of the identified anthocyanin compounds of C1 (delphinidin-3-*O*-glucoside), C2 (cyanidin-3-*O*-glucoside) and C3 (cyanidin-3-*O*-pentoside). Each graphical illustration shows the time degradation effects (0–190 h) of each *T* tested (4, 25, 40, 55, and 70 °C). Points are the experimental data of the different *pHs* tested (●2, ○3.5, ◆5, ◇6.5 and ★8) and lines (—) show the results predicted by Eq. (1). The parametric results and correlation coefficients obtained after fitting each kinetic degradation at each of the *T* and *pH* values tested by Eq. (1) are presented in Table 2. In all cases the statistical description was significant and the prediction of the anthocyanins content stability in solution by Eq. (1) showed highly consistent R^2 values. When observing the patterns of the kinetic parametric values *k* and *r* (Table 2), it can be observed that the kinetic parameter value of *k* remain constant at each value of *T* and *pH*, meanwhile the kinetic parameter *r* is the one that takes into account all the effects caused by the changes of *T* and *pH*.

3.2.2. Multivariable analysis for the global comprehension of the anthocyanins stability

To be able to describe those effects in a multivariate form, the degradation rate parameter of Eq. (1) (*r*) assumes all the perturbation effects caused by the *pH* and *T* variables. The increase in *pH* and *T* units causes an exponential increase on the degradation rate of the stability of anthocyanin compounds. The *T* effect behaves following the Arrhenius equation presented in Eq. (2). However, the *pH* effect cannot be described by any standard physical-chemical function, because the main mechanisms behind the *pH* in basic chemical reactions or complex living organisms are dissimilar and heterogeneous. For this particular

A: INDIVIDUAL ANALYSIS
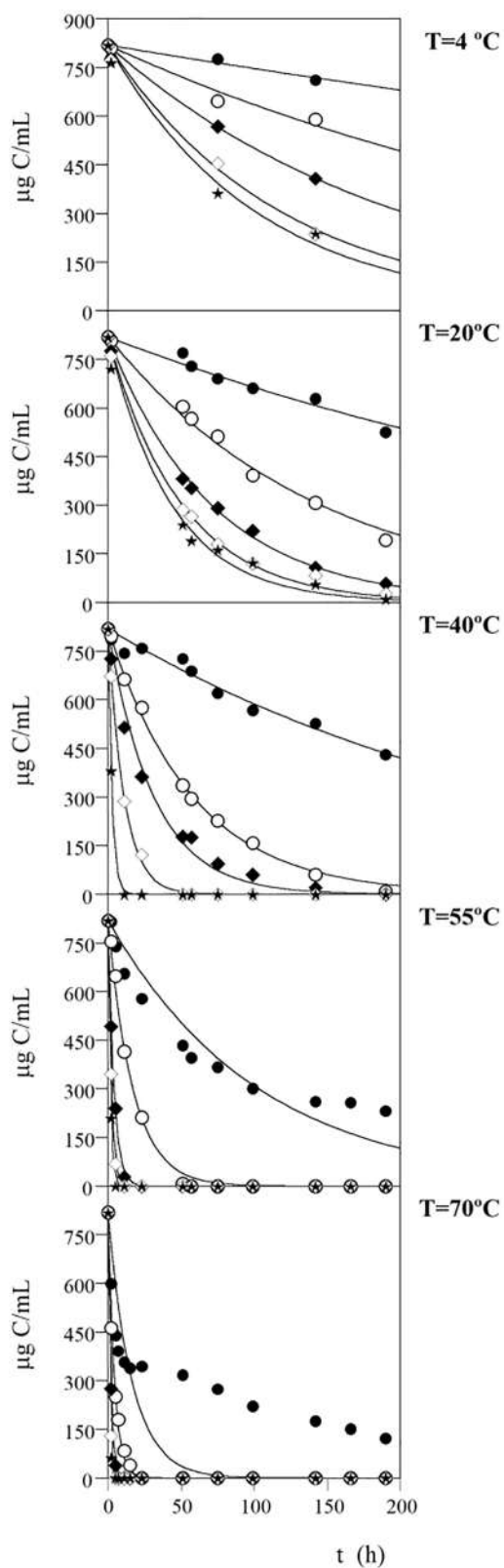
B: MULTIVARIABLE ANALYSIS

B1: Parametric pattern
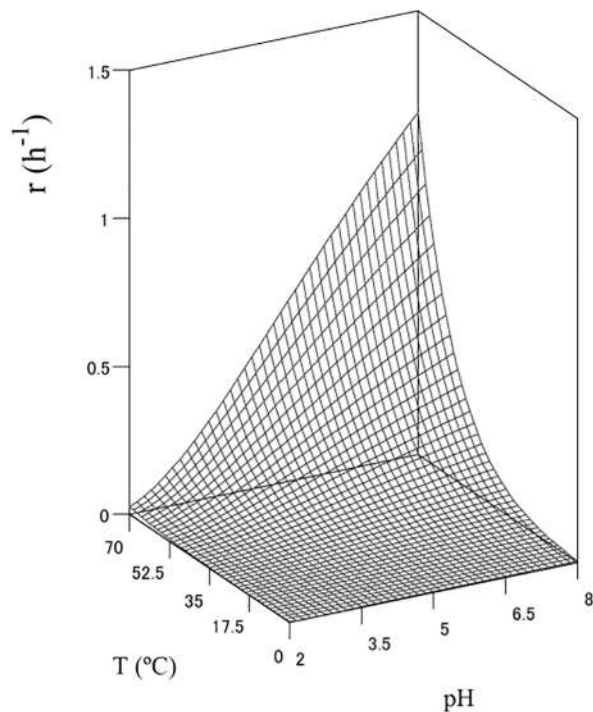
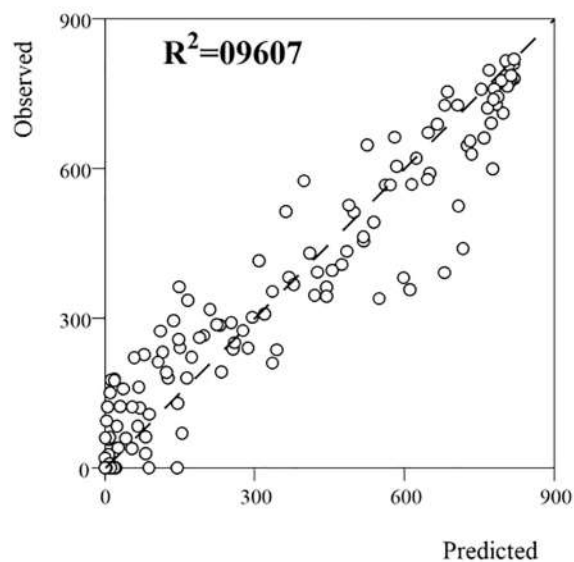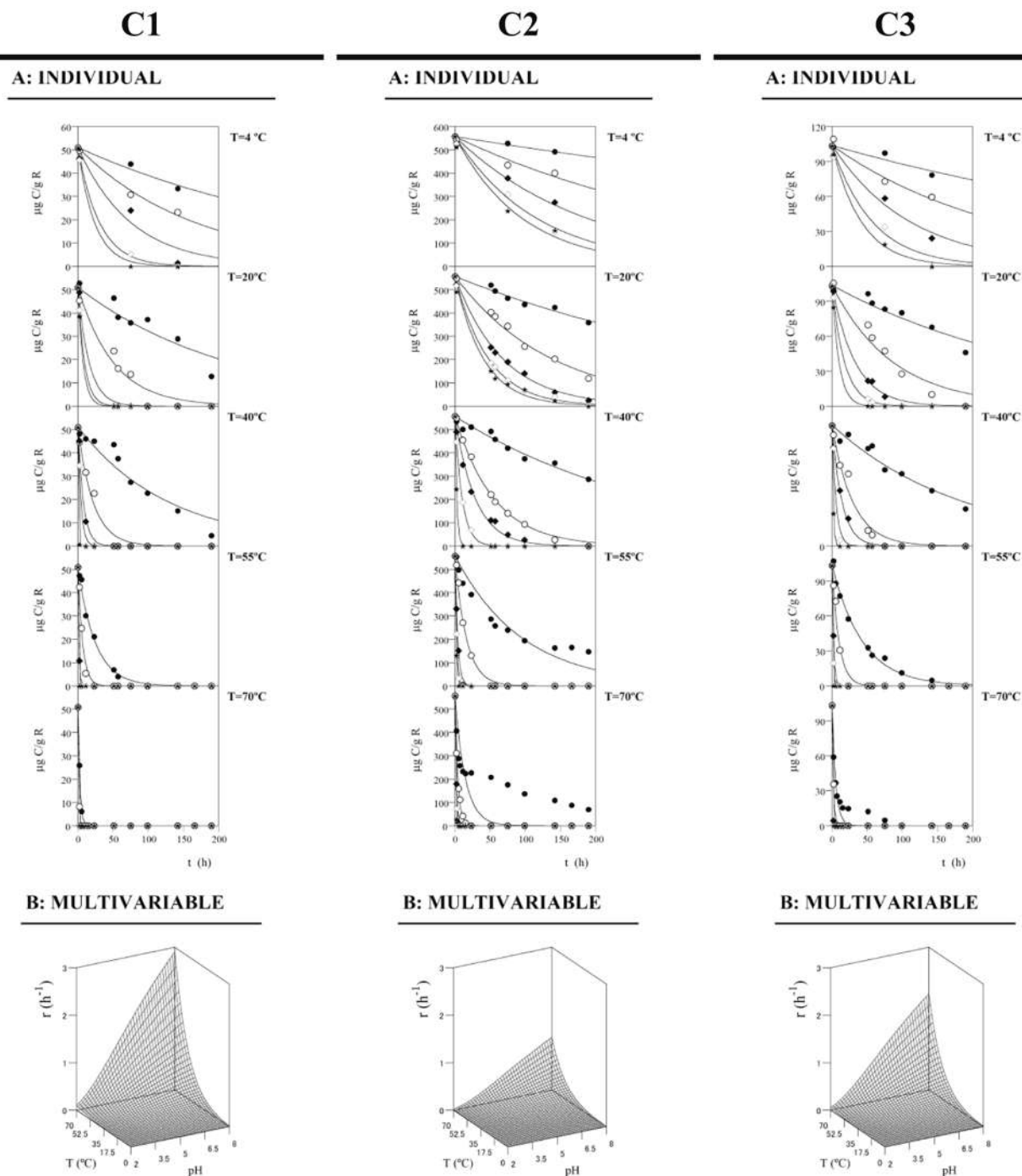## B2: Experimental data and modelled

(caption on next page)

Fig. 2. Total anthocyanins stability as function of the *t*, *T* and *pH* in aqueous solution systems simulating food matrices. Section **A** shows the individual time-dependent graphical analysis of the stability results based on the anthocyanins content as function of the *T* and *pH*. Each graph shows the time degradation effects (0–190 h) of each *T* tested (5, 25, 40, 55 and 70 °C). Points are the experimental data of the different *pHs* tested (●2, ○3.5, ◆5, ◊6.5 and ★8) and lines (—) the results predicted by Eq. (1). The parametric results and correlation coefficients are presented in Table 2. Section **B** shows the global multivariable fitting results of applying Eq. (5) to describe the full multivariable data: **B1** shows the parametric net surface pattern of the kinetic *r* as a function of their respective affecting variables (*pH* and *T*); and **B2** shows the correlation between the experimental values and the predicted ones obtained with the multivariable model presented in Eq. (5).

Fig. 3. Individual stability of delphinidin-3-*O*-glucoside (C1), cyanidin-3-*O*-glucoside (C2) and cyanidin-3-*O*-pentoside (C3) as function of the *t*, *T* and *pH* in aqueous solution systems simulating food matrices. Two sub-sections for each compound are represented as in Fig. 2. Section **A** shows the individual time-dependent graphical analysis of the stability results based on the anthocyanins content as function of the *T* and *pH*. Each graph shows the time degradation effects (0–190 h) of each *T* tested (5, 25, 40, 55 and 70 °C). Points are the experimental data of the different *pHs* tested (●2, ○3.5, ◆5, ◊6.5 and ★8) and lines (—) the results predicted by Eq. (1). The parametric results and correlation coefficients are presented in Table 2. Section **B** shows the global multivariable fitting results of applying Eq. (5) to describe the full multivariable data of the parametric net surface pattern of the kinetic *r* as a function of their respective affecting variables (*pH* and *T*).

Table 2

Results of the parametric and confidence intervals of the total anthocyanins, delphinidin-3-glucoside (C1), cyanidin-3-glucoside (C2) and cyanidin-3-pentoside (C3) content fitted to the time dependent model presented in Eq. (1) at different pH and T conditions when evaluating the stability during the process for obtaining the enriched extract.

T	pH	Total $k(t)$ ($\mu g/g$ R)	$r(t)$ (h^{-1})	R^2	C1 $k(t)$ ($\mu g/g$ R)	$r(t)$ (h^{-1})	R^2	C2 $k(t)$ ($\mu g/g$ R)	$r(t)$ (h^{-1})	R^2	C3 $k(t)$ ($\mu g/g$ R)	$r(t)$ (h^{-1})	R^2
4.0	2.0	818.9 ± 66.28	0.001 ± 0.001	0.909	51.4 ± 4.47	0.003 ± 0.001	0.870	557.0 ± 38.43	0.001 ± 0.001	0.890	103.7 ± 9.23	0.002 ± 0.000	0.890
4.0	3.5	818.9 ± 79.46	0.003 ± 0.001	0.970	51.4 ± 5.10	0.006 ± 0.001	0.992	557.0 ± 53.59	0.003 ± 0.001	0.962	103.7 ± 10.11	0.004 ± 0.000	0.975
4.0	5.0	818.9 ± 81.41	0.005 ± 0.002	0.994	51.4 ± 4.89	0.013 ± 0.001	0.952	557.0 ± 55.41	0.005 ± 0.001	0.995	103.7 ± 10.13	0.009 ± 0.000	0.976
4.0	6.5	818.9 ± 81.48	0.008 ± 0.003	0.995	51.4 ± 5.13	0.033 ± 0.001	0.998	557.0 ± 55.31	0.009 ± 0.002	0.993	103.7 ± 10.19	0.017 ± 0.001	0.983
4.0	8.0	818.9 ± 81.15	0.010 ± 0.003	0.991	51.4 ± 5.12	0.044 ± 0.001	0.997	557.0 ± 55.12	0.010 ± 0.002	0.990	103.7 ± 10.35	0.024 ± 0.001	0.998
20.0	2.0	818.9 ± 79.25	0.002 ± 0.001	0.968	51.4 ± 4.62	0.005 ± 0.001	0.899	557.0 ± 53.90	0.002 ± 0.001	0.968	103.7 ± 9.53	0.003 ± 0.000	0.919
20.0	3.5	818.9 ± 81.34	0.007 ± 0.002	0.993	51.4 ± 4.96	0.020 ± 0.001	0.965	557.0 ± 55.21	0.007 ± 0.002	0.991	103.7 ± 10.06	0.012 ± 0.000	0.970
20.0	5.0	818.9 ± 81.77	0.014 ± 0.005	0.998	51.4 ± 5.12	0.064 ± 0.001	0.997	557.0 ± 55.56	0.015 ± 0.003	0.997	103.7 ± 10.34	0.031 ± 0.001	0.997
20.0	6.5	818.9 ± 81.73	0.020 ± 0.006	0.998	51.4 ± 5.14	0.111 ± 0.002	1.000	557.0 ± 55.63	0.021 ± 0.005	0.999	103.7 ± 10.37	0.057 ± 0.002	1.000
20.0	8.0	818.9 ± 81.36	0.023 ± 0.007	0.993	51.4 ± 5.14	0.143 ± 0.003	1.000	557.0 ± 55.42	0.025 ± 0.006	0.995	103.7 ± 10.37	0.102 ± 0.004	1.000
40.0	2.0	818.9 ± 79.24	0.003 ± 0.001	0.967	51.4 ± 4.78	0.008 ± 0.001	0.930	557.0 ± 53.64	0.003 ± 0.001	0.963	103.7 ± 9.79	0.005 ± 0.000	0.944
40.0	3.5	818.9 ± 81.75	0.017 ± 0.006	0.998	51.4 ± 5.05	0.047 ± 0.001	0.984	557.0 ± 55.62	0.018 ± 0.004	0.999	103.7 ± 10.17	0.034 ± 0.001	0.980
40.0	5.0	818.9 ± 81.34	0.032 ± 0.010	0.993	51.4 ± 5.09	0.129 ± 0.003	0.991	557.0 ± 55.39	0.035 ± 0.008	0.994	103.7 ± 10.34	0.071 ± 0.003	0.997
40.0	6.5	818.9 ± 81.83	0.092 ± 0.030	0.999	51.4 ± 5.11	0.237 ± 0.005	0.994	557.0 ± 55.67	0.098 ± 0.022	0.999	103.7 ± 10.23	0.177 ± 0.007	0.986
40.0	8.0	818.9 ± 81.88	0.385 ± 0.126	1.000	51.4 ± 5.14	2.250 ± 0.046	1.000	557.0 ± 55.69	0.412 ± 0.092	1.000	103.7 ± 10.37	0.659 ± 0.027	1.000
55.0	2.0	818.9 ± 77.79	0.010 ± 0.003	0.950	51.4 ± 5.11	0.041 ± 0.001	0.994	557.0 ± 53.18	0.010 ± 0.002	0.955	103.7 ± 10.29	0.023 ± 0.001	0.992
55.0	3.5	818.9 ± 81.71	0.059 ± 0.019	0.998	51.4 ± 5.09	0.155 ± 0.003	0.991	557.0 ± 55.52	0.062 ± 0.014	0.997	103.7 ± 10.26	0.102 ± 0.004	0.989
55.0	5.0	818.9 ± 81.84	0.254 ± 0.083	0.999	51.4 ± 5.14	0.791 ± 0.016	1.000	557.0 ± 55.60	0.268 ± 0.060	0.998	103.7 ± 10.28	0.498 ± 0.020	0.991
55.0	6.5	818.9 ± 81.84	0.449 ± 0.147	0.999	51.4 ± 5.14	6.688 ± 0.137	1.000	557.0 ± 55.63	0.481 ± 0.107	0.999	103.7 ± 10.37	0.843 ± 0.035	1.000
55.0	8.0	818.9 ± 81.82	0.699 ± 0.229	0.999	51.4 ± 5.14	12.894 ± 0.265	1.000	557.0 ± 55.66	0.740 ± 0.165	0.999	103.7 ± 10.37	4.784 ± 0.198	1.000
70.0	2.0	818.9 ± 67.27	0.062 ± 0.017	0.821	51.4 ± 5.11	0.393 ± 0.008	0.994	557.0 ± 46.19	0.068 ± 0.013	0.829	103.7 ± 9.97	0.194 ± 0.008	0.961
70.0	3.5	818.9 ± 81.55	0.237 ± 0.077	0.996	51.4 ± 5.14	0.922 ± 0.019	1.000	557.0 ± 55.56	0.253 ± 0.056	0.997	103.7 ± 10.34	0.572 ± 0.024	0.997
70.0	5.0	818.9 ± 81.85	0.561 ± 0.184	0.999	51.4 ± 5.14	6.271 ± 0.129	1.000	557.0 ± 55.62	0.592 ± 0.132	0.999	103.7 ± 10.37	1.591 ± 0.066	1.000
70.0	6.5	818.9 ± 81.89	0.927 ± 0.304	1.000	51.4 ± 5.14	5.635 ± 0.116	1.000	557.0 ± 55.52	0.836 ± 0.186	0.997	103.7 ± 10.37	4.967 ± 0.206	1.000
70.0	8.0	818.9 ± 81.90	1.288 ± 0.422	1.000	51.4 ± 5.14	4.943 ± 0.102	1.000	557.0 ± 55.70	1.517 ± 0.338	1.000	103.7 ± 10.37	4.285 ± 0.178	1.000

case, the *pH* effect follows a positive exponential relation as described by Eq. (3). Therefore, the general solution presented in Eq. (4) is reduced to a simpler solution in which only the kinetic parameter *r* is assuming the effects caused by the variables. In conclusion, the global multivariable model that controls the effect of *t*, *pH* and *T* on the stability in aqueous system can be established by substituting the *r* parameter of Eq. (1) with the equations leading the effect of the variables *T* (Eq. (2)) and the *pH* (Eq. (3)), as follows:

$$e(t, pH, T) = k \exp(-p \exp(-\frac{Ea}{RT} + bpH)t) \tag{5}$$

When substituting the *r* parameter by the multiplicative results of Eqs. (2) and (3), the new resulting expression share a pre-exponential factor (*A* and *s*) and their use in conjunction will be redundant therefore, a new factor is described and noted as *p*. All other parametric notations are as defined in the material and methods section. Section B of Figs. 2 and 3 show the global multivariable fitting results of applying Eq. (5) to describe the full multivariable data.

The parametric results for the different multivariable analysis are:

- The resulting parameters of the total anthocyanin content analysis were $k = 819.00 \pm 56.1 \,\mu g/g$ R, $p = 59.32 \pm 11.2$, $Ea = 4.35 \times 10^{+9} \pm 0.98 \times 10^{+9}$ kJ and $b = 10.05 \pm 3.5$ obtaining a R^2 values of 0.9577.
- For C1 were $k = 50.16 \pm 4.3 \,\mu g/g$ R, $p = 57.10 \pm 9.7$, $Ea = 4.35 \times 10^{+9} \pm 1.21 \times 10^{+9}$ kJ and $b = 8.91 \pm 2.3$ obtaining a R^2 values of 0.9396.
- For C2 were $k = 527.35 \pm 116.4 \,\mu g/g$ R, $p = 59.38 \pm 7.8$, $Ea = 4.35 \times 10^{+9} \pm 0.46 \times 10^{+9}$ kJ and $b = 10.23 \pm 3.2$ obtaining a R^2 values of 0.9590.
- For C3 were $k = 101.20 \pm 31.4 \,\mu g/g$ R, $p = 57.95 \pm 7.6$, $Ea = 4.35 \times 10^{+9} \pm 0.44 \times 10^{+9}$ kJ and $b = 9.42 \pm 3.5$ obtaining a R^2 values of 0.9534.

In all cases the statistical description was significant and the prediction of the anthocyanin content stability in solution by Eq. (5) showed highly consistent R^2 values. The multivariable analysis of the kinetic parameter *r* as a function of their respective affecting variables (*pH* and *T*) presented in the subsection B of Figs. 2 and 3, show the 3D graphical surface response for the degradation rate of the total anthocyanins content and for the individual content of the identified anthocyanin compounds (C1, C2 and C3). The conclusions are in accordance with previous results reported (Komatsu et al., 2014; Li et al., 2012; Li et al., 2011), revealing that at $T < 20\,°C$ and $pH < 3.5$ the extract is more stable lowering as much as possible the degradation rate of anthocyanin compounds.

In the aqueous solution system, it proved to be highly dependent on the three variables studied. Compounds decayed completely over a period of time at different *pH* and *T*. This phenomenon was also detected by other authors that studied the stability of catechin and derivatives from other matrices such as green tea and cacao (Komatsu et al., 2014; Li et al., 2012; Zhu et al., 2002, Zhu et al., 1997). In similar terms with other authors (Li et al., 2012), results indicated that anthocyanin extracts in aqueous solution remained stable at a *pH* value lower than 3.5 and temperatures below 30 °C for a period of 72 h. Even at high thermal process conditions (70 °C) with a *pH* lower than 3.5, the anthocyanins content is detected during 1 h period without great losses. These results may limit the anthocyanin extract direct application, favouring acid foods as some chesses, fruit juice, vegetable/fruit products, mayonnaises and yogurts.

The key issue lies down behind the fact that anthocyanins undergo kinetic degradation during thermal processing and that the increase of the *pH* causes molecular changes in detriment of its colour properties (Komatsu et al., 2014; Ruiz-Rodríguez et al., 2011). The analytical solution of such a system through mathematical models is important and necessary, but not exempt of complexity due to the heterogeneous

responses of the variables involved. Achieving a successful mathematical model solution would allow to control most factors that affect the system, helping to standardize the key variables for producing stable plant-based extracts and therefore, to optimize the complete extraction process.

The analysis of the anthocyanin compounds stability from the strawberry tree fruits is crucial for predicting the shelf life behaviour of the compounds in various processing situations. In fact, food processing or other processes are factors that affect directly on the integrity of the molecules. Controlling the conditions of *t*, *pH* and *T* among others are essential aspects for keeping the process efficiency and for obtaining high quality products. Mathematical models were developed and multiple graphical plots were conducted to establish and illustrate the optimum values of the independent variables studied. Thus, the kinetic models could be used for calculating shelf-life and predicting compounds stability at given *pH* and *T* conditions for aqueous systems. The optimal stability conditions for anthocyanins content in aqueous solution remained intact at $pH < 3.5$ and $T < 30\,°C$ for a period of at least 72 h. Moreover, using the optimal processing conditions, it is possible to produce functional extracts with high potential as nutraceuticals or as active ingredients in the design of functional foods, which can be also extended to other industrial fields such as pharmaceutical and cosmeceutical industries.

3.3. Incorporation of the anthocyanins rich extract as a natural colorant additive in wafers: Colour parameters, pH, nutritional composition and antioxidant activity of the samples along storage time

The bakery industry represents an important economic sector and is currently in great growth and constant innovation. Wafers are well-known cakes and consumed worldwide. Thus, their preparation using natural colorants instead of artificial ones, is a representative case study for the bakery sector. However, it is important to evaluate the colour changes caused in the food matrix within the storage time, as well as the effects in other parameters such as pH, nutritional composition and the preservative function, evaluated using antioxidant activity assays.

Part A of Table 3 shows the result values obtained for each of the evaluated colour parameter (L^*, a^* and b^*) in each one of the food samples during the storage period (6 days). The results presented in Table 3 (part A) demonstrate that the incorporation of *A. unedo* extract rich in cyanidin-3-*O*-glucoside caused slight changes in the wafers when compared to the control wafer, along the different storage time. In visual terms, the *A. unedo* extract provides a slightly golden colour to the wafer (Fig. 1, sub-Fig. 3.*a*) when compared to the control wafer (Fig. 1, sub-Fig. 3.*b*). These results are in accordance with those produced by other authors (Debonne, Van Bockstaele, Philips, De Leyn, & Eeckhout, 2017), when evaluating the colorimetric parameters in pastry and baking products, revealing that it is necessary to consider that the colour of the crust is directly related to the temperature and cooking time and not entirely related to the products used.

- Parts B, C, D and E of Table 3 show the *pH* values, macronutrients content, individual sugar contents and energy of the control wafers and of the wafers whit the *A. unedo* extract rich in cyanidin-3-*O*-glucoside during the self-life period of the product. As a bakery product which has been baked with temperature, moisture values (Table 3) were expected to be quite low. It is possible to verify that the carbohydrates are the most abundant macronutrients in wafers. The results show that the incorporation of the extract did not cause significant changes in relation to the control sample, for all the studied storage times. Three individual sugars were detected in the samples: fructose, glucose and sucrose (Fig. A1), with a high prevalence of the disaccharide. Significant differences were detected only for fructose and glucose after 3 and 6 days of storage, whereas the wafers incorporated with the extract always showed higher amounts of these sugars when compared to the control wafers. This

Table 3
Results of colour parameters, pH, nutritional composition, free sugars, fatty acids and antioxidant activity of wafer samples.

Parameters	0 Days				3 Days			6 Days		
		Control	AU	t-test	Control	AU	t-test	Control	AU	t-test
A) Colour parameters										
L^*		52.6 ± 0.6	52 ± 1	0.91	50.0 ± 0.4	54 ± 2	0.191	50.5 ± 0.4	54 ± 2	0.341
a^*		18.1 ± 0.5	16 ± 1	0.168	19.5 ± 0.1	15.3 ± 0.5	0.005	18.2 ± 0.5	15.6 ± 0.4	0.02
b^*		36.8 ± 0.7	35 ± 1	0.149	36.1 ± 0.6	38 ± 1	0.114	35.1 ± 0.5	36 ± 1	0.533
B) pH value										
pH		5.64 ± 0.09	5.3 ± 0.1	0.009	5.58 ± 0.04	5.7 ± 0.3	0.329	5.48 ± 0.06	5.9 ± 0.5	0.185
C) Nutritional composition										
Moisture	(g/100 g fw)	11.42 ± 0.08	11.25 ± 0.09	0.058	11.5 ± 0.2	11.9 ± 0.1	0.054	11.4 ± 0.2	10.9 ± 0.1	0.018
Ash	(g/100 g fw)	0.018 ± 0.01	0.018 ± 0.01	0.682	0.020 ± 0.01	0.017 ± 0.01	0.205	0.017 ± 0.01	0.018 ± 0.01	0.396
Fat	(g/100 g fw)	21.7 ± 0.5	22.5 ± 0.1	0.044	22.6 ± 0.7	21.5 ± 0.9	0.17	22.4 ± 0.2	21.7 ± 0.2	0.026
Proteins	(g/100 g fw)	9.6 ± 0.3	9.48 ± 0.09	0.388	8.47 ± 0.07	9.0 ± 0.2	0.005	9.45 ± 0.5	9.0 ± 0.1	0.096
Total sugars	(g/100 g fw)	57.3 ± 0.4	56.8 ± 0.1	0.123	57.4 ± 0.6	57.6 ± 0.8	0.764	56.8 ± 0.4	58.3 ± 0.2	0.002
Energy	(kcal/100 g fw)	463 ± 2	467 ± 1	0.027	467 ± 3	460 ± 4	0.099	466 ± 1	465 ± 1	0.203
D) Free sugars										
Fructose	(g/100 g fw)	0.32 ± 0.01	0.64 ± 0.09	0.001	0.35 ± 0.01	0.76 ± 0.003	< 0.001	0.33 ± 0.01	0.69 ± 0.001	< 0.001
Glucose	(g/100 g fw)	0.38 ± 0.01	0.51 ± 0.06	0.005	0.39 ± 0.02	0.58 ± 0.004	< 0.001	0.31 ± 0.02	0.53 ± 0.003	< 0.001
Sucrose	(g/100 g fw)	28.1 ± 0.2	28.3 ± 0.9	0.702	28.4 ± 0.4	29.2 ± 0.7	0.06	28.17 ± 0.07	30.0 ± 0.7	0.004
Total	(g/100 g fw)	28.8 ± 0.2	29 ± 1	0.216	29.1 ± 0.4	30.6 ± 0.7	0.011	28.82 ± 0.05	31.2 ± 0.7	0.001
E) Fatty acids										
C12:0	(%)	3.3 ± 0.1	3.22 ± 0.09	0.332	3.1 ± 0.2	3.21 ± 0.07	0.234	3.28 ± 0.08	3.3 ± 0.1	0.728
C14:0	(%)	1.65 ± 0.03	1.65 ± 0.02	0.898	1.59 ± 0.06	1.63 ± 0.03	0.322	1.68 ± 0.03	1.67 ± 0.03	0.851
C16:0	(%)	30.8 ± 0.4	30.8 ± 0.4	0.942	29.8 ± 0.3	30.5 ± 0.5	0.073	31.4 ± 0.4	31.4 ± 0.5	0.839
C18:0	(%)	30.9 ± 0.3	31.6 ± 0.1	0.042	30.8 ± 0.5	31 ± 1	0.736	29.9 ± 0.5	31.0 ± 0.5	0.055
C18:2n6	(%)	30.4 ± 0.2	29.7 ± 0.3	0.036	31.9 ± 0.5	31.3 ± 0.4	0.121	30.9 ± 0.2	29.8 ± 0.4	0.021
C18:3n3	(%)	1.28 ± 0.04	1.37 ± 0.02	0.053	1.30 ± 0.03	1.25 ± 0.09	0.459	1.376 ± 0.01	1.30 ± 0.09	0.236
SFA	(%)	67.9 ± 0.2	68.5 ± 0.3	0.046	66.4 ± 0.5	67.1 ± 0.4	0.138	67.4 ± 0.2	68.5 ± 0.5	0.03
MUFA	(%)	0.34 ± 0.03	0.38 ± 0.01	0.162	0.35 ± 0.01	0.39 ± 0.01	0.024	0.34 ± 0.04	0.38 ± 0.01	0.19
PUFA	(%)	31.7 ± 0.2	31.1 ± 0.3	0.041	33.2 ± 0.5	32.5 ± 0.4	0.125	32.2 ± 0.2	31.1 ± 0.5	0.027
F) Antioxidant activity										
DPPH activity	(mg/mL)	> 200	43.3 ± 0.6	< 0.001	> 200	43.5 ± 0.5	< 0.001	> 200	57 ± 1	< 0.001
Reducing power	(mg/mL)	15.0 ± 0.4	14 ± 0.1	< 0.001	21.7 ± 0.8	14.42 ± 0.20	< 0.001	23.9 ± 0.3	15.9 ± 0.4	< 0.001

Control- wafer without extract and AU- wafers with *A. unedo* extract rich in cyanidin-3-*O*-glucoside. In each line and for each storage time a Studeńs *t*-test was used to determine the significant difference between two different samples, with α = 0.05. L^*, a^* and b^* represent colour parameters. SFA- Saturated fatty acids; MUFA- Monounsaturated fatty acids; PUFA- Polyunsaturated fatty acids. Antioxidant activity was evaluated in terms of EC_{50} values that correspond to the sample concentration achieving 50% of antioxidant activity or 0.5 of absorbance in reducing power assay.

fact may be related with the presence of free sugars in the *A. unedo* extract.

- Table 3E shows the six most abundant fatty acids detected in wafer samples. Although fourteen fatty acids were identified in the studied samples (Fig. A1), eight were detected only in trace amounts (data not shown). The most abundant fatty acids were palmitic acid (C16:0), stearic acid (C18:0) and linoleic acid (C18:2n6). In this work, it was verified that the saturated fatty acids appear in higher quantity than the unsaturated counterparts, and the incorporation of the extract did not cause significant changes in the fatty acids profile when compared to the control wafers at any storage period. The amount of extract added was in a low amount and as such it would be expected that no changes are made to the fatty acid profile of the wafers, since the shelf life was very short and therefore over time there were also no changes.

- Finally, the antioxidant activity results (preservation potential of the extract rich in anthocyanins) based on the DPPH radical scavenging activity and reducing power of the wafers samples during the shelf-life period are presented in Table 3F. The incorporation of the extract obtained from *A. unedo* and rich in cyanidin-3-*O*-glucoside provides significantly beneficial properties to the tested food matrix as compared to the control wafers. This is in agreement with the results obtained in previous studies where chestnut flowers were incorporated into "económicos" cakes (Carocho et al., 2015), aqueous extracts of fennel and chamomile in cookies (Caleja, Barros, Antonio, Oliveira, & Ferreira, 2017) and in a study using a catechin-rich extract obtained from *A. unedo* incorporated into bread (Takwa

et al., 2018). In general, it was concluded that the incorporation of these natural ingredients introduces beneficial properties to the tested food products.

As demonstrated in other studies involving natural extracts with the aim of replacing artificial additives (Carocho et al., 2015; Caleja, et al., 2017), the key lies down behind the preservation of the beneficial properties of the extracts without altering the organoleptic characteristics of the original product. Therefore, as a function of the results presented in Table 3, the extract from *A. unedo* rich in cyanidin-3-*O*-glucoside is able to provide colorant properties with functional antioxidant properties without altering the main organoleptic characteristics of the food sample, demonstrating the potential of *A. unedo* fruit extracts for industrial applications.

4. Conclusions

There are no productive applications found at an industry level for the fruits of *Arbutus unedo* L. (Ericaceae family), because this plant is mainly used as an ornamental plant. Spontaneous growth by seedlings are found along the Mediterranean region easily. Most of the fruit production is discarded, because it only reaches a pleasant flavour during a short period of time and only minor traditional uses have been described (jams, wines and liqueurs). The edible reddish sweet fruit produced contains a diverse source of health promoting compounds, such as tocopherols, carbohydrates, sugars, and phenolic compounds. Additionally, given the evidence that the fruits contain a good amount

of anthocyanins, and also that this raw material is easy to obtain in good quantities in the areas where they are abundant, it may be interesting to use them as a new source of anthocyanins, which contributes, favours and promotes the use of these compounds as a natural colorant. Therefore, valorising, producing added-value extract rich in anthocyanins and understanding the stability patterns of this compounds with interest for the food technology field, from this underused fruit, could be of interest for the industrial sector and research community.

The present results provide information for: i) potential industrial application of extracts from *A. unedo* fruits, as alternative source of anthocyanins to be used as natural colorant ingredients with bioactive properties; ii) shelf-life predictions of the extract rich in anthocyanins (mainly cyanidin-3-*O*-glucoside) at specific conditions of temperature and pH. Overall, the incorporation of the *A. unedo* extract gave a more attractive colour to the wafers and improved the antioxidant activity, without causing significant changes in the nutritional profile of the wafers.

Acknowledgements

Appendix A. Supplementary data

Supplementary data to this article can be found online at https://doi.org/10.1016/j.foodchem.2018.09.099.

References

AOAC International. (2016). Official methods of analysis of AOAC International. In W. Dr. George & J. Latimer (Eds.). (20th ed.).

Barros, L., Carvalho, A. M., Morais, J. S., & Ferreira, I. C. F. R. (2010). Strawberry-tree, blackthorn and rose fruits: Detailed characterisation in nutrients and phytochemicals with antioxidant properties. *Food Chemistry, 120*(1), 247–254.

Barros, L., Dueñas, M., Dias, M. I., Sousa, M. J., Santos-Buelga, C., & Ferreira, I. C. F. R. (2013). Phenolic profiles of cultivated, in vitro cultured and commercial samples of *Melissa officinalis* L. infusions. *Food Chemistry, 136*(1), 1–8.

Caleja, C., Barros, L., Antonio, A. L., Carocho, M., Oliveira, M. B. P. P., & Ferreira, I. C. F. R. (2016). Fortification of yogurts with different antioxidant preservatives: A comparative study between natural and synthetic additives. *Food Chemistry, 210*, 262–268.

Caleja, C., Barros, L., Antonio, A. L., Oliveira, M. B. P. P., & Ferreira, I. C. F. R. (2017). A comparative study between natural and synthetic antioxidants: Evaluation of their performance after incorporation into biscuits. *Food Chemistry, 216*, 342–346.

Carocho, M., Barreira, J. C. M., Barros, L., Bento, A., Cámara, M., Morales, P., & Ferreira, I. C. F. R. (2015). Traditional pastry with chestnut flowers as natural ingredients: An approach of the effects on nutritional value and chemical composition. *Journal of Food Composition and Analysis, 44*, 93–101.

Carocho, M., Barreiro, M. F., Morales, P., & Ferreira, I. C. F. R. (2014). Adding molecules to food, pros and cons: A review on synthetic and natural food additives. *Comprehensive Reviews in Food Science and Food Safety, 13*(4), 377–399.

Carocho, M., & Ferreira, I. C. F. R. (2013). The role of phenolic compounds in the fight against cancer–a review. *Anti-Cancer Agents in Medicinal Chemistry, 13*(8), 1236–1258.

Cavalcanti, R. N., Santos, D. T., & Meireles, M. A. A. (2011). Non-thermal stabilization mechanisms of anthocyanins in model and food systems-An overview. *Food Research International, 44*(2), 499–509.

Cevallos-Casals, B. A., & Cisneros-Zevallos, L. (2004). Stability of anthocyanin-based aqueous extracts of Andean purple corn and red-fleshed sweet potato compared to synthetic and natural colorants. *Food Chemistry, 86*(1), 69–77.

Clifford, M. N. (2000). Anthocyanins – nature, occurrence and dietary burden. *Journal of the Science of Food and Agriculture, 80*(7), 1063–1072.

Debonne, E., Van Bockstaele, F., Philips, E., De Leyn, I., & Eeckhout, M. (2017). Impact of par-baking and storage conditions on the quality of par-baked and fully baked bread. *LWT – Food Science and Technology, 78*, 16–22.

Demeule, M., Michaud-Levesque, J., Annabi, B., Gingras, D., Boivin, D., Jodoin, J., ... Béliveau, R. (2002). Green tea catechins as novel antitumor and antiangiogenic compounds. *Current Medicinal Chemistry. Anti-Cancer Agents, 2*, 441–463.

Ding, M., Feng, R., Wang, S. Y., Bowman, L., Lu, Y., Qian, Y., ... Shi, X. (2006). Cyanidin-3-glucoside, a natural product derived from blackberry, exhibits chemopreventive and chemotherapeutic activity. *Journal of Biological Chemistry, 281*(25), 17359–17368.

Esatbeyoglu, T., Wagner, A. E., Schini-Kerth, V., & Rimbach, G. (2015). Betanin-A food colorant with biological activity. *Molecular Nutrition and Food Research, 59*(1), 36–47.

Garzón, G. A. (2008). Las antocianinas como colorantes naturales y compuestos bioactivos: Revisión. *Acta Biológica Colombiana, 13*(3), 27–36.

Ge, Q., & Ma, X. (2013). Composition and antioxidant activity of anthocyanins isolated from Yunnan edible rose (An ning). *Food Science and Human Wellness, 2*(2), 68–74.

Gironés-Vilaplana, A., Baenas, N., Villaño, D., Speisky, H., García-Viguera, C., & Moreno, D. A. (2014). Evaluation of Latin-American fruits rich in phytochemicals with biological effects. *Journal of Functional Foods, 7*(1), 599–608.

Guimarães, R., Barros, L., Calhelha, R. C., Carvalho, A. M., Queiroz, M. J. R. P., & Ferreira, I. C. F. R. (2014). Bioactivity of different enriched phenolic extracts of wild fruits from Northeastern Portugal: A comparative study. *Plant Foods for Human Nutrition, 69*(1), 37–42.

Guimaraes, R., Barros, L., Carvalho, A. M., & Ferreira, I. C. F. R. (2010). Studies on chemical constituents and bioactivity of *Rosa micrantha*: An alternative antioxidants source for food, pharmaceutical, or cosmetic applications. *Journal of Agricultural and Food Chemistry, 58*(10), 6277–6284.

Guimarães, R., Barros, L., Dueñas, M., Carvalho, A. M., Queiroz, M. J. R. P., Santos-Buelga, C., & Ferreira, I. C. F. R. (2013). Characterisation of phenolic compounds in wild fruits from Northeastern Portugal. *Food Chemistry, 141*, 3721–3730.

Ibañez, F. C., Torre, P., & Irigoyen, A. (2003). Aditivos alimentarios. *Universitas Navarrensis*, 1–10.

Jiménez, A., Caleja, C., Prieto, M. A., Barreiro, M. F., Barros, L., & Ferreira, I. C. F. R. (2018). Optimization and comparison of heat and ultrasound assisted extraction techniques to obtain anthocyanin compounds from *Arbutus unedo* L. fruits. *Food Chemistry, 264*, 81–91.

Komatsu, Y., Suematsu, S., Hisanobu, Y., Saigo, H., Matsuda, R., & Hara, K. (2014). Effects of pH and temperature on reaction kinetics of catechins in green tea infusion. *Bioscience, Biotechnology and Biochemistry, 57*(6), 907–910.

Labbé, D., Têtu, B., Trudel, D., & Bazinet, L. (2008). Catechin stability of EGC- and EGCG-enriched tea drinks produced by a two-step extraction procedure. *Food Chemistry, 111*, 139–143.

Li, N., Taylor, L. S., Ferruzzi, M. G., & Mauer, L. J. (2012). Kinetic study of catechin stability: Effects of pH, concentration, and temperature. *Journal of Agricultural and Food Chemistry, 60*, 12531–12539.

Li, N., Taylor, L. S., & Mauer, L. J. (2011). Degradation kinetics of catechins in green tea powder: Effects of temperature and relative humidity. *Journal of Agricultural and Food Chemistry, 59*(11), 6082–6090.

Mak, Y. W., Chuah, L. O., Ahmad, R., & Bhat, R. (2013). Antioxidant and antibacterial activities of hibiscus (Hibiscus rosa-sinensis L.) and Cassia (Senna bicapsularis L.) flower extracts. *Journal of King Saud University – Science, 25*(4), 275–282.

Martins, N., Roriz, C. L., Morales, P., Barros, L., & Ferreira, I. C. F. R. (2016). Food colorants: Challenges, opportunities and current desires of agro-industries to ensure consumer expectations and regulatory practices. *Trends in Food Science and Technology, 52*, 1–15.

Miguel, M. G., Faleiro, M. L., Guerreiro, A. C., & Antunes, M. D. (2014). *Arbutus unedo* L.: Chemical and biological properties. *Molecules, 19*(10), 1579–15823.

Pinela, J., Prieto, M. A., Carvalho, A. M., Barreiro, M. F., Oliveira, M. B. P., Barros, L., & Ferreira, I. C. F. R. (2016). Microwave-assisted extraction of phenolic acids and flavonoids and production of antioxidant ingredients from tomato: A nutraceutical-oriented optimization study. *Separation and Purification Technology, 164*, 114–124.

Prieto, M. A., Vázquez, J. A., & Murado, M. A. (2012a). A simple pseudo-mechanistic model for the response characterization and quantification of the copper-induced oxidative LDL method. *Free Radical Biology and Medicine, 53*, S245.

Prieto, M. A., Vázquez, J. A., & Murado, M. A. (2012b). Comparison of several mathematical models for describing the joint effect of temperature and ph on glucanex activity. *Biotechnology Progress, 28*(2), 372–381.

Prior, R. L., & Wu, X. (2006). Anthocyanins: Structural characteristics that result in unique metabolic patterns and biological activities. *Free Radical Research, 40*(10), 1014–1028.

Ruiz-Rodríguez, B.-M., Morales, P., Fernández-Ruiz, V., Sánchez-Mata, M.-C., Cámara, M., Díez-Marqués, C., ... Tardío, J. (2011). Valorization of wild strawberry-tree fruits (*Arbutus unedo* L.) through nutritional assessment and natural production data. *Food Research International, 44*(5), 1244–1253.

Sang, J. J., Sang, J. J., Ma, Q., Hou, X. Fang, & Li, C. Qin (2017). Extraction optimization and identification of anthocyanins from *Nitraria tangutorun* Bobr. seed meal and establishment of a green analytical method of anthocyanins. *Food Chemistry, 218*, 386–395.

Sarmento, A., Barros, L., Fernandes, Â., Carvalho, A. M., & Ferreira, I. C. (2015). Valorization of traditional foods: Nutritional and bioactive properties of *Cicer arietinum* L. and *Lathyrus sativus* L. pulses. *Journal of the Science of Food and Agriculture, 95*(1), 179–185.

Soković, M., Glamočlija, J., Marin, P. D., Brkić, D., & van Griensven, L. J. L. D. (2010). Antibacterial effects of the essential oils of commonly consumed medicinal herbs using an in vitro model. *Molecules, 15*(11), 7532–7546.

Soković, M., & van Griensven, L. J. L. D. (2006). Antimicrobial activity of essential oils

and their components against the three major pathogens of the cultivated button mushroom, *Agaricus bisporus. European Journal of Plant Pathology, 116*(3), 211–224.

Su, Y. L., Leung, L. K., Huang, Y., & Chen, Z. Y. (2003). Stability of tea theaflavins and catechins. *Food Chemistry, 83*, 189–195.

Takwa, S., Caleja, C., Barreira, J. C. M., Soković, M., Achour, L., Barros, L., & Ferreira, I. C. F. R. (2018). *Arbutus unedo* L. and *Ocimum basilicum* L. as sources of natural preservatives for food industry: A case study using loaf bread. *LWT – Food Science and Technology, 88*(Supplement C), 47–55.

Timberlake, C. F., & Henry, B. S. (1988). Anthocyanins as natural food colorants. *Progress in Clinical and Biological Research, 280*, 107–121.

Ziani, B. E. C., Calhelha, R. C., Barreira, J. C. M., Barros, L., Hazzit, M., & Ferreira, I. C. F. R. (2015). Bioactive properties of medicinal plants from the Algerian flora: Selecting the species with the highest potential in view of application purposes. *Industrial Crops and Products, 77*, 582–589.

Zhu, Q. Y., Holt, R. R., Lazarus, S. A., Ensunsa, J. L., Hammerstone, J. F., Schmitz, H. H., & Keen, C. L. (2002). Stability of the flavan-3-ols epicatechin and catechin and related dimeric procyanidins derived from cocoa. *Journal of Agricultural and Food Chemistry, 50*(6), 1700–1705.

Zhu, Q. Y., Zhang, A., Tsang, D., Huang, Y., & Chen, Z. (1997). Stability of Green Tea Catechins, 4624–4628.

Ziyyat, A., Mekhfi, H., Bnouham, M., Tahri, A., Legssyer, A., Hoerter, J., & Fischmeister, R. (2002). *Arbutus unedo* induces endothelium-dependent relaxation of the isolated rat aorta. *Phytotherapy Research, 16*, 572–575.

Incorporation of natural colorants obtained from edible flowers in yogurts

Tânia C.S.P. Pires[a,b], Maria Inês Dias[a], Lillian Barros[a], João C.M. Barreira[a],
Celestino Santos-Buelga[b], Isabel C.F.R. Ferreira[a,*]

[a] *Centro de Investigação de Montanha (CIMO), Instituto Politécnico de Bragança, Campus de Santa Apolónia, 5300-253 Bragança, Portugal*
[b] *Grupo de Investigación en Polifenoles (GIP-USAL), Facultad de Farmacia, Universidad de Salamanca, Campus Miguel de Unamuno s/n, 37007 Salamanca, Spain*

A B S T R A C T

The substitution of artificial dyes by natural colouring agents is among the top concerns of food industry to fulfil current consuming trends, justifying the prospection of novel natural sources of these compounds. Herein, the hydrophilic extracts from rose, cornflower and dahlia were tested as potential substitutes to E163 (anthocyanin extract). Besides comparing the colouring capacity, the potential occurrence of changes in the chemical composition of yogurts (nutritional parameters, free sugars and fatty acids) was also assessed throughout storage (up to 7 days) and compared with a "blank" (free of any additive) yogurt formulation. In general, yogurts prepared with flower extracts, presented similar nutritional value and free sugars profile to those prepared with E163 and to the "blank" yogurt. Nevertheless, rose extract turned out to be the most suitable alternative to E163 as these two groups of yogurts had similar nutritional composition, free sugars and fatty acids composition, besides presenting close scores in colour parameters.

1. Introduction

Fermented milk is a dairy product processed by lactic fermentation, which ends up by coagulating milk casein due to the acidification process (pH values around 4.6). Among different fermented dairy products, yogurt is certainly one of the most popular, being widely consumed all over the world due to its organoleptic and nutritional properties (Arioui, Ait Saada, & Cheriguene, 2017; Caleja et al., 2016).

Some yogurt formulations are prepared using specific additives, such as exemplified by colorants. However, the recent concerns about the safety of artificial colorants in food products, has encouraged the development and application of natural colorants, which are generally considered safer than artificial ones (Pop, Lupea, Popa, & Gruescu, 2010). Anthocyanins are authorised food colorants (E163 in EU) and have previously been evaluated by the Joint FAO/WHO Expert Committee on Food Additives (JECFA) in 1982 and by the EU Scientific Committee for Food (SCF) in 1975 and 1997 (Pop et al., 2010; Rodriguez-Amaya, 2016). Anthocyanins are water-soluble pigments isolated from plants, being responsible for the blue, purple, and red colour of many plant tissues. These phenolic compounds are widely found in fruits (especially berries), as well as flowers and leaves, mainly linked to sugar units. Their sugar-free counterparts (anthocyanidins) are based on the flavylium cation, which might present different substitution patterns originating the diversity of anthocyanidins found in

nature (Hidalgo & Almajano, 2017). Among the 17 natural anthocyanidins, cyanidin, delphinidin, petunidin, peonidin, pelargonidin and malvidin, are the major forms in most species (Hidalgo & Almajano, 2017).

In what concerns the application of anthocyanins in food products, there are some previous reports describing the incorporation of rose (*Rosa damascena*) petals extracts in yogurt (*e.g.*, Chanukya & Rastogi, 2016). Owing to the previously evidenced suitability of *R. damascena* as a colour ring agent in yogurt, we selected that species as one of the plant sources of anthocyanins to be incorporated in the yogurt formulations prepared in the lab. Likewise, we selected the flowers of *Centaurea cyanus* L. (cornflower), mainly due to its richness in cyanidin 3-*O*-(6-*O*-succinylglucoside)-5-*O*-glucoside (Takeda et al., 2005), but also in other bioactive phenolic compounds such as apigenin-glucuronide (Pires, Dias, Barros, & Ferreira, 2017) and *Dahlia mignon* (dahlia), which also presents a rich composition in different phenolic compounds like naringenin-3-*O*-glucoside, kaempferol-pentosyl-rhamnosyl-hexoside or apigenin-hexoside (Deguchi, Ohno, Hosokawa, Tatsuzawa, & Doi, 2013; Pires et al., 2018).

The selection and purchase of food products are greatly influenced by sensory expectations (Spence, Levitan, Shankar, & Zampini, 2010). Visual perception deliver so called quality cues, perceived prior to actual consumption and give hints of the quality attributes that are apparent during the consumption (Jantathai, Sungsri-in, Mukprasirt, &

Duerrschmid, 2014; Spence et al., 2010). Colour plays an important role in the development of food preferences and sensory perception (Jantathai et al., 2014).

Nevertheless, colour is not important only in what concerns the product appearance. In fact, some colouring agents may have important functions beyond their primary effect. Anthocyanins, for instance, might have beneficial health effects due to their antioxidant, anti-inflammatory, anticancer, and anti-diabetic properties, thereby being of great interest to the food industry (Rodriguez-Amaya, 2016). However, it is also necessary to take into account that anthocyanins might degrade or react in food systems to form complex reaction products, leading to a mixture of products in addition to the parent anthocyanins (Rodriguez-Amaya, 2016). The intensity and stability of anthocyanins when used as food additives are influenced by pH, structure, concentration, co-pigmentation and metal complexing, as well as temperature, light, oxygen, acetaldehyde, ascorbic acid, sugars and their degradation products, sulphur dioxide, amino acids and catechins. Still, when low pH conditions are maintained, anthocyanins are relatively stable (EFSA, 2013; Rodriguez-Amaya, 2016).

Accordingly, the aim of the present study was to develop a new colouring strategy in yogurt products using natural anthocyanin rich extracts obtained from edible flower petals of *Dalia mignon*, *Centaurea cyanus* L. and *Rosa damascena* "Alexandria" mixed with *Rosa gallica* "French" draft in *Rosa canina*. These flowers were firstly characterized and quantified regarding the anthocyanin content, thought an HPLC-DAD-ESI/MS system. Additionally, the chromatic stability was evaluated by performing the evaluation studies (nutritional parameters, free sugars, fatty acids, anthocyanin content, and colour parameter) in yogurt formulation at two different periods (preparation day and after 7 days of storage).

2. Materials and methods

2.1. Samples

Dried commercial samples of petals of *Dahlia mignon*, rose resulting from *R. damascena* 'Alexandria' and *R. gallica* 'Francesa' draft in *R. canina*, and *Centaurea cyanus* L. were provided by RBR foods (Castro D'aire, Portugal).

In order to prepare the extracts, samples were reduced to powder (20 mesh) and were extracted by maceration (25 °C, 150 rpm, 1 h) using a stirring plate (VELP scientific, Keyland Court, NY, USA) by adding 1 g of dry material to 50 mL of distilled water. Afterwards, the mixture was filtered through Whatman filter paper No. 4, frozen and lyophilized. The lyophilized extracts obtained were used as natural additives.

2.2. Anthocyanin compounds identification by HPLC-DAD-ESI/MS

The chromatographic data of anthocyanin compounds were acquired from a Dionex Ultimate 3000 system (Thermo Scientific, San Jose, CA, USA), coupled to diode array, using 520 nm as preference wavelength, and to a mass spectrometer (MS, Linear Ion Trap LTQ XL mass spectrometer, Thermo Finnigan, San Jose, CA, USA) operating in the positive mode (Gonçalves et al., 2017). Retention times, UV–Vis and mass spectra were compared with available standards and with literature data to identify the anthocyanin's. Calibration curves of the available anthocyanin standards were constructed based on the UV signal to perform quantitative analysis, in case of an unavailable commercial standards, the compounds were quantified *via* the calibration curves of the most similar available standards. The results were expressed as µg/g of dry extract.

2.3. Fortification of yogurts with natural and commercial colorant additives

2.3.1. Incorporation process

The base formulation yogurts (fat 3.8%; protein 5.0% and

carbohydrates 4.7%) were purchased at the local market. Five groups (three samples/group) of yogurts (70 g each) were prepared, with three replicates of each: i) control samples (BY); ii) yogurts with commercial colorant, E 163 (AY); iii) yogurts with rose petals extract (RY); iv) yogurts with *Centaurea cyanus* L. petals extract (CY); v) yogurts with *Dahlia mignon* petals extract (DY). All colorants were added to a portion of 70 g of yogurt and were prepared in duplicate. The E163 colorant was added at a 0.02% concentration; in the case of yogurts added with petals extracts, slightly higher concentrations of each extract (0.05% for dahlia extract; 0.15% for rose extract; 0.10% for centaurea extract) were added (the quantity was added until an evident change in colour was obtained).

2.3.2. Nutritional and chemical composition

The proximate composition was determined according to AOAC procedures (AOAC, 2016), including protein (991.02), crude fat (989.05) and ash (935.42) contents. Crude protein (N × 6.25) was determined by the Kjeldahl method; ash content was estimated by subjecting the sample to incineration at 600 ± 15 °C for 5 h, while crude fat was determined using a Soxhlet apparatus with petroleum ether as recycling solvent and total carbohydrate was estimated by difference. The total energy was calculated using the following equation: Energy (kcal) = 4 × (g protein + g carbohydrates) + 9 × (g fat).

Free sugars were determined by high performance liquid chromatography coupled to a refraction index detector (HPLC-RI; Knauer, Smartline system 1000, Berlin, Germany), using melezitose as an internal standard. All the mentioned procedures were previously described by the authors (Barros, Pereira, & Ferreira, 2013; Dias et al., 2015).

The fatty acids were determined by gas chromatography coupled with a flame ionization detector (GC-FID/capillary column, DANI model GC 1000, Contone, Switzerland), a split/splitless injector and a Macherey–Nagel column. The identification of fatty acids was performed by comparing the relative retention times of FAME peaks from samples with commercial standards (Barros et al., 2013; Dias et al., 2015).

Anthocyanins were determined in the yogurt sample by extracting 3 g of dry yogurt with water at 25 °C, 150 rpm during 1 h, followed by filtration through a Whatman filter paper No. 4. The remaining residue was re-extracted with an additional portion of water mixture, stored at −20 °C and lyophilized for further analysis. The lyophilized extracts were analysed using the HPLC-DAD-ESI/MS system mentioned above.

2.4. Physico-chemical parameters

The colour was measured in triplicate for each sample using a colorimeter (model CR-400, Konica Minolta Sensing Inc., Tokyo, Japan). The CIE L*, a* and b* colour space values were registered using a data software "Spectra Magic Nx" (version CM-S100W 2.03.0006), using the illuminant C and diaphragm aperture of 8 mm (Fernandes et al., 2012). The pH values of the samples was measured directly with a HI 99161 pH-meter (Hanna Instruments, Woonsocket, Rhode Island, USA).

2.5. Statistical analysis

All statistical tests were performed at a 5% significance level using IBM SPSS Statistics for Windows, version 22.0. (IBM Corp., Armonk, NY, USA).

Data were expressed as mean ± standard deviation, maintaining the significant numbers allowed by the magnitude of the corresponding standard deviation.

An analysis of variance (ANOVA) with type III sums of squares was performed using the general linear model (GLM) procedure to compare the parameters evaluated in the prepared yogurts. The dependent variables were analysed using 2-way ANOVA with the factors "yogurt formulation" (YF) and "storage" (SE). When a statistically significant

interaction was detected among the two factors, their effect was evaluated by checking estimated marginal means plots for all levels of each factor. On the contrary, if no statistical significant interaction was found, means were compared using Tukey's multiple comparison test, after verifying the homogeneity of variances through Levene's test.

In addition, a linear discriminant analysis (LDA) was used to have a better understanding about the YF overall effect. A stepwise technique was applied, considering the Wilks' Λ test with the usual probabilities of F (3.84 to enter and 2.71 to be removed) for variable selection. Only variables with a statistically significant classification performance ($p < 0.050$) were maintained by the statistical model. The significant independent variables were selected following the stepwise method of LDA. This procedure is based in sequential forward selection and backward elimination steps, where the inclusion of a new variable requires verifying the significance of all previously selected variables (Zielinski et al., 2014). The main purpose was estimating the relationship between the single categorical dependent variables (yogurt formulations) and the quantitative independent variables (results obtained in the laboratorial assays). The LDA outputs allowed determining which independent variables contributed more to the differences in the average score profiles of different YF. A leaving-one-out cross validation procedure was carried out to assess the model performance.

3. Results and discussion

3.1. Anthocyanin profile characterization

Owing to the powerful colouring capacity of anthocyanins, these compounds were thoroughly characterized in the extracts obtained from the petals of each selected species. The extraction yields (mg of anthocyanin per 100 g of petals) obtained for each sample extract were: ~53% for dahlia; ~46% for rose; and ~23% for centaurea samples.

Nine anthocyanin compounds were detected in dahlia, two in rose and eight in centaurea extracts. Peak characteristics, tentative identification and compound quantification are presented in Table 1. Cyanidin (Cy; peaks **1**, **2**, **3**, **4**, **6**, **10**, **11**, **13**, **15**, and **17**), pelargonidin (Pg; peaks **8**, **9**, **12**, **16**, and **18**), and delphinidin (Dp; peaks **5** and **7**) were identified as main aglycones, based on the observation of their characteristic fragments in MS^2 spectra. As reviewed by Castañeda-Ovando, Pacheco-Hernández, Páez-Hernández, Rodríguez, and Galán-Vidal (2009), these non-methylated anthocyanidins are the most commonly found in flowers, being cyanidin derivatives the most abundant in the analysed samples.

The conjugated bonds of anthocyanins, the glycosylated form of anthocyanidins, result in red, blue, and purple-coloured plants (Khoo, Azlan, Tang, & Lim, 2017). Several foods, like yoghurt, are considered healthy, but they lack important components such as phenolic compounds. Therefore, the incorporation of plant extracts rich in anthocyanins in these fermented products might impart a desirable red colour, while enhancing their potential health effect (Mourtzinos et al., 2018).

Before incorporating the flower extracts in yogurts, their profiles in anthocyanins were thoroughly characterized. Peak **1**, detected in rose and centaurea samples, was positively identified as cyanidin 3,5-di-*O*-glucoside based on the HPLC-DAD-MS results and comparison with our database library. This compound was already described as the main anthocyanin in petals of *R. damascena* (Velioglu & Mazza, 1991) and *R. hybrida* (Lee, Lee, & Choung, 2011) used with edible purposes, as well as in flowers from different *Centaurea* species (Mishio, Takeda, & Iwashina, 2015), highlighting its suitability to be incorporated in yogurt formulations. Peak **2**, found in rose samples, was also positively identified as cyanidin-3-*O*-glucoside according with its retention time and mass spectral data by comparison with a standard. The presence of this reddish-purple anthocyanin was also reported in rose hips (*R. canina*) previously Hvattum (2002).

Peak **4** ([M]$^+$ at *m/z* 711) was the majority anthocyanin in centaurea samples. Its MS^2 spectra yielded fragments at *m/z* 549 (-162 mu, loss of a hexose), 449 (-262 mu, loss of succinylhexose) and 287 (cyanidin), coherent with an identity as Cy-3-*O*-(6″-succinylglucoside)-5-*O*-glucoside, a compound consistently identified in centaurea flowers also referred to as centaurocyanin (Mishio et al., 2015; Kôsaku; Takeda & Tominaga, 1983), and whose combination with a flavone glycoside

Table 1
Retention time (Rt), wavelengths of maximum absorption in the visible region (λ_{max}), mass spectral data, tentative identification, and quantification of anthocyanins in dahlia, rose, and centaurea extracts. Results are presented as mean $\pm$ standard deviation.

Peak	Rt (min)	λ_{max} (nm)	Molecular ion (*m/z*)	MS^2 (*m/z*)	Tentative identification	Quantification (µg/g extract)
Rose						
1	11.5	514	611	449(10),287(100)	Cyanidin 3,5-di-*O*-glucoside[A]	13.19 ± 0.01
2	18.5	516	449	287 (100)	Cyanidin-3-*O*-glucoside[A]	0.131 ± 0.004
					Total Anthocyanins	**13.326 ± 0.002**
Centaurea						
1	11.7	512	611	449(5),287(100)	Cyanidin 3,5-di-*O*-glucoside[A]	5.5 ± 0.2
3	18.03	516	697	535(62),449(8),287(46)	Cyanidin 3-*O*-(6″-malonylglucoside)-5-*O*-glucoside[A]	6.2 ± 0.3
4	20.38	516	711	549(3),449(48),287(100)	Cyanidin 3-*O*-(6″-succinylglucoside)-5-*O*-glucoside[A]	11.2 ± 0.5
5	29.6	518	465	303 (100)	Delphinidin-hexoside[C]	1.5 ± 0.2
6	31.5	518	463	287 (100)	Cyanidin-glucuronide[A]	0.85 ± 0.06
7	32.6	518	561	303 (100)	Delphinidin-malonylhexoside[C]	tr
8	38.1	501	695	609(9),433(2),271(82)	Pelargonidin 3-*O*-(6″-succinylglucoside)-5-*O*-glucoside[B]	0.18 ± 0.01
9	39.2	502	519	271 (100)	Pelargonidin-malonylhexoside[B]	0.17 ± 0.01
					Total Anthocyanins	**26 ± 1**
Dahlia						
10	11.6	516	449	287 (100)	Cyanidin-hexoside[A]	2.98 ± 0.01
11	13.4	504	449	287 (100)	Cyanidin-hexoside[A]	2.654 ± 0.001
12	15.1	514	579	271 (100)	Pelargonidin-rutinoside[B]	1.4 ± 0.1
13	17.2	514	491	287 (100)	Cyanidin-acetylhexoside[A]	5.36 ± 0.01
14	19.4	501	431	269 (100)	Methylapigeninidin-hexoside[A]	4.1 ± 0.1
15	20.8	518	595	287 (100)	Cyanidin-rutinoside[A]	0.8 ± 0.1
16	28.5	504	595	271 (100)	Pelargonidin 3,5-di-*O*-glucoside[B]	0.8 ± 0.1
17	31.5	518	491	287 (100)	Cyanidin-acetylhexoside[A]	0.33 ± 0.02
18	32.7	516	433	271 (100)	Pelargonidin-hexoside[B]	0.450 ± 0.001
					Total Anthocyanins	**18.8 ± 0.2**

tr-trace amounts; Standard calibration curves: A – cyanidin-3-*O*-glucoside ($y = 243287x - 1E+06$; $R^2 = 0.995$); B – pelargonidin-3-*O*-glucoside ($y = 276117x - 480418$; $R^2 = 0.9979$); C– delphinidin-3-*O*-glucoside ($y = 557274x + 126.24$; $R^2 = 0.997$).

Table 2

Nutritional composition (g/100 g fresh weight) and energy values (kcal/100 g fresh weight) for different yogurt formulations (YF) and storage effect (SE). Results are presented as mean ± standard deviation.[a]

		Water	Fat	Protein	Ash	Carbohydrates	Galactose	Lactose	Energy
YF	**BY**	85.0 ± 0.4	3.3 ± 0.1	5.3 ± 0.3	0.79 ± 0.03	5.6 ± 0.1	0.69 ± 0.01[c]	4.7 ± 0.1	73 ± 2
	RY	84.8 ± 0.4	3.3 ± 0.2	5.3 ± 0.2	0.85 ± 0.01	5.8 ± 0.2	0.71 ± 0.04[bc]	4.7 ± 0.2	74 ± 3
	DY	85.0 ± 0.1	3.4 ± 0.1	5.4 ± 0.1	0.86 ± 0.02	5.4 ± 0.1	0.71 ± 0.01[b]	4.8 ± 0.1	73 ± 1
	CY	84.8 ± 0.1	3.2 ± 0.1	5.4 ± 0.1	0.86 ± 0.02	5.7 ± 0.1	0.76 ± 0.02[a]	4.8 ± 0.1	74 ± 1
	AY	84.9 ± 0.2	3.4 ± 0.1	5.3 ± 0.1	0.82 ± 0.02	5.5 ± 0.1	0.72 ± 0.02[b]	4.9 ± 0.1	74 ± 1
	ANOVA p-value (n = 18)[b]	0.083	0.001	0.039	< 0.001	< 0.001	< 0.001	< 0.001	0.632
SE	**0 days**	85.0 ± 0.2	3.3 ± 0.1	5.3 ± 0.2	0.84 ± 0.04	5.6 ± 0.2	0.73 ± 0.03	4.8 ± 0.1	73 ± 1
	7 days	84.8 ± 0.3	3.4 ± 0.1	5.4 ± 0.1	0.84 ± 0.03	5.6 ± 0.2	0.71 ± 0.03	4.8 ± 0.1	74 ± 2
	ANOVA p-value (n = 45)[c]	0.056	0.061	0.119	0.763	0.258	0.100	0.408	0.081
YF × SE	p-value (n = 90)[d]	< 0.001	< 0.001	< 0.001	< 0.001	< 0.001	0.272	< 0.001	< 0.001

[a] Results are reported as mean values of each YF, aggregating results from 0 to 7 days, and mean values of SE, combining all YF.
[b] If $p < 0.05$, the corresponding parameter presented a significantly different value for at least one YF.
[c] If $p < 0.05$, the corresponding parameter presented a significant difference among stored and non-stored yogurts.
[d] In this table, the interaction among factors was significant in all cases; thereby no multiple comparisons could be performed.

Table 3

Physicochemical parameters (CIE L^*, a^* and b^* and pH values) for different yogurt formulations (YF) and storage effect (SE). Results are presented as mean ± standard deviation.[a]

		L^*	a^*	b^*	pH
YF	**BY**	93 ± 1	−3.5 ± 0.1	9.8 ± 0.4	4.3 ± 0.1
	RY	88 ± 1	2.2 ± 0.1	9.0 ± 0.3	4.3 ± 0.1
	DY	84 ± 1	2.1 ± 0.3	17.7 ± 0.4	4.4 ± 0.1
	CY	90 ± 1	−1.1 ± 0.2	9.5 ± 0.5	4.2 ± 0.1
	AY	89 ± 1	3.1 ± 0.5	6.5 ± 0.5	4.8 ± 0.1
	ANOVA p-value (n = 18)[b]	< 0.001	< 0.001	< 0.001	< 0.001
SE	**0 days**	88 ± 3	1 ± 3	10 ± 3	4.4 ± 0.2
	7 days	89 ± 3	0 ± 2	11 ± 3	4.4 ± 0.2
	ANOVA p-value (n = 45)[c]	0.056	0.250	0.312	0.946
IF × ST	p-value (n = 90)[d]	< 0.001	< 0.001	< 0.001	0.867

[a] Results are reported as mean values of each YF, aggregating results from 0 to 7 days, and mean values of SE, combining all YF.
[b] If $p < 0.05$, the corresponding parameter presented a significantly different value for at least one YF.
[c] If $p < 0.05$, the corresponding parameter presented a significant difference among stored and non-stored yogurts.
[d] In this table, the interaction among factors was significant in all cases; thereby no multiple comparisons could be performed.

and metal ions give rise to protocyanin, a stable complex pigment considered to be the main responsible for the blue colour of *Centaurea cyanus* flowers (Kosaku Takeda et al., 2005). This compound could have interesting colouring properties to be used as a natural additive in food products. Similarly, mass spectral characteristics of peak **3**, with a molecular ion $[M]^+$ at m/z 697 and MS^2 fragments at m/z 535 (−162 mu, loss of a hexose), 449 (−248 mu, loss of malonylhexose) and 287 (cyanidin), allowed tentatively assigning it as Cy-3-*O*-(6″-malonylglucoside)-5-*O*-glucoside owing to its previous identification in flowers from different *Centaurea* species (Mishio et al., 2015). Peak **6** ($[M]^+$ at m/z 463) was another cyanidin derivative, tentatively identified as Cy-*O*-glucuronide based on the loss of 176 mu (a glucuronyl moiety) to yield the unique MS^2 product ion at m/z 287.

Peaks **8** and **9** in centaurea samples were associated to pelargonidin derivatives based on their characteristic absorption spectra showing λ_{max} at 501 nm and the fragment ion observed at m/z 271 (Pg). Peak **8** ($[M]^+$ at m/z 695), with similar fragmentation behaviour as peak 4, was identified as Pg-3-*O*-(6″-succinylglucoside)-5-*O*-glucoside, previously described in *Centaurea cyanus* flowers by Kosaku Takeda, Kumegawa, Harborne, and Self (1988). Peak **9** ($[M]^+$ at m/z 519) was tentatively assigned as a Pg-*O*-malonylhexoside based on the loss of 248

mu (malonylhexoside) to yield the aglycone ion at m/z 271. Pelargonidin differs from most anthocyanidins as it might provide an orange hue to flowers and red to some of the fruits and berries (Jaakola, 2013; Khoo et al., 2017), having also demonstrated a notable anti-inflammatory effect (Duarte et al., 2018). In a similar way, peak **7** ($[M]^+$ at m/z 561), yielding a unique MS^2 fragment at m/z 303 (−248 mu) was associated to delphinidin-*O*-malonylhexoside, whereas **peak 5** ($[M]^+$ at m/z 465) was assigned as a Dp-*O*-hexoside; a possible identity as Dp-3-*O*-glucoside was excluded by comparison with peak characteristics with our database library. Delphinidin appears as a purple pigment in the nature, and the blue hue of flowers is often due this pigment, which was previously reported for its anti-inflammatory, anti-oxidant, and anti-tumorigenic activities (Ko et al., 2015), making it specially interesting as an ingredient of innovative food formulations (Khoo et al., 2017).

Similar reasoning was applied to identify anthocyanins in dahlia samples as cyanidin (peaks **10**, **11**, **13**, **15** and **17**) and pelargonidin derivatives (peaks **12**, **16** and **18**), which were previously reported in dahlia flowers (Deguchi et al., 2013; Kosaku; Takeda, Harborne, & Self, 1986; Yamaguchi et al., 1999). The presence of Pg-3,5-diglucoside in flowers of *Dahlia variabilis* was identified by Yamaguchi et al. (1999) and Deguchi et al. (2013), which could correspond to peak **16** ($[M]^+$ at m/z 595) in our samples. For the remaining compounds (peaks **10**, **11**, **12**, **13**, **15**, **17, and 18**), no conclusions about the precise identity of the anthocyanins could be obtained, and the glycoside moieties were assigned based on the mass losses observed in the MS^2 spectra, as hexosides (−162 mu), acetylhexosides (−204 mu) or deoxyhexosylhexosides (−308 mu). Curiously, none of the observed peak losses indicates the presence of malonylglucosides, a type of derivatives usually reported in dahlia flowers (Deguchi et al., 2013; Kosaku; Takeda et al., 1986; Yamaguchi et al., 1999). Cy-acetylhexoside (peak **13**) was the most abundant compound in dahlia, representing the main responsible for the coloration of this edible flowers. In addition to improve the sensory characteristics of yogurt, that cyanidin might be a promising antiglycation agent for preventing or ameliorating AGEs-mediated diabetic complications (Suantawee, Cheng, & Adisakwattana, 2016). Finally, peak **14** presented a molecular ion $[M]^+$ at m/z 431 and a unique MS^2 fragment at m/z 269, which could match the mass of methylapigeninidin, so that it might be associated to a methylapigeninidin-hexoside, a pigment reported in red sorghum (Wu & Prior, 2005). Nevertheless, the absorption spectrum of peak **14** would not be coherent with such an identity, as the maximum absorption in the visible region of that compound should be expected around 470 nm (Awika, 2008; Yang, Dykes, & Awika, 2014). Thus, the identity of this peak as a 3-deoxyanthocyanin is uncertain, although in case it is confirmed it would be the first description of this type of pigments in dahlia flowers.

In general, these flowers have a great potential to be used as natural

Table 4
Fatty acids profile (relative percentage) of yogurt formulations (YF) and storage effect (SE). Results are presented as mean ± standard deviation.[a]

		C4:0	C6:0	C8:0	C10:0	C12:0	C14:0	C15:0	C16:0	C16:1	C18:0	C18:1n9	C18:2n6	C18:3n3	SFA	MUFA	PUFA
YF	BY	1.3 ± 0.2	1.7 ± 0.1	1.3 ± 0.1	2.9 ± 0.1	3.6 ± 0.1	11.9 ± 0.4	1.4 ± 0.1	35 ± 1	1.4 ± 0.1	11.0 ± 0.2	21 ± 1	2.3 ± 0.1	1.5 ± 0.1	71 ± 1	23 ± 2	5.0 ± 0.1
	RY	0.8 ± 0.1	1.4 ± 0.1	1.2 ± 0.1	2.8 ± 0.1	3.6 ± 0.1	12.2 ± 0.2	1.5 ± 0.1	36 ± 1	1.5 ± 0.1	11.5 ± 0.1	20 ± 1	2.2 ± 0.1	1.3 ± 0.1	72 ± 1	23 ± 1	4.6 ± 0.2
	DY	1.0 ± 0.1	1.4 ± 0.1	1.1 ± 0.1	2.7 ± 0.1	3.5 ± 0.1	12.1 ± 0.1	1.5 ± 0.1	36 ± 1	1.5 ± 0.1	11.5 ± 0.2	21 ± 1	2.3 ± 0.1	1.5 ± 0.1	72 ± 1	23 ± 1	5.1 ± 0.1
	CY	1.1 ± 0.1	1.5 ± 0.1	1.1 ± 0.1	2.7 ± 0.1	3.6 ± 0.1	12.0 ± 0.1	1.5 ± 0.1	36 ± 1	1.5 ± 0.1	11.5 ± 0.1	20 ± 1	2.5 ± 0.2	1.5 ± 0.1	72 ± 1	23 ± 1	5.3 ± 0.2
	AY	1.2 ± 0.1	1.6 ± 0.1	1.2 ± 0.1	2.8 ± 0.1	3.7 ± 0.1	12.0 ± 0.3	1.5 ± 0.1	35 ± 1	1.4 ± 0.1	11.3 ± 0.1	21 ± 1	2.3 ± 0.1	1.4 ± 0.1	72 ± 1	23 ± 1	4.9 ± 0.2
	ANOVA p-value (n = 18)[b]	< 0.001	< 0.001	< 0.001	< 0.001	< 0.001	0.002	< 0.001	< 0.001	< 0.001	< 0.001	0.133	< 0.001	< 0.001	0.180	0.125	< 0.001
SE	0 days	1.1 ± 0.2	1.4 ± 0.1	1.1 ± 0.1	2.7 ± 0.1	3.5 ± 0.1	11.9 ± 0.3	1.5 ± 0.1	35 ± 1	1.5 ± 0.1	11.3 ± 0.3	21 ± 1	2.3 ± 0.1	1.5 ± 0.1	71 ± 1	23 ± 1	5.0 ± 0.2
	7 days	1.0 ± 0.3	1.6 ± 0.1	1.2 ± 0.1	2.8 ± 0.1	3.6 ± 0.1	12.2 ± 0.2	1.5 ± 0.1	36 ± 2	1.5 ± 0.1	11.4 ± 0.1	20 ± 1	2.3 ± 0.1	1.4 ± 0.1	72 ± 1	22 ± 1	5.0 ± 0.1
	t-student p-value (n = 45)[c]	0.018	< 0.001	< 0.001	< 0.001	< 0.001	< 0.001	0.737	0.001	0.984	0.213	< 0.001	0.063	< 0.001	< 0.001	< 0.001	0.532
IF × ST	p-value (n = 90)[d]	< 0.001	< 0.001	< 0.001	< 0.001	< 0.001	< 0.001	< 0.001	< 0.001	< 0.001	< 0.001	< 0.001	< 0.001	< 0.001	< 0.001	< 0.001	< 0.001

[a] Results are reported as mean values of each YF, aggregating results from 0 to 7 days, and mean values of SE, combining all YF.
[b] If $p < 0.05$, the corresponding parameter presented a significantly different value for at least one YF.
[c] If $p < 0.05$, the corresponding parameter presented a significant difference among stored and non-stored yogurts.
[d] In this table, the interaction among factors was significant in all cases; thereby no multiple comparisons could be performed.

colorants, being an excellent source of anthocyanins to develop innovative products with new sensorial and bioactive characteristics.

3.2. Characterization of different fortified yogurts

Natural additives are generally considered as producing no harmful effects on consumers' health, contrarily to some artificial compounds (Carocho, Barreiro, Morales, & Ferreira, 2014). Nevertheless, the acceptability of these products is highly dependent on their appearance and rheological properties (Caleja et al., 2016; Santillán-Urquiza, Méndez-Rojas, & Vélez-Ruiz, 2017). In what concerns yogurt, similarly to several other food products, colour is a determining factor. Bearing this in mind, different plant species were selected as potential sources of colourants to be incorporated in yogurt. Yogurts prepared with different flower extracts were compared with each other and also with yogurts added with a commercial anthocyanin extract (E163, authorised by EFSA). In addition, a set of yogurts were used exactly as bought (free of any colouring agent), functioning as the "blank" yogurt control.

Besides comparing different yogurt formulations (YF), their stability throughout storage was also evaluated, specifically by performing the same evaluation assays on the preparation day and after 7 days of storage (SE).

Since the effect of each factor (YF or SE) might be affected by the second factor level (*i.e.*, different storage effects according on each YF, or *vice versa*), the interaction (YF × SE) was also evaluated. In all cases where a significant interaction was found ($p < 0.050$), the multiple comparisons could not be performed. In those cases, the overall conclusions were obtained from the corresponding estimated marginal means (EMM) plots.

Starting by analysing the results for nutritional parameters (Table 2), a significant interaction among YF and SE (YF × SE) was found in all cases, thereby indicating that each YF reacted differently to storage. Considering each factor individually, YF-related differences were significant in most cases, except water and energy, while SE had no significant effect in any case. In either case, the nutritional profile is very similar among all tested samples, with water as the main component (≈ 85 g/100 g), followed by carbohydrates (slightly higher in RY and CY and lower in DY) and protein (a bit higher in CY and lower in RY), both corresponding to ≈ 5.5 g/100 g), fat (≈ 3.2 g/100 g in CY to 3.4 g/100 g DY and AY) and ash (< 0.9 g/100 g in all yogurts). This profile resulted in energy values around 74 kcal/100 g in all cases. Actually, owing to the low quantity of colorant added, it was not expectable to have differences of high magnitude among different YF, particularly in what concerns fat amounts (the flower extracts were prepared with water). Nevertheless, the plant species used in the extraction procedures had different nutritional composition (Pires et al., 2017), causing some minor changes in the corresponding yogurts. Even so, these results validate the maintenance of the nutritional quality of natural yogurt (herein identified as BY).

In what concerns individual sugars, lactose was the main compound (≈ 4.8 g/100 g, with slightly higher values in AY). Minor levels of galactose were also quantified, varying form the maximum values detected in CY (0.76 g/100 g) to the lowest in BY (0.69 g/100 g).

More significant differences were, as observable in Table 3, obtained in the case of colour parameters, which is in line with the main purpose of this work. Yogurts free of any additive (BY) showed the highest L^* values, followed by CY, AY, RY and DY. On the contrary, BY presented the lowest a^* values, while AY, RY and DY reached the highest (without significantly different values among them). On the other hand, the absence of significant differences for a^* values among AY, RY and DY, indicate that rose and dahlia extracts might be potential alternatives to E163.

Fatty acids profiles, especially for their potential usefulness as indicators of suitable conservation conditions, were also characterized (Barreira, Pereira, Oliveira, & Ferreira, 2010; Pereira et al., 2016). All fatty acids quantified in relative percentages above 1% are presented in
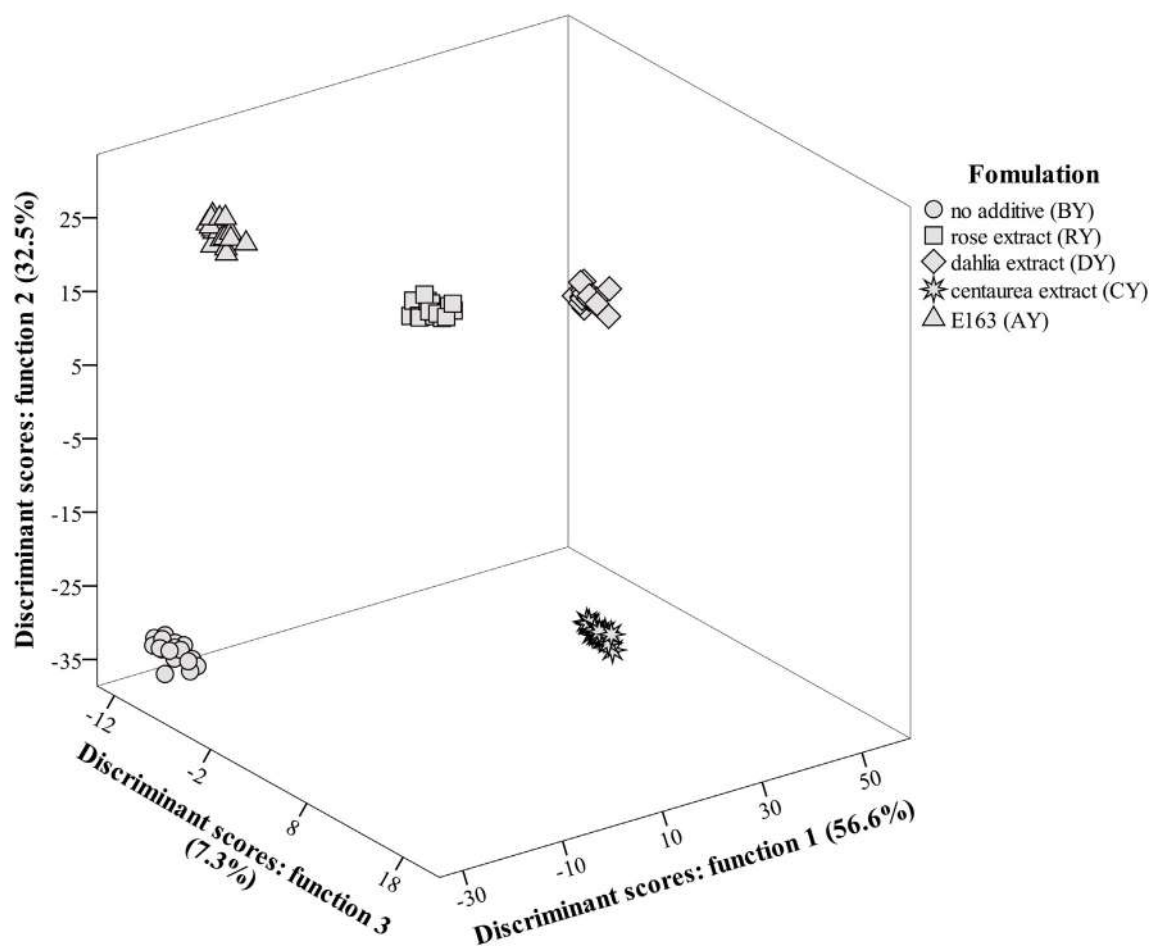
Fig. 1. Three-dimensional distribution of YF markers according to the canonical discriminant functions coefficients defined from different yogurt parameters.

Table 4, but the complete profiles included also C11:0, C13:0, C14:1, C17:0, C17:1, C18:3n6, C20:0, C20:1, C20:4n6, C20:5n3, C22:0, C23:0, C24:0 (however, all fatty acids were included in the Linear Discussion Analysis discussed in the next section).

Since milk was the main source of fatty acids in yogurt, and bearing in mind, once again, that the added extracts were aqueous, the high similarity among YF is coherent. Nevertheless, C18:1n9 ($p = 0.133$), SFA ($p = 0.180$) and MUFA ($p = 0.125$) were the only cases with no significant differences among tested YF, most likely because the added extracts might have different effectiveness in preventing the oxidation of specific fatty acids throughout time.

Since the interaction among factors (YF $\times$ SE) the next conclusions were obtained from the EMM plots (data not shown): BY presented higher percentages of C4:0 (1.3%), C6:0 (1.7%), C8:0 (1.3%), and C10:0 (2.9%), while C15:0 (1.5%), C16:1 (1.5%), C18:0 (11.5%), C18:2n6 (2.5%) and PUFA (5.3%) showed the highest values in CY. Yogurts prepared with rose extract (RY), on the other hand, had the highest percentages of C14:0 (12.2%) and C16:0 (36%), whilst C12:0 was slightly higher in AY (3.7%).

In what concerns SE effect, almost all tabled fatty acids showed significant differences, except in the cases of C15:0 ($p = 0.737$), C16:1 ($p = 0.984$), C18:0 ($p = 0.213$), C18:2n6 ($p = 0.063$) and PUFA ($p = 0.532$). In stored samples, C6:0, C8:0, C10:0, C12:0, C14:0, C16:0 and SFA were quantified in higher percentages, while C4:0, C18:1n9, C19:3n3 and MUFA tended to present higher values in non-stored samples, thereby generally corroborating the higher resistance of saturated forms to storage.

3.3. Linear discriminant analysis

Despite the statistical significance of differences among different YF, we decided to verify if the magnitude of the detected differences was high enough to discriminate each YF. Accordingly, a linear discriminant analysis (LDA) was applied to find the variables with highest contribution to discriminate each YF.

The first three discriminant functions included 97.7% (first function: 61.4%; second function: 30.0%; third function: 6.3%) of the observed variance (Fig. 1). From the 41 variables under analysis, the discriminant model selected b^*, a^*, L^*, pH, C4:0, C8:0, C13:0, C16:1, C17:1, C18:3n3, C18:3n6, C20:1, C20:4n6, C20:5n3, C23:0, C24:0 and PUFA as those having discriminant ability, which clearly indicates that fatty acids and colour parameters were the variables with highest dissimilarity among the prepared YF.

In what concerns the correlations among functions and variables, function 1 was highly correlated with b^* and L^*, placing markers corresponding to DY and BY in the farthest positions due to their differences in both parameters (the highest b^* value was measured in DY, while the maximum L^* was measured in BY). Function 2, in turn, was mostly correlated with a^*, mostly separating markers corresponding to AY and RY (positive end of the axis) from BY (negative end of the axis). Function 3 also contributed to separate the markers of each YF, being especially effective in separating BY and CY. Owing to the higher proximity of their markers according to the three plotted discriminant functions RY and AY showed the highest similarity among the assayed parameters.

In the performed LDA, the classification performance was 100% accurate, either for original grouped cases, as well as for the cross-

validated grouped cases.

4. Conclusion

Overall, the natural extracts with highest potential as alternatives to E163 resulted to be RY, considering the main purpose of colouring yogurts in the yellow-orange series. In addition to the provided colour, these groups of yogurts (AY and RY) showed very similar nutritional value, free sugars and fatty acids composition.

Conflicts of interest

The authors declare that they have no conflicts of interest.

References

AOAC (2016). In W. George, & J. Latimer (Eds.). *Official methods of analysis of AOAC international - 20th edition*(20th ed.). AOAC International.

Arioui, F., Ait Saada, D., & Cheriguene, A. (2017). Physicochemical and sensory quality of yogurt incorporated with pectin from peel of *Citrus sinensis*. *Food Sciences and Nutrition, 5*(2), 358–364. https://doi.org/10.1002/fsn3.400.

Awika, J. M. (2008). Behavior of 3-deoxyanthocyanidins in the presence of phenolic copigments. *Food Research International, 41*(5), 532–538.

Barreira, J. C. M., Pereira, J. A., Oliveira, M. B. P. P., & Ferreira, I. C. F. R. (2010). Sugars profiles of different chestnut (*Castanea sativa* Mill.) and almond (*Prunus dulcis*) cultivars by HPLC-RI. *Plant Foods for Human Nutrition, 65*(1), 38–43. https://doi.org/10.1007/s11130-009-0147-7.

Barros, L., Pereira, C., & Ferreira, I. C. F. R. (2013). Optimized analysis of organic acids in edible mushrooms from Portugal by ultra fast liquid chromatography and photodiode array detection. *Food Analytical Methods, 6*(1), 309–316. https://doi.org/10.1007/s12161-012-9443-1.

Caleja, C., Barros, L., Antonio, A. L., Carocho, M., Oliveira, M. B. P. P., & Ferreira, I. C. F. R. (2016). Fortification of yogurts with different antioxidant preservatives: A comparative study between natural and synthetic additives. *Food Chemistry, 210*, 262–268. https://doi.org/10.1016/j.foodchem.2016.04.114.

Carocho, M., Barreiro, M. F., Morales, P., & Ferreira, I. C. F. R. (2014). Adding molecules to food, pros and cons: A review on synthetic and natural food additives. *Comprehensive Reviews in Food Science and Food Safety, 13*(4), 377–399. https://doi.org/10.1111/1541-4337.12065.

Castañeda-Ovando, A., Pacheco-Hernández, M. de L., Páez-Hernández, M. E., Rodríguez, J. A., & Galán-Vidal, C. A. (2009, April). *Chemical studies of anthocyanins: A review. Food chemistry.* Elsevierhttps://doi.org/10.1016/j.foodchem.2008.09.001.

Chanukya, B. S., & Rastogi, N. K. (2016). A comparison of thermal processing, freeze drying and forward osmosis for the downstream processing of anthocyanin from rose petals. 40(6 OP-Journal of Food Processing & Preservation. Dec 2016, Vol. 40 Issue 6, p1289, 8 p.), 1289. https://doi.org/10.1111/jfpp.12714.

Deguchi, A., Ohno, S., Hosokawa, M., Tatsuzawa, F., & Doi, M. (2013). Endogenous post-transcriptional gene silencing of flavone synthase resulting in high accumulation of anthocyanins in black dahlia cultivars. *Planta, 237*(5), 1325–1335. https://doi.org/10.1007/s00425-013-1848-6.

Dias, M. I., Barros, L., Morales, P., Sánchez-Mata, M. C., Oliveira, M. B. P. P., & Ferreira, I. C. F. (2015). Nutritional parameters of infusions and decoctions obtained from *Fragaria vesca* L. roots and vegetative parts. *Lebensmittel-Wissenschaft und -Technologie-Food Science and Technology, 62*(1), 32–38. https://doi.org/10.1016/j.lwt.2015.01.034.

Duarte, L. J., Chaves, V. C., Nascimento, M. V. P., dos, S., Calvete, E., Li, M., et al. (2018). Molecular mechanism of action of Pelargonidin-3-*O*-glucoside, the main anthocyanin responsible for the anti-inflammatory effect of strawberry fruits. *Food Chemistry, 247*, 56–65. https://doi.org/10.1016/j.foodchem.2017.12.015.

E.F.S.A (2013). Scientific Opinion on the re-evaluation of anthocyanins (E 163) as a food additive. *EFSA Journal, 11*(4), 3145. https://doi.org/10.2903/j.efsa.2013.3145.

Fernandes, Â., Antonio, A. L., Barreira, J. C. M., Oliveira, M. B. P. P., Martins, A., & Ferreira, I. C. F. R. (2012). Effects of gamma irradiation on physical parameters of *Lactarius deliciosus* wild edible mushrooms. *Postharvest Biology and Technology, 74*, 79–84. https://doi.org/10.1016/j.postharvbio.2012.06.019.

Gonçalves, G. A., Soares, A. A., Correa, R. C. G., Barros, L., Haminiuk, C. W. I., Peralta, R. M., et al. (2017). Merlot grape pomace hydroalcoholic extract improves the oxidative and inflammatory states of rats with adjuvant-induced arthritis. *Journal of Functional Foods, 33*, 408–418.

Hidalgo, G.-I., & Almajano, M. P. (2017). *Red fruits: Extraction of antioxidants, phenolic content, and radical scavenging determination: A review.* https://doi.org/10.3390/antiox6010007.

Hvattum, E. (2002). Determination of phenolic compounds in rose hip (*Rosa canina*) using liquid chromatography coupled to electrospray ionisation tandem mass spectrometry and diode-array detection. *Rapid Communications in Mass Spectrometry, 16*(7), 655–662. https://doi.org/10.1002/rcm.622.

Jaakola, L. (2013). New insights into the regulation of anthocyanin biosynthesis in fruits. *Trends in Plant Science, 18*(9), 477–483. https://doi.org/10.1016/J.TPLANTS.2013.06.003.

Jantathai, S., Sungsri-in, M., Mukprasirt, A., & Duerrschmid, K. (2014). Sensory expectations and perceptions of austrian and Thai consumers: A case study with six colored Thai desserts. *Food Research International, 64*, 65–73. https://doi.org/10.1016/j.foodres.2014.06.007.

Khoo, H. E., Azlan, A., Tang, S. T., & Lim, S. M. (2017). Anthocyanidins and anthocyanins: Colored pigments as food, pharmaceutical ingredients, and the potential health benefits. *Food & Nutrition Research, 61*(1), 1361779. https://doi.org/10.1080/16546628.2017.1361779.

Ko, H., Jeong, M.-H., Jeon, H., Sung, G.-J., So, Y., Kim, I., et al. (2015). Delphinidin sensitizes prostate cancer cells to TRAIL-induced apoptosis, by inducing DR5 and causing caspase-mediated HDAC3 cleavage. *Oncotarget, 6*(12), 9970–9984. https://doi.org/10.18632/oncotarget.3667.

Lee, J. H., Lee, H.-J., & Choung, M.-G. (2011). Anthocyanin compositions and biological activities from the red petals of Korean edible rose (*Rosa hybrida* cv. Noblered). *Food Chemistry, 129*(2), 272–278. https://doi.org/10.1016/J.FOODCHEM.2011.04.040.

Mishio, T., Takeda, K., & Iwashina, T. (2015). Anthocyanins and other flavonoids as flower pigments from eleven Centaurea species. *Natural Product Communications, 10*(3), 447–450.

Mourtzinos, I., Prodromidis, P., Grigorakis, S., Makris, D. P., Biliaderis, C. G., & Moschakis, T. (2018). Natural food colourants derived from onion wastes: Application in a yoghurt product. *Electrophoresis, 1–28*https://doi.org/10.1002/elps.201800073.

Pereira, E., Barros, L., Barreira, J. C. M., Carvalho, A. M., Antonio, A. L., & Ferreira, I. C. F. R. (2016). Electron beam and gamma irradiation as feasible conservation technologies for wild *Arenaria Montana* L.: Effects on chemical and antioxidant parameters. *Innovative Food Science & Emerging Technologies, 36*, 269–276. https://doi.org/10.1016/j.ifset.2016.07.012.

Pires, T. S. C. P., Dias, M. I., Barros, L., Calhelha, R. C., Alves, M. J., Oliveira, M. B. P. P., et al. (2018). Edible flowers as sources of phenolic compounds with bioactive potential. *Food Research International, 105*, 580–588.

Pires, T. C. S. P., Dias, M. I., Barros, L., & Ferreira, I. C. F. R. (2017). Nutritional and chemical characterization of edible petals and corresponding infusions: Valorization as new food ingredients. *Food Chemistry, 220*, 337–343. https://doi.org/10.1016/j.foodchem.2016.10.026.

Pop, M., Lupea, A. X., Popa, S., & Gruescu, C. (2010). *Colour of bilberry (Vaccinium myrtillus fruits) extracts.* https://doi.org/10.1080/10942910902894898.

Rodriguez-Amaya, D. B. (2016). Natural food pigments and colorants. *Current Opinion in Food Science, 7*, 20–26. https://doi.org/10.1016/j.cofs.2015.08.004.

Santillán-Urquiza, E., Méndez-Rojas, M.Á., & Vélez-Ruiz, J. F. (2017). Fortification of yogurt with nano and micro sized calcium, iron and zinc, effect on the physico-chemical and rheological properties. *Lebensmittel-Wissenschaft und -Technologie- Food Science and Technology, 80*, 462–469. https://doi.org/10.1016/j.lwt.2017.03.025.

Spence, C., Levitan, C. A., Shankar, M. U., & Zampini, M. (2010). Does food color influence taste and flavor perception in humans? *Chemosensory Perception, 3*(1), 68–84. https://doi.org/10.1007/s12078-010-9067-z.

Suantawee, T., Cheng, H., & Adisakwattana, S. (2016). Protective effect of cyanidin against glucose- and methylglyoxal-induced protein glycation and oxidative DNA damage. *International Journal of Biological Macromolecules, 93*, 814–821. https://doi.org/10.1016/j.ijbiomac.2016.09.059.

Takeda, K., Harborne, J. B., & Self, R. (1986). Identification and distribution of malonated anthocyanins in plants of the compositae. *Phytochemistry, 25*(6), 1337–1342.

Takeda, K., Kumegawa, C., Harborne, J. B., & Self, R. (1988). Pelargonidin 3-(6″-succinyl glucoside)-5-glucoside from pink *Centaurea cyanus* flowers. *Phytochemistry, 27*(4), 1228–1229.

Takeda, K., Osakabe, A., Saito, S., Furuyama, D., Tomita, A., Kojima, Y., et al. (2005). Components of protocyanin, a blue pigment from the blue flowers of *Centaurea cyanus*. *Phytochemistry, 66*(13), 1607–1613. https://doi.org/10.1016/j.phytochem.2005.04.002.

Takeda, K., & Tominaga, S. (1983). The anthocyanin in blue flowers of C*entaurea cyanus. Botanical Magazine Tokyo, 96*(4), 359–363.

Vecioglu, Y. S., & Mazza, G. (1991). Characterization of flavonoids in petals of *Rosa damascena* by HPLC and spectral analysis. *Journal of Agricultural and Food Chemistry, 39*(3), 463–467.

Wu, X., & Prior, R. L. (2005). Identification and characterization of anthocyanins by high-performance liquid chromatography-electrospray ionization-tandem mass spectrometry in common foods in the United States: Vegetables, nuts, and grains. *Journal of Agricultural and Food Chemistry, 53*(8), 3101–3113. https://doi.org/10.1021/

jf0478861.

Yamaguchi, M.-A., Oshida, N., Nakayama, M., Koshioka, M., Yamaguchi, Y., & Ino, I. (1999). Anthocyanidin 3-glucoside malonyltransferase from Dahlia variabilis. *Phytochemistry, 52*(1), 15–18. https://doi.org/10.1016/S0031-9422(99)00099-0.

Yang, L., Dykes, L., & Awika, J. M. (2014). Thermal stability of 3-deoxyanthocyanidin pigments. *Food Chemistry, 160,* 246–254.

Zielinski, A. A. F., Haminiuk, C. W. I., Alberti, A., Nogueira, A., Demiate, I. M., & Granato, D. (2014). A comparative study of the phenolic compounds and the in vitro antioxidant activity of different Brazilian teas using multivariate statistical techniques. *Food Research International, 60,* 246–254. https://doi.org/10.1016/j.foodres.2013.09.010.

Gomphrena globosa L. as a novel source of food-grade betacyanins: Incorporation in ice-cream and comparison with beet-root extracts and commercial betalains

Custódio Lobo Roriz[a,b], João C.M. Barreira[a], Patricia Morales[b], Lillian Barros[a], Isabel C.F.R. Ferreira[a,*]

[a] *Centro de Investigação de Montanha (CIMO), Instituto Politécnico de Bragança, Campus de Santa Apolónia, 5300-253 Bragança, Portugal*
[b] *Dpto. Nutrición y Bromatología II, Facultad de Farmacia, Universidad Complutense de Madrid (UCM), Plaza Ramón y Cajal, s/n. E-28040, Madrid, Spain*

ARTICLE INFO

ABSTRACT

Currently, there are some examples of natural colourants with commercial use. However, these colourants are usually under-exploited, besides being obtained from a reduced number of plant or algal species. Accordingly, we propose using betalains obtained from an alternative plant species, *Gomphrena globosa*, which have a powerful colouring activity besides being strong antioxidants, as a novel ice-cream colourant. For comparison purposes, other ice-cream formulations were prepared, namely without colourants, added with commercial betalain or with *Beta vulgaris* extract. Besides evaluating the colour parameters $L*$, $a*$ and $b*$, the nutritional parameters, individual sugars and fatty acids profiles were also studied. These parameters were evaluated throughout time, up to a maximum of 60 days of freeze ($-22\,°C$) storage. Betacyanin quantification of each formulation was also performed to determine its maintenance along storage. In general, ice-creams prepared with *G. globosa* were similar (considering nutritional, colour, individual sugars and fatty acids profiles) to those including *B. vulgaris* extract, thereby validating the suitability of this alternative plant as a source of food colourants, particularly as ice-cream colourants. Furthermore, the positive effects induced by the addition of this natural colourant were maintained throughout storage time, as indicated by the markers distribution in the linear discriminant analysis.

1. Introduction

The importance of food appearance might be considered as being as important as its taste, being often considered as a top indicator of the overall quality of food (Bridle & Timberlake, 1997, pp. 103–109). Nowadays, the complex processing that most food products are submitted to might cause some unwanted changes to their visual appearance, especially by causing a fading effect in their colour (González, Gallego, & Valcárcel, 2002). In addition, there is growing concern about the health effects potentially induced by food, which is increasingly being considered as having the double purpose of satisfying nutritional needs, while exerting disease-preventing effects. This overall trend represents the main foundation of the functional foods market, in which novel food products, able to provide new consuming experiences, are continuously being developed (Edmonds, Wadhwa, & Wibisono, 2013). When these products are developed with the main purpose of achieving specific functional properties, foods poor in bioactive compounds present higher necessity of improvement. In this sense, ice-cream, a

product with high consumption level, would certainly benefit from the incorporation of bioactive natural substances, particularly if these substances could simultaneously improve its appearance (Edmonds et al., 2013). In general, frozen dairy desserts, such as ice-creams, are complex colloidal systems that consist in a combination of milk, sweeteners, emulsifiers, stabilizers, colouring and flavouring agents (Soukoulis, Lyroni, & Tzia, 2010). Despite the generalized use of artificial substances, most of these agents could be obtained from natural sources, making the resulting products very appealing to the consumers (Erkaya, Dağdemir, & Sengül, 2012).

In the case of colouring agents, and owing to the important role of colour when enjoying any food product or as a potential indicator of food quality (Bridle & Timberlake, 1997, pp. 103–109), it is mandatory to find natural-based colourants, particularly if the associated compounds might exert any kind of bioactivity. This becomes even more important if we remind that most artificial compounds are often regarded as causing several secondary and harmful effects, such as allergenic or intolerance reactions (Wissgott & Bortlik, 1996).

Despite the diversity of natural dyes (*e.g.*, carotenoids, anthocyanins or betalains) in the market (Carocho, Morales, & Ferreira, 2015), most are far from being used according to their full potential, besides being obtained from a reduced number of natural sources. Betalains, which can be divided in red-violet betacyanins and yellow-orange betaxanthins, are a good example of under-exploited natural food colourants. Furthermore, betacyanins are almost exclusively obtained from beetroot, despite the availability of other alternative sources (Roriz, Barros, Prieto, Morales, & Ferreira, 2017). Besides their colouring capacity, these pigments have a high antioxidant activity, exerting also different chemopreventive effects (Spórna-kucab & Jagodzi, 2017). *Gomphrena globosa* L. presents a multitude of phytochemicals with interest, such as tocopherols, sugars and organic acids (Roriz, Barros, Carvalho, & Ferreira, 2014). In addition to these compounds, other substances with antioxidant properties have been identified in this plant, in particular bioactive substances such as phenolic compounds, but also molecules that can confer colour, such as betacyanins (Roriz, Barros, Carvalho, Santos-Buelga, & Ferreira, 2014). Herein, betacyanins extracted from the purple flowers of *Gomphrena globosa* L. (Amaranthaceae) were evaluated as colouring/functionalizing agents in ice-cream formulations, aiming to verify its potential improvement in colour parameters, as well as its effect on nutritional composition, individual sugars and fatty acids profiles. In order to acquire comprehensive conclusions, other ice-cream formulations were prepared namely, ice-cream without any colouring agent, ice-cream incorporated with commercial betalains and ice-cream added with beet-root extract. Betacyanin quantification of each formulation was also performed in order to determine its maintenance along storage. All parameters were analysed in five different moments: preparation day, and after 15, 30, 45 and 60 days (considered as the maximum desired storage limit, for this type of ice-cream) of storage ($-22\,°C$).

2. Material and methods

2.1. Standard and reagents

Acetonitrile (HPLC grade) was obtained from Lab-Scan (Lisbon, Portugal). The standard betalain and the fatty acids methyl ester (FAME) reference standard mixture 37 (standard 47885-U) was purchased from Sigma-Aldrich (St. Louis, MO, USA). Other reagents and solvents (analytical grade) were obtained from common sources. Milk (UHT entire milk Continente, composition per 100 mL: 273 KJ, or 65 Kcal energetic value; 3.6 g of lipids of which 2.3 are unsaturated; 4.9 g of carbohydrates, being the majority sugars; 3.3 g of protein; and 0.1 g of salt) and double cream (UHT cream Continente; composition per 100 mL: 1385 KJ, or 336 Kcal energetic value; 35 g of lipids of which 20 g are unsaturated; 3 g of carbohydrates; 2 g of protein; and 0.1 g of salt) were purchased at a local supermarket (Continente, Portugal). Water was treated in a Milli-Q water purification system (TGI Pure Water Systems, Greenville, SC, USA).

2.2. Sample collection

Gomphrena globosa L. samples were obtained from Ervital, a company established in a mountain region with high biodiversity, holding a vast collection of certified plant materials from different origins, obtained from sustainable harvesting of spontaneous local species and organic farming of exogenous ones. The botanical identification of the samples was confirmed by a botanical expert, responsible for the medicinal plant collection of *Escola Superior Agrária* herbarium (BRESA), Polytechnic Institute of Bragança (Trás-os-Montes, Portugal). After identification, samples were subjected to a mechanical treatment to separate the pigmented floral parts (bracts and bracteoles) from the inflorescences.

2.3. Sample preparation

2.3.1. Ultrasound assisted extraction (UAE)

The *G. globosa* extract enriched in betacyanins was obtained by UAE (QSonica sonicators, model CL-334, Newtown, CT, USA), working at 500 W, for 22 min, using water as the extraction solvent and a liquid-to-solid ratio of 5 g/L, as described by (Roriz, Barros, Prieto, Barreiro, et al., 2017).

2.3.2. Preparation of B. vulgaris extract

B. vulgaris extract obtained by UAE, was further filtrated and frozen prior to its lyophilization (FreeZone 4.5, Labconco, Kansas City, MO, USA), in order to obtain a dry extract.

2.4. Incorporation of the natural food colorant in the ice-cream

2.4.1. a) Ice-cream preparation

Ice-cream was prepared from a base recipe: 240 g of sugar were mixed with 500 mL of milk (UHT entire milk, Continente, Portugal), in order to dissolve the sugar. Meanwhile, 1000 mL of double cream (UHT cream, Continente, Portugal) were used to obtain whipped cream, which was previously added to the mixture. The final batter was left to stand for 12 h, further divided in four batches, each placed in an ice-cream machine equipment (Ice-cream Maker SECN 12 A1, SilverCrest, Hamburg, Germany).

2.4.2. b) Colouring agent addition

The ice-cream batches were identified as: i) control (ice-cream without colouring agents); ii) ice-cream added with betalain standard (200 mg, *i.e.* ≈ 46 mg/100 g ice-cream); iii) ice-cream with *G. globosa* extract (670 mg, *i.e.* ≈ 154 mg/100 g ice-cream); iv) ice-cream with *Beta vulgaris* extract (670 mg, *i.e.* ≈ 154 mg/100 g ice-cream).

The amount of each ingredient was added in order to obtain the desired colour. Moreover, the added quantities were different because commercial betalain (Sigma-Aldrich, St. Louis, MO, USA) is an isolated compound, obviously with a higher degree of purity in comparison with the extracts from *G. globosa* and *B. vulgaris*. *B. vulgaris* extract was obtained by grinding the sample with 10% of water, followed by a filtration step and freeze prior to its lyophilization (FreeZone 4.5, Labconco, Kansas City, MO, USA).

The samples were analysed immediately after preparation and after: 15, 30, 45 and 60 days (maximum desired storage limit for this type of ice-cream) of storage at $-22\,°C$.

2.5. Nutritional composition and physico-chemical analyses

2.5.1. Nutritional parameters

The samples were also analysed for proximate composition (moisture, protein, fat, ash and carbohydrates) using the AOAC procedures (AOAC, 2016). Crude protein content (N × 6.38) was estimated by the Kjeldahl method (AOAC 978.04, AOAC, 2016); crude fat was determined by Rose-Gottlieb method (AOAC 905.02, AOAC, 2016); ash content was determined by incineration at $600 \pm 15\,°C$ (AOAC 923.03, AOAC, 2016); total carbohydrates were calculated by difference, taking into account moisture content, and the results were expressed in fresh weight. Total energy was calculated according to the following equation: Energy (kcal) = 4 × (g proteins + g carbohydrates) + 9 × (g lipids).

2.5.2. Individual sugars

Free sugars were detected by high performance liquid chromatography (HPLC) coupled to a refractive index detector. Sugars were identified by comparison with standards and further quantified (g/100 g of ice-cream) by the internal standard (melezitose) method (Barros et al., 2013).

2.5.3. Colour parameters

The CIE colour parameters were measured in three different points for each sample using a colorimeter (model CR-400, Konica Minolta Sensing Inc., Tokyo, Japan), and the average value of the different points was considered to determine this parameter. The illuminant C and a diaphragm aperture of 8 mm were selected. The Hunter colour L*, $a*$ and $b*$ values were registered using the data software "Spectra Magic Nx" (version CM-S100W 2.03.0006, Konica Minolta Company, Japan). The instrument was calibrated to standard white tiles before analysis (Spectra Magic NX Instruction Manual, Konica Minolta Sensing, Inc. (ver. 2.0), 2009, Japan) (Fernandes et al., 2012).

2.5.4. Fatty acids

Fatty acids were analysed by gas chromatography (GC) coupled to a flame ionization detector (FID) at 260 °C, using a DANI model GC 1000 instrument equipped with a split/splitless injector and a Macherey-Nagel (Duren, Germany) column (50% cyanopropyl-methyl-50% phenylmethylpolysiloxane, 30 m × 0.32 mm i.d. × 0.25 μm df). The oven temperature programme was as follows: the initial temperature of the column was 50 °C, held for 2 min, then a 30 °C/min ramp to 125 °C, 5 °C/min ramp to 160 °C, 20 °C/min ramp to 180 °C, 3 °C/min ramp to 200 °C, 20 °C/min ramp to 220 °C and held for 15 min. The carrier gas (hydrogen) flow-rate was 4.0 mL/min (0.61 bar), measured at 50 °C. Split injection (1:40) was carried out at 250 °C. Fatty acid identification was made by comparing the relative retention times of FAME peaks from samples with standards. The results were recorded and processed using the CSW 1.7 Software (DataApex 1.7) and expressed in relative percentage of each fatty acid (Barros et al., 2013).

2.5.5. Betacyanins

For betacyanins' determination an HPLC-DAD-ESI/MS analyses was performed with a Dionex Ultimate 3000 UPLC instrument (Thermo Scientific, San Jose, CA, USA) coupled with a diode-array detector and a mass spectrometer, as previously described by (Roriz, Barros, Prieto, Morales, et al., 2017). The separation was carried out in a Waters Spherisorb S3 ODS-2 C18, (3 μm, 4.6 mm × 150 mm, Waters, Milford, MA, USA) column operating at 35 °C and the solvents used were: (A) 0.1% trifluoracetic acid (TFA) in water and (B) acetonitrile, using a gradient flow elution method. Betacyanins maximum absorbance is 530 nm, therefore this was the preference wavelength used to record all chromatograms. For quantitative analysis, a calibration curve was obtained based on gomphrenin III and betalain.

2.6. Evaluation of hepatotoxicity

The different extracts, the commercial standard and the final ice-cream formulations (maximal tested concentration: 400 μg/mL) were evaluated regarding their hepatotoxicity, following a methodology previously described (Abreu et al., 2011) and using porcine liver, which was acquired from certified abattoirs. A phase-contrast microscope was used to monitor the growth of the cell cultures. They were sub-cultured and plated in 96 well plates (density of 1.0×10^4 cells/well). Dulbecco's Modified Eagle Medium (DMEM) was used, with 10% of foetal bovine serum (FBS), 100 U/mL of penicillin and 100 μg/mL of streptomycin. Ellipticine was used as a positive control, and the results were expressed in GI_{50} values (growth inhibition values) in μg/mL (sample concentration that inhibited 50% of the net cell growth).

2.7. Statistical analysis

All statistical tests were performed with IBM SPSS Statistics for Windows, version 22.0 (IBM Corp., Armonk, NY, USA) considering a 5% significance level. Data were expressed as mean ± standard deviation (the number of significant numbers was maintained according to the standard deviation magnitude).

For each ice cream formulation, three different samples were used.

Each of these samples was further analysed in triplicate. A 2-way analysis of variance (ANOVA) with type III sums, using the general linear model (GLM) procedure was applied to compare all parameters among different ice-cream formulations (IF) or storage times (ST). Besides evaluating the effect of each factor, their interaction was also assessed. When no statistical significant interaction was found, the means were compared using Tukey's multiple comparison test, with a previous assessment of the equality of variances through a Levene's test. Otherwise, differences were analysed in the estimated marginal means plots obtained for all levels of each factor.

In addition, a linear discriminant analysis (LDA) was used to compare the effect of IF and ST over all parameters simultaneously. A stepwise technique was applied, based on the Wilks' Ʌ test with the usual probabilities of F (3.84 to enter and 2.71 to be removed) for variable selection. Only variables with a statistically significant classification performance ($p < 0.050$) were maintained by the statistical model. This statistical classification tool was performed to estimate the relationship between single categorical dependent variables (ice-cream formulations) and the quantitative independent variables (results obtained in laboratorial assays). A leaving-one-out cross validation procedure was carried out to assess the model performance.

3. Results and discussion

Owing to the high consumers' acceptability, there are several studies reporting tentative improvements in ice-cream recipes, either by substituting its main ingredients, especially sugars (Moriano & Alamprese, 2017; Soukoulis & Tzia, 2017), or by adding compounds with different biological activity, *e.g.*, probiotics (Chaikham & Rattanasena, 2017; dos Santos Cruxen et al., 2017) or antioxidants (Sanguigni, Manco, Sorge, Gnessi, & Francomano, 2016). There is an increasing tendency towards using natural extracts in recent studies (Carocho, Barreiro, Morales, & Ferreira, 2014; dos Santos Cruxen et al., 2017), for instance to replace the artificial dyes commonly utilized in ice-cream, as shown in a recent study reporting the presence of 18 artificial dyes in different ice-cream formulations (Machewad, Chatge, Chappalwar, Jadhav, & Chappalwar, 2012; Martin, Oberson, Meschiari, & Munari, 2016). The industrial use of natural extracts might represent an effective answer to the current consumers' concerns, who are gradually preferring food products prepared with natural additives instead of artificial compounds, often associated with unwanted effects.

Bearing this in mind, four different ice-cream formulations: i) control ice-cream (CI, ice-cream with no added colourants); ii) ice-cream added with betalain standard (BSI); iii) ice-cream with *G. globosa* extract (GGI); and iv) ice-cream with *B. vulgaris* extract (BVI), were characterized. In addition to the preparation day, this comparative study was extended to four storage periods, namely: 15, 30, 45 and 60 days at − 22 °C.

As explained in the Materials and methods section, the effect of storage time (ST) was evaluated after a previous aggregation of results obtained for all formulations in a determined period; likewise, the effect of ice-cream formulation (IF) was evaluated after combining the results of all storage periods in each specific IF. This approach is expected to allow concluding which is best colouring agent, independently of ST, as well as the main changes along storage in differently formulated ice-creams. This is, in our opinion, the most useful information pertaining potential industrial applications. Since ST effect could depend on the ice-cream formulation (IF), and *vice-versa*, the interaction among both factors was also studied, in addition to evaluating the significance of each individual factor. In all cases where a significant ($p < 0.050$) interaction was found, not allowing the statistical classification of results, differences induced by each factor (if significant) were described according to the estimated marginal means (EMM) plots.

The nutritional composition and energy values for different ice-cream formulations (IF) and storage times (ST) are presented in Table 1. In terms of nutritional composition (Table 1), the interaction among IF

Table 1

Nutritional composition (g/100 g fresh weight) and energy values (kcal/100 g fresh weight) for different ice-cream formulations (IF) and storage times (ST). Results are presented as mean ± standard deviation.[1]

		Water	Fat	Protein	Ash	Carbohydrates	Sucrose	Lactose	Energy
IF	CI	59 ± 1	14 ± 2	5.0 ± 0.2	0.35 ± 0.05	22 ± 2	19 ± 1	2.5 ± 0.3	234 ± 13
	BSI	59 ± 1	15 ± 1	5.1 ± 0.3	0.35 ± 0.05	21 ± 1	18 ± 1	2.5 ± 0.3	239 ± 6
	GGI	59 ± 1	15 ± 1	5.1 ± 0.4	0.37 ± 0.05	21 ± 1	18 ± 1	2.5 ± 0.3	239 ± 7
	BVI	63 ± 1	13 ± 1	5.8 ± 0.3	0.37 ± 0.05	18 ± 1	16 ± 1	2.3 ± 0.3	212 ± 7
	ANOVA p-value (n = 45)[2]	< 0.001	< 0.001	< 0.001	0.243	< 0.001	< 0.001	0.036	< 0.001
ST	0 days	60 ± 1	14 ± 1	5.3 ± 0.4	0.43 ± 0.05	20 ± 1	17 ± 1	2.7 ± 0.3	227 ± 8
	15 days	60 ± 1	15 ± 1	5.3 ± 0.5	0.32 ± 0.04	20 ± 2	18 ± 1	2.3 ± 0.2	236 ± 8
	30 days	61 ± 2	12 ± 2	5.1 ± 0.4	0.42 ± 0.05	21 ± 3	18 ± 1	2.6 ± 0.3	212 ± 11
	45 days	60 ± 2	15 ± 1	5.3 ± 0.5	0.28 ± 0.05	20 ± 2	18 ± 1	2.4 ± 0.2	236 ± 11
	60 days	60 ± 2	14 ± 1	5.3 ± 0.5	0.36 ± 0.04	20 ± 2	18 ± 1	2.2 ± 0.2	227 ± 15
	ANOVA p-value (n = 36)[3]	0.026	< 0.001	0.219	< 0.001	< 0.001	0.002	< 0.001	< 0.001
IF × ST	p-value (n = 180)[4]	< 0.001	< 0.001	< 0.001	< 0.001	< 0.001	< 0.001	< 0.001	< 0.001

[1] Results are reported as mean values of each ice-cream formulation (IF), including results from 0, 15, 30, 45 and 60 days, and mean values of each storage time (ST), considering all IF in each ST.
[2] If $p < 0.05$, the corresponding parameter presented a significantly different value for at least one IF.
[3] If $p < 0.05$, the corresponding parameter presented a significantly different value for at least one ST.
[4] In this table, the interaction among factors was significant in all cases; thereby no multiple comparisons could be performed.

Table 2

Colour parameters measured in different ice-cream formulations (IF) and storage times (ST). Results are presented as mean ± standard deviation.[1]

		Fresh			Lyophilized		
		L*	a*	b*	L*	a*	b*
IF	CI	94 ± 1	−2.5 ± 0.2	13 ± 1	95 ± 1	−2.3 ± 0.2	11 ± 1
	BSI	93 ± 1	2.0 ± 0.2	8.1 ± 0.4	94 ± 1	1.7 ± 0.3	8 ± 1
	GGI	86 ± 3	8 ± 1	2.4 ± 0.3	87 ± 2	8 ± 1	2.5 ± 0.3
	BVI	85 ± 2	10 ± 2	3.0 ± 0.4	87 ± 1	10 ± 1	3.4 ± 0.4
	ANOVA p-value (n = 45)[2]	< 0.001	< 0.001	< 0.001	< 0.001	< 0.001	< 0.001
ST	0 days	91 ± 3	4 ± 4	7 ± 5	91 ± 3	4 ± 4	6 ± 4
	15 days	90 ± 4	4 ± 6	7 ± 5	90 ± 5	5 ± 5	6 ± 3
	30 days	89 ± 5	5 ± 5	7 ± 4	91 ± 5	4 ± 5	6 ± 3
	45 days	88 ± 5	4 ± 5	6 ± 4	91 ± 3	4 ± 5	6 ± 4
	60 days	89 ± 5	4 ± 5	6 ± 4	90 ± 4	4 ± 5	6 ± 3
	ANOVA p-value (n = 36)[3]	0.030	0.824	0.879	0.854	0.912	0.985
IF × ST	p-value (n = 180)[4]	< 0.001	< 0.001	< 0.001	< 0.001	< 0.001	< 0.001

[1] Results are reported as mean values of each ice-cream formulation (IF), including results from 0, 15, 30, 45 and 60 days, and mean values of each storage time (ST), considering all IF in each ST.
[2] If $p < 0.05$, the corresponding parameter presented a significantly different value for at least one IF.
[3] If $p < 0.05$, the corresponding parameter presented a significantly different value for at least one ST.
[4] In this table, the interaction among factors was significant in all cases; thereby, no multiple comparisons could be performed.

and ST had a significant influence in all evaluated parameters, thereby indicating that the effect of ST over water, fat, protein, ash, carbohydrates (which in this case corresponds to total soluble sugar content) and energy values varied according to each IF. Regarding the effect of each factor *per se*, it was also significant in most cases, except for protein ($p = 0.219$) along ST and ash ($p = 0.243$) among different IF. Despite not being possible to present the statistical classification, some general tendencies were obtained from the EMM plots. Among different IF, ice-creams incorporating the *B. vulgaris* extract showed the highest contents in water (63 ± 1 g/100 g) and protein (5.8 ± 0.3 g/100 g) and the lowest levels of carbohydrates (18 ± 1 g/100 g), sucrose (16 ± 1 g/100 g) and energy (212 ± 7 kcal/100 g). These results were somehow surprising, since the same batter was used to prepare all ice-cream formulations, and the incorporation of different colouring additives, owing to the low added quantities, should not interfere with nutritional values. Nevertheless, it might be speculated that ice-cream formulations prepared with *B. vulgaris* were not as stable as the remaining ones, since the presented values correspond to the average values obtained in each storage period. In what regards the effect of ST, 15 days and 45 days stored ice-creams presented the highest fat contents (15 ± 1 g/100 g), whilst those stored during 30 days had the lowest energy levels (210 ± 11 kcal/100 g).

In general, the nutritional profile is in agreement with the reported in typical ice-cream formulation (dos Santos Cruxen et al., 2017), except for protein contents that were detected herein, which were higher than commonly reported values (2.5–4.5 g/100 g) in ice-cream (Erkaya et al., 2012; Senaka Ranadheera, Evans, Adams, & Baines, 2013; Silva, Bezerra, Santos, & Correia, 2015). Protein content is important to the textural properties (emulsification, aeration, water retention, and viscosity) (Cheng, Ma, Li, Yan, & Cui, 2015), while carbohydrates, mainly sucrose and lactose, are essential to improve taste and retaining aromas (Karaman et al., 2014).

Table 3
Major fatty acids (relative percentage > 0.5%) of different ice-cream formulations (IF) and storage times (ST). Results are presented as mean ± standard deviation.[1]

		C6:0	C8:0	C10:0	C12:0	C14:0	C14:1	C15:0	C16:0	C16:1	C17:0	C18:0	C18:1n9	C18:2n6	SFA	MUFA	PUFA
IF	CI	3.2 ± 0.4	1.7 ± 0.2	3.3 ± 0.3	3.9 ± 0.2	11.1 ± 0.4	1.0 ± 0.1	1.1 ± 0.1	32 ± 1	1.4 ± 0.1	0.7 ± 0.1	11.9 ± 0.1	25 ± 1	3.1 ± 0.2	69 ± 1	27 ± 1	3.9 ± 0.2
	BSI	3.2 ± 0.3	1.7 ± 0.1	3.4 ± 0.2	4.1 ± 0.2	11.3 ± 0.3	1.0 ± 0.1	1.1 ± 0.1	32 ± 1	1.5 ± 0.1	0.7 ± 0.1	11.8 ± 0.1	24 ± 1	3.1 ± 0.2	70 ± 1	27 ± 1	3.9 ± 0.3
	GGI	3.2 ± 0.2	1.7 ± 0.1	3.3 ± 0.2	4.0 ± 0.3	11.2 ± 0.4	1.0 ± 0.1	1.1 ± 0.1	32 ± 1	1.4 ± 0.1	0.7 ± 0.1	11.9 ± 0.1	24 ± 1	3.1 ± 0.2	70 ± 1	27 ± 1	3.9 ± 0.2
	BVI	3.3 ± 0.4	1.7 ± 0.2	3.3 ± 0.2	4.0 ± 0.2	11.1 ± 0.3	1.0 ± 0.1	1.0 ± 0.1	32 ± 1	1.5 ± 0.1	0.7 ± 0.1	11.8 ± 0.1	24 ± 1	3.1 ± 0.1	69 ± 1	27 ± 1	3.9 ± 0.2
	ANOVA p-value (n = 18)[2]	0.360	0.849	0.217	0.051	0.039	0.084	0.833	0.402	0.003	0.141	0.193	0.002	0.615	0.072	0.073	0.494
ST	0 days	3.3 ± 0.2	1.7 ± 0.1	3.2 ± 0.2	4.0 ± 0.2	11.2 ± 0.3	1.0 ± 0.1	1.1 ± 0.1	32 ± 1	1.5 ± 0.1	0.7 ± 0.1	11.9 ± 0.1	24 ± 1	3.1 ± 0.2	69 ± 1	27 ± 1	3.9 ± 0.2
	15 days	2.9 ± 0.3	1.6 ± 0.1	3.2 ± 0.1	4.0 ± 0.2	11.3 ± 0.4	1.0 ± 0.1	1.0 ± 0.1	33 ± 1	1.4 ± 0.1	0.7 ± 0.1	12.0 ± 0.3	24 ± 1	3.0 ± 0.2	70 ± 1	27 ± 1	3.8 ± 0.2
	30 days	3.4 ± 0.2	1.7 ± 0.1	3.4 ± 0.2	4.0 ± 0.2	11.1 ± 0.2	1.0 ± 0.1	1.0 ± 0.1	32 ± 1	1.4 ± 0.1	0.7 ± 0.1	11.8 ± 0.4	24 ± 1	3.1 ± 0.2	69 ± 1	27 ± 1	3.9 ± 0.2
	45 days	3.3 ± 0.3	1.8 ± 0.2	3.5 ± 0.3	4.2 ± 0.2	11.3 ± 0.4	1.0 ± 0.1	1.1 ± 0.1	32 ± 1	1.4 ± 0.1	0.7 ± 0.1	11.7 ± 0.3	24 ± 1	3.1 ± 0.2	70 ± 1	27 ± 1	3.9 ± 0.3
	60 days	3.3 ± 0.5	1.7 ± 0.2	3.3 ± 0.2	3.9 ± 0.2	10.9 ± 0.4	1.0 ± 0.1	1.1 ± 0.1	32 ± 1	1.5 ± 0.1	0.7 ± 0.1	11.8 ± 0.3	24 ± 1	3.2 ± 0.1	69 ± 1	27 ± 1	4.0 ± 0.2
	ANOVA p-value (n = 36)[3]	< 0.001	< 0.001	< 0.001	< 0.001	< 0.001	0.180	0.107	< 0.001	< 0.001	0.111	0.009	0.271	< 0.001	0.009	0.108	0.177
IF×ST	p-value (n = 72)[4]	< 0.001	< 0.001	< 0.001	< 0.001	0.001	0.307	0.258	0.001	< 0.001	0.135	0.002	< 0.001	< 0.001	< 0.001	< 0.001	< 0.001

[1] Results are reported as mean values of each ice-cream formulation (IF), including results from 0, 15, 30, 45 and 60 days, and mean values of each storage time (ST), considering all IF in each ST.
[2] If p < 0.05, the corresponding parameter presented a significantly different value for at least one IF.
[3] If p < 0.05, the corresponding parameter presented a significantly different value for at least one ST.
[4] If p < 0.05, the interaction among factors is significant; in this case, no multiple comparisons can be performed.
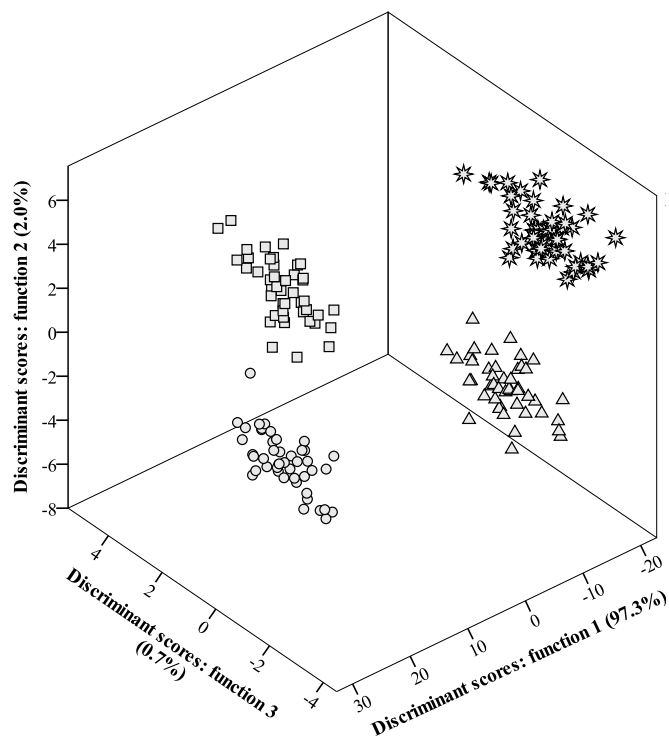
Fig. 1. Spatial distribution of IF markers distributed according to the canonical discriminant functions coefficients defined from results obtained in the laboratorial assays. CI: control ice-cream (○); BSI: ice-cream added with betalain standard (□); GGI: ice-cream with *G. globosa* extract (△); BVI: ice-cream with *B. vulgaris* extract (✳).
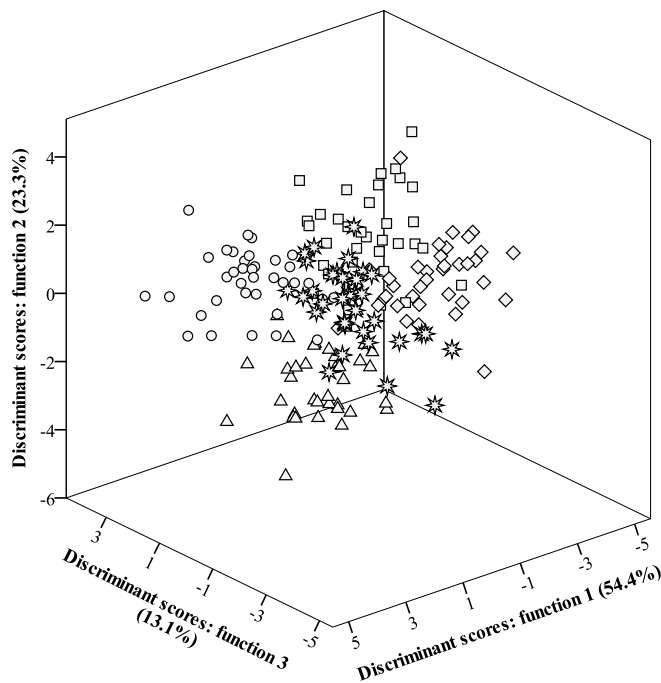
Fig. 2. Spatial distribution of ST markers distributed according to the canonical discriminant functions coefficients defined from results obtained in the laboratorial assays. 0 days: ○; 15 days: □; 30 days: △; 45 days: BVI: ◇; 60 days: ✳.

Table 2 presents the colour parameters measured for different IF and ST. Considering the main purpose of this work, finding an alternative natural colouring agent for ice-cream, the parameters lightness (L^*), redness (a^*) and blueness (b^*) were evaluated in fresh and lyophilized forms of all IF throughout ST (Table 2). In line with the

observed in nutritional composition, the studied factors, IF and ST, had a cooperative ($p < 0.001$) effect over colour parameters. However, the effect of ST was not significant in most cases, except $L*$ value in fresh samples ($p = 0.030$), while differences among different IF (as it might have been anticipated) were significant in all cases. In general, $L*$ and $b*$ presented the highest values in CI samples, fresh and lyophilized, which on the other hand showed the lowest $a*$ values, owing to the absence of any colouring agent. Concerning IF added with colourants, BSI presented higher $L*$ and $b*$ values, while GGI and BVI were characterized as having the highest $a*$ values. The lower values of $L*$ in GGI and BVI might be explained by the fact that both ingredients are natural extracts, therefore potentially presenting some opacity, as these were not purified compounds.

The major fatty acids of different IF and storage times are shown in Table 3. The profiles in fatty acids were influenced by ST, especially in the cases of short-chain fatty acids and unsaturated ones. Nevertheless, and despite their statistical significance, the observed differences correspond only to slight variations in the percentages of each fatty acid, which did not seem to be relevant enough to the overall quality of ice-creams. This hypothesis is corroborated by the effect of IF, which was only significant in the cases of C14:0, C16:1, C18:1 and MUFA. Likewise, the interaction among factors was not significant for C14:1, C15:0 and C17:0; however, since the individual effect of ST and IF was not significant in these cases, the statistical classification could not be presented. The analysis of the EMM plots of each fatty acid did not allow obtaining overall tendencies, except for the generally higher percentages of C12:0 in ice-creams stored for 45 days, C13:0 in non-stored ice-creams and C16:0 in ice-creams stored during 15 days.

In addition to the tabled fatty acids, C11:0, C13:0, C18:3n3, C20:0, C20:3n6 and C20:4n6 were also detected, but in percentages lower than 0.5%. Nevertheless, all quantified fatty acids were included in the linear discriminant analyses discussed in the next section.

Furthermore, the extracts, the commercial standard and the ice-cream samples did not show hepatotoxicity up to the maximal assayed concentration (400 µg/mL) as indicated by the results obtained with the PLP2 cell line (isolated from porcine liver). The quantities of betacyanins were also maintained along ST, as it was validated according to the chromatographic results from HPLC-DAD-ESI/MS, showing their suitability as potentially useful stable colouring agents.

3.1. Linear discriminant analysis

After comparing the evaluated parameters one by one, weighing the significance of changes caused by either IF or ST, a linear discriminant analysis was applied to find the parameters suffering the highest changes in each IF or ST. This was specifically achieved by assessing the linkage between IF or ST (categorical dependent variables) and the matrix of obtained results (quantitative independent variables).

Fig. 1 presents the spatial distribution of IF markers distributed according to the canonical discriminant functions coefficients defined from results obtained in the laboratorial assays. In what concerns the IF effect, the three defined discriminant functions included 100.0% (first function: 97.3%; second function: 2.0%; third function: 0.7%) of the observed variance (Fig. 1). From the 36 analysed variables, the model selected 17: water, protein, sucrose, energy, $L*$(fresh and lyophilized), $a*$(fresh and lyophilized), $b*$(fresh and lyophilized), C6:0, C10:0, C11:0, C13:0, C16:1, C18:1 and C20:4 as those having discriminant effect. As it might be concluded, function 1 included a considerably high percentage of variance, thereby indicating that the variables more correlated with this function (specifically $b*$ in lyophilized samples, $b*$ in fresh samples and $a*$ in fresh samples) were the ones presenting the highest changes within different IF. Accordingly, function 1 separated mostly one group (high $b*$ values) formed by CI and BSI from a second group (high $a*$ values) formed by GGI and BVI. Function 2, on the other hand, was more highly correlated to water, sucrose and protein contents, being effective in separating markers corresponding to BVI. Finally,

function 3, despite the low percentage of explained variance, was useful to separate CI from BSI, mostly due to their differences in $L*$ (fresh and lyophilized), $a*$ (lyophilized) and energy values. The classification performance was 100% accurate, either for original grouped cases, as well as for the cross-validated grouped cases.

The spatial distribution of ST markers scattered according to the canonical discriminant functions coefficients defined from results obtained in the laboratorial assays is presented in Fig. 2. A completely different outcome was obtained when comparing the effect ST of all parameters simultaneously. In fact, the differences observed in each ST (0, 15, 30, 45 and 60 days) were not enough to discriminate their corresponding markers (Fig. 2). Actually, several results were misclassified (*i.e.*, results from a determined storage time were classified as belonging to a different period) by the leave-one-out validation procedure, proving that ST, up to the assayed periods, did not act as a significant source of variability for nutritional and colour parameters, probably due to the low storage temperature ($-22\,^{\circ}$C).

4. Conclusion

Overall, the extracts obtained from *G. globosa* might be a suitable alternative as natural colouring agents for ice-cream, as the obtained results in GGI and BVI were quite similar. Comparing both studied factors, ST and IF had significant effects in most nutritional parameters, while colour parameters were not affected by ST (except for $L*$ in lyophilized samples), contrarily to fatty acids, which were mainly altered by ST, showing only minor changes among different IF. Nevertheless, and as evidenced by LDA outputs, the effects of IF were more pronounced than those induced by ST, since markers were only clustered according to the levels of each factor in the case of IF.

References

Abreu, R. M. V., Ferreira, I. C. F. R., Calhelha, R. C., Lima, R. T., Vasconcelos, M. H., Adega, F., et al. (2011). Anti-hepatocellular carcinoma activity using human HepG2 cells and hepatotoxicity of 6-substituted methyl 3-aminothieno[3,2-b]pyridine-2-carboxylate derivatives: In vitro evaluation, cell cycle analysis and QSAR studies. *European Journal of Medicinal Chemistry, 46*(12), 5800–5806. http://doi.org/10.1016/j.ejmech.2011.09.029.

AOAC (2016). *AOAC Official Methods of Analysis* (20th ed.). AOAC International.

Barros, L., Pereira, E., Calhelha, R. C., Dueñas, M., Carvalho, A. M., Santos-Buelga, C., et al. (2013). Bioactivity and chemical characterization in hydrophilic and lipophilic compounds of Chenopodium ambrosioides L. *Journal of Functional Foods, 5*(4), 1732–1740. http://doi.org/10.1016/j.jff.2013.07.019.

Bridle, P., & Timberlake, C. F. (1997). *Anthocyanins as natural food colours-selected aspects.* 58(1).

Carocho, M., Barreiro, M. F., Morales, P., & Ferreira, I. C. F. R. (2014). Adding molecules to food, pros and cons: A review on synthetic and natural food additives. *Comprehensive Reviews in Food Science and Food Safety*. http://doi.org/10.1111/1541-4337.12065.

Carocho, M., Morales, P., & Ferreira, I. C. F. R. (2015). Natural food additives: Quo vadis? *Trends in Food Science & Technology, 45*(2), 284–295. http://doi.org/10.1016/j.tifs.2015.06.007.

Chaikham, P., & Rattanasena, P. (2017). Combined effects of low-fat ice cream supplemented with probiotics on colon microfloral communities and their metabolites during fermentation in a human gut reactor. *Food Bioscience, 17*, 35–41. http://doi.org/10.1016/j.fbio.2016.12.005.

Cheng, J., Ma, Y., Li, X., Yan, T., & Cui, J. (2015). Effects of milk protein-polysaccharide interactions on the stability of ice cream mix model systems. *Food Hydrocolloids, 45*, 327–336. http://doi.org/10.1016/j.foodhyd.2014.11.027.

Edmonds, L., Wadhwa, S. S., & Wibisono, R. (2013). Producing ice cream using a

substantial amount of juice from kiwifruit with green, gold or red fl esh. *FRIN, 50*(2), 647–656. http://doi.org/10.1016/j.foodres.2011.05.030.

Erkaya, T., Dağdemir, E., & Sengül, M. (2012). Influence of Cape gooseberry (Physalis peruviana L.) addition on the chemical and sensory characteristics and mineral concentrations of ice cream. *Food Research International, 45*(1), 331–335. http://doi.org/10.1016/j.foodres.2011.09.013.

Fernandes, Â., Antonio, A. L., Barreira, J. C. M., Oliveira, M. B. P. P., Martins, A., & Ferreira, I. C. F. R. (2012). Effects of gamma irradiation on physical parameters of Lactarius deliciosus wild edible mushrooms. *Postharvest Biology and Technology, 74*, 79–84. http://doi.org/10.1016/j.postharvbio.2012.06.019.

González, M., Gallego, M., & Valcárcel, M. (2002). Automatic screening method for the rapid and simple discrimination between synthetic and natural colorants in foods. *Analytica Chimica Acta, 464*, 237–247.

Karaman, S., Toker, Ö. S., Yüksel, F., Çam, M., Kayacier, A., & Dogan, M. (2014). Physicochemical, bioactive, and sensory properties of persimmon-based ice cream: Technique for order preference by similarity to ideal solution to determine optimum concentration. *Journal of Dairy Science, 97*(1), 97–110. http://doi.org/10.3168/jds.2013-7111.

Machewad, G., Chatge, P., Chappalwar, V., Jadhav, B., & Chappalwar, A. (2012). Studies on extraction of safflower pigments and its utilization in ice cream. *Journal of Food Processing & Technology, 3*, 172–174.

Martin, F., Oberson, J. M., Meschiari, M., & Munari, C. (2016). Determination of 18 water-soluble artificial dyes by LC-MS in selected matrices. *Food Chemistry, 197*, 1249–1255. http://doi.org/10.1016/j.foodchem.2015.11.067.

Moriano, M. E., & Alamprese, C. (2017). Honey, trehalose and erythritol as sucrose-alternative sweeteners for artisanal ice cream. A pilot study. *LWT - Food Science and Technology, 75*, 329–334. http://doi.org/10.1016/j.lwt.2016.08.057.

Roriz, C. L., Barros, L., Carvalho, A. M., & Ferreira, I. C. F. R. (2014). HPLC-profiles of tocopherols, sugars, and organic acids in three medicinal plants consumed as infusions. *International Journal of Food Science, 2014*(5)http://doi.org/10.1155/2014/241481.

Roriz, C. L., Barros, L., Carvalho, A. M., Santos-Buelga, C., & Ferreira, I. C. F. R. F. R. (2014). Pterospartum tridentatum, Gomphrena globosa and cymbopogon citratus: A phytochemical study focused on antioxidant compounds. *Food Research International, 62*, 684–693. http://doi.org/10.1016/j.foodres.2014.04.036.

Roriz, C. L., Barros, L., Prieto, M. A., Barreiro, M. F., Morales, P., & Ferreira, I. C. F. R. (2017). Modern extraction techniques optimized to extract betacyanins from Gomphrena globosa L. *Industrial Crops and Products, 105*(May), 29–40. http://doi.org/10.1016/j.indcrop.2017.05.008.

Roriz, C. L., Barros, L., Prieto, M. A., Morales, P., & Ferreira, I. C. F. R. (2017). *Floral parts of Gomphrena globosa L. as a novel alternative source of betacyanins: Optimization of the extraction using response surface methodology*, Vol. 229, 223–234. http://doi.org/10.1016/j.foodchem.2017.02.073.

Sanguigni, V., Manco, M., Sorge, R., Gnessi, L., & Francomano, D. (2016). Natural antioxidant ice cream acutely reduces oxidative stress and improves vascular function and physical performance in healthy individuals. *Nutrition (Burbank, Los Angeles County, Calif.), 33*, 1–9. http://doi.org/10.1016/j.nut.2016.07.008.

dos Santos Cruxen, C. E., Hoffmann, J. F., Zandoná, G. P., Fiorentini, Â. M., Rombaldi, C. V., & Chaves, F. C. (2017). Probiotic butiá (Butia odorata) ice cream: Development, characterization, stability of bioactive compounds, and viability of Bifidobacterium lactis during storage. *LWT - Food Science and Technology, 75*, 379–385. http://doi.org/10.1016/j.lwt.2016.09.011.

Senaka Ranadheera, C., Evans, C. A., Adams, M. C., & Baines, S. K. (2013). Production of probiotic ice cream from goat's milk and effect of packaging materials on product quality. *Small Ruminant Research, 112*(1–3), 174–180. http://doi.org/10.1016/j.smallrumres.2012.12.020.

Silva, P. D. L. da, Bezerra, M. de F., Santos, K. M. O. dos, & Correia, R. T. P. (2015). Potentially probiotic ice cream from goat's milk: Characterization and cell viability during processing, storage and simulated gastrointestinal conditions. *LWT - Food Science and Technology, 62*(1), 452–457. http://doi.org/10.1016/j.lwt.2014.02.055.

Soukoulis, C., Lyroni, E., & Tzia, C. (2010). Sensory pro fi ling and hedonic judgement of probiotic ice cream as a function of hydrocolloids, yogurt and milk fat content. *LWT - Food Science and Technology, 43*(9), 1351–1358. http://doi.org/10.1016/j.lwt.2010.05.006.

Soukoulis, C., & Tzia, C. (2018). Grape, raisin and sugarcane molasses as potential partial sucrose substitutes in chocolate ice creat: milk: A feasibility study. *International Dairy Journal, 76*, 18–29. https://doi.org/10.1016/j.idairyj.2017.08.004.

Spórna-kucab, A., & Jagodzi, J. (2017). *Separation of betacyanins from purple flowers of Gomphrena globosa*, Vol. 1489, 51–57. http://doi.org/10.1016/j.chroma.2017.01.064.

Wissgott, U., & Bortlik, K. I. (1996). Prospects for new natural food colorants. *Trends in Food Science & Technology, 7*(9), 298–302. http://doi.org/10.1016/0924-2244(96)20007-X.

Optimization of heat- and ultrasound-assisted extraction of anthocyanins from *Hibiscus sabdariffa* calyces for natural food colorants

José Pinela[a], M.A. Prieto[a,b], Eliana Pereira[a], Inès Jabeur[a], Maria Filomena Barreiro[a,c], Lillian Barros[a], Isabel C.F.R. Ferreira[a,*]

[a] *Centro de Investigação de Montanha (CIMO), Instituto Politécnico de Bragança, Campus de Santa Apolónia, 5300-253 Bragança, Portugal*
[b] *Nutrition and Bromatology Group, Faculty of Food Science and Technology, University of Vigo, Ourense Campus, E32004 Ourense, Spain*
[c] *Laboratory of Separation and Reaction Engineering – Laboratory of Catalysis and Materials (LSRE-LCM), Polytechnic Institute of Bragança, Campus de Santa Apolónia, 5300-253 Bragança, Portugal*

ARTICLE INFO

ABSTRACT

Heat- and ultrasound-assisted extraction methods were applied to recover anthocyanins from *Hibiscus sabdariffa* calyces. The extraction variables, time (t), ethanol proportion (S), and temperature (T) or ultrasonic power (P), were combined in a 5-level experimental design and analysed by response surface methodology for process optimization. The delphinidin-3-*O*-sambubioside ($C1$) and cyanidin-3-*O*-sambubioside ($C2$) levels were monitored by LC-DAD-ESI/MS^n and used as response criteria. The developed models were successfully fitted to the experimental data and used to determine optimal extraction conditions. UAE was the most efficient method yielding 51.76 mg $C1 + C2$/g R under optimal conditions ($t = 26.1$ min, $P = 296.6$ W and $S = 39.1\%$ ethanol, v/v). The dose-response effects of the solid/liquid ratio on the extraction rate were also determined. The anthocyanin levels herein reported are higher than those found in the literature, which support the potential use of *H. sabdariffa* as a sustainable source of natural colorants with application in different industrial sectors.

1. Introduction

The globalization of the industrial food sector, together with consumer's awareness about the existence of bio-based alternatives to the artificial additives, nowadays massively used, and with potential toxic effects in humans, has promoted the demand for food products formulated with natural ingredients recovered from plant materials (Carocho, Morales, & Ferreira, 2015; Martins, Roriz, Morales, Barros, & Ferreira, 2016). The scientific research in this area has gained international prominence (Almeida et al., 2018; Carocho et al., 2016; Pinela et al., 2017), as it is still necessary to expand the range of natural options and find new sources (e.g., plants, algae and insects), as well as to develop sustainable processes for an efficient recovery of the target compounds (e.g., anthocyanins, carotenoids, and beet derivatives).

The global food colouring market has grown rapidly in recent years and it is expected to continue growing by 10% to 15% annually (Carle & Schweiggert, 2016). The colour, in addition to be an important food sensory attribute, often related to flavour, safety and overall quality, also greatly influences product's marketing success. At the same time, there is a growing interest in replacing the artificially obtained colorants by natural counterparts, since the former have been associated

with adverse health effects, including hyperkinesis, skin rashes, tumours, kidney damage and migraine, among others (Ramesh & Muthuraman, 2018). Natural colorants can also provide an extensive range of colours, with the advantage of being innocuous and can provide beneficial health effects (Castañeda-Ovando, Pacheco-Hernández, Páez-Hernández, Rodríguez, & Galán-Vidal, 2009). However, the high stability and low cost of the synthetic food colorants have limited the use of the natural counterparts by the industrial sector (Carocho et al., 2015). Moreover, there are only few natural alternatives approved by federal authorities (Martins et al., 2016).

Plants are an interesting source of natural pigments endowed with colouring potential and bioactivities (Jabeur et al., 2017). Among them, *Hibiscus sabdariffa* L. (Fam. Malvaceae), also known as roselle, is an annual medicinal shrub relatively easy to grow and used worldwide by the food and pharmaceutical industries (Da-Costa-Rocha, Bonnlaender, Sievers, Pischel, & Heinrich, 2014). It comprises two main varieties, the *altissima* Wester, cultivated for the jute-like fibre, and the *sabdariffa*, generally pigmented and cultivated for the edible calyces used in the preparation of herbal teas and beverages, and a number of pastry products (Sharma et al., 2016). In folk medicine, *H. sabdariffa* calyx infusions are used for their diuretic, febrifugal and hypotensive effects,

---

and for helping to lower body temperature; while other preparations are used for treating sore throats and coughs, liver, cardiac and nerve diseases, and genital problems (Da-Costa-Rocha et al., 2014). Some of these traditional uses have been validated by scientific studies, which have shown that calyx extracts have strong antioxidant and anti-hypertensive capacities, together with antihypercholesterolaemic, antinociceptive, and antipyretic effects, among others (Ali, Al Wabel, & Blunden, 2005; Da-Costa-Rocha et al., 2014). Therefore, this plant has high potential to be used in the development of new functional and therapeutic products.

Most of the phytochemical studies on the *H. sabdariffa* constituents have been directed towards the characterization of pigments, namely anthocyanins (Ali et al., 2005; Beye, Hiligsmann, Tounkara, & Thonart, 2017; Jabeur et al., 2017). Delphinidin-3-glucoside, cyanidin-3-gluco-side, and in particular delphinidin-3-sambubioside (hibiscin) and cya-nidin-3-sambubioside (gossypicyanin) have been identified in calyx extracts (Alarcón-Alonso et al., 2012; Beye et al., 2017; Salazar-González, Vergara-Balderas, Ortega-Regules, & Guerrero-Beltrán, 2012). These anthocyanins are responsible for the characteristic red colour of the *H. sabdariffa* calyces and can be recovered for subsequent use as colorants in different industrial sectors.

In order to turn bio-based colorants into real and efficient alternatives to the widely used artificial analogues, it is necessary to find promising sources for their extraction and develop sustainable recovery processes. Today, several technologies are available to enhance extraction, including ultrasounds (López et al., 2018), microwaves (Liazid, Guerrero, Cantos, Palma, & Barroso, 2011), pulsed electric fields, and pressurized and supercritical fluids (Corrales, Toepfl, Butz, Knorr, & Tauscher, 2008; Garcia-Mendoza et al., 2017). Among them, ultrasound-assisted extraction (UAE) brings significant benefits over conventional heating methods in terms of time and solvent consumption and extraction yield (Chemat et al., 2017a; Marić et al., 2018). This "green" processing technique also reduces energy and water consumption, allows recycling of by-products through bio-refining, and ensures a safe and high quality product (Chemat et al., 2017a). In addition, UAE has been recognised as suitable for industrial applications (Vilkhu, Mawson, Simons, & Bates, 2008). However, the efficiency of these processes is affected by process variables (e.g., time, temperature, ultrasonic power and solvent). Therefore, it is necessary to use appropriate experimental designs and optimization tools to determine the optimal extraction conditions leading to the best responses in terms of recovering of target compounds.

This study was performed aiming at optimizing the recovery of the two major anthocyanins found in *H. sabdariffa* calyces by heat- and ultrasound-assisted extraction processes to serve as natural colorants (a workflow scheme is presented in Fig. A1). The three most relevant independent variables for each process were combined in a circumscribed central composite design, and response surface methodology (RSM) was used for process optimization. It is thus intended to identify which method and extraction conditions are the most suitable to extract these colouring compounds.

2. Material and methods

2.1. Plant material

Dried flowers of *H. sabdariffa* were supplied by a local company (Pragmático Aroma Lda, Alfândega da Fé, Bragança, Portugal) that produces medicinal and aromatic plants with organic certification. According to the producers, the plant material was dehydrated in a drying chamber with controlled conditions of temperature, relative humidity and air velocity, in order to ensure the quality of the final product. The red flower calyx consisting of 5 large sepals with a collar (epicalyx) of 8 to 12 slim, pointed bracts (or bracteoles) around the base was handpicked and reduced to a fine powder (~20 mesh). The powdered samples were kept at -80 °C until further use.

2.2. Extraction methods

2.2.1. Heat-assisted extraction

The heat-assisted extraction (HAE) was performed in a thermostated water bath using sealed vessels to avoid solvent evaporation. The dry powder samples (0.6 g) were mixed with 20 mL of solvent (ethanol:water mixtures) and processed under continuous electromagnetic stirring according to the experimental design presented in Table A1. The extraction time (t, 55–150 min), temperature (T, 20–90 °C) and ethanol proportion (S, 0–100%) were the considered independent variables. The solid/liquid ratio (S/L) was kept constant (30 g/L). After extraction, the mixture was centrifuged (6000 rpm for 10 min at room temperature) and the supernatant filtered through Whatman filter paper No. 4.

2.2.2. Ultrasound-assisted extraction

The ultrasound-assisted extraction (UAE) was performed using an ultrasonic equipment (QSonica sonicators, model CL-334, Newtown, CT, USA). The dry powder samples (1.5 g) were placed in a beaker with 50 mL of solvent (ethanol: water mixtures) and processed according to the experimental design presented in Table A1. The extraction time (t, 3–36.5 min), ultrasonic power (P, 100–500 W; at a frequency of 20 kHz) and ethanol proportion (S 0–100%) were the considered independent variables. The solid/liquid ratio (S/L, 30 g/L) and the temperature (30–35 °C) were kept constant during extraction. Then, the mixtures were centrifuged (6000 rpm for 10 min at room temperature) and the supernatant was filtered through Whatman filter paper No. 4.

A probe system was used for extraction because it delivers the ultrasonic intensity on a small surface compared to an ultrasonic bath, thus being more powerful and widely used for sonication of small volumes of sample (Chemat et al., 2017a; Sicaire et al., 2016). The probe was immersed directly into the reaction beaker (containing the solvent and the sample) so that less attenuation could happen. A special care was taken because of the fast rise of the temperature in the reaction system.

2.3. Determination of extraction yield

The residue or extract weight resulting from each extraction was determined gravimetrically using crucibles, subjected firstly to a partial evaporation of the water at 60 °C and then to heat treatment at 100 °C for 24 h. The results were expressed in percentage (%, w/w).

2.4. Chromatographic analysis of anthocyanins

Each obtained solution was subjected to solvent evaporation at 35 °C and the obtained residue redissolved in water and filtered through a 0.22-m disposable LC filter disk. The chromatographic analysis was performed in a Dionex Ultimate 3000 UPLC system (Thermo Scientific, San Jose, CA, USA) equipped with a diode array detector coupled with an electrospray ionization mass detector (LC-DAD-ESI/MSⁿ), as previously described by Jabeur et al. (2017). Detection was carried out with a DAD (520 nm as the preferred wavelength) and a MS (Linear Ion Trap LTQ XL mass spectrometer, Thermo Finnigan, San Jose, CA, USA) equipped with an ESI source, working in positive mode. The anthocyanins were characterized according to their UV–Vis and mass spectra, and quantification was performed through a calibration curve performed using cyanidin-3-glucoside standard ($y = 243287x - 1E6$; $R^2 = 0.995$). The results were expressed as mg/g of plant material (P) or residue (R).

2.5. Extraction optimization by response surface methodology

2.5.1. Experimental design

A five-level circumscribed central composite design (CCCD) with three independent variables [X_1 (t, min), X_2 (T, °C or P, W) and X_3 (S,

%)] was applied to optimize the extraction of anthocyanins from *H. sabdariffa* calyces by HAE and UAE. The *CCCD* included 14 independent combinations and 6 replicates at the centre of the experimental design, chosen to maximize the predictive capacity of the models. In addition, the experimental points were generated on a sphere around the centre point to ensure that the variation of the model prediction is constant for all points equidistant from the centre. The experimental runs were randomized to minimize the effect of unexpected variability in the observed responses.

2.5.2. Response criteria used to understand the extraction behaviour

The extraction yield and levels of delphinidin-3-*O*-sambubioside (*C*1) and cyanidin-3-*O*-sambubioside (*C*2), as well as the total amount resulting from the sum of both compounds (*CT*), were the four response variables considered for the RSM optimization. In addition, the anthocyanin content was expressed using the Y_1 (mg/g P dw) and Y_2 (mg/g R) response formats in order to determine the concentration present in the dried plant material and in the obtained residue or extract, respectively.

2.5.3. Mathematical model

The response surface models were fitted by means of least squares calculation using the following second-order polynomial equation:

$$Y = b_0 + \sum_{i=1}^{n} b_i X_i + \sum_{\substack{i=1 \\ j>1}}^{n=1} \sum_{j=2}^{n} b_{ij} X_i X_j + \sum_{i=1}^{n} b_{ii} X_i^2$$

(1)

where *Y* is the dependent (response) variable to be modelled, X_i and X_j define the independent variables, b_0 is the constant coefficient, b_i the coefficient of the linear effect, b_{ij} the coefficient of the interaction effect, b_{ii} the coefficient of the quadratic effect, and *n* is the number of variables.

2.5.4. Procedure to optimize the variables to a maximum response

The maximization of the model-produced responses was achieved using a simple method tool to solve non-linear problems (Heleno et al., 2016; Pinela et al., 2016). Limitations were made to the variable coded values to avoid unnatural conditions (i.e., time < 0).

2.6. Dose-response analysis of the solid/liquid ratio effect

After optimizing the experimental conditions for the variables X_1, X_2 and X_3, the solid/liquid ratio (*S/L*, g/L) was included as the fourth variable (X_4) to be optimized in order to design more productive and sustainable processes, as demanded by the industrial sector. The response effects as function of the *S/L* variation showed linear trends and were depicted using a general linear equation with intercept ($Y = b + m \cdot S/L$), where *Y* is the used response criteria (i.e. if Y_1 the units would be mg/g P dw) and *b* and *m* are the parameters (intercept and slope, respectively). The rate of the process parameter (*m*, if assessing the Y_1 response criterion the units would be mg/g P per g/L) provides information related to the extraction as function of *S/L* increase. Positive values will indicate an increase in the extraction responses, whereas negative values will designate a decrease in the extraction efficiency, as the *S/L* increase.

2.7. Fitting procedures and statistical analysis

The statistical analysis of the experimental results and models fitting was performed in three steps, using a Microsoft Excel spreadsheet, as follows:

(1) The measurement of the coefficients was achieved using the non-linear least-square (quasi-Newton) method provided by the macro "*Solver*" (Kemmer & Keller, 2010), by minimization of the sum of

the quadratic differences between the observed and model-predicted values.

(2) The significance of the coefficients was obtained *via "SolverAid"* macro (de Levie, 2012) to determine the parametric confidence intervals. The terms that were not statistically significant (*p*-value > 0.05) were excluded to simplify the model.

(3) The model reliability was confirmed by applying the following criteria: (a) the Fisher *F*-test ($\alpha = 0.05$) was used to determine the consistency of the constructed models to describe the obtained data (Shi & Tsai, 2002); (b) the "*SolverStat*" macro was used to make an assessment of the parameter and model prediction uncertainties (Comuzzi, Polese, Melchior, Portanova, & Tolazzi, 2003); (c) R^2 was determined to explain the variability proportion of the dependent variable obtained by the model.

3. Results and discussion

3.1. Experimental data for RSM optimization

Although some previous studies on the extraction of anthocyanins from *H. sabdariffa* calyces can be found in literature, no reports detailing the optimal conditions maximizing their extraction are presently available. In addition, the compositional diversity of anthocyanins' natural sources (e.g., fruits, flowers, leaves, stems and roots) does not allow to directly extrapolate the extraction conditions of these pigments from previously studied sources. Therefore, it is important to conduct independent studies to maximize the extraction of anthocyanins from *H. sabdariffa*, by selecting the relevant variables for each selected extraction method. Table 1 provides a bibliographical summary of the delphinidin-3-*O*-sambubioside, cyanidin-3-*O*-sambubioside and total anthocyanin levels in *H. sabdariffa* and other major plant sources, as well as the conditions used for their extraction. Although important conclusions can be derived from this summary, the results may be highly dependent on dissimilarities not foreseen in these studies, where certain variables remaining constant, together with raw-material's variability, can definitely influence the extraction process. Therefore, the first approach to optimize the efficiency of the HAE and UAE processes to recover anthocyanins from *H. sabdariffa* calyces consisted of the application of RSM coupled to a CCCD design with five levels of variation for the three independent variables as follows: *t* (30–150 min), *T* (30–90 °C) and *S* (0–100%) for HAE and *t* (3–45 min), *P* (100–500 W) and *S* (0–100%) for UAE. A detailed description of the coded and natural values of the selected variables for each extraction method in the CCCD design is presented in Table A1. The different steps carried out in this optimization study are illustrated in Fig. A1.

According to previous studies, high *P* can cause major alterations in plant materials by inducing greater shear forces, which result from the oscillation and collapse of cavitation bubble within the solvent. As a consequence, critical temperature and pressure are generated, inducing the formation of free radicals that can attack target metabolites and lead to their degradation (Chemat et al., 2017; Meullemiestre, Breil, Abert-Vian, & Chemat, 2016). However, this independent variable was optimized in order to apply the minimum power required to achieve the best results.

The experimental values obtained under the 20 runs of the five-level CCCD design applied to the HAE and UAE processes used in the recovery of anthocyanins from *H. sabdariffa* calyces are presented in Table 2. The different response criteria used (*yield*, Y_1 and Y_2) are of interest for industrial sectors dealing with the recovering of high added-value compounds from plant materials to be used as natural colorants, or other bio-based ingredients, providing information concerning the amount of plant material needed to obtain a certain quantity of the target compounds, and the concentration of these compounds in the produced extracts.

The extraction yield ranged from 34.45 to 62.80% and 14.38–56.21% for HAE and UAE, respectively (Table 2). In both cases,

Table 1
Bibliographical summary of the delphinidin-3-O-sambubioside, cyanidin-3-O-sambubioside and total anthocyanin levels in *H. sabdariffa* and other major plant species, and conditions used in their extraction.

Plant material	Extraction conditions					Solvent	Acidification	Content		Reference
Species and common name	Used part	T (°C)	P (W)	t (min)	S/L (g/L)	Solvent type and proportion (v/v)		(mg/g)		
Delphinidin-3-O-sambubioside										
Hibiscus sabdariffa L. (roselle)	Calyx	~25	–	120	100	Water	–	0.55 ± 0.07	R	Salazar-González et al. (2012)
Hibiscus sabdariffa L. (roselle)	Calyx	100	–	5	5	Water	–	7.0 ± 0.2	R	Jabeur et al. (2017)
Hibiscus sabdariffa L. (roselle)	Calyx	100	–	10	10	Water	–	4.11 ± 1.47	R	Sindi et al. (2014)
Hibiscus sabdariffa L. (roselle)	Calyx	100	–	10	10	Water	1% formic acid	3.68 ± 0.34	R	Sindi et al. (2014)
Hibiscus sabdariffa L. (roselle)	Calyx	~25	–	120	100	Ethanol/water (50:50)	–	1.33 ± 0.21	R	Salazar-González et al. (2012)
Hibiscus sabdariffa L. (roselle)	Calyx	~25	–	120	100	Ethanol/water (70:30)	–	0.80 ± 0.14	R	Salazar-González et al. (2012)
Hibiscus sabdariffa L. (roselle)	Calyx	25	–	60 × 2	33.3	Ethanol/water (80:20)	–	7.03 ± 0.04	R	Jabeur et al. (2017)
Hibiscus sabdariffa L. (roselle)	Calyx	~25	–	120	100	Ethanol/water (96:4)	–	0.17 ± 0.02	R	Salazar-González et al. (2012)
Hibiscus sabdariffa L. (roselle)	Calyx	~25	–	120	100	Ethanol/acidified water (85:15)	1.5 N HCl	0.50 ± 0.10	R	Salazar-González et al. (2012)
Hibiscus sabdariffa L. (roselle)	Calyx	64,7	–	10	10	Methanol	–	2.26 ± 0.07	R	Sindi et al. (2014)
Hibiscus sabdariffa L. (roselle)	Calyx	64,7	–	10	10	Methanol	1% formic acid	2.41 ± 0.09	R	Sindi et al. (2014)
Hibiscus sabdariffa L. (roselle)	Calyx	50	–	30 × 3	20	Water	–	16.1–21.2	P dw	Ifie et al. (2018)
Hibiscus sabdariffa L. (roselle)	Calyx	~25	–	60 + 60 × 5	83.3	Acetone + acetone/acidified water (70:30)	4% formic acid	3.54–9.19	P dw	Beye et al. (2017)
Vaccinium myrtillus L. (bilberry)	Fruit	–	–	–	–	Methanol	0.5% HCl	0.26	R	Du, Jerz, and Winterhalter (2004)
Aristotelia chilensis L. (maqui)	Fruit	~25	?	60 × 2	100	Methanol/water (70:30)	1% formic acid	0.19–0.73	P dw	Gironés-Vilaplana et al. (2014)
Cyanidin-3-O-sambubioside										
Hibiscus sabdariffa L. (roselle)	Calyx	~25	–	120	100	Water	–	0.31 ± 0.04	R	Salazar-González et al. (2012)
Hibiscus sabdariffa L. (roselle)	Calyx	100	–	5	5	Water	–	4.08 ± 0.07	R	Jabeur et al. (2017)
Hibiscus sabdariffa L. (roselle)	Calyx	100	–	10	10	Water	–	3.81 ± 1.21	R	Sindi et al. (2014)
Hibiscus sabdariffa L. (roselle)	Calyx	100	–	10	10	Water	1% formic acid	2.98 ± 0.21	R	Sindi et al. (2014)
Hibiscus sabdariffa L. (roselle)	Calyx	~25	–	120	100	Ethanol/water (50:50)	–	0.75 ± 0.09	R	Salazar-González et al. (2012)
Hibiscus sabdariffa L. (roselle)	Calyx	~25	–	120	100	Ethanol/water (70:30)	–	0.45 ± 0.09	R	Salazar-González et al. (2012)
Hibiscus sabdariffa L. (roselle)	Calyx	25	–	60 × 2	33.3	Ethanol/water (80:20)	–	4.40 ± 0.02	R	Jabeur et al. (2017)
Hibiscus sabdariffa L. (roselle)	Calyx	~25	–	120	100	Ethanol/water (96:4)	–	0.11 ± 0.01	R	Salazar-González et al. (2012)
Hibiscus sabdariffa L. (roselle)	Calyx	~25	–	120	100	Ethanol/acidified water (85:15)	1.5 N HCl	0.27 ± 0.06	R	Salazar-González et al. (2012)
Hibiscus sabdariffa L. (roselle)	Calyx	64,7	–	10	10	Methanol	–	1.96 ± 0.03	R	Sindi et al. (2014)
Hibiscus sabdariffa L. (roselle)	Calyx	64,7	–	10	10	Methanol	1% formic acid	2.10 ± 0.02	R	Sindi et al. (2014)
Hibiscus sabdariffa L. (roselle)	Calyx	50	–	30 × 3	20	Water	–	3.06–5.17	P dw	Ifie et al. (2018)
Hibiscus sabdariffa L. (roselle)	Calyx	~25	–	60 + 60 × 5	83.3	Acetone + acetone/acidified water (70:30)	4% formic acid	2.52–4.72	P dw	Beye et al. (2017)
Vaccinium myrtillus L. (bilberry)	Fruit	–	*	–	–	Methanol	0.5% HCl	0.15	R	Du et al. (2004)
Aristotelia chilensis L. (maqui)	Fruit	~25	*	60 × 2	100	Methanol/water (70:30)	1% formic acid	0.23–0.82	P dw	Gironés-Vilaplana et al. (2014)
Ribes rubrum L. (red currant)	Fruit	–	–	? × 10	14	Methanol	1% HCl	0.43–0.60	P dw[1]	Yang, Zheng, Laaksonen, Tahvonen, and Kallio (2013)
Vigna unguiculata ssp. *sesquipedalis* L. (yard-long bean)	Purple pod	4	–	2880	50	Methanol/water (40:60)	0.1% HCl	0.16	P dw	Tae et al. (2010)
Total anthocyanin content										
Hibiscus sabdariffa L. (roselle)	Calyx	100	–	5	5	Water	–	12.3 ± 0.3	R	Jabeur et al. (2017)
Hibiscus sabdariffa L. (roselle)	Calyx	100	–	10	10	Water	–	8.53	R	Sindi et al. (2014)
Hibiscus sabdariffa L. (roselle)	Calyx	100	–	10	10	Water	1% formic acid	7.36	R	Sindi et al. (2014)
Hibiscus sabdariffa L. (roselle)	Calyx	25	–	60 × 2	33.3	Ethanol/water (80:20)	–	12.9 ± 0.1	R	Jabeur et al. (2017)
Hibiscus sabdariffa L. (roselle)	Calyx	64,7	–	10	10	Methanol	–	4.88	R	Sindi et al. (2014)
Hibiscus sabdariffa L. (roselle)	Calyx	64,7	–	10	10	Methanol	1% formic acid	5.14	R	Sindi et al. (2014)
Hibiscus sabdariffa L. (roselle)	Petals	35	–	120 × 2	2.5	Methanol	0.1% HCl	33.92 ± 3.16	R	Zhang et al. (2014)
Hibiscus sabdariffa L. (roselle)	Calyx	50	–	30 × 3	20	Water	–	19.57–27.10	P dw	Ifie et al. (2018)
Hibiscus sabdariffa L. (roselle)	Calyx	~25	–	60 + 60 × 5	83.3	Acetone + acetone/acidified water (70:30)	4% formic acid	6.88–15.29	P dw	Beye et al. (2017)
Arbutus unedo L. (strawberry tree)	Fruit	< 35	215.1	21.8	50	Ethanol/water (64.3:35.7)	0.05% HCl	0.49 ± 0.03	R	López et al. (2018)
Aristotelia chilensis L. (maqui)	Fruit	~25	*	60 × 2	100	Methanol/water (70:30)	1% formic acid	6.14–9.84	P dw	Gironés-Vilaplana et al. (2014)

Table 1 (*continued*)

Plant material	Extraction conditions					Solvent		Content	Reference
Species and common name	Used part	T (°C)	P (W)	t (min)	S/L (g/L)	Solvent type and proportion (v/v)	Acidification	(mg/g)	
Ipomoea batatas L. (purple sweet potato)	Tuber	60	–	90	100	Ethanol/water (80:20)	0.1% HCl	2.18 ± 0.03 P dw	Cai et al. (2016)
Ipomoea batatas L. (purple sweet potato)	Tuber	50	200	45	100	Ethanol/water (90:10)	0.1% HCl	2.29 ± 0.05 P dw	Cai et al. (2016)
Prunus avium L. (sweet cherry)	Fruit	37		90	100	Methanol or ethanol	0.1% 12 N HCl	2.49 ± 0.04 P fw	Blackhall et al. (2018)
Vigna unguiculata ssp. *sesquipedalis* L. (yard-long bean)	Purple pod	4	–	2880	50	Methanol/water (40:60)	0.1% HCl	8.81 P dw	Tae et al. (2010)

P: Plant material; R: residue or extract; dw: dry weight; fw: fresh weight.

[1] Converted from a fresh weight value.

* Samples sonicated in an ultrasonic bath (power not indicated).

the higher values were achieved with the run 12, which combined the following conditions: $t = 90$ min, $T = 90$ °C and $S = 50\%$ for HAE, and $t = 24$ min, $T = 500$ W and $S = 50\%$ for UAE. In general, HAE originated the highest experimental yields, translated in higher amounts of residue or crude extract. A lower yield (28.3%) was obtained by Alarcón-Alonso et al. (2012) when using water at 55 °C with 2 h of extraction.

As described by other authors (Ifie, Ifie, Ibitoye, Marshall, & Williamson, 2018; Jabeur et al., 2017; Sindi, Marshall, & Morgan, 2014), $C1$ predominated over $C2$ in all cases (Table 2), with levels ranging from 1,02–6.88 mg/g P and 0.43–2.11 mg/g P for HAE and from 1.26 to 14.31 mg/g P and 0.92–7.29 mg/g P for UAE, respectively. The highest total content (CT) was achieved with the runs 13 (8.99 mg/g P) and 10 (21.48 mg/g P) of the HAE and UAE processes, respectively. Beye et al. (2017) recovered up to 9.19 mg $C1$/g P and 4.72 mg $C2$/g P from dried calyces of *H. sabdariffa* cultivars grown in Senegal, when subjected to a 60-min extraction with acetone followed by five more 60-min extraction cycles with acetone/acidified water (70:30, v/v; 4% formic acid). Higher levels of $C1$ (up to 21.2 mg/g P), but lower of $C2$ (up to 5.17 mg/g P) were obtained by Ifie et al. (2018) in dried calyces of a dark red variety of *H. sabdariffa* cultivated in Ibadan, South-Western Nigeria, in comparison with the quantities found in our samples harvested in north-eastern Portugal. These contents were obtained by three successive aqueous extractions of 30-min duration at 50 °C.

The CT content in the obtained residue ranged from 3.41 to 12.44 mg/g R and 14.39–47.93 mg/g R for HAE and UAE, respectively (Table 2). In general, these levels are higher than those found in the literature (Table 1). Salazar-González et al. (2012) obtained up to 2.08 mg CT/g P (1.33 mg $C1$/g and 0.75 mg $C2$/g) when performing a 120-min extraction with ethanol:water mixtures (50:50, v/v) at a S/L of 100 g/L and room temperature. Up to 7.92 mg CT/g R (4.11 mg $C1$/g and 3.81 mg $C2$/g) were achieved by Sindi et al. (2014) with aqueous extractions of 10 min at 100 °C. In another study, Jabeur et al. (2017) quantified 11.08 mg/g R (7.0 mg $C1$ + 4.08 mg C_2) in extracts obtained by addition of boiling water (at 100 °C) to the samples and subsequent maceration for 5 min at room temperature (process known as infusion).

3.2. Theoretical response surface models

The parametric values obtained by fitting the response values (Table 2) to the second-order polynomial model of Eq. (1) using a nonlinear algorithm are presented in Table A2 (Eqs. (2)–(15)). These values translate the response patterns and are useful for developing mathematical models (Table A3), which indicate the complexity of the possible scenarios. However, not all Eq. (1) parameters were used in the development of the models since some coefficients were non-significant (*ns*); the significant ones were assessed at a 95% confidence level ($\alpha = 0.05$). The statistic lack-of-fit, used to test the adequacy of the obtained models, revealed that no considerable improvement was achieved by the inclusion of the statistically *ns* parametric values. The agreement between the experimental and predicted values provided an acceptable explanation of the obtained results (Table 2). Additionally, residues were randomly scattered around zero and no grouped data or auto-correlations were observed. The obtained coefficients of determination (R^2) were higher than 0.94 and 0.86 in the cases of HAE and UAE, respectively (Table A2), which indicates that the variability of each response can be explained by the independent variables involved in the process. Therefore, the models proved to be applicable and were used in the later prediction and optimization steps. Although the obtained model coefficients are empirical and cannot be associated with physical or chemical significance, they are useful to predict the outcome of untested experimental conditions (Ranic et al., 2014). Moreover, the sign of the parametric values determines part of the response; for positive effects, the response is higher at the high level, and when a factor has a negative effect, the response is lower at the high level. The higher of the parametric value, the more significant the weight of the

Table 2

Experimental CCCD design and results for the HAE and UAE processes used in the extraction of delphinidin-3-O-sambubioside ($C1$), cyanidin-3-O-sambubioside (C_2), and total anthocyanins (C_T) from *H. sabdariffa* calyces. The extraction yield is given as percentage (%) and the anthocyanin content is expressed as mg/g of plant material (Y_1, mg/g P dw) and mg/g of residue (Y_2, mg/g R). The independent variables, natural values and ranges are presented in Table A1.

| | Experimental design | | | | | | | | | Heat-assisted extraction (HAE) | | | | | | | Ultrasound-assisted extraction (UAE) | | | | | | |
| | Coded values | | | HAE | | | UAE | | | Residue | Individual anthocyanins | | | | Total anthocyanins | | Residue | Individual anthocyanins | | | | Total anthocyanins | |
	X_1	X_2	X_3	X_1: t min	X_2: T °C	X_3: S %	X_1: t min	X_2: P W	X_3: S %	Yield	Y_1C_1	Y_1C_2	Y_2C_1	Y_2C_2	Y_1C_T	Y_2C_T	Yield	Y_1C_1	Y_1C_2	Y_2C_1	Y_2C_2	Y_1C_T	Y_2C_T
1	−1	−1	−1	54.3	42.2	20.3	11.5	181.1	20.3	51.85	5.01	1.67	9.67	3.22	6.68	12.89	18.78	5.16	2.59	27.45	15.54	7.75	42.99
2	1	−1	−1	125.7	42.2	20.3	36.5	181.1	20.3	55.67	4.72	1.86	8.47	3.34	6.58	11.82	35.24	9.14	3.08	25.94	9.84	12.22	35.78
3	−1	1	−1	54.3	77.9	20.3	11.5	418.9	20.3	53.80	4.28	1.86	7.96	3.46	6.14	11.42	27.16	3.18	3.90	11.71	16.17	7.08	27.88
4	1	1	−1	125.7	77.9	20.3	36.5	418.9	20.3	59.73	4.37	1.79	7.32	3.00	6.16	10.32	49.27	12.51	5.79	25.39	13.23	18.30	38.62
5	−1	−1	1	54.3	42.2	79.8	11.5	181.1	79.7	42.92	1.66	0.66	3.88	1.54	2.33	5.42	16.35	3.75	0.97	22.93	6.67	4.72	29.60
6	1	−1	1	125.7	42.2	79.8	36.5	181.1	79.7	43.44	1.70	0.61	3.92	1.39	2.31	5.32	39.00	5.26	3.00	13.49	8.67	8.26	22.16
7	−1	1	1	54.3	77.9	79.8	11.5	418.9	79.7	51.55	1.50	0.57	2.92	1.11	2.08	4.03	14.38	1.26	0.92	8.78	7.16	2.18	15.94
8	1	1	1	125.7	77.9	79.8	36.5	418.9	79.7	50.12	1.51	0.51	3.02	1.02	2.03	4.04	51.24	9.06	5.01	17.68	11.01	14.07	28.68
9	−1.68	0	0	30	60	50	3	300	50	46.29	1.10	0.84	2.37	1.82	1.94	4.19	23.28	6.62	2.04	28.45	9.88	8.67	38.33
10	1.68	0	0	150	60	50	45	300	50	49.00	1.10	0.78	2.26	1.59	1.88	3.84	55.38	14.31	7.17	25.84	14.58	21.48	40.41
11	0	−1.68	0	90	30	50	24	100	50	55.82	1.54	1.03	2.76	1.85	2.57	4.61	15.71	3.06	1.52	19.48	10.88	4.58	30.36
12	0	1.68	0	90	90	50	24	500	50	62.80	1.21	0.93	1.93	1.48	2.14	3.41	56.21	12.73	4.80	22.65	9.62	17.53	32.26
13	0	0	−1.68	90	60	0	24	300	0	55.30	6.88	2.11	12.44	3.82	8.99	16.26	30.03	7.26	2.61	24.17	9.77	9.86	33.94
14	0	0	1.68	90	60	100	24	300	100	34.45	1.31	0.43	3.82	1.26	1.75	5.07	32.69	3.21	1.33	9.82	4.57	4.54	14.39
15	0	0	0	90	60	50	24	300	50	55.22	1.06	0.91	1.92	1.64	1.97	3.56	37.23	10.06	6.68	27.02	20.19	16.74	47.21
16	0	0	0	90	60	50	24	300	50	55.37	1.02	0.96	1.84	1.73	1.98	3.57	37.36	10.28	6.54	27.51	19.71	16.82	47.22
17	0	0	0	90	60	50	24	300	50	57.32	1.34	0.96	2.33	1.68	2.30	4.01	37.49	10.14	6.76	27.06	20.30	16.90	47.35
18	0	0	0	90	60	50	24	300	50	56.72	1.23	0.89	2.16	1.58	2.12	3.74	38.51	10.25	7.29	26.61	21.32	17.54	47.93
19	0	0	0	90	60	50	24	300	50	51.10	1.21	0.91	2.36	1.79	2.12	4.15	38.08	10.35	6.92	27.19	20.44	17.27	47.63
20	0	0	0	90	60	50	24	300	50	56.12	1.25	0.92	2.23	1.63	2.17	3.86	37.90	10.49	6.68	27.66	19.83	17.16	47.49

governing variable is.

Certain features regarding the overall effects of the independent variables were inferred from the complexity of the parametric values, i.e. the variables were ordered in a decreasing form as a function of its significance in the extraction processes as follows: $S >> T > t$ for HAE; $S > P > t$ for the Y_2 response formats of UAE; and $t > P > S$ for the extraction yield of UAE. It was also possible to observe that all the evaluated responses were significantly affected by linear and quadratic effects, whose values were particularly higher for the variable S (with some exceptions, since, although the linear effects of the variable t were negligible in most cases in the HAE process, the corresponding values for the Y_1 response formats and extraction yield in the UAE process were quite high). The parametric values also revealed that strong interactions occurred in the UAE process, mainly between the variables $t \times P$. In turn, the interactions $t \times T$ and $P \times S$ were of minor relevance in the HAE and UAE processes, respectively. These results justify the use of RSM as an optimization tool, since one-variable-at-a-time approaches do not allow to assess the existence of interactive effects, which makes it difficult to determine optimum values.

To make all these combined effects more explicit and to visually describe the extraction trends, the results were presented in the response surface graphs discussed below.

3.3. Response surface analysis: Efficiency of the extraction conditions and methods

Fig. 1 shows the 3D response surface graphs of the extraction yield (residue) and total anthocyanin content (expressed in terms of mg/g of

plant material (Y_1) and mg/g of residue (Y_2)) obtained for both extraction methods (HAE and UAE). The net surfaces were predicted with the second-order polynomial model of Eq. (1), whose model equations are presented in Table A3. The binary actions between the variables are displayed when the excluded variable is positioned at the centre of the experimental domain (Table A1). Additionally, the goodness of fit of the model is illustrated by the ability to simulate response changes between the observed and predicted data, and the residual distribution as a function of each variable. In turn, Fig. 2 shows the 2D contour graphs resulting from the projections of the 3D response surfaces in the XY plane. These projections focused the optimal extraction conditions obtained for the residue (*yield*), delphinidin-3-*O*-sambubioside (*C1*) and cyanidin-3-*O*-sambubioside (*C2*), depending on the used extraction method. For each anthocyanin, the result is expressed in terms of mg/g of plant material (Y_1) and mg/g of residue (Y_2) to visually describe the extraction trends. The binary actions between variables are displayed when the excluded variable is positioned at the individual optimum (Table 3).

3.3.1. Extraction yield

After analysing the response surface and contour graphs shown in Figs. 1 and 2, it was possible to draw some conclusions regarding the effects of the independent variables on the extraction yield. For HAE, the variable S originated the most marked curvatures on the net surfaces, followed by the variable t. In the first case, the extraction was promoted with the increase in ethanol proportion up to 35% with subsequent decrease. The variable t had a comparable behaviour, since the medium-long extraction times were the most suitable ones. In turn,
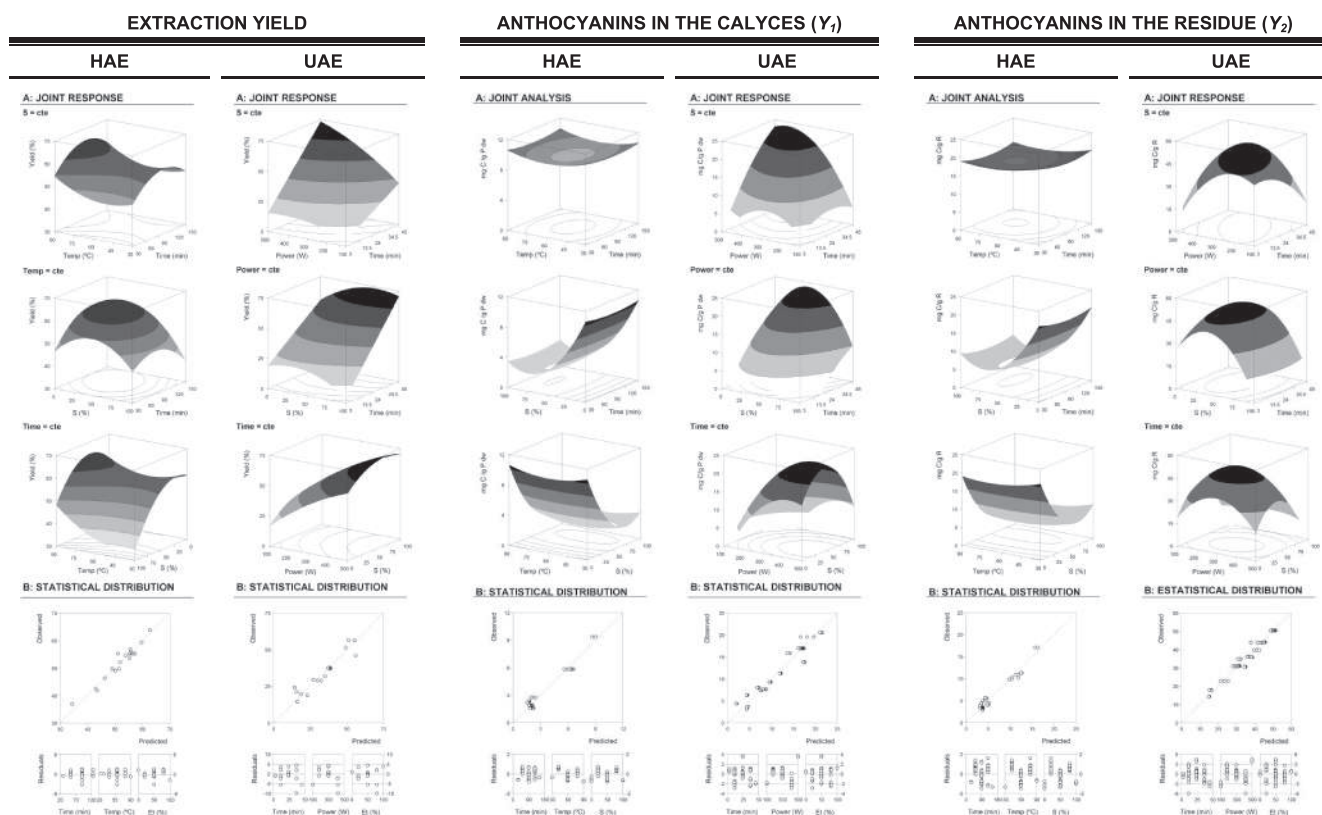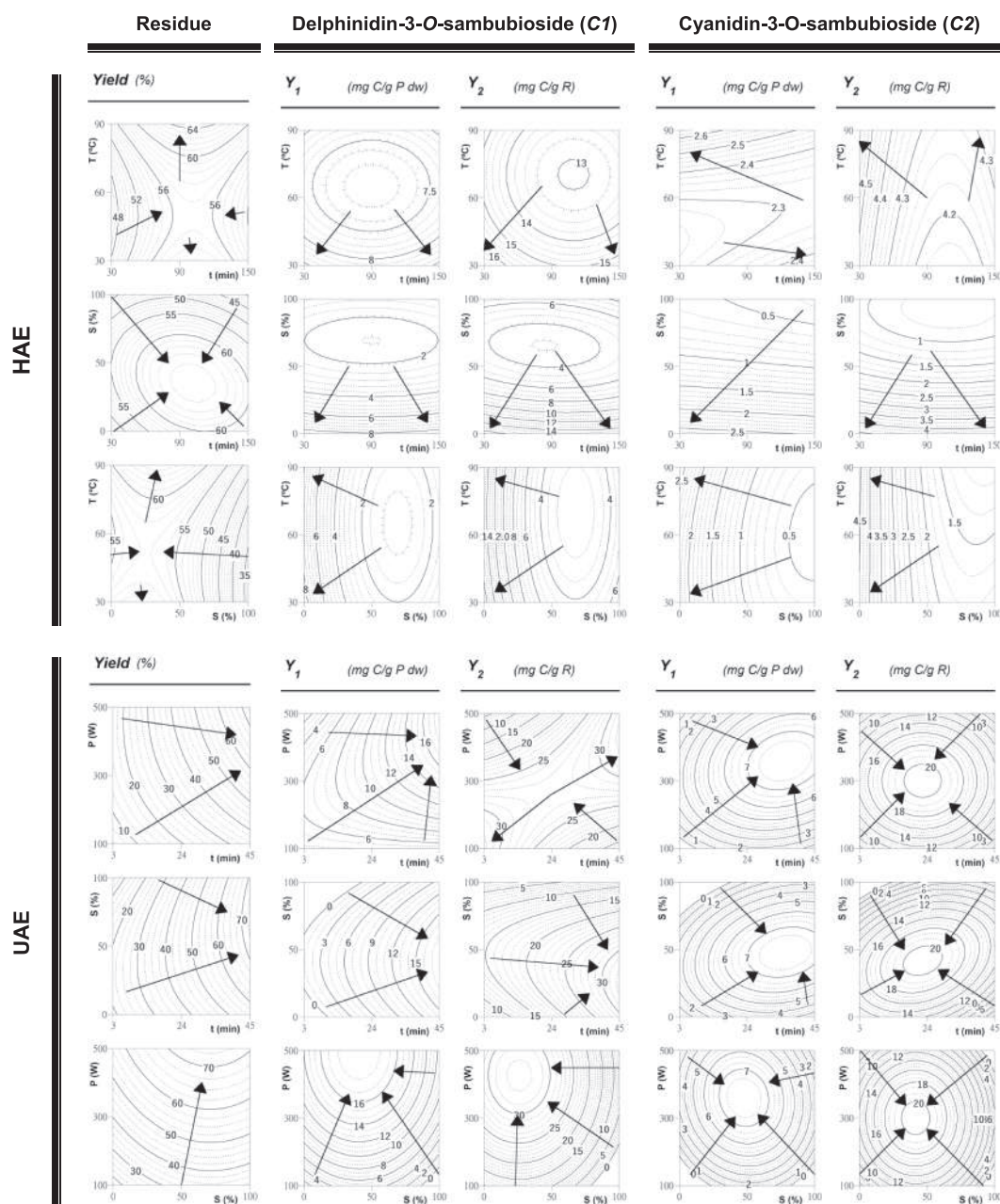

Fig. 1. Response surface graphs of the extraction yield (residue, %) and total anthocyanin content (expressed in terms of mg/g of plant material (Y_1) and mg/g of residue (Y_2)), obtained for both extraction methods (HAE and UAE). Part A: Joint graphical analysis as a function of the involved variables. Each net surface represents the 3D response surface predicted with the second-order polynomial model of Eq. (1) as a function of each variable and described by the equations given in Table A3. The binary actions between the variables are presented when the excluded variable is positioned at the centre of the experimental domain (Table A1). The experimental design and results are presented in Table 2 and the estimated parametric values are shown in Table A2. Part B: Illustration of the goodness of fit through two graphical statistic criteria, namely the ability to simulate response changes between the observed and predicted data, and the residual distribution as a function of each variable.

Fig. 2. 2D contour graphs focusing the optimal points for the extraction yield (residue) and levels of delphinidin-3-*O*-sambubioside (*C*1) and cyanidin-3-*O*-sambubioside (*C*2) obtained by HAE and UAE. For each anthocyanin, the result is expressed in terms of mg/g of plant material (Y_1) and mg/g of residue (Y_2) to visually describe the extraction trends. Each contour graph represents the projection of the theoretical 3D response surface predicted by the second-order polynomial model of Eq. (1) in the XY plane. The binary actions between variables are presented when the excluded variable is positioned at the individual optimum (Table 3). The experimental design and results are presented in Table 2 and the estimated parametric values are shown in Table A2.

higher T provided the highest extraction yields. The amount of residue was also affected by the interaction of the variable S with t (negative interaction) and T (positive interaction) (Table A2). In the UAE process, the most marked response surface curvatures were caused by the tested ranges of t and P, whose increase led to the higher extraction yields (Table A2). Additionally, the obtained yield was also promoted by the strong positive interaction between t and the other two variables (Table A2). Therefore, based on the optimal extraction conditions presented in Table 3, it was observed that HAE required a longer t and a lower S than UAE (while both methods required the highest tested T or P) to obtain optimum response values. The best yield (73.30 ± 4.51%) was

obtained with the UAE process under the following conditions: $t = 45.0$ min, $P = 500.0$ W, and $S = 71.4\%$ ethanol, v/v. Comparable results were obtained by López et al. (2018) when optimizing the HAE and UAE of anthocyanins from *Arbutus unedo* fruits, as they also associated the highest extraction yields with UAE process.

3.3.2. Anthocyanin contents

The variable S was the one that affected most the HAE of anthocyanins from *H. sabdariffa* calyces (Table A2), as verified from the obtained extraction yield with this method. Its significance is visually highlighted in the response surface graphs (Fig. 1), which show that the

Table 3

Operating conditions that maximize the amounts of residue (*yield*), delphinidin-3-*O*-sambubioside (*C1*), cyanidin-3-*O*-sambubioside (C_2), and total anthocyanins (C_T) extracted from *H. sabdariffa* calyces as a function of the extraction method (HAE and UAE) and response value format (Y_1, mg/g P, and Y_2, mg/g R).

Criteria			Optimal extraction conditions			Response optimum		
			X_1: t (min)	X_2: T (°C) or P(W)	X_3: S (%)			
(A) Individual optimal extraction conditions								
HAE	*Yield*		101.5	90.0	35.4	64.74	± 3.60	%
	Y_1	C1	30.0	30.0	0.0	8.57	± 2.07	mg C1/g P dw
		C2	30.0	90.0	0.0	2.66	± 1.15	mg C2/g P dw
		CT	30.0	30.0	0.0	10.61	± 3.26	mg CT/g P dw
	Y_2	C1	30.0	30.0	0.0	16.81	± 2.37	mg C1/g R
		C2	30.0	90.0	0.0	4.59	± 1.24	mg C2/g R
		CT	30.0	30.0	0.0	20.86	± 1.24	mg CT/g R
UAE	*Yield*		45.0	500.0	71.4	73.30	± 4.51	%
	Y_1	C1	45.0	500.0	40.9	17.90	± 2.44	mg C1/g P dw
		C2	36.0	360.0	47.9	7.64	± 1.13	mg C2/g P dw
		CT	45.0	432.3	42.8	23.83	± 2.44	mg CT/g P dw
	Y_2	C1	45.0	426.9	26.1	32.39	± 3.29	mg C1/g R
		C2	22.7	300.0	41.7	20.55	± 3.21	mg C2/g R
		CT	26.1	296.6	39.1	51.76	± 3.70	mg CT/g R
(B) Global optimal extraction conditions								
HAE	*Yield*		30.0	30.0	0.0	44.85	± 8.12	%
	Y_1	C1				8.55	± 1.73	mg C1/g P dw
		C2				2.26	± 0.29	mg C2/g P dw
		CT				10.60	± 1.11	mg CT/g P dw
	Y_2	C1				16.79	± 2.18	mg C1/g R
		C2				4.47	± 0.86	mg C2/g R
		CT				20.83	± 2.76	mg CT/g R
UAE	*Yield*		42.9	386.3	46.1	61.21	± 6.21	%
	Y_1	C1				16.17	± 1.22	mg C1/g P dw
		C2				7.38	± 1.91	mg C2/g P dw
		CT				23.08	± 2.96	mg CT/g P dw
	Y_2	C1				29.72	± 3.19	mg C1/g R
		C2				12.76	± 1.91	mg C2/g R
		CT				47.57	± 4.37	mg CT/g R

higher amounts were obtained when water (*S* = 0%) was used as the extraction solvent. In turn, the effects of *t* and *T* were less marked, with the lowest tested ranges leading to the highest total anthocyanin values. For this method, the extraction conditions originating the higher response values were similar, regardless of the considered response format, except for the variable *T*. Table 3 shows that it was possible to obtain 8.57 ± 2.07 mg/g P and 2.66 ± 1.15 mg/g P of *C1* and *C*2 from *H. sabdariffa* calyces, respectively, when applying the following HAE conditions: *t* = 45.0 min, *S* = 0.0% ethanol, v/v, and *T* = 30 or 90 °C for *C1* and *C*2, respectively. The residue or extract obtained under the same extraction conditions contained approximately the double amount of *C1* (16.81 ± 2.37 mg/g R) and *C*2 (4.59 ± 1.24 mg/g R).

The extraction of anthocyanins followed a different trend when using UAE. Fig. 1 shows that all variables caused accented response surface curvatures, as also indicated by the corresponding parametric values (Table A2). Moreover, contrary to the one verified for HAE, the extraction conditions differed according to the considered response format. However, in both cases, there was a strong *t* × *P* interaction with a positive impact on the obtained total anthocyanin contents, especially for Y_2. Interactions between *t* and *S* were also noted. Applying this method, it was possible to recover 17.90 ± 2.44 mg/g P and 7.64 ± 1.13 mg/g P of *C1* and *C*2, respectively, from the dried red flower calyces (Table 3). In turn, 1 g of residue contained 32.39 ± 3.29 mg of *C1* and 20.55 ± 3.21 mg of *C*2 when using the following conditions: *t* = 45.0 min, *P* = 426.9 W and *S* = 26.1% ethanol, v/v, and *t* = 22.7 min, *P* = 300.0 W and *S* = 41.7% ethanol, v/v, respectively. All these values were much higher than those obtained by HAE (approximately twice). Moreover, the effectiveness of the applied UAE process was highlighted since the obtained anthocyanin

levels are much higher than those reported in other studies (Table 1).

The *H. sabdariffa* calyces are a promising source of anthocyanins for potential use as natural red colorants, since the amounts achieved by applying the optimal extraction conditions are superior to those already found in the fruits of *Prunus avium* L. (sweet cherry, 2.49 mg/g P fw) (Blackhall, Berry, Davies, & Walls, 2018) and *Aristotelia chilensis* L. (maqui, 9.84 mg/g P dw) (Gironés-Vilaplana et al., 2014), tubers of *Ipomoea batatas* L. (purple sweet potato, 2.29 mg/g P dw) (Cai et al., 2016), and purple pods of *Vigna unguiculata* ssp. *sesquipedalis* L. (yard-long bean, 8.81 mg/g P dw) (Tae et al., 2010). The anthocyanin-based colorants can replace the artificial counterparts and provide health-promoting effects (Castañeda-Ovando, de Pacheco-Hernández, & Páez-Hernández, Rodríguez, & Galán-Vidal, 2009; Martins et al., 2016).

### 3.3.3. Efficiency of HAE vs. UAE

As discussed above, the extraction of anthocyanins from the red flower calyces of *H. sabdariffa* was differently affected by the tested HAE and UAE methods. The highest yields were obtained using the non-conventional UAE method, which promotes the rupture of the plant tissue through cavitation forces and enhances the solvent entrance into the cells with consequent release of the intracellular compounds into the solvent, thus intensifying mass transfer phenomena (Antonio et al., 2016; Misra et al., 2017). This method yielded 51.76 ± 3.70 mg *CT*/g R when applying: *t* = 26.1 min, *P* = 296.6 W, and *S* = 39.1% ethanol, v/v, whereas HAE originated 20.86 ± 1.24 mg *CT*/g R when: *t* = 30.0 min, *T* = 30.0 °C, and *S* = 0.0% ethanol, v/v. These optimized methods shared some similarities in terms of *T* (~30 °C) and *t* (26–30 min), thus indicating that the lower HAE values were not caused by thermal degradation of these compounds. In contrast, the response
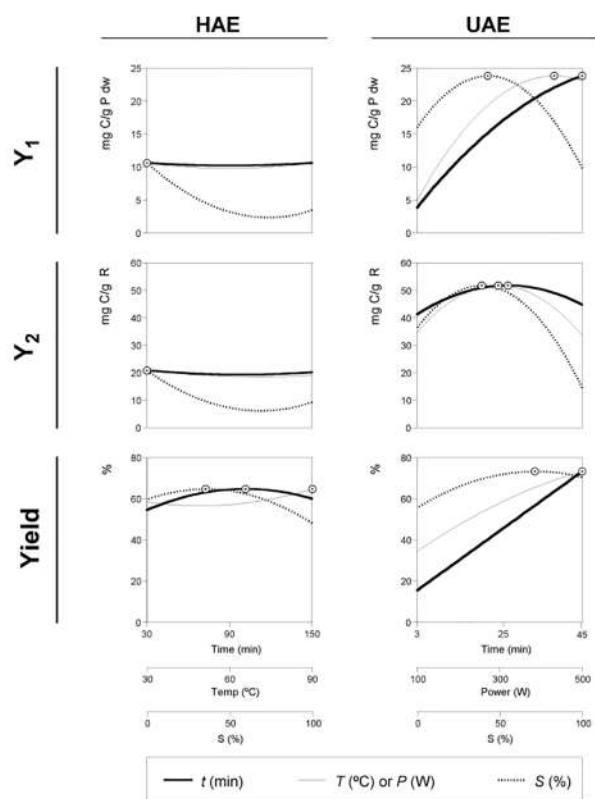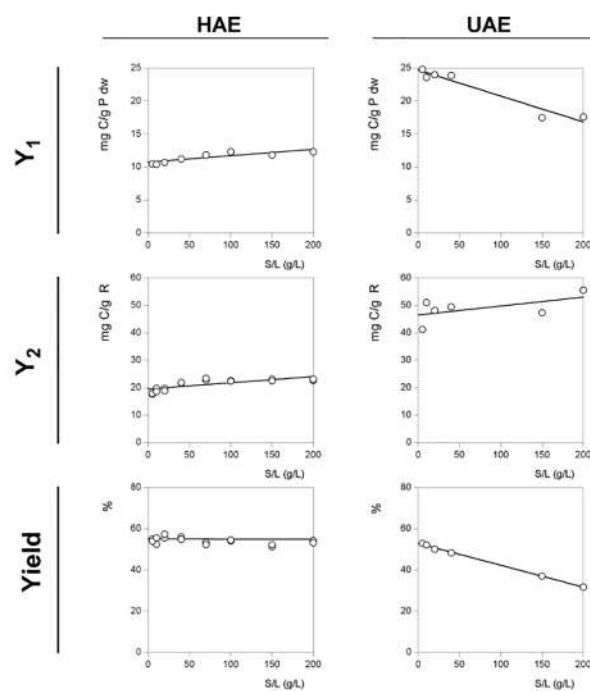
Fig. 3. Summary representation of the effects of the four-variable considered in the HAE and UAE processes. Part A: 2D individual responses and optimum values (⊙) of the three variables determined for the total anthocyanin content (*CT*) in mg/g P (Y_1) and mg/g R (Y_2) and the extraction yield (%). In each graph, each independent variable was positioned at the optimal value of the other two variables (Table 3). Lines and dots were generated by the second-order polynomial model of Eq. (1) (Table A3). Part B: Dose-response analysis of the solid/liquid ratio (*S/L*) at the optimal extraction conditions of the other three variables (Table 3). Dots (○) represent the experimental values and lines show the pattern predicted by linear equation (parametric values in Table A4).

optimum of UAE was achieved with the application of ultrasound and a higher ethanol proportion (meaning higher energy and solvent costs), while water was a suitable solvent for HAE. Nevertheless, the different maximum values achievable by each method are quite different and must be considered when selecting the most appropriate one.

In order to determine the most cost-effective option, it would be interesting to perform a life-cycle cost analysis (LCCA), not only of the sole extraction process as an individual unit operation, but considering the entire supply chain, including the production and harvesting of the plant material, equipment investment, natural resources and energy consumption, and environment hazardous emissions. A comparative LCCA between conventional solvent extraction and innovative methods using microwaves and ultrasounds was performed by Kyriakopoulou, Papadaki, and Krokida (2015), which found UAE the most viable and environmental friendly method to recover β-carotene from microalgae. In our study, the effects of the *S/L* variable were investigated to obtain more information about the efficiency of each extraction method.

3.3.4. Optimal extraction conditions for maximizing the responses criteria

Although the effects described above provided a guiding range of conditions maximizing the defined responses, optimal values can be determined using a simple method tool to solve nonlinear problems. The results of the application of this simple procedure are presented in Table 3 (part A), in which the extraction conditions that maximize each response in individual and global terms are provided. Additionally, Fig. 3 (part A) summarizes the information derived from the

mathematical equations, where 2D graphs are presented as a function of all assessed variables. These variables were positioned at the optimal global values of the other two variables (Table 3) (part B). For the three variables optimized for the recovery of total anthocyanins (*CT*) in mg/g P (Y_1) and mg/g R (Y_2) and extraction yield (%), the predicted individual responses are represented by lines and optimum values by points (⊙). The determined global optimal extraction conditions were experimentally tested to confirm the accuracy of the presented results and to assess the dose-response effect of the *S/L* variable.

3.4. Dose-response analysis of the solid/liquid ratio at the optimum conditions

Reduced extraction time and low solvent consumption are some of the desired requirements when designing novel extraction methods. The solvent volume should be sufficient only to dissolve the target compounds and promote mass transfer (Pinela et al., 2016). At industrial scale, higher solid/liquid ratios (*S/L*) are desirable to maximize the extraction yield with minimal solvent consumption, thus making the process more productive and sustainable. The extraction rate is also affected by the mass transfer resistance associated with the matrix structure (Marco, Agnese, & Giuseppe, 2012). The studies on *S/L* were performed at the global optimal conditions predicted by the polynomial models obtained for each extraction technique as previously described. Preliminary results indicated that the experimental limit value was proximal to 200 g/L. Therefore, the experiment was designed to assess

the dose-response effects of the S/L variable between 5 g/L and 200 g/L.

Fig. 3 (part B) shows the dose-responses analysis of S/L at the optimal global extraction conditions of the other three variables (Table 3 part B), where it is also possible to observe that the responses achieved by HAE and UAE are consistent with those previously obtained. In these 2D representations, dots (○) represent the experimental values and lines show the pattern predicted by a simple linear relation with intercept (parametric values in Table A4). Based on the parametric values presented in Table A4, a consistency was found between the CT values (for both Y_1 and Y_2 response formats) and those previously obtained for HAE and UAE (Table 3). Consequently, the dose response is explained by the slope (m) of the linear relation. Negative values of m describe decreasing extraction patterns as the S/L increases, and positive values describe increasing extraction patterns as the S/L increases, while a constant pattern is shown when the m value is ns (or zero). As can be observed, two cases showed negative m values (the extraction efficiency increases as the S/L rate decreases), and one case showed non-significant values, or a zero value of m (the efficiency doesn't change as the S/L increases). In all the other cases the m showed positive values (the efficiency increases as the S/L increases). The reliability of the obtained linear fittings is strongly consistent. In fact, high coefficients of determination were obtained ($R^2 \geq 0.94$) indicating a good agreement between predicted patterns and the obtained experimental data, validating the mathematical analysis selected to describe the reached solutions. The conclusions derived from this analysis are described below:

– For the Y_1 value format, the parametric values for HAE were $b = 10.76 \pm 1.31$ mg CT/g P dw and $m = 0.0097 \pm 0.001$, with $R^2 = 0.9510$; while for UAE, $b = 24.47 \pm 2.37$ mg CT/g P dw and $m = -0.0393 \pm 0.019$, with $R^2 = 0.9765$. For the HAE process, as the S/L increases, the extraction also slightly increases, leading to an increment of ~15% in the extracted compounds, when changing from 5 g/L (lower tested value) to 200 g/L (maximum tested experimental value). On the other hand, the observed decrease for UAE is relatively strong, which means that the increase of 1 g/L implies the loss of 0.0393 ± 0.019 mg CT/g P dw. Such values produce losses of ~25% when applying 200 g/L, comparatively with the tested lower value. Therefore, when working at the most economically attractive S/L value (200 g/L), both solutions will reach similar results.

– For the Y_2 value format, the parametric values for HAE were $b = 19.53 \pm 1.38$ mg CT/g R and $m = 0.0225 \pm 0.0091$, with $R^2 = 0.9434$; while for UAE, $b = 46.26 \pm 2.74$ mg CT/g R and $m = 0.0325 \pm 0.0098$, with $R^2 = 0.9674$. The positive m values show that the S/L increase leads to an increase in the extraction ability, conducting to a maximum extraction value when using 200 g/L. Nevertheless, the quantity extracted by UAE is nearly 3-fold superior to the quantity obtained by HAE.

– For the $Yield$ value format, the parametric values for HAE were $b = 55.14 \pm 3.56\%$ and a ns value of m (i.e., the obtained amount of residue does not vary as a function of the S/L increase), with $R^2 = 0.9794$; whereas for UAE, $b = 52.20 \pm 2.98\%$ and $m = -0.106 \pm 0.007$, with $R^2 = 0.9975$.

These results are in accordance with the ones reported in the literature, where UAE has been identified as a technique with potential to improve the extraction yield through the intensification of the mass transfer between the plant material and the solvent (Tomšik et al., 2016). Probably, the implosion of the cavitation bubbles generated during sonication led to an improved cell disruption and particle breakdown, which facilitated the release of the extractable compounds and allowed a greater penetration of the solvent into the sample matrix, thus increasing the contact surface area between the solid and liquid phases (Chemat et al., 2017b; Tomšik et al., 2016). However, in order to propose a more accurate sonication mechanism and to visualize the effects, it would be interesting to investigate different mechanisms

involved during UAE, such as fragmentation, erosion, capillarity, detexturation and sonoporation, as well as the influencing parameters (Chemat et al., 2017b). Therefore, macroscopic and cyto-histochemical analyses, scanning electron microscopy (SEM), and environmental scanning electron microscopy (e-SEM), among other observations, should be performed (Khadhraoui et al., 2018).

The concept of "green extraction" is aligned with the societal challenges of the 21st century, to protect both the consumers and environment. This approach also promotes competition in the industrial sector, making it more innovative, efficient and sustainable (Chemat et al., 2017a; Khadhraoui et al., 2018; Sicaire et al., 2016). Therefore, the UAE process herein optimized can be adopted by industrials interested in replacing their traditional extraction process with this more ecological and competitive method. For this, experiments should be conducted from the laboratory to pilot-scale, to lead to the implementation of UAE at the industrial-scale (using countercurrent extractors) (Chemat et al., 2017a; Sicaire et al., 2016), which will be of great importance to recover pigments, aromas and antioxidants from plant materials (in this case, anthocyanins from *H. sabdariffa* calyces). However, UAE finds other relevant applications in the food, nutraceutical, pharmaceutical and bioenergy industries (Chemat et al., 2017a, 2017b; Meullemiestre et al., 2016; Sicaire et al., 2016).

4. Conclusions

Nowadays, consumers are increasingly choosing food products formulated with natural additives due to the understanding of the strong relation between health and diet. Therefore, it is important for the industrial food sector to find novel sources and efficient extraction methods to support the production of bio-based ingredients, including colorants. In this study, two extraction methods were applied, and optimized by combining the effects of three relevant independent variables, to maximize the recovery of anthocyanins from the red calyces of *H. sabdariffa*. The achieved experimental data were successfully fitted to the theoretical models used to determine the optimal extraction conditions. UAE was the most efficient method; it allowed to recover 23.83 ± 2.44 mg of the target anthocyanins per 1 g of dried plant material and obtain 51.76 mg of these pigments in 1 g of residue (or extract). For the S/L variable, whose effects were assessed at the optimum conditions, firstly determined for the defined three variables, the positive m values obtained for Y_2 showed that the S/L increase leads to an increase in the extraction ability, conducting to maximum values at 200 g/L. Furthermore, the amount of anthocyanins obtained by UAE was nearly 3-fold higher than the amount obtained by HAE. According to these results, it can be stated that *H. sabdariffa* calyces can be used as a viable source of anthocyanins to produce bio-based colouring agents, being one of the richest anthocyanin containing sources reported in the literature. In addition, this bench-scale application study can support the scale-up of natural colorants production, which is of interest to industrial suppliers of the food, pharmaceutical and cosmetic sectors, among others.

Appendix A. Supplementary material

Supplementary data to this article can be found online at https://doi.org/10.1016/j.foodchem.2018.09.118.

References

Alarcón-Alonso, J., Zamilpa, A., Aguilar, F. A., Herrera-Ruiz, M., Tortoriello, J., & Jimenez-Ferrer, E. (2012). Pharmacological characterization of the diuretic effect of *Hibiscus sabdariffa* Linn (Malvaceae) extract. *Journal of Ethnopharmacology, 139*(3), 751–756.

Ali, B. H., Al Wabel, N., & Blunden, G. (2005). Phytochemical, pharmacological and toxicological aspects of *Hibiscus sabdariffa* L.: A review. *Phytotherapy Research, 19*(5), 369–375.

Almeida, H. H. S., Barros, L., Barreira, J. C. M., Calhelha, R. C., Heleno, S. A., Sayer, C., ... Ferreira, I. C. F. R. (2018). Bioactive evaluation and application of different formulations of the natural colorant curcumin (E100) in a hydrophilic matrix (yogurt). *Food Chemistry, 261*, 224–232.

Antonio, A. L., Pereira, E., Pinela, J., Heleno, S., Pereira, C., & Ferreira, I. C. F. R. (2016). Determination of antioxidant compounds in foodstuff. *Food safety: Innovative analytical tools for safety assessment* (pp. 179–220). Hoboken, NJ, USA: John Wiley & Sons Inc.

Beye, C., Hiligsmann, S., Tounkara, L. S., & Thonart, P. (2017). Anthocyanin content of two *Hibiscus sabdariffa* cultivars grown in Senegal. *Agronomie Africaine, 29*(1), 63–68.

Blackhall, M. L., Berry, R., Davies, N. W., & Walls, J. T. (2018). Optimized extraction of anthocyanins from Reid Fruits' *Prunus avium* 'Lapins' cherries. *Food Chemistry, 256*, 280–285.

Cai, Z., Qu, Z., Lan, Y., Zhao, S., Ma, X., Wan, Q., ... Li, P. (2016). Conventional, ultrasound-assisted, and accelerated-solvent extractions of anthocyanins from purple sweet potatoes. *Food Chemistry, 197*, 266–272.

Carle, R., & Schweiggert, R. M. (2016). *Handbook on natural pigments in food and beverages: Industrial applications for improving food color* (1st ed.). Woodhead Publishing.

Carocho, M., Barros, L., Barreira, J. C. M., Calhelha, R. C., Soković, M., Fernández-Ruiz, V., ... Ferreira, I. C. F. R. (2016). Basil as functional and preserving ingredient in "Serra da Estrela" cheese. *Food Chemistry, 207*, 51–59.

Carocho, M., Morales, P., & Ferreira, I. C. F. R. (2015). Natural food additives: Quo vadis? *Trends in Food Science & Technology, 45*(2), 284–295.

Castañeda-Ovando, A., Pacheco-Hernández, M.de L., Páez-Hernández, M. E., Rodríguez, J. A., & Galán-Vidal, C. A. (2009). Chemical studies of anthocyanins: A review. *Food Chemistry, 113*(4), 859–871.

Chemat, F., Rombaut, N., Meullemiestre, A., Turk, M., Perino, S., Fabiano-Tixier, A.-S., & Abert-Vian, M. (2017a). Review of green food processing techniques. Preservation, transformation, and extraction. *Innovative Food Science & Emerging Technologies, 41*, 357–377.

Chemat, F., Rombaut, N., Sicaire, A. G., Meullemiestre, A., Fabiano-Tixier, A. S., & Abert-Vian, M. (2017b). Ultrasound assisted extraction of food and natural products. Mechanisms, techniques, combinations, protocols and applications. A review. *Ultrasonics Sonochemistry, 34*, 540–560.

Comuzzi, C., Polese, P., Melchior, A., Portanova, R., & Tolazzi, M. (2003). SOLVERSTAT: A new utility for multipurpose analysis. An application to the investigation of dioxygenated Co(II) complex formation in dimethylsulfoxide solution. *Talanta, 59*(1), 67–80.

Corrales, M., Toepfl, S., Butz, P., Knorr, D., & Tauscher, B. (2008). Extraction of anthocyanins from grape by-products assisted by ultrasonics, high hydrostatic pressure or pulsed electric fields: A comparison. *Innovative Food Science and Emerging Technologies, 9*(1), 85–91.

Da-Costa-Rocha, I., Bonnlaender, B., Sievers, H., Pischel, I., & Heinrich, M. (2014). *Hibiscus sabdariffa* L. - A phytochemical and pharmacological review. *Food Chemistry, 165*, 424–443.

de Levie, R. (2012). *Advanced excel for scientific data analysis* (3rd ed.). Atlantic Academic LLC.

Du, Q., Jerz, G., & Winterhalter, P. (2004). Isolation of two anthocyanin sambubiosides from bilberry (*Vaccinium myrtillus*) by high-speed counter-current chromatography. *Journal of Chromatography A, 1045*(1–2), 59–63.

Garcia-Mendoza, M.del P., Espinosa-Pardo, F. A., Baseggio, A. M., Barbero, G. F., Maróstica Junior, M. R., Rostagno, M. A., & Martínez, J. (2017). Extraction of phenolic compounds and anthocyanins from juçara (*Euterpe edulis* Mart.) residues using pressurized liquids and supercritical fluids. *The Journal of Supercritical Fluids, 119*, 9–16.

Gironés-Vilaplana, A., Baenas, N., Villaño, D., Speisky, H., García-Viguera, C., & Moreno, D. A. (2014). Evaluation of Latin-American fruits rich in phytochemicals with biological effects. *Journal of Functional Foods, 7*(1), 599–608.

Heleno, S. A., Diz, P., Prieto, M. A., Barros, L., Rodrigues, A., Barreiro, M. F., & Ferreira, I. C. F. R. (2016). Optimization of ultrasound-assisted extraction to obtain mycosterols from *Agaricus bisporus* L. by response surface methodology and comparison with conventional Soxhlet extraction. *Food Chemistry, 197*, 1054–1063.

Ifie, I., Ifie, B. E., Ibitoye, D. O., Marshall, L. J., & Williamson, G. (2018). Seasonal variation in *Hibiscus sabdariffa* (Roselle) calyx phytochemical profile, soluble solids and α-glucosidase inhibition. *Food Chemistry, 261*, 164–168.

Jabeur, I., Pereira, E., Barros, L., Calhelha, R. C., Soković, M., Oliveira, M. B. P. P., & Ferreira, I. C. F. R. (2017). *Hibiscus sabdariffa* L. as a source of nutrients, bioactive compounds and colouring agents. *Food Research International, 100*, 717–723.

Kemmer, G., & Keller, S. (2010). Nonlinear least-squares data fitting in excel spreadsheets. *Nature Protocols, 5*(2), 267–281.

Khadhraoui, B., Turk, M., Fabiano-Tixier, A. S., Petitcolas, E., Robinet, P., Imbert, R., ... Chemat, F. (2018). Histo-cytochemistry and scanning electron microscopy for studying spatial and temporal extraction of metabolites induced by ultrasound. Towards chain detexturation mechanism. *Ultrasonics Sonochemistry, 42*, 482–492.

Kyriakopoulou, K., Papadaki, S., & Krokida, M. (2015). Life cycle analysis of β-carotene extraction techniques. *Journal of Food Engineering, 167*, 51–58.

Liazid, A., Guerrero, R. F., Cantos, E., Palma, M., & Barroso, C. G. (2011). Microwave assisted extraction of anthocyanins from grape skins. *Food Chemistry, 124*(3), 1238–1243.

López, C. J., Caleja, C., Prieto, M. A., Barreiro, M. F., Barros, L., & Ferreira, I. C. F. R. (2018). Optimization and comparison of heat and ultrasound assisted extraction techniques to obtain anthocyanin compounds from *Arbutus unedo* L. fruits. *Food Chemistry, 264*, 81–91.

Marco, B., Agnese, C., & Giuseppe, T. (2012). Quality preservation and cost effectiveness in the extraction of nutraceutically – Relevant fractions from microbial and vegetal matrices. In B. Valdez (Ed.). *Scientific, health and social aspects of the food industry* (pp. 488). InTech.

Marić, M., Grassino, A. N., Zhu, Z., Barba, F. J., Brnčić, M., & Rimac Brnčić, S. (2018). An overview of the traditional and innovative approaches for pectin extraction from plant food wastes and by-products: Ultrasound-, microwave-, and enzyme-assisted extraction. *Trends Food Science & Technology, 76*, 28–37.

Martins, N., Roriz, C. L., Morales, P., Barros, L., & Ferreira, I. C. F. R. (2016). Food colorants: Challenges, opportunities and current desires of agro-industries to ensure consumer expectations and regulatory practices. *Trends in Food Science & Technology, 52*, 1–15.

Meullemiestre, A., Breil, C., Abert-Vian, M., & Chemat, F. (2016). Microwave, ultrasound, thermal treatments, and bead milling as intensification techniques for extraction of lipids from oleaginous *Yarrowia lipolytica* yeast for a biojetfuel application. *Bioresource Technology, 211*, 190–199.

Misra, N. N., Martynenko, A., Chemat, F., Paniwnyk, L., Barba, F. J., & Jambrak, A. R. (2017). Thermodynamics, transport phenomena, and electrochemistry of external field-assisted nonthermal food technologies. *Critical Reviews in Food Science and Nutrition*, 1–32.

Pinela, J., Prieto, M. A., Barreiro, M. F., Carvalho, A. M., Oliveira, M. B. P. P., Curran, T. P., & Ferreira, I. C. F. R. (2017). Valorisation of tomato wastes for development of nutrient-rich antioxidant ingredients: A sustainable approach towards the needs of the today's society. *Innovative Food Science & Emerging Technologies, 41*, 160–171.

Pinela, J., Prieto, M. A., Barreiro, M. F., Carvalho, A. M., Oliveira, M. B. P. P., Vázquez, J. A., & Ferreira, I. C. F. R. (2016). Optimization of microwave-assisted extraction of hydrophilic and lipophilic antioxidants from a surplus tomato crop by response surface methodology. *Food and Bioproducts Processing, 98*, 283–298.

Ramesh, M., & Muthuraman, A. (2018). Flavoring and coloring agents: Health risks and potential problems. In A. M. Grumezescu, & A. M. Holban (Eds.). *Natural and artificial flavoring agents and food dyes* (pp. 1–28). Academic Press.

Ranic, M., Nikolic, M., Pavlovic, M., Buntic, A., Siler-Marinkovic, S., & Dimitrijevic-Brankovic, S. (2014). Optimization of microwave-assisted extraction of natural antioxidants from spent espresso coffee grounds by response surface methodology. *Journal of Cleaner Production, 80*, 69–79.

Salazar-González, C., Vergara-Balderas, F. T., Ortega-Regules, A. E., & Guerrero-Beltrán, J.Á. (2012). Antioxidant properties and color of *Hibiscus sabdariffa* extracts. *Ciencia e Investigación Agraria, 39*(1), 79–90.

Sharma, H. K., Sarkar, M., Choudhary, S. B., Kumar, A. A., Maruthi, R. T., Mitra, J., & Karmakar, P. G. (2016). Diversity analysis based on agro-morphological traits and microsatellite based markers in global germplasm collections of roselle (*Hibiscus sabdariffa* L.). *Industrial Crops and Products, 89*, 303–315.

Shi, P., & Tsai, C.-L. (2002). Regression model selection - A residual likelihood approach. *Journal of the Royal Statistical Society: Series B (Statistical Methodology), 64*(2), 237–252.

Sicaire, A.-G., Vian, M. A., Fine, F., Carré, P., Tostain, S., & Chemat, F. (2016). Ultrasound induced green solvent extraction of oil from oleaginous seeds. *Ultrasonics Sonochemistry, 31,* 319–329.

Sindi, H. A., Marshall, L. J., & Morgan, M. R. A. (2014). Comparative chemical and biochemical analysis of extracts of *Hibiscus sabdariffa. Food Chemistry, 164,* 23–29.

Tae, J. H., Lee, M. H., Park, C. H., Pae, S. B., Shim, K. B. O., Ko, J. M., ... Park, K. Y. (2010). Identification and characterization of anthocyanins in yard-long beans (*Vigna unguiculata* ssp. *sesquipedalis* L.) by high-performance liquid chromatography with diode array detection and electrospray ionization/mass spectrometry (HPLC-DAD-ESI. *Journal of Agricultural and Food Chemistry, 58*(4), 2571–2576.

Tomšik, A., Pavlić, B., Vladić, J., Ramić, M., Brindza, J., & Vidović, S. (2016). Optimization of ultrasound-assisted extraction of bioactive compounds from wild garlic (*Allium ursinum* L.). *Ultrasonics Sonochemistry, 29,* 502–511.

Vilkhu, K., Mawson, R., Simons, L., & Bates, D. (2008). Applications and opportunities for ultrasound assisted extraction in the food industry - A review. *Innovative Food Science and Emerging Technologies, 9*(2), 161–169.

Yang, B., Zheng, J., Laaksonen, O., Tahvonen, R., & Kallio, H. (2013). Effects of latitude and weather conditions on phenolic compounds in currant (*Ribes* spp.) cultivars. *Journal of Agricultural and Food Chemistry, 61*(14), 3517–3532.

Zhang, B., Mao, G., Zheng, D., Zhao, T., Zou, Y., Qu, H., ... Wu, X. (2014). Separation, identification, antioxidant, and anti-tumor activities of *Hibiscus sabdariffa* L. extracts. *Separation Science and Technology, 49*(9), 1379–1388.

Optimization of the Extraction Process to Obtain a Colorant Ingredient from Leaves of *Ocimum basilicum* var. *purpurascens*

Filipa Fernandes [1], Eliana Pereira [1], Miguel A. Prieto [1,2], Ricardo C. Calhelha [1], Ana Ćirić [3], Marina Soković [3], Jesus Simal-Gandara [2], Lillian Barros [1,*] and Isabel C. F. R. Ferreira [1,*]

1   Centro de Investigação de Montanha (CIMO), Instituto Politécnico de Bragança, Campus de Santa Apolónia, 5300-253 Bragança, Portugal; filipafernandes1994@outlook.com (F.F.); eliana@ipb.pt (E.P.); mprieto@ipb.pt (M.A.P.); calhelha@ipb.pt (R.C.C.)
2   Nutrition and Bromatology Group, Department of Analytical and Food Chemistry, Faculty of Food Science and Technology, University of Vigo—Ourense Campus, E-32004 Ourense, Spain; jsimal@uvigo.es
3   University of Belgrade, Department of Plant Physiology, Institute for Biological Research "Siniša Stanković", Bulevar Despota Stefana 142, 11000 Belgrade, Serbia; rancic@ibiss.bg.ac.rs (A.Ć.); mris@ibiss.bg.ac.rs (M.S.)
*   Correspondence: lillian@ipb.pt (L.B.); iferreira@ipb.pt (I.C.F.R.F.); Tel.: +351-273-303285 (L.B.); +351-273-303219 (I.C.F.R.F.)

Abstract: Heat-Assisted Extraction (HAE) was used for the optimized production of an extract rich in anthocyanin compounds from *Ocimum basilicum* var. *purpurascens* leaves. The optimization was performed using the response surface methodology employing a central composite experimental design with five-levels for each of the assessed variables. The independent variables studied were the extraction time (t, 20–120 min), temperature (T, 25–85 °C), and solvent (S, 0–100% of ethanol, *v/v*). Anthocyanin compounds were analysed by HPLC-DAD-ESI/MS and the extraction yields were used as response variables. Theoretical models were developed for the obtained experimental data, then the models were validated by a selected number of statistical tests, and finally, those models were used in the prediction and optimization steps. The optimal HAE conditions for the extraction of anthocyanin compounds were: $t = 65.37 \pm 3.62$ min, $T = 85.00 \pm 1.17$ °C and $S = 62.50 \pm 4.24\%$, and originated 114.74 ± 0.58 TA mg/g of extract. This study highlighted the red rubin basil leaves as a promising natural matrix to extract pigmented compounds, using green solvents and reduced extraction times. The extract rich in anthocyanins also showed antimicrobial and anti-proliferative properties against four human tumor cell lines, without any toxicity on a primary porcine liver cell line.

Keywords: natural colorants; anthocyanins; *Ocimum basilicum* var. *purpurascens* leaves; red rubin basil; Heat-Assisted Extraction; extraction optimization

1. Introduction

Consumers' interest in food quality has been increasing, selecting foods with health benefits. Colour is the main organoleptic attribute in the selection and acceptance of foods [1,2]. Some vegetable matrices are composed by natural pigments, attracting much attention from the scientific community and leading to studies to characterize these compounds and explore their subsequent application, not only in the food industry as natural colorants, but also in the pharmaceutical sector, as antioxidants [3–5].

Anthocyanins are natural pigment studied worldwide; however, when these compounds are incorporated in food products, there are several intrinsic and extrinsic factors that affect and influence

their stability [6]. The pH is an important parameter, because it is crucial in the determination of the anthocyanin colour, which shows a significant pigmentation variability. In aqueous medium, they are red at pH = 1–3, colourless at pH = 4–5, purple at pH = 6–7, blue at pH = 7–8, and yellow at pH = 8–9 [3,7]. Other variables to be taken into account in anthocyanins' stability are the handling and storage temperature, the chemical composition of target products (presence of enzymes, proteins, metal ions and even other flavonoids), and exposure to light and oxygen [3].

The use of anthocyanins as food colorants is approved in several countries [8] and according to the Regulation (EU) nr 1129/2011 of the Commission of 11 November 2011, their application is authorised in numerous food products and processes, such as cured cheeses and cheese products of red marbled paste, vegetables in vinegar, oil or brine (except olives), jams, jellies and marmalades, fruit-flavored breakfast cereals, fish pastes and crustaceans, pre-cooked crustaceans, and smoked fish, among other products. The acceptable daily intake (ADI) is not regulated, which means that sufficient quantity can be added to food products to achieve the desired coloration effect [9].

Anthocyanins can be found in numerous natural sources, especially in fruits, cereals, leaves, flowers, and roots, such as in the leaves of *Ocimum basilicum* var. *purpurascens* (red rubin basil) [10]. Red rubin basil belongs to the *Lamiaceae* family, being a variety of *Ocimum basilicum*, and is used not only as an ornamental plant, but also in traditional medicine [10–12].

In order to apply sustainable extraction methodologies at an industrial level, mathematical studies are performed to maximize the extraction of compounds from natural matrices [13,14]. The patterns of the response variables of the extraction method, such as processing temperature, time and solvent [13,14] can be evaluated using the response surface methodology (RSM). This technique allows to save time, reagents and reduce the operational costs, meanwhile increases the efficiency of the optimization process. Aiming to promote the applicability of natural pigments present in the *Ocimum basilicum* var. *pupurascens* leaves at an industrial level, this work optimized the HAE extraction of anthocyanin compounds, particularly cyanidin and pelargonidin derivatives using Response Surface Methodology (RSM).

2. Results

2.1. Response Criteria for the RSM Analysis

The HPLC anthocyanin profile of the red rubin basil leaves extract from experimental run number 18 is shown in Figure 1. Up to 13 anthocyanin compounds were identified (Table 1) based their chromatographic characteristics (UV-Vis, mass spectral fragmentation patterns) and literature information [15,16].
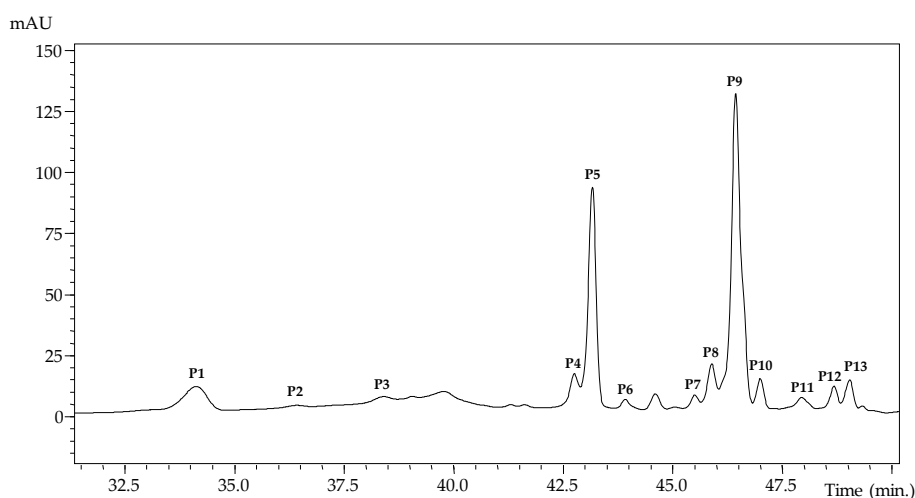
Figure 1. HPLC profile of anthocyanin molecules found in red rubin basil leaves extract obtained in the data set number 18 (as described in Table 2).

Table 1. Retention time (Rt), wavelengths of maximum absorption in the UV-Vis region (λ_{max}), and tentative identification of anthocyanin compounds in *O. basilicum* var. *purpurascens* (mean $\pm$ SD).

Peak	Rt (min)	λ_{max} (nm)	$[M + H]^+$	Main Fragment ESI-MSn [Intensity (%)]	Tentative Identification
P1	34.1	520	919	757(49),449(6),287(13)	Cyanidin-3-(p-coumaroyl-6′-caffeoyl)sophoroside isomer 1 [A]
P2	36.4	520	919	757(49),449(6),287(13)	Cyanidin-3-(p-coumaroyl-6′-caffeoyl)sophoroside isomer 2 [A]
P3	38.4	522	1005	757(6),535(11),287(11)	Cyanidin-3-(6-p-coumaroyl)sophoroside-5-(6-malonyl)glucoside [A]
P4	42.8	522	757	595(100),449(11),287(61)	Cyanidin-3-(6-p-coumaroyl)glucoside-5-glucoside [A]
P5	43.2	530	1081	919(15),449(6),287(6)	Cyanidin-3-(6-p-coumaroyl-6′-caffeoyl)-5-glucoside isomer1 [A]
P6	43.9	532	1167	919(44),757(5),287(20)	Cyanidin-3-(6-p-coumaroyl-6′-caffeoyl)sophoroside-5-(6-malonyl)glucoside isomer 1 [A]
P7	44.6	530	1167	919(27),757(5),287(6)	Cyanidin-3-(6 p-coumaroyl-6′-caffeoyl)sophoroside-5-(6-malonyl)glucoside isomer 2 [A]
P8	45.5	530	1081	919(100),449(11),287(20)	Cyanidin-3-(6-p-coumaroyl-6′-caffeoyl)sophoroside-5-glucoside isomer2 [A]
P9	45.9	530	1065	903(20),449(5),287(3)	Cyanidin-3-(6,6′-di p-coumaroyl)sophoroside-5-glucoside [A]
P10	46.4	526	1151	989(10),903(5),287(5)	Cyanidin-3-(6,6′-di p-coumaroyl)sophoroside-5-(6-malonyl)glucoside [A]
P11	47.0	514	1049	887(33),433(9),271(5)	Pelargonidin-3-(6,6′-di p-coumaroyl)sophoroside-5-glucoside [B]
P12	48.0	526	1167	1005(63),919(23),449(8),287(13)	Cyanidin-3-(6-p-coumaroyl-X-malonyl-6′-caffeoyl)sophoroside-5-glucoside [A]
P13	48.7	530	1151	989(28),449(17),287(5)	Cyanidin-3-(6-p-coumaroyl-X-malonyl-6′-p-coumaroyl)sophoroside-5-glucoside [A]

Calibration curves used: [A]- cyanidin-3-*O*-glucoside (y = 97,787x − 743,469; R^2 = 0.999); [B]- pelargonidin-3-*O*-glucoside (y = 43,781x − 275,315; R^2 = 0.999).

Figure 2 shows a summary of the diverse stages used for optimization procedure, in order to recover the anthocyanin compounds from the red rubin basil leaves. The experimental values of the 28 experimental runs of the circumscribed central composite design (*CCCD*) design are presented in Table 2.
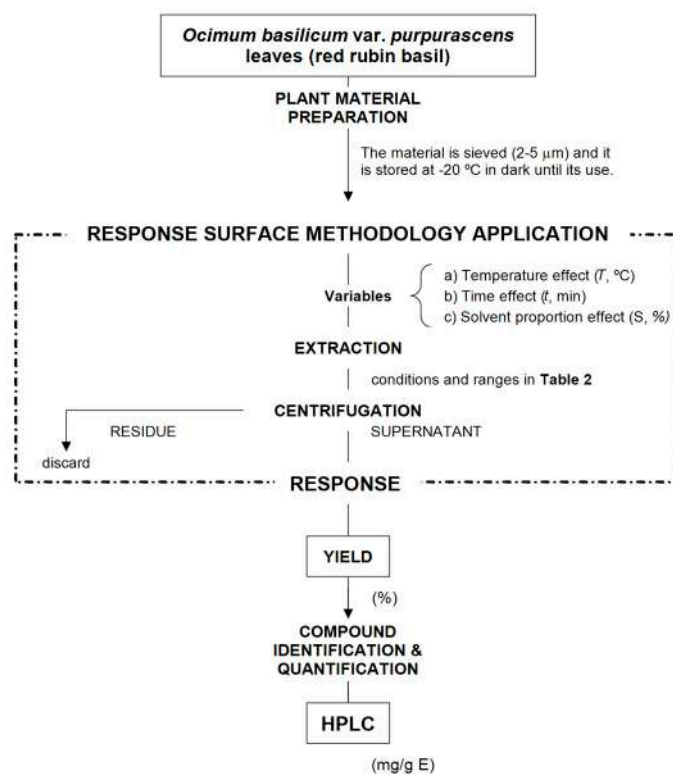
Figure 2. Diagram of the different steps carried out for optimizing the conditions that maximize the extraction responses of the anthocyanin compounds and the total extracted residue (Yield, %).

Table 2. The first part describes the experimental design that was applied in this work. The independent variables are presented in coded and natural values. The second part shows the response values for the detected anthocyanin compounds (mg/g E) and extraction yield (%) achieved for all the 28 experimental conditions performed for the HAE by the RSM design.

															Five-Level *CCCD* Experimental Design														
	Runs	1	2	3	4	5	6	7	8	9	10	11	12	13	14	15	16	17	18	19	20	21	22	23	24	25	26	27	28
Coded values	X_1: Time (t)	−1	−1	−1	−1	1	1	1	1	1.68	−1.68	0	0	0	0	−1.68	−1.68	−1.68	−1.68	1.68	1.68	1.68	1.68	0	0	0	0	0	0
	X_2: Temp. (T)	−1	−1	1	1	−1	−1	1	1	0	0	−1.68	1.68	0	0	−1.68	−1.68	1.68	1.68	−1.68	−1.68	1.68	1.68	0	0	0	0	0	0
	X_3: Solvent (S)	−1	1	−1	1	−1	1	−1	1	0	0	0	0	−1.68	1.68	−1.68	1.68	−1.68	1.68	−1.68	1.68	−1.68	1.68	0	0	0	0	0	0
Natural values	X_1: t (min)	40.3	40.3	40.3	40.3	99.7	99.7	99.7	99.7	120.0	20.0	70.0	70.0	70.0	70.0	20.0	20.0	20.0	20.0	120.0	120.0	120.0	120.0	70.0	70.0	70.0	70.0	70.0	70.0
	X_2: T (°C)	37.2	37.2	72.8	72.8	37.2	37.2	72.8	72.8	55.0	55.0	25.0	85.0	55.0	55.0	25.0	25.0	85.0	85.0	25.0	25.0	85.0	85.0	55.0	55.0	55.0	55.0	55.0	55.0
	X_3: S (%)	20.3	79.7	20.3	79.7	20.3	79.7	20.3	79.7	50.0	50.0	50.0	50.0	0.0	100.0	0.0	100.0	0.0	100.0	0.0	100.0	0.0	100.0	50.0	50.0	50.0	50.0	50.0	50.0
																Response Variables for RSM Application														
	P1	3.34	5.61	4.50	5.75	3.41	5.80	3.55	4.96	3.93	5.08	5.05	5.52	3.17	5.78	1.96	6.36	4.56	5.83	2.27	5.86	1.42	5.11	4.93	4.91	5.34	5.35	5.24	4.84
	P2	2.47	4.24	2.64	4.15	2.38	4.27	2.26	3.72	2.55	3.32	3.15	2.92	2.31	5.31	1.78	4.85	2.50	4.11	1.83	4.22	1.45	3.83	3.43	3.54	3.47	3.48	3.44	3.29
	P3	3.94	5.53	4.71	5.37	3.60	6.52	3.90	5.78	3.93	4.89	5.29	5.74	2.81	5.13	2.10	4.25	2.98	3.16	1.59	4.63	1.48	5.42	6.33	7.04	6.70	6.71	6.94	6.67
	P4	2.95	5.68	2.82	5.05	2.93	6.60	2.71	5.01	3.70	4.26	4.98	4.97	1.66	4.60	1.79	5.27	1.47	4.67	1.59	4.61	1.39	5.12	4.59	4.57	4.78	4.79	4.40	4.42
	P5	7.61	13.13	8.39	13.66	7.30	13.00	8.15	13.66	10.54	12.68	15.27	17.09	2.64	9.81	1.87	8.32	1.47	10.19	1.59	8.67	1.39	11.07	16.99	16.40	17.62	17.66	15.93	16.40
	P6	3.47	5.69	3.78	5.34	3.48	4.99	3.52	5.02	3.91	5.09	5.68	5.74	1.70	4.01	1.74	4.70	1.47	3.76	1.59	3.99	1.37	3.25	6.35	6.10	6.62	6.64	6.34	6.31
	P7	2.52	4.25	2.62	3.98	2.43	3.59	2.41	3.62	3.12	3.52	3.80	3.64	1.75	4.07	1.74	4.83	1.91	3.98	1.59	4.07	1.37	3.28	3.73	3.75	3.85	3.86	3.69	3.69
	P8	3.53	5.93	3.67	5.39	3.40	6.22	3.36	5.03	3.95	5.09	5.42	5.28	1.96	3.84	1.85	4.65	1.47	3.82	1.59	3.96	1.37	3.49	5.86	5.64	5.88	5.89	6.01	5.57
	P9	5.10	8.37	5.33	7.82	4.78	8.55	4.94	7.82	5.46	7.15	8.25	8.59	2.07	5.44	1.94	5.27	1.47	4.98	1.59	4.70	1.40	5.41	9.99	9.52	10.25	10.27	9.49	9.71
	P10	14.92	21.10	16.36	24.14	14.84	18.68	16.01	24.14	21.50	23.40	26.73	30.48	6.96	14.17	2.29	9.46	2.35	13.48	1.59	10.19	1.43	17.38	32.57	32.82	33.99	34.06	32.48	33.27
	P11	10.18	14.08	13.19	15.07	9.34	12.26	10.90	13.27	12.83	17.10	16.97	19.23	5.98	5.71	2.31	5.13	5.67	5.26	1.27	4.82	1.16	5.32	20.04	19.79	20.91	20.95	21.22	19.94
	P12	2.91	4.60	3.27	4.31	2.66	4.10	2.76	3.81	3.22	4.13	4.19	4.26	2.20	4.09	1.92	4.80	2.74	4.17	1.59	4.29	1.41	3.54	3.93	3.80	3.83	3.84	3.94	3.83
	P13	4.84	7.26	5.77	6.99	4.30	7.53	4.89	6.72	5.63	7.31	7.30	7.85	2.73	4.57	2.08	4.75	3.32	4.12	1.59	4.08	1.40	4.15	8.06	8.08	8.34	8.36	8.75	8.38
	TAC	67.78	105.46	77.06	107.01	64.86	102.12	69.37	102.56	84.25	103.00	112.07	121.30	37.96	76.52	25.38	72.65	33.37	71.53	21.22	68.10	18.04	76.37	116.79	115.97	111.59	111.85	117.87	116.32
	Yield	36.35	28.58	38.26	31.41	36.08	29.95	39.41	32.14	38.12	37.53	34.75	37.90	38.84	18.08	35.62	13.22	38.27	17.80	35.42	16.52	41.00	20.24	35.68	34.54	35.68	35.61	35.54	35.40

P: anthocyanin compound; TAC: Total anthocyanin content.

The content in individual (**P1** to **P13**) and grouped (TAC – total anthocyanin compounds) anthocyanin compounds were used as criteria to maximize their content and to optimize the extraction conditions of HAE from red rubin basil leaves under RSM assessment. The values of the extraction yield were also considered, and ranged from 13.22 to 41.00%, with the experimental runs no. 16 and 21, respectively (Table 2). In total, 15 response variables are taking into account for the optimization processes.

2.2. Theoretical Response Surface Models

Evaluating the precision of theoretical models to predict and comprehended the effects of independent variables in some response variable is necessary. This, as in many research fields, is achieved by fitting these models to the experimental values. In this study, a non-linear algorithm (least-squares estimates) has been used to adjust the response values (Table 2) to a second order polynomial model. The estimated coefficient values obtained from the polynomial model of Equation (1) and the coefficient of correlation (R^2) for each parametric response of the extraction process are shown in Table 3.

$$y = b_0 + \sum_{i=1}^{n} b_i X_i + \sum_{\substack{i=1 \\ j>i}}^{n-1} \sum_{j=2}^{n} b_{ij} X_i X_J + \sum_{i=1}^{n} b_{ii} X_i^2 \tag{1}$$

The parametric values obtained, not only it allows to translate response patterns, it also helps to undestand the complexity of the possible interactions between variables. However, some of the parameters of Equation (1) whose coefficients were non-significant (*ns*) at a 95% confidence level ($\alpha = 0.05$) were not used for building the model. By means of the statistic lack of fit it is possible to prove the adequacy of the obtained models and in this way it was demonstrated that a considerable improvement was not achieved by means of the inclusion of the statistically *ns* parametric values. Each of the 15 assessed responses can be seen in models in Table 4 getting in all cases R^2 coefficients higher than 0.92 (Table 3). According to this value, it can be said that the percentage of variability of each response can be explained by the model.These workable models were applied in the subsequent prediction and optimization steps, with a good agreement between the experimental and predicted values, which indicates that the variation is explained by the independent variables.

Although the obtained model coefficients (Table 3) cannot be associated with physical or chemical significance and are empirical, they can however be used to predict the results of untested extraction conditions [17]. As the effect sign marks the performance of the response, if a factor has a positive effect, the response is higher at the high level. On the other hand, the response is lower at the high level when a factor has a negative effect. Therefore, the weight of the corresponding variable will be more important the higher the absolute value of a coefficient. Certain characteristics relating to the general effects of the variables based on mathematical expressions can be observed in Table 4. The relevance of the significant parametric values can be order as a function of the variables involved in a decreasing form as $S > t \gg T$. Previous authors that work with similar matrices [14], have concluded that the most relevant variable on the HAE extraction of bioactive compounds is *S*. As for the study of the linear, quadratic, and interactive parametric effects of the developed equations, it allowed to conclude that all these parameters play an important and significant role in all evaluated responses. For the linear effect, the variables *S* and *t* had strong values, while the effect of *T* was less important in almost all cases. All independent variables had moderate quadratic or nonlinear effects. As for the interactions of the variable (*tT*, *TS* and *tS*), these were of minor importance. The results obtained were represented in the response surface plots that can be seen below so that in this way one can see in a more obvious way the combined effects as well as to be able to visually describe the tendencies of extraction. The optimal HAE conditions, that maximize their retrieval from red rubin basil leaves, are presented in Table 3.

Table 3. Estimated coefficients and R^2 determined for the models obtained for individual and grouped anthocyanin compounds and extraction yield (Table 3), and optimal HAE conditions and response values.

Response variables	Intercept	Linear Effect			Quadratic Effect			Interactive Effect			R^2	t (min)	T (°C)	S (%)	Optimum
	b_0	b_1 (t)	b_2 (T)	b_3 (S)	b_{11} (t^2)	b_{22} (T^2)	b_{33} (S^2)	b_{12} (tT)	b_{13} (tS)	b_{23} (TS)					
P1	5.06 ± 0.15	−0.28 ± 0.09	ns	0.92 ± 0.09	−0.16 ± 0.11	ns	−0.17 ± 0.11	−0.17 ± 0.06	0.07 ± 0.06	−0.15 ± 0.06	0.9441	81.06 ± 2.08	20.00 ± 1.73	100.00 ± 1.58	6.56 ± 0.31
P2	3.37 ± 0.10	−0.15 ± 0.06	ns	0.76 ± 0.06	−0.20 ± 0.07	ns	0.11 ± 0.07	−0.04 ± 0.00	ns	−0.07 ± 0.04	0.9556	64.04 ± 5.07	20.00 ± 0.43	100.00 ± 9.11	5.15 ± 0.36
P3	31.23 ± 1.68	ns	0.96 ± 0.95	ns	−2.14 ± 1.15	ns	−5.40 ± 1.15	ns	0.98 ± 0.68	ns	0.9359	70.00 ± 3.94	90.00 ± 6.07	50.00 ± 3.80	32.85 ± 2.47
P4	4.65 ± 0.19	ns	−0.20 ± 0.11	1.06 ± 0.11	−0.11 ± 0.01	ns	−0.41 ± 0.13	ns	ns	ns	0.9225	70.00 ± 5.49	20.00 ± 1.94	88.44 ± 5.39	5.67 ± 1.05
P5	15.59 ± 0.62	ns	0.33 ± 0.22	2.42 ± 0.35	−0.95 ± 0.42	ns	−2.85 ± 0.42	ns	ns	ns	0.9449	70.00 ± 1.26	90.00 ± 5.25	62.60 ± 5.86	16.66 ± 1.76
P6	5.90 ± 0.27	−0.16 ± 0.15	−0.10 ± 0.01	0.74 ± 0.15	−0.31 ± 0.18	ns	−0.89 ± 0.18	ns	ns	ns	0.9336	62.47 ± 1.24	20.00 ± 0.31	62.27 ± 3.93	6.24 ± 0.56
P7	3.63 ± 0.08	−0.16 ± 0.05	−0.09 ± 0.05	0.70 ± 0.05	−0.08 ± 0.06	ns	−0.23 ± 0.06	ns	ns	−0.07 ± 0.03	0.9701	40.93 ± 1.60	20.00 ± 1.49	100.00 ± 6.12	4.59 ± 0.34
P8	5.59 ± 0.18	−0.13 ± 0.10	−0.14 ± 0.10	0.77 ± 0.10	−0.23 ± 0.12	ns	−0.80 ± 0.12	ns	ns	ns	0.9456	61.55 ± 4.64	20.00 ± 1.03	64.30 ± 1.89	6.03 ± 0.55
P9	9.06 ± 0.43	ns	−0.12 ± 0.02	1.15 ± 0.24	−0.62 ± 0.30	ns	−1.52 ± 0.30	ns	ns	ns	0.9286	70.00 ± 1.16	20.00 ± 1.24	61.18 ± 2.85	9.47 ± 1.32
P10	29.87 ± 1.32	ns	0.85 ± 0.74	2.89 ± 0.74	−2.07 ± 0.91	ns	−6.27 ± 0.91	ns	ns	ns	0.9377	70.00 ± 1.42	90.00 ± 2.46	56.85 ± 0.94	31.63 ± 2.42
P11	8.93 ± 0.25	−0.32 ± 0.14	−0.12 ± 0.14	0.63 ± 0.14	−0.47 ± 0.17	ns	−1.64 ± 0.17	ns	ns	−0.10 ± 0.01	0.9359	59.99 ± 5.19	20.00 ± 0.59	57.18 ± 0.16	9.28 ± 0.38
P12	3.91 ± 0.06	−0.22 ± 0.03	−0.03 ± 0.03	0.65 ± 0.03	−0.06 ± 0.04	ns	−0.25 ± 0.04	−0.05 ± 0.02	ns	−0.09 ± 0.02	0.9757	36.49 ± 0.30	20.00 ± 1.21	98.54 ± 9.29	4.71 ± 0.20
P13	7.93 ± 0.20	−0.26 ± 0.11	−0.16 ± 0.11	0.73 ± 0.11	−0.37 ± 0.03	ns	−1.37 ± 0.13	ns	0.09 ± 0.08	−0.10 ± 0.01	0.9451	60.74 ± 0.00	20.00 ± 1.30	59.46 ± 0.04	8.38 ± 0.29
TAC	109.78 ± 2.73	−1.93 ± 1.54	1.07 ± 0.32	14.30 ± 1.54	−6.20 ± 1.87	ns	−17.00 ± 1.87	ns	ns	ns	0.9577	65.37 ± 3.62	90.00 ± 1.17	62.50 ± 4.24	114.74 ± 0.58
Yield	36.43 ± 1.46	0.49 ± 0.88	1.19 ± 0.87	−5.56 ± 0.87	ns	ns	−3.09 ± 0.84	ns	ns	ns	0.9592	120.00 ± 2.62	90.00 ± 7.72	23.23 ± 0.91	41.77 ± 1.59

ns: non-significant coefficient; R^2: Correlation coefficient; **P**: anthocyanin compound; TAC: total anthocyanin content.

Table 4. Mathematical models produced after fitting Equation (1) to the data set (individual and grouped values).

Anthocyanin Compounds	Equations	Equation Numbers
P1	$Y_{P1} = 5.06 - 0.28t + 0.92S - 0.16t^2 - 0.17S^2 - 0.17tT + 0.07tS - 0.15TS$	Equation (2)
P2	$Y_{P2} = 3.37 - 0.15t + 0.76S - 0.20t^2 - 0.11S^2 - 0.04tT - 0.07tS$	Equation (3)
P3	$Y_{P3} = 31.23 + 0.96T - 2.14t^2 - 5.40S^2 + 0.98tS$	Equation (4)
P4	$Y_{P4} = 4.65 - 0.20T + 1.06S - 0.11t^2 - 0.41S^2$	Equation (5)
P5	$Y_{P5} = 15.59 + 0.33T + 2.42S - 0.95t^2 - 2.85S^2$	Equation (6)
P6	$Y_{P6} = 5.90 - 0.16t - 0.10T + 0.74S - 0.31t^2 - 0.89S^2$	Equation (7)
P7	$Y_{P7} = 3.63 - 0.16t - 0.09T + 0.70S - 0.08t^2 - 0.23S^2 - 0,07TS$	Equation (8)
P8	$Y_{P8} = 5.59 - 0.13t - 0.14 + 0.77S - 0.23t^2 - 0.80S^2$	Equation (9)
P9	$Y_{P9} = 9.06 - 0.12T + 1.15S - 0.62t^2 - 1.52S^2$	Equation (10)
P10	$Y_{P10} = 29.87 + 0.85T + 2.89S - 2.07t^2 - 6.27S^2$	Equation (11)
P11	$Y_{P11} = 8.93 - 0.32t - 0.12 + 0.63S - 0.47t^2 - 1.64S^2 - 0,10TS$	Equation (12)
P12	$Y_{P12} = 3.91 - 0.22t - 0.03T + 0.65S - 0.06t^2 - 0.25S^2 - 0,05tT - 0,09TS$	Equation (13)
P13	$Y_{P13} = 7.93 - 0.26t - 0.16T + 0.73S - 0.37t^2 - 1.37S^2 + 0.09tS - 0.10TS$	Equation (14)
TAC	$Y_{TAC} = 109.78 - 1.93t + 1.07T + 14.30S - 6.20t^2 - 17.00S^2$	Equation (15)
Yield	$Y_{Yield} = 36.43 + 0.49t + 1.19T - 5.56S - 3.09S^2$	Equation (16)

2.3. Final Effects of the Studied Conditions of HAE on the Target Responses and Optimal Values that Maximize the Responses

Figure 3 shows the response surface plots of extraction yield, *TAC* and two other representative anthocyanins extracted (**P1** and **P10**), as well as their statistical analysis. Inspecting the given surface plots of the extraction yield (Figure 3), it is conceivable to confirm that the measure of removed material increments to an ideal point and afterward, by and large, it diminishes as a component of the included variables. Subsequently, the ideal values can be found similar to a solitary point, which permits figuring the extraction conditions that lead to the most extreme flat out. This behaviour is common to almost all responses, allowing us to determine the conditions that maximize the responses. In consequence, the ideal extraction values for the reactions shown in Figure 3 were determined for the HAE conditions (Table 3), as summarized below:

For yield, the optimal HAE conditions were: $t = 120.00 \pm 2.62$ min, $T = 85.00 \pm 7.72$ °C and 23.23 ± 0.91% of ethanol (v/v), and produced 41.77 ± 1.59%.

For TAC, the optimal HAE conditions were: $t = 65.37 \pm 3.62$ min, $T = 85.00 \pm 1.17$ °C and 62.50 ± 4.24% of ethanol (v/v), and produced 114.74 ± 0.58 mg/g of E.

For **P1**, the optimal HAE conditions were: $t = 81.06 \pm 2.08$ min, $T = 25.00 \pm 1.73$ °C and 100.00 ± 1.58% of ethanol (v/v), and produced 6.56 ± 0.31 mg/g of E.

For **P10**, the optimal HAE conditions were: $t = 70.00 \pm 1.42$ min, $T = 85.00 \pm 2.46$ °C and 56.85 ± 0.94% of ethanol (v/v), and produced 31.63 ± 2.42 mg/g of E.

It is well-known that the utilization of high values of ethanol in the solvent, increases the extraction of bioactive compounds from plant materials [13]. The effects of the independent variables on the extraction of individual anthocyanin compounds from red rubin basil leaves are represented in 2D in Figure 4. The processing conditions that generated optimal response values (⊙) are numerically described in Table 3. The identified anthocyanin compounds were organized as a function of the maximum amount achieved (mg/g of extract) in a decreasing order as follows: **P3** (32.85) > **P10** (31.63) >> **P5** (16.66) >> **P9** (9.47) > **P11** (9.28) > **P13** (8.38) > **P1** (6.56) > **P6** (6.24) > **P8** (6.03) > **P4** (5.67) > **P2** (5.15) > **P7** (4.59) > **P2** (4.71).
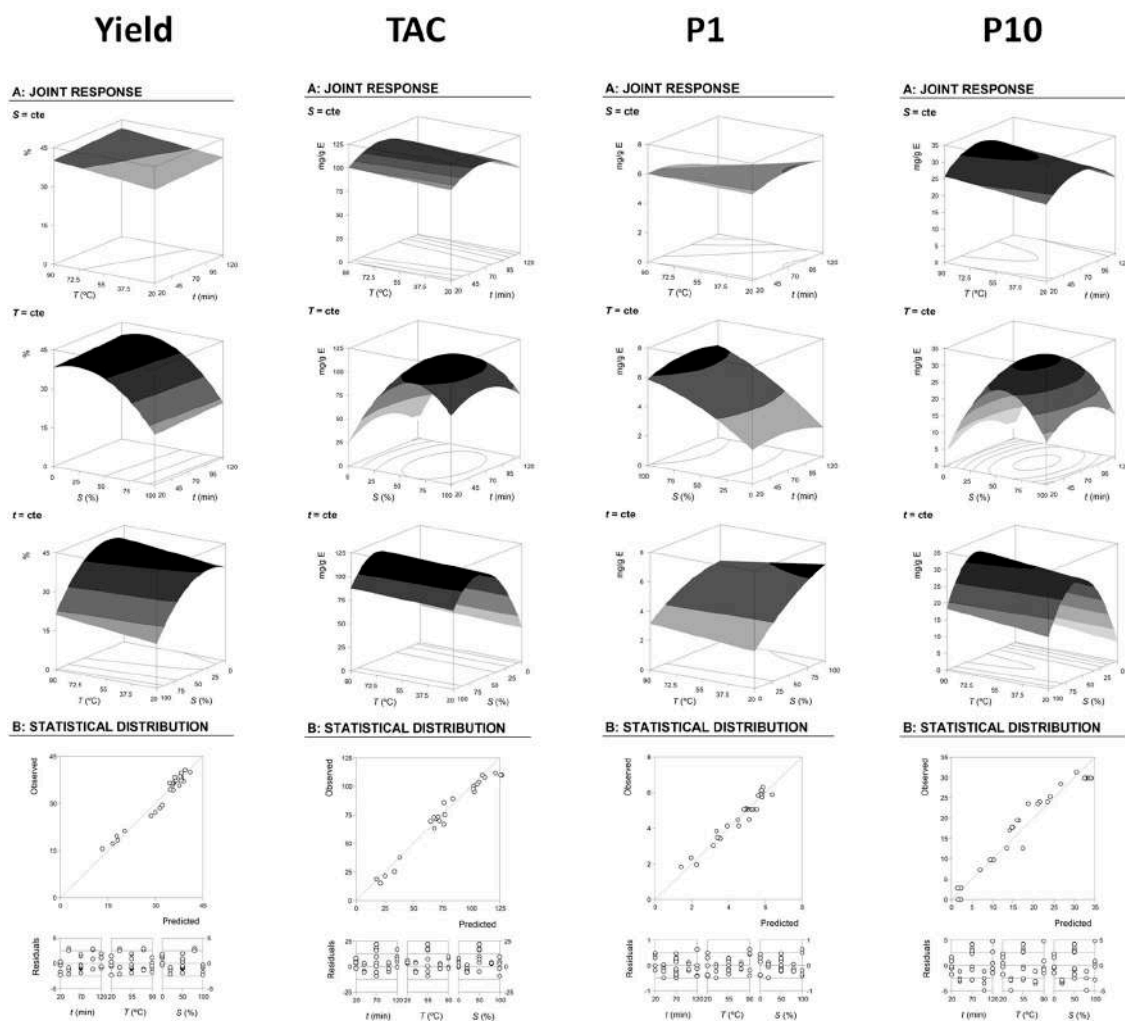
Figure 3. Illustrative representation of the extraction yield and grouped anthocyanin compounds (total anthocyanin acids, total flavonoids and total anthocyanin compounds) responses. The part A shows the 3D description as a function of each independent variable. The surfaces were constructed using the values presented in Table 3 and described by Equation (1). In each graph, the excluded variable was positioned at the optimum of their experimental domain (Table 3). Part B shows a summary of the goodness of fit using the observed/predicted and the residual distribution plots as a function of each variable.
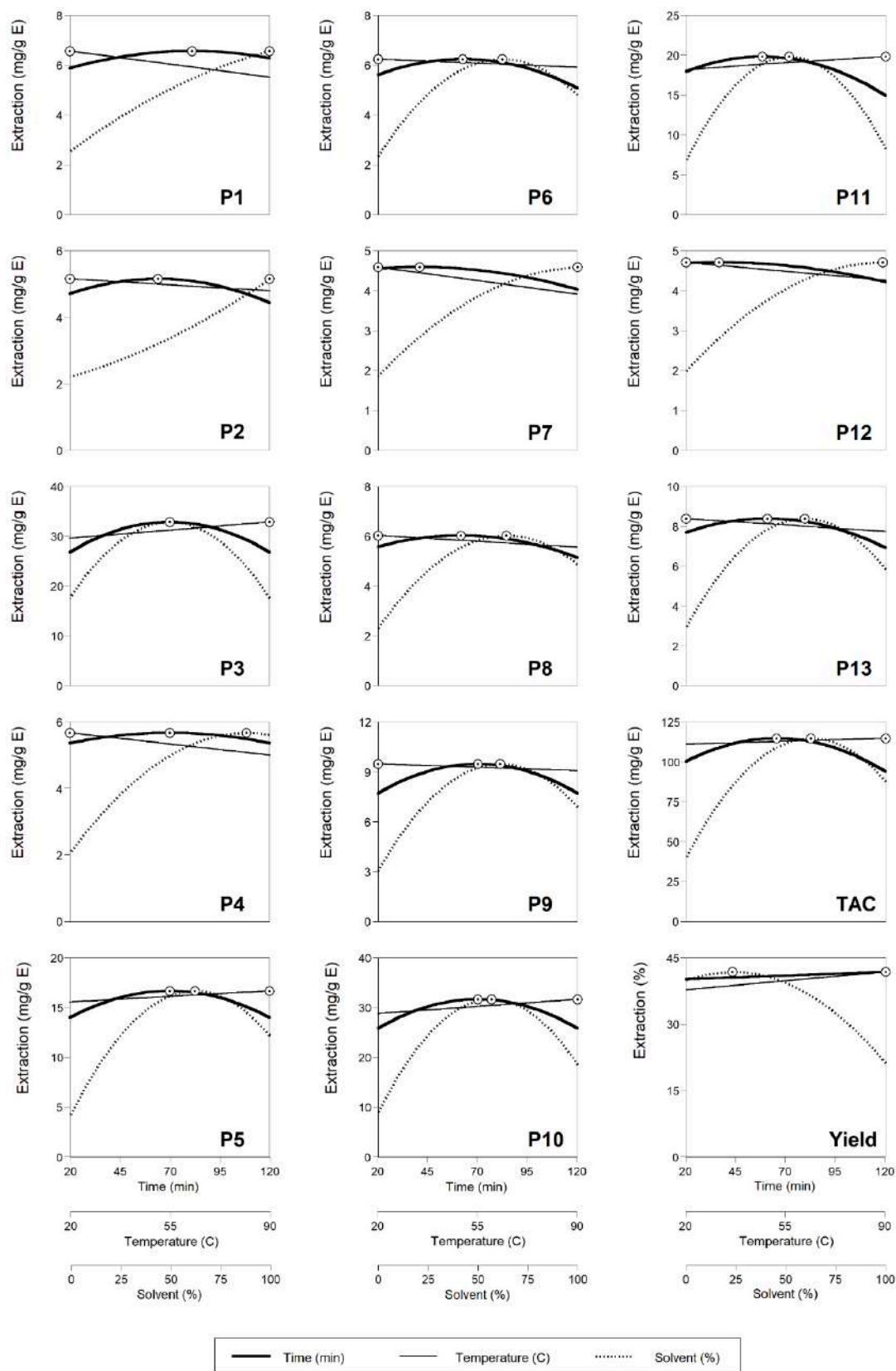
Figure 4. 2D graphical response of the effects of the independent variables on the extraction of anthocyanin compounds from red rubin basil leaves (see Figure 1 for peak identification). Dots (⊙) represent the optimal values. In each plot, each independent variable was positioned at the optimal value of the other two variables (Table 3).

The greater extraction values achieved under these optimized conditions highlight the suitability of HAE with RSM as an innovative process to recover a greater amount of anthocyanin compounds from red rubin basil leaves using shorter processing times and greener solvents.

2.4. Clustering of Anthocyanin Compounds According to the HAE Conditions that Maximize their Extraction

The maximum values for the response values of the different anthocyanin compounds and their concentrations if extracted under the optimal HAE conditions of the other compounds (Table 3) are presented in Table 5. The values of subparagraph (B) is the ratio of the optimum value of each compound between the maximum of the other compounds. When two compounds show values of 100%, i.e., the coefficient is 1, under the same conditions of HAE means that the optimal response value for both is in the same conditions. As example, the compounds **P1**, **P2**, **P4**, **P7** and **P12** were clustered in C1 under the same HAE conditions (Figure 5). By cons, if the coefficient is different from 1, it means that the conditions that are optimal for the extraction of a compound are not for the other (compounds **1** and **13**).

Table 5. Maximum response values of each anthocyanin compound and their values at the optimal processing conditions of the other compounds presented in Table 3.

(A) Maximum Response Values (mg/g of Extract) of the Individual Anthocyanin Compounds												
Peak:	P1	P2	P3	P4	P5	P6	P7	P8	P9	P10	P11	P12	P13
Optimum:	6.56	5.15	32.85	5.67	16.66	6.24	4.59	6.03	9.47	31.63	9.28	4.71	8.38

(B) Values of each Anthocyanin Compound at the Optimal Conditions of the other Compounds													
	P1	P2	P3	P4	P5	P6	P7	P8	P9	P10	P11	P12	P13
P1	1	0.99	0.77	0.96	0.81	0.84	0.95	0.85	0.83	0.79	0.81	0.94	0.82
P2	0.99	1	0.65	0.91	0.71	0.73	0.98	0.74	0.72	0.68	0.70	0.95	0.71
P3	0.45	0.42	1	0.63	0.97	0.87	0.33	0.85	0.88	0.99	0.88	0.33	0.88
P4	0.99	0.99	0.76	1	0.83	0.94	0.97	0.95	0.94	0.80	0.92	0.97	0.93
P5	0.65	0.66	0.97	0.80	1	0.93	0.61	0.93	0.93	0.99	0.92	0.61	0.93
P6	0.75	0.77	0.92	0.89	0.94	1	0.74	1.00	1.00	0.94	1.00	0.75	1.00
P7	0.97	0.99	0.76	0.97	0.80	0.90	1	0.91	0.88	0.79	0.87	1.00	0.88
P8	0.79	0.81	0.89	0.91	0.92	1.00	0.79	1	1.00	0.91	0.99	0.80	1.00
P9	0.72	0.72	0.93	0.86	0.96	1.00	0.66	0.99	1	0.95	0.99	0.66	0.99
P10	0.48	0.49	0.99	0.69	0.99	0.90	0.43	0.89	0.91	1	0.90	0.44	0.90
P11	0.61	0.63	0.94	0.80	0.93	0.99	0.61	0.99	0.99	0.94	1	0.63	1.00
P12	0.97	0.99	0.82	0.98	0.85	0.91	1.00	0.92	0.90	0.84	0.89	1	0.90
P13	0.69	0.70	0.91	0.84	0.91	1.00	0.67	1.00	1.00	0.92	1.00	0.68	1
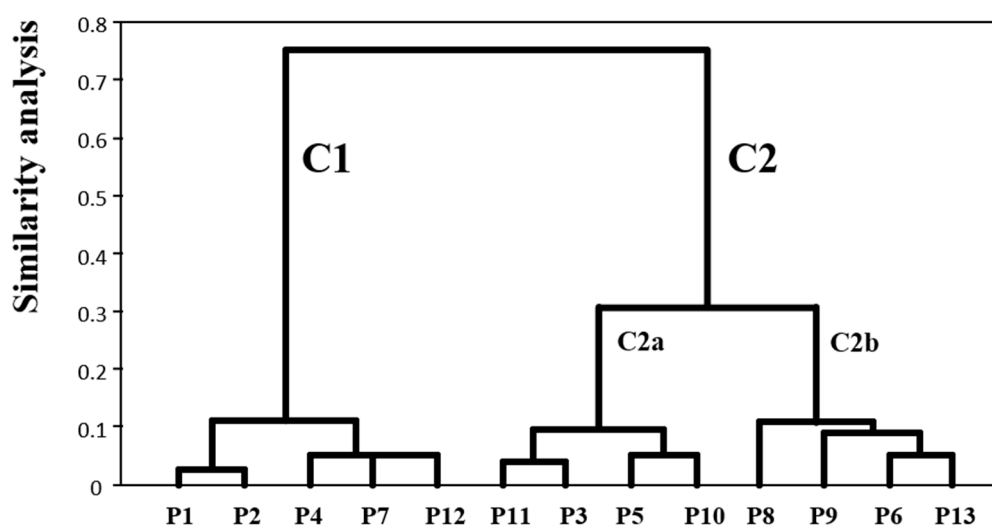
Figure 5. HCA dendrogram of anthocyanin compounds according to the HAE conditions that maximize their extraction from red rubin basil leaves.

In Table 5 it can be observed the formation of different groups of compounds of anthocyanin with maximum response values in conditions of HAE extraction similar. The division in these groups was made possible by the complete data set of Table 5 and by performing a multi objective optimization problem using an appropriate clustering algorithm. The results of Hierarchical Cluster Analysis (HCA) are presented in Figure 5. In the HCA dendrogram, the shorter distance between compounds, the higher similarity in terms of conditions that favour their extraction. Moreover, compounds belonging to the same group are better extracted under similar HAE conditions. Two significant clusters (C1 and C2), being the C2 divided in turn into 2 subgroups (a and b). Other less important subgroups were created, but they can be considered as a residual noise produced by the algorithm.

Cluster C1 included the compounds **P1**, **P2**, **P4**, **P7** and **P12**. The extraction of these compounds for maximize by medium *t*, high *S* and low/high *T* (Table 3 and Figure 3). The subgroups were mainly differentiated by the *T* values.

Cluster C2 included all other compounds **P11**, **P3**, **P5**, **P10**, **P8**, **P9**, **P6** and **P13**, which were subdivided in C2a and C2b. For maximizing the extraction of the compounds in C2a low *T* and medium *S* was used. On the other hand, the compounds in C2b was maximized when using high *T* and medium *S*.

Although it was expected that if the compounds have similar chemical characteristics also would have similar HAE conditions, the HCA analysis was an interesting and innovative approach in the field of extraction of high added-value compound from natural sources since this analysis highlighted suitable HAE conditions for maximize the simultaneous recovery of specific groups of compounds from red rubin basil leaves.

2.5. Dose-Response Analysis of the Solid-to-Liquid Effect at the Optimum Conditions

Thanks to the precise results obtained by HPLC, the *S/L* effect was tested under the optimal conditions provided for each extractive technique by the polynomial models, using the amount of anthocyanin as response. As confirmed by the preliminary results (data not shown), the maximum experimental value is close to 30 g/L, since at higher values of *S/L* it is observed experimental stirring, so an experiment was designed for each extractive process in which to check the *S/L* behaviour at values between 1 and 30 g/L. The obtained results are consistent with previous responses. It was observed that the effect caused by the *S/L* ratio follows a simple linear model with an intercept, and that this model follows a slightly decreasing pattern proportional to the increase of *S/L* in all the assays. However, that pattern, explained by the parametric coefficient of the slope, was non-significant with a confidence interval level of 95 % ($\alpha = 0.05$) and the decreasing effect was not taken into account for further analysis. In conclusion, it can be affirmed that the increase in the *S/L* ratio has very little effect on the *TAC* extraction, besides that saturation effects were not observed at any value below 30 g/L.

2.6. Evaluation of the Colorant Potential of the Extract Rich in Anthocyanin Compounds Obtained under Optimum Conditions from Leaves of O. basilicum var. purpurascens

The results of the chromatic analysis in the CIE *L*a*b** colour space of the extract rich in anthocyanins present in the leaves of *O. basilicum* var. *purpurascens* are shown in Table 6. The colour of the pigmented extract showed an *L** value, lightness (0 to 100), of 20.5 ± 0.5; and in parameters *a** (colour intensity from green to red (−120 to 120)) and *b** (colour is evaluated at the intensity level from blue to yellow (−120 to 120)), the values were 33.0 ± 0.1 and 8.2 ± 0.4, respectively.

For a better understanding of the colour values, these were converted to RGB values and the colour obtained from the extract, red-berry, can be visualized. These results can be justified by the presence of anthocyanin compounds in the extract, which, in addition to having darker shades, are also characterized by blue, red and purple tones. The concentration of total anthocyanin compounds, obtained in the optimized extract, was similar to that predicted by the model.

Table 6. Amount of anthocyanins (cyanidin and pelargonidin derivatives) and color parameters under optimal conditions (mean ± SD).

Quantification (mg/g E)	L*	a*	b*	Conversion Color to RGB Values
115.4 ± 0.4	20.5 ± 0.5	33.0 ± 0.1	8.2 ± 0.4	

L* lightness; a* chromatic axis from green (−) to red (+); b* chromatic axis from blue (−) to yellow (+).

2.7. Evaluation of the Bioactive Properties of the Extract Rich in Anthocyanin Compounds Obtained under Optimal Conditions from Leaves of O. basilicum var. purpurascens

2.7.1. Antimicrobial Activity

Table 7 shows the results of the antimicrobial activity obtained from the extract rich in anthocyanins present in the leaves of *O. basilicum* var. *purpurascens*. The results demonstrate antibacterial activity of the pigmented extract for all microorganisms' strains. In this way, the best results are obtained against *Bacillus cereus* (*B.c.*) (MIC = 0.037 mg/mL; MBC = 0.075 mg/mL) and *Escherichia coli* (*E.c.*) (MIC = 0.037 mg/mL; MBC = 0.075 mg/mL) strains. However, the pigmented extract also showed a high activity against *Listeria monocytogenes* (*L.m.*) (MIC = 0.05 mg/mL; MBC = 0.075 mg/mL), *Staphylococcus aureus* (*S.a.*), *Enterobacter cloacae* (*En.cl.*) (MIC = 0.075 mg/mL, MBC = 0.15 mg/mL), and *Salmonella typhimirium* (*S.t.*) (MIC = 0.15 mg/mL; MBC= 0.30 mg/mL).

Table 7. Antibacterial activity (MIC and MBC, mg/mL) and antifungal activity (MIC and MFC, mg/mL) of the anthocyanins rich extract obtained under optimal extraction conditions.

Antibacterial Activity							
		B.c.	S.a.	L.m.	E.c.	En.cl.	S.t.
Anthocyanins rich extract	MIC	0.037	0.075	0.05	0.037	0.075	0.15
	MBC	0.075	0.15	0.075	0.075	0.15	0.30
Streptomycin [1]	MIC	0.10	0.04	0.20	0.20	0.20	0.20
	MBC	0.20	0.10	0.30	0.30	0.30	0.30
Ampicillin [1]	MIC	0.25	0.25	0.40	0.40	0.25	0.75
	MBC	0.40	0.45	0.50	0.50	0.50	1.20
Antifungal Activity							
		A.fun.	A.o.	A.n.	P.f.	P.o	P.v.c.
Anthocyanins rich extract	MIC	0.037	0.002	0.075	0.075	0.30	0.30
	MFC	0.075	0.075	0.15	0.15	0.45	0.45
Ketoconazole [1]	MIC	0.25	0.20	0.20	0.20	2.50	0.20
	MFC	0.50	0.50	0.50	0.50	3.50	0.30
Bifonazole [1]	MIC	0.15	0.10	0.15	0.20	0.20	0.10
	MFC	0.20	0.20	0.20	0.25	0.25	0.20

[1] Positive controls. *B.c.*: *Bacillus cereus*; *S.a.*: *Staphylococcus aureus*; *L.m.*: *Listeria monocytogenes*; *E.c.*: *Escherichia coli*; *En.cl.*: *Enterobacter cloacae*; *S.t.*: *Salmonella typhimurium*; *A.fum.*: *Aspergillus fumigatus*; *A.o.*: *Aspergillus ochraceus*; *A.n.*: *Aspergillus niger*; *P.f.*: *Penicillium funiculosum*; *P.o.*: *Penicillium ochrochloron*; *P.v.c.*: *Penicillium verrucosum* var. *cyclopium*. MIC—minimum inhibitory concentration; MBC—minimum bactericidal concentration; MFC—minimum fungicidal concentration.

Regarding antifungal activity, the extract showed a high potential against most of the tested fungi. *Aspergillus ochraceus* (*A.o.*) was the most susceptible species to the extract (MIC = 0.002 mg/mL; MFC = 0.075 mg/mL); however, no antifungal activity was observed against *Penicillium verrucosum* var. *cyclopium* (*P.v.c.*) (MIC = 0.30 mg/mL; MFC = 0.45 mg/mL). These results indicated a promising antimicrobial activity, and this can be explained due to the high concentration of anthocyanin compounds that have a high antimicrobial potential [18].

2.7.2. Cytotoxic Activity

Table 8 shows the results obtained in the cytotoxicity evaluation assays in extracts rich in anthocyanin compounds, obtained through optimal extraction conditions. The extract exhibited anti-proliferative capacity in HeLa (GI_{50} = 213 ± 9 µg/mL) and HepG2 (GI_{50} = 198 ± 9 µg/mL) tumour cell lines.

Table 8. Cytotoxic activity of the anthocyanins rich extract obtained under optimal extraction conditions (mean ± SD).

Tumor Cell Lines	Concentrations (GI_{50} Values, µg/mL)
MCF-7 (breast carcinoma)	>400
NCI-H460 (lung carcinoma)	>400
HeLa (cervical carcinoma)	213 ± 9
HepG2 (hepatocellular carcinoma)	198 ± 9
Non-Tumour Cells	
PLP2 (non-tumor porcine liver primary cells)	>400

GI_{50} values - concentration that inhibited 50% of cell growth. Ellipticin GI_{50} (positive control): 1.21 µg/mL (MCF-7), 1.03 µg/mL (NCI-H460), 0.91 µg/mL (HeLa), 1.10 µg/mL HepG2) and 2.29 µg/mL (PLP2).

These results may also be explained by the high levels of anthocyanin compounds present in the extract, since these molecules have been described, by several authors, as a potential anti-proliferative agent in tumor cell lines [19]. Regarding the assay performed on primary non-tumor cell culture (PLP2), the extract evidenced the absence of toxicity up to the maximal tested concentration (GI_{50} > 400 µg/mL).

3. Materials and Methods

3.1. Samples

Ocimum basilicum var. *purpurascens* (Lamiaceae) variety was obtained in Cantinho das Aromáticas, Vila Nova de Gaia, Portugal. The samples acquired were planted to grow in greenhouse at the Polytechnic Institute of Bragança and then collected (September 2017). The fresh leaves were separated through a mechanical procedure, posteriorly lyophilized (FreeZone 4.5, Labconco, Kansas City, MO, USA), reduced to a fine and homogeneous dried powder (~20 mesh) and stored protected from light and heat.

3.2. Heat-Assisted Extraction

Heat-Assisted Extraction (HAE) was performed in a water reactor agitated internally with a Cimarec^{TM} Magnetic Stirrer at a constant speed (~500 *rpm*, Thermo Scientific, San Jose, CA, USA), following a procedure previously performed by Roriz et al. [20]. The powdered samples (300 mg) were extracted with solvent (20 mL of ethanol/water) under diverse conditions, as previously defined by the established RSM plan (Table 2). The ranges of the experimental design were: time (*t* or X_1, 20 to 120 min), temperature (*T* or X_2, 25 to 85 °C) and ethanol content (*S* or X_3, 0 to 100%). The solid-to-liquid ratio (*S/L*) was kept at 15 g/L for all conditions.

When all the individual extraction conditions were carried out, the samples were immediately centrifuged (4750× *g* during 20 min at 10 °C) and filtered (paper filter Whatman n° 4) to eliminate the non-dissolved material. The supernatant was collected and divided in two portions for HPLC and extraction yield analysis. The portion separated for HPLC analysis (2 mL) was filtered through a LC filter disk (0.22 µm), whereas the portion for the extraction yield determination (5 mL) was dried at 105 °C during 48 h and thereafter weighted.

3.3. Calculation of the Extraction Yield

The extraction yields (%) were calculated based on the dry weight (crude extract) obtained after evaporation of the solvent. In all cases, the filtrates were concentrated at 35 °C in a rotary evaporator (Büchi R-210, Flawil, Switzerland) under reduced pressure and the aqueous phase was then lyophilised to obtain a dried extract.

3.4. Chromatographic Analysis of Anthocyanin Compounds

The samples were analysed using Dionex Ultimate 3000 UPLC (Thermo Scientific, San Jose, CA, USA) coupled to a diode de array detector (chromatograms recorded at 520 nm) and to a Linear Ion Trap LTQ XL mass spectrometer (Thermo Finnigan, San Jose, CA, USA) equipped with an ESI source working in positive mode, following a procedure previously reported [21]. Quantitative analysis was performed using a calibration curve obtained using cyanidin-3-glucoside (y = 97,787x − 743,469; R^2 = 0.9993) and pelargonidin-3-glucoside (y = 43,781x − 275,315; R^2 = 0.9989) and results were expressed in mg per g of extract (mg/g E).

3.5. Experimental Design, Modelling and Optimization

3.5.1. Experimental Design

A RSM of five-level *CCCD* of 28 runs with 6 replicated values at centre points was applied to optimize the HAE conditions for the extraction of anthocyanin compounds. Coded and natural values of the independent variables X_1 (processing time (t), min), X_2 (temperature (T), °C) and X_3 (solvent (S), % of ethanol, *v/v*) are presented in Table 1.

3.5.2. Mathematical Modelling

The response surface models were fitted by means of least-squares calculation using the following second-order polynomial equation with interactive terms (Equation (1)). In this equation, Y represents the dependent variable (response variable) to be modelled, X_i and X_j are the independent variables, b_0 is the constant coefficient, bi is the coefficient of linear effect, b_{ij} is the coefficient of interaction effect, b_{ii} is the coefficient of quadratic effect, and n is the number of variables. The extraction yield and the individual and grouped anthocyanin compounds, 13 individual compounds plus the total anthocyanin content (*TAC*), were used as dependent variables.

3.5.3. Maximization of the Responses

For the extraction yield and the recovery of phenolic compounds responses, a *simplex* method was used for maximize the models developed of Equation (1) [22]. In all cases, restrictions were added to limit the values of the conditions assessed.

3.6. Gropping the Responses by Cluster Analyses

A cluster analysis was performed to group the anthocyanin compounds according to the extraction conditions that maximize their response values using the Excel add-in "XLSTAT 2016" (Addinsoft, Barcelana, Spain). A comparative agglomerative hierarchical clustering analysis (HCA) with automatic truncation based on entropy and Pearson correlation coefficient were used for clustering (similarity analysis).

3.7. Fitting Procedures and Statistical Analysis

Fitting procedures, coefficient estimates and statistical calculations were performed as previously described by Prieto and Vázquez [23]. In brief: (a) fitting procedure by nonlinear least-square (quasi-Newton) as provided by the Excel add-in "Solver"; (b) coefficient intervals determination by the Excel add-in "SolverAid"; and (c) the model consistency by common statistical tests for each

model developed: (i) the Fisher F-test (α = 0.05); (ii) parametric assessment by the Excel add-in ";SolverStat"; (iii) the determination of R^2.

3.8. Preparation of the Extract Rich in Anthocyanin Compounds Obtained under Optimum Conditions from the Leaves of O. basilicum var. purpurascens

For the preparation of an extract rich in anthocyanin compounds, extraction from the leaves of *O. basilicum* var. *purpurascens* was performed, following the previously optimized procedure (Table 1). The samples (300 mg) were placed together ethanol/water (20 mL, 55:45, *v/v*) acidified with 0.25% citric acid (pH = 3) in a glass vial with a stopper. The extraction followed established conditions of temperature (T = 72 °C) and time (60 min). After the procedure described, the sample was centrifuged (Centurion K24OR, West Sussex, UK) at 5000 rpm for 5 min at 10 °C. They were then filtered through filter paper (Whatman n° 4) to remove suspended solids. The ethanol fraction was removed at a temperature of 35 °C and the aqueous fraction obtained was frozen and lyophilized (FreeZone 4.5), affording an extract rich in anthocyanin compounds. The lyophilized extract was stored away from the light for further analysis.

3.9. Evaluation of the Colorant Potential of the Extract Rich in Anthocyanin Compounds Obtained under Optimum Conditions from the Leaves of O. basilicum var. purpurascens

The evaluation of the colorant potential of the extract was carried out by measuring the colour and the measurement of the colouring compounds by chromatography, in order to corroborate the data provided by the MRS. The colour was measured using a colorimeter (model CR-400, Konica Minolta Sensing, Inc., Osaka, Japan) with an adapter for granular materials (model CR-A50), according to a procedure described by Pereira et al. [24]. The measurements were made in the CIE *L*a*b** colour space, using the illuminant C and a diaphragm aperture of 8 mm. Data were processed with the "Spectra Magic Nx" (version CM-S100W 2.03.0006 software, Konica Minolta). Quantitation of anthocyanin compounds was accomplished by chromatography using an HPLC-DAD-ESI/MS system as described in Section 3.4.

3.10. Evaluation of the Bioactive Properties of the Extract Rich in Anthocyanin Compounds Obtained under Optimal Conditions from the Leaves of O. basilicum var. purpurascens.

3.10.1. Antimicrobial Activity

The antimicrobial activity was evaluated using the methodology described by Carocho et al. [25]. Gram-negative (*Enterobacter cloacae* (American Type Culture Collection (ATCC) 35030), *Escherichia coli* (ATCC 35210) and *Salmonella typhimurium* (ATCC 13311)) and Gram-positive (*Bacillus cereus* (clinical isolate), *Listeria monocytogenes* (NCTC (National collection of type cultures) 7973) and *Staphylococcus aureus* (ATCC 6538)) bacteria strains were used. For the calculation of the minimum inhibitory (MIC) and minimum bactericidal (MBC) concentrations, the microdilution method was applied and the results were expressed in mg/mL.

For the antifungal activity, a procedure previously described by Carocho et al. [25] was followed. *Aspergillus fumigatus* (ATCC 1022), *Aspergillus niger* (ATCC 6275), *Aspergillus ochraceus* (ATCC 12066), *Penicillium funiculosum* (ATCC 36839), *Penicillium ochrochloron* (ATCC 9112) and *Penicillium verrucosum* var. *cyclopium* (food isolate) were used. Minimum inhibitory concentration (MIC) and minimum fungicidal concentration (MFC) were also determined by using the microdilution method and the results were also expressed in mg/mL.

3.10.2. Cytotoxic Activity

The evaluation of the cytotoxic potential of the extract rich in anthocyanin compounds was performed by the Sulfarodamine B (SRB) assay previously described by Barros et al. [26] MCF-7 (breast carcinoma), NCI-H460 (lung carcinoma), HeLa (cervical carcinoma) and HepG2 (hepatocellular

carcinoma) were used as human tumor cell lines. For the hepatotoxicity assay, the extract rich in anthocyanin compounds was tested in a primary non-tumor cell culture obtained from porcine liver (PLP2).

Ellipticine (Sigma-Aldrich, St. Louis, MO, USA) was used as the positive control and the results were expressed as GI_{50} values (sample concentration that inhibits the growth of cells by 50%), and expressed in μg/mL.

4. Conclusions

Colorants are one of the most important additives in terms of marketing, because their presence in food products is considered the principal factor influencing customer choice. To the authors' best knowledge, the potential industrial use of the anthocyanin compounds from red rubin basil leaves have not been explored previously. In such a context, the present work presents a new rapid method to extract anthocyanin compounds from red rubin basil leaves. RSM and other mathematical strategies were successfully employed to optimize extraction conditions that maximize the anthocyanin recovery to produce a rich extract with potential for industrial application as a natural colouring additive.

The scientific literature shows clear evidence that extraction procedures of target compounds from plant-based products, must be assessed individually. Therefore, a nonstop effort needs to be performed, because agro-industrial and food sectors are looking for byproduct valorisation into added-value products. However, in order to take full advantage of the technological advances, the extraction conditions need to be optimized. Mathematical solutions, such as RSM tools, could increase the efficiency and profitability of the process and help to change conventional extraction approaches.

In this study, the suitability of HAE for extracting anthocyanin compounds from red rubin basil leaves was demonstrated and the variables of *t*, *T* and *S* were combined in a five-level *CCCD* design coupled to RSM for optimization. According to the results, a good agreement between experimental and theoretical results was observed. In general, the recovery of anthocyanin compounds was maximized when high temperatures, high ethanol concentrations and medium extraction times were applied, validating this Heat-Assisted Extraction.

The colour analysis in the pigmented extract revealed interesting values, showing dark tones, more directed to a red tonality. It was also evident the antimicrobial and anti-proliferative potential against several strains and tumour cell lines, respectively, without presenting toxicity for non-tumor cells.

These results should promote interest in conducting further studies on *O. basilicum* varieties, highlighting the potential of ruby red basil as a potential source of natural and bioactive ingredients with application in several industrial factors, namely in the food and pharmaceutical areas.

Conflicts of Interest: The authors declare they have no conflict of interest.

References

1. Hoefkens, C.; Verbeke, W. Consumers' health-related motive orientations and reactions to claims about dietary calcium. *Nutrients* **2013**, *5*, 82–96. [CrossRef] [PubMed]
2. Martins, N.; Roriz, C.L.; Morales, P.; Barros, L.; Ferreira, I.C.F.R. Food colorants: Challenges, opportunities and current desires of agro-industries to ensure consumer expectations and regulatory practices. *Trends Food Sci. Technol.* **2016**, *52*, 1–15. [CrossRef]

3. Rodriguez-Amaya, D.B. Natural food pigments and colorants. *Curr. Opin. Food Sci.* **2016**, *7*, 20–26. [CrossRef]

4. Neri-Numa, I.A.; Pessoa, M.G.; Paulino, B.N.; Pastore, G.M. Genipin: A natural blue pigment for food and health purposes. *Trends Food Sci. Technol.* **2017**, *67*, 271–279. [CrossRef]

5. Almeida, H.H.S.; Barros, L.; Barreira, J.C.M.; Calhelha, R.C.; Heleno, S.A.; Sayer, C.; Miranda, C.G.; Leimann, F.V.; Barreiro, M.F.; Ferreira, I.C.F.R. Bioactive evaluation and application of different formulations of the natural colorant curcumin (E100) in a hydrophilic matrix (yogurt). *Food Chem.* **2018**, *261*, 224–232. [CrossRef] [PubMed]

6. Sigurdson, G.T.; Tang, P.; Giusti, M.M. Natural Colorants: Food Colorants from Natural Sources. *Annu. Rev. Food Sci. Technol* **2017**, *8*, 261–280. [CrossRef] [PubMed]

7. Ananga, A.; Georgiev, V.; Ochieng, J.; Phills, B.; Tsolov, V. Production of Anthocyanins in Grape Cell Cultures: A Potential Source of Raw Material for Pharmaceutical, Food, and Cosmetic Industries. In *The Mediterranean Genetic Code—Grapevine and Olive*; IntechOpen: London, UK, 2013; pp. 247–287.

8. Gerardi, C.; Tommasi, N.; Albano, C.; Blando, F.; Rescio, L.; Pinthus, E.; Mita, G. *Prunus mahaleb* L. fruit extracts: a novel source for natural food pigments. *Eur Food Res. Technol.* **2015**, *241*, 683–695. [CrossRef]

9. Jornal Oficial da União Europeia. Regulamento (UE) N°1129/2011. *Eur. Food Res. Technol.* **2011**, *25*.

10. Flanigan, P.M.; Niemeyer, E.D. Effect of cultivar on phenolic levels, anthocyanin composition, and antioxidant properties in purple basil (*Ocimum basilicum* L.). *Food Chem.* **2014**, *164*, 518–526. [CrossRef]

11. Da Silva, F.J.; Nascimento, A.B.; Barbosa, L.N.; Magalhães, H.M. In vitro cultivation of purple basil *Ocimum basilicum* L. 'red rubin' at different levels of salts, charcoal, sucrose and potassium iodine. *Aust. J. Crop Sci.* **2017**, *11*, 1137–1145. [CrossRef]

12. El-Ziat, R.A.; Swaefy, H.M.; Esmail, S.E.A. The Response of Red Rubin Basil Plant to Organic Fertilizer and Humic Acid versus Chemical Fertilizers. *Middle East. J. Agric. Res.* **2018**, *7*, 740–751.

13. Alexandre, E.M.C.; Araújo, P.; Duarte, M.F.; de Freitas, V.; Pintado, M.; Saraiva, J.A. High-pressure assisted extraction of bioactive compounds from industrial fermented fig by-product. *Int. J. Food Sci. Technol.* **2017**, *54*, 2519–2531. [CrossRef]

14. Alexandre, E.M.C.; Araújo, P.; Duarte, M.F.; de Freitas, V.; Pintado, M.; Saraiva, J.A. Experimental design, modeling, and optimization of high-pressure-assisted extraction of bioactive compounds from pomegranate peel. *Food Bioprocess Tech.* **2017**, *10*, 886–900. [CrossRef]

15. Luna, M.C.; Bekhradi, F.; Ferreres, F.; Jordán, M.J.; Delshad, M.; Gil, M.I. Effect of Water Stress and Storage Time on Anthocyanins and Other Phenolics of Different Genotypes of Fresh Sweet Basil. *J. Agric. Food Chem* **2015**, *63*, 9223–9231. [CrossRef] [PubMed]

16. Phippen, W.B.; Simon, J.E. Anthocyanins in Basil (*Ocimum basilicum* L.). *J. Agric. Food Chem.* **1998**, *46*, 1734–1738. [CrossRef]

17. Ranic, M.; Nikolic, M.; Pavlovic, M.; Buntic, A.; Siler-Marinkovic, S.; Dimitrijevic-Brankovic, S. Optimization of microwave-assisted extraction of natural antioxidants from spent espresso coffee grounds by response surface methodology. *J. Clean. Prod.* **2014**, *80*, 69–79. [CrossRef]

18. Sun, X.-H.; Zhou, T.-T.; Wei, C.-H.; Lan, W.-Q.; Zhao, Y.; Pan, Y.-J.; Wu, V.C.H. Antibacterial effect and mechanism of anthocyanin rich Chinese wild blueberry extract on various foodborne pathogens. *Food Control* **2018**, *94*, 155–161. [CrossRef]

19. Zhou, L.; Wang, H.; Yi, J.; Yang, B.; Li, M.; He, D.; Yang, W.; Zhang, Y.; Ni, H. Anti-tumor properties of anthocyanins from *Lonicera caerulea* 'Beilei' fruit on human hepatocellular carcinoma: In vitro and in vivo study. *Biomed. Pharmacother.* **2018**, *104*, 520–529. [CrossRef]

20. Roriz, C.L.; Barros, L.; Prieto, M.A.; Morales, P.; Ferreira, I.C.F.R. Floral parts of *Gomphrena globosa* L. as a novel alternative source of betacyanins: Optimization of the extraction using response surface methodology. *Food Chem.* **2017**, *229*, 223–234. [CrossRef]

21. Gonçalves, G.A.; Soares, A.A.; Correa, R.C.G.; Barros, L.; Haminiuk, C.W.I.; Peralta, R.M.; Ferreira, I.C.F.R.; Bracht, A. Merlot grape pomace hydroalcoholic extract improves the oxidative and inflammatory states of rats with adjuvant-induced arthritis. *J. Funct. Foods* **2017**, *33*, 408–418. [CrossRef]

22. Vieira, V.; Prieto, M.A.; Barros, L.; Coutinho, J.A.P.; Ferreira, O.; Ferreira, I.C.F.R. Optimization and comparison of maceration and microwave extraction systems for the production of phenolic compounds from *Juglans regia* L. for the valorization of walnut leaves. *Ind. Crops Prod.* **2017**, *107*, 341–352. [CrossRef]

23. Prieto, M.A.; Vázquez, J.A. In vitro determination of the lipophilic and hydrophilic antioxidant capacity of unroasted coffee bean extracts and their synergistic and antagonistic effects. *Food Res. Int.* **2014**, *62*, 1183–1196. [CrossRef]

24. Pereira, E.; Antonio, A.L.; Barreira, J.C.M.; Barros, L.; Bento, A.; Ferreira, I.C.F.R. Gamma irradiation as a practical alternative to preserve the chemical and bioactive wholesomeness of widely used aromatic plants. *Food Res. Int.* **2015**, *67*, 338–348. [CrossRef]

25. Carocho, M.; Barros, L.; Calhelha, R.C.; Ćirić, A.; Soković, M.; Santos-Buelga, C.; Morales, P.; Ferreira, I.C.F.R. *Melissa officinalis* L. decoctions as functional beverages: a bioactive approach and chemical characterization. *Food Funct.* **2015**, *6*, 2240–2248. [CrossRef] [PubMed]

26. Barros, L.; Pereira, E.; Calhelha, R.C.; Dueñas, M.; Carvalho, A.M.; Santos-Buelga, C.; Ferreira, I.C.F.R. Bioactivity and chemical characterization in hydrophilic and lipophilic compounds of *Chenopodium ambrosioides* L. *J. Funct. Foods* **2013**, *5*, 1732–1740. [CrossRef]

Sample Availability: Samples are available from the authors.

Recovery of bioactive anthocyanin pigments from *Ficus carica* L. peel by heat, microwave, and ultrasound based extraction techniques

Emanueli Backes[a,b], Carla Pereira[a], Lillian Barros[a], M.A. Prieto[a,c], Aziza Kamal Genena[d], Maria Filomena Barreiro[a,b], Isabel C.F.R. Ferreira[a,*]

[a] *Centro de Investigação de Montanha (CIMO), Instituto Politécnico de Bragança, Campus de Santa Apolónia, 5300-253 Bragança, Portugal*
[b] *Laboratory of Separation and Reaction Engineering, Laboratory of Catalysis and Materials (LSRE-LCM), Polytechnic Institute of Bragança, Campus Santa Apolónia, 5300-253 Bragança, Portugal*
[c] *Nutrition and Bromatology Group, Faculty of Food Science and Technology, University of Vigo, Ourense Campus, E32004 Ourense, Spain.*
[d] *Departamento Acadêmico de Alimentos (DAALM), Universidade Tecnológica Federal do Paraná, Campus Medianeira, 85884-000 Paraná, Brazil*

ARTICLE INFO

ABSTRACT

Due to its coloration, the fig (*Ficus carica* L.) peel, a by-product of fruit processing and/or consumption, is a potential source of anthocyanin compounds. In the present study different extraction techniques (heat, ultrasound, and microwave) were compared aiming to recover the anthocyanin pigments and optimize its extraction conditions. A response surface methodology tool with three factors and five levels for each factor was used according to a circumscribed central composite design. The variables tested for the heat and microwave extraction methods were time, temperature, and solvent proportion (ethanol/water ratio), meanwhile, for the ultrasound method, the variables tested were the ultrasonic power, time, and solvent proportion. The anthocyanin composition of the extract was determined by HPLC-DAD-ESI/MS, and the used criteria responses were: i) quantification of cyanidin 3-rutinoside (C) in the extracted residue (mg C/g R) and in the dried peel (mg C/g P dw), and the extraction yield of the obtained residue (g R/g P dw). Ultrasound extraction was the most effective method, yielding 3.82 mg C/g R at the optimal global extraction conditions (21 min, 310 W, and 100% of ethanol). Additionally, the solid-to-liquid ratio effect was studied at the optimal conditions, using a dose-response format, in view of its plausible transference to industrial level. For the ultrasound method, an increased non-linear relationship was observed for concentrations in the range 5 to 200 g/L, being the optimal solution close to 150 g/L. In brief, the obtained results show the potential of fig peels as a source of anthocyanin pigments, with potential uses in various industrial fields, such as food, pharmaceutical, and cosmetic.

1. Introduction

Figs are the infructescences of a tree belonging to the family of Moraceae, called *Ficus carica* L., with extensive production in the Mediterranean region (Palassarou et al., 2017). When mature, the fig can acquire different colouring hues depending on its cultivar, which range from green to black-violet as a function of the anthocyanin concentration in the infructescence peel (Wang, Cui, Vainstein, Chen, & Ma, 2017). Recent studies have shown that the fig peel contains anthocyanins at levels higher than the ones present in most of their typical natural sources (Harzallah, Bhouri, Amri, Soltana, & Hammami, 2016; Vallejo, Marín, & Tomás-Barberán, 2012). Figs consumption varies with the region, but for industrial purposes it is mostly used peeled (Harzallah et al., 2016), which makes the fig peel a potential by-

product that can be valorised in the recovering of anthocyanin pigments.

In the last decade, researchers have proved that the regular consumption of artificial colouring agents can cause several adverse toxicological side effects on humans, such as allergic reactions, minor health disorders, and behavioural changes (Fattore et al., 2016; Montesano et al., 2008; Salem et al., 2014). Faced with this problem, and driven by consumer's needs, the food industry is decreasing the amount of used artificial colorants and, whenever possible, replacing them by more innocuous natural counterparts. These natural solutions are, not only harmless to humans when regularly consumed, but also exhibit a complementary range of important bioactivities, with beneficial health effects. These include antioxidant activity, protection against cellular oxidation, anti-inflammatory capacity, and prevention

---

* Corresponding author.
  E-mail address: iferreira@ipb.pt (I.C.F.R. Ferreira).

of chronic non-transmissible diseases, among others (Gowd, Jia, & Chen, 2017; Rodriguez-Amaya, 2016). Therefore, the attention given by the industrial sector to these natural colorant alternatives is increasing over time, due to the urge need to find reliable solutions to replace the prevalent artificial ones. Other important features, such as the possible variation of anthocyanin chemical structure (Ongkowijoyo, Luna-Vital, & Gonzalez de Mejia, 2018) that allow the existence of a high variety of colorations, together with their high solubility in water (Rustioni, Di Meo, Guillaume, Failla, & Trouillas, 2013), rises the interest to screen different raw-material sources, able to reach industrial scale and contribute to make these natural solutions viable (Salem et al., 2014).

A huge array of solid-liquid extraction procedures are available to recover compounds of interest from natural matrices (Chemat et al., 2017; Montesano et al., 2008; Zhu et al., 2017). Briefly, the solid-liquid extraction consists in keeping the solid sample (usually in powder form) in direct contact with a solvent for a specific time, and by applying a certain level of energy (conventional heat, ultrasound or microwave radiation, pressure, etc.) (Fattore et al., 2016; García-Moreno et al., 2014; Zhu et al., 2016). The common solid-liquid procedures comprise the conventional methods, such as Soxhlet and heat assisted extraction (HAE, also known as maceration). These methods are easy to apply and relatively inexpensive; nevertheless several authors have pointed out some disadvantages, which are mainly associated with their application at industrial level, i.e. the use of large amounts of solvent and long extraction times (Azmir et al., 2013).

Nowadays, modern solid-liquid extraction technologies are available, such as microwave and ultrasound assisted extraction (MAE and UAE), which are perceived as more sustainable, green techniques and efficient solutions for industrial application, in particular UAE (Chemat et al., 2017; Dai & Mumper, 2010). However, conventional methods are still important at industrial level, mainly due to the lack of comparative results showing the advantages of the alternative modern techniques. For instance, the UAE can improve the recovery of bioactive components, mainly the ones that are sensitive to heat at prolonged extraction times, by keeping these variables at low levels. UAE is an effective extraction technique, in comparison to conventional methods, because the ultrasound radiation is able to disrupt cellular walls allowing a better penetration of solvents in the matrix material, thus improving mass transfer and increasing cell's content release (Bonfigli, Godoy, Reinheimer, & Scenna, 2017; Chemat, Rombaut, Sicaire, et al., 2017). On the other hand, MAE is a process in which the applied energy accelerates the extraction (Tsatsop, Djiobie, Kenmogne, Regonne, & Ngassoum, 2016). This method has a good performance in terms of extraction yield, solvent consumption, and extraction time, being considered a potential substitute for conventional methods (Chan, Yusoff, & Ngoh, 2013; Meullemiestre, Breil, Abert-Vian, & Chemat, 2016).

The recovery of natural components from vegetable matrices for implementation as food ingredients must be made under the best extraction conditions to promote its application at industrial scale and compete against the low economic cost of producing artificial dyes. The particularities of the aforementioned extraction methods, and their effectiveness, cannot be applied in a generalized way to all matrices, demanding specific optimization for each case (Jacotet-Navarro et al., 2016). Moreover, several factors may affect anthocyanin stability and, consequently, their deterioration rate, reinforcing the importance of determining the conditions that maximize the extraction yield of these compounds (Estupiñan, Schwartz, & Garzón, 2011). In this context, the response surface methodology (RSM) arises as an important statistical method to optimize the extraction conditions and maximize responses (Sang, Sang, Ma, Hou, & Li, 2017). The RSM consists in an assembly of mathematical and statistical techniques, helping to describe process patterns (e.g. extraction patterns) of any data set and perform predictions. The RSM procedure is essential when responses are interactively influenced by different factors, its application simplifies the system performance and optimizes the extraction conditions while maximizing the responses assessed (Bezerra et al., 2008).

Thus, the present study aims to optimize and compare anthocyanin extraction, from the peel of *F. carica* infructescences, through different extraction methodologies (HAE, UAE, and MAE). For that purpose, the joint effect of the identified relevant variables for each technique will be described through RSM. This study will allow to achieve the optimal conditions to recover anthocyanins, important pigments with a large range of colours and various industrial applications, from this natural source.

2. Material and methods

2.1. Samples, standards and reagents

The infructescences of *F. carica* were obtained in a local production at the municipality of Bragança, in Trás-os-Montes, Northeast of Portugal. They were peeled, and the peels lyophilized (FreeZone 4.5, Labconco, Kansas City, MO, USA), powdered to 20 mesh size, and stored in the freezer at -20 °C for subsequent extractions assays.

PA grade ethanol, hydrogen chloride, formic acid, citric acid, and HPLC grade acetonitrile were acquired from Fisher Scientific (Lisbon, Portugal). Water was treated in a Milli-Q water purification system (TGI Pure Water Systems, Greenville, SC, USA).

2.2. Description of the extraction techniques and associated relevant variables

The relevant variables to be considered in the optimization study by RSM were time (t, min), temperature (T, °C), and solvent proportion (S, % v/v of ethanol in hydroalcoholic mixtures) for HAE and MAE extraction methods. For the UAE method, ultrasonic power (P, W), together with t and S were used. For all the extraction techniques, the solid-to-liquid ratio (S/L) was kept constant (50 g/L). Next, the technical requirements for each technique are briefly described.

2.2.1. Heat-assisted extraction (HAE)

The lyophilized powdered peel samples (1 g) were placed in a beaker with 20 mL of solvent acidified with citric acid (pH = 3). The beaker was placed in a thermostatic water bath (Bath Shaker, OVAN, Barcelona, Spain) and the mixture was kept under continuous electromagnetic stirring (Cimarec™ Magnetic, Thermo Scientific, San Jose, CA, USA) for the required t. The variables and tested ranges were: t (X_1, 5–68.8 min), T (X_2, 20–90 °C), and S (X_3, 0–100%).

2.2.2. Microwave-assisted extraction (MAE)

The MAE process was performed in a Biotage Initiator Microwave (Biotage® Initiator+, Uppsala, Sweden) using closed vessels. The lyophilized powdered peel samples (0.5 g) were introduced in a closed reaction vessel with 10 mL of acidified solvent (pH 3, using citric acid). The variables of pressure and T are correlated in the microwave extraction and only one can be used to maximize the responses. The effect of T was used letting the other one reach the corresponding values. The microwave power was set in all cases at a constant value of 400 W. Another important issue in the microwave extraction systems is the time interval needed to reach the selected T (value that increases as the T increases). For the conditions used, the time interval was always < 20 s, therefore, under this quick heating process, time interval was neglected considering only the studied extraction t range. In consequence, the tested variables and ranges were t (X_1, 5–35 min), T (X_2, 40–115 °C) and S (X_3, 0–100%).

2.2.3. Ultrasound-assisted extraction (UAE)

The UAE was studied in a QSonica sonicators equipment (CL-334, Newtown, CT, USA) using a reaction vessel of 50 mL of the acidified solvent (pH 3, using citric acid) and 2.5 g of lyophilized powdered. The tested variables and ranges were at t (X_1, 5–55 min), P (X_2, 100–400 W) and S (X_3, 0–100%). The T was monitored to ensure that the reaction

was always below 30–35 °C.

2.3. Anthocyanin identification and quantification

The extraction solutions were centrifuged (600 rpm for 20 min) and filtered through a paper filter n° 4 to remove the suspended solids. The solvent was then evaporated at 35 °C (rotary evaporator Büchi R-210, Flawil, Switzerland) and the extracted residue gravimetrically quantified. Afterwards, it was re-dissolved in acidified water (citric acid solution with pH 3) and filtered through a LC filter disk (0.22 μm) to a 1.5 mL amber vial. This solution was analysed by high-performance liquid chromatography (Dionex UltiMate 3000 UPLC, Thermo Scientific, San Jose, CA, USA), coupled to a DAD (using 520 nm as the preferred wavelength), and to a mass spectrometer working in positive mode using a Linear Ion Trap LTQ XL mass spectrometer (Thermo Finnigan, San Jose, CA, USA) equipped with an ESI source (Gonçalves et al., 2017). Data acquisition was performed using the Xcalibur® data system (Thermo Finnigan, San Jose, CA, USA) and quantitative analysis was performed from a 5-level calibration curve obtained from the injection of known concentrations of cyanidin 3-rutinoside ($Y = 146,924 \times - 671,583$; $R^2 = 0.9989$).

2.4. Experimental design, model analysis, and statistical evaluation

2.4.1. RSM experimental design

To centre correctly the experimental design preliminary trials were conducted based in one-at-the-time analysis of the studied variables for each of the selected techniques. After those preliminary analysis (data not presented), the relevant ranges were selected for each one of the studied techniques and presented in Table A1 (supplemental material). The experimental design used was the *circumscribed central composite design* (CCCD) with 28 response combinations using five levels for each variable.

2.4.2. Responses applied to analyse the results

The extraction results were expressed in three response formats (Y): Y_1, mg of cyanidin 3-rutinoside (C) obtained in the extracted dried weight residue (R; mg C/g R), which was specifically used to evaluate the purity of the target compound in the extract; Y_2, mg of C per g of peel (P) dry matter (mg C/g P dw), specifically used to analyse the extraction yield in C; and Y_2/Y_1, obtained by dividing the responses Y_2 and Y_1, which provides information regarding the extraction yield in R (g of R/g P dw).

2.4.3. Mathematical model to describe the responses

The RSM data was fitted by means of least-squares calculation using the following second-order polynomial equation:

$$Y = b_0 + \sum_{i=1}^{n} b_i X_i + \sum_{\substack{i=1 \\ j>i}}^{n-1} \sum_{j=2}^{n} b_{ij} X_i X_j + \sum_{i=1}^{n} b_{ii} X_i^2 \tag{1}$$

where Y is the dependent variable (response) to be modelled, X_i and X_j define the independent variables, b_0 is the constant coefficient, b_i is the coefficient of linear effect, b_{ij} is the coefficient of interaction effect, b_{ii} is the coefficient of quadratic effect, and n is the number of variables. As responses, the three response formats were used: Y_1 (mg C/g R), Y_2 (mg C/g P dw), and Y_2/Y_1 (g R/g P dw).

2.4.4. Procedure to optimize the variables to a maximum response

To optimize the extraction conditions and maximize the responses, a simplex method was used. The predictive model obtained by RSM was employed under non-linear system with restrictions to avoid variables with unnatural physical conditions (i.e., $t \geq 0$) and a maximization was obtained (Vieira et al., 2017).

2.5. Dose-response description of the solid-to-liquid ratio effect

The analysis of the solid-to-liquid ratio (S/L or X_4, expressed in g/L) was performed by a dose-response at the optimal conditions of the variables found by the RSM (X_1, X_2, and X_3). The aim was to achieve the S/L conditions that leads to a more productive processes for industrial applications. To depict the response effect as function of the S/L, the Weibull (W) equation (Prieto, Curran, Gowen, & Vázquez, 2015) for increasing (↑) and decreasing (↓) responses was used (with some parametric modifications to fit the searched purposes):

$$\uparrow W(X_4) = K \exp\left[\ln\left(1 - \frac{n}{100}\right)\left(\frac{X_4}{m_n}\right)^a\right] or \downarrow W(X_4)$$

$$= K - K \exp\left[\ln\left(1 - \frac{n}{100}\right)\left(\frac{X_4}{m_n}\right)^a\right] \tag{2}$$

where K is the maximum extraction value (i.e., if Y_2 the units would be in mg C/g P dw), a is a shape parameter related to the maximum slope of the response, n is any desired level between 0 and 100% of the response (Y_1, Y_2, and Y_2/Y_1) that would be achieved and m_n would be the S/L value (X_4) for the selected n response level (m_{10}, m_{25}, m_{75}, m_{95}, etc.). For example, if the n value is selected as 99%, the m_n parameter will display de S/L needed to achieve the 99% of the assessed response ($m_{99\%}$). When the response shows increasing patterns (↑), the Weibull equation that is used to describe the response will present a m_n parameter of $n = 99$%. When the response shows decreasing patterns (↓), a m_n parameter with $n = 50$% will be used. These different levels of the responses as a function of their increasing or decreasing patterns are logical relations of the intrinsic solutions for industrial purposes. When the response increases, it is logical to know the maximum S/L leading to a 99% level of the assessed response ($m_{99\%}$). However, when the response decreases, the value of $m_{99\%}$ will tend to zero, therefore, it seems to be logical to search for values not decreasing our response more than the half of the maximum (such as $m_{50\%}$). If other m_n is required, Eq. (2) can be modified to produce any other desirable result. However, the selected values for the parameters K and m_n will provide key information related to the pattern of the response to assess the effect of the S/L.

2.6. Numerical methods, statistical analysis, and graphical illustrations

Fitting procedures, coefficient estimates, and statistical calculations were achieved as previously described by other authors (Prieto & Vázquez, 2014). In brief, a) the parameter's determination was accomplished using the quasi-Newton algorithm (least-square) by running the integrated macro 'Solver' in Microsoft Excel by minimizing the differences between observed and predicted values; b) the coefficient significance was evaluated using the 'SolverAid' macro to determine their intervals ($\alpha = 0.05$); and c) the model consistency was checked by means of several statistical criteria: ci) the Fisher F-test ($\alpha = 0.05$) was used to assess the adequacy of the models to describe the observed data; cii) the 'SolverStat' macro was used to assess parameter and model prediction uncertainties (Murado & Prieto, 2013); and ciii) the R^2 value was interpreted as the amount of variability of the dependent variable that is explained by the model.

3. Results and discussion

3.1. Optimization of the RSM analysis using the 3 relevant variables for each extraction technique

3.1.1. Preliminary experiments to select the relevant variables and ranges for designing an appropriate RSM

The extraction of target compounds from natural matrices requires specific considerations due to the intrinsic features and stability of these compounds, and such analysis cannot be extrapolated from similar sources. An in-depth extraction study is required to determine the best

solid-to-liquid extraction method, and operating conditions, for the extraction of target compounds from a certain natural matrix, otherwise, results may lead to erroneous conclusions.

The anthocyanin profile of fig peel extracts was obtained by HPLC-DAD-ESI/MS is presented in Fig. A1. Among another minor component, cyanidin 3-rutinoside ([M-H]$^-$ at m/z 595), which is the molecule responsible for the colorant capacity, was identified. To maximize the extraction of cyanidin 3-rutinoside (C), it is indispensable to identify the effects of variables on responses. A minimum time, energy, and solvent consumption, in order to achieve the most cost-effective and profitable extraction system, is intended (Dai & Mumper, 2010). The RSM design allows optimizing all the variables simultaneously considering interactive effects and predicting the most efficient conditions. Based on the tested experimental range and by using second order polynomial models with interactions, the RSM technique provides for the selected responses used as criteria, a truthful description and the optimal conditions that maximize/minimize them (Bezerra et al., 2008; Ferreira et al., 2007; Kalil & Maugeri, 2000). When applying RSM, the initial difficulties are to select the important involved factors and their relevant experimental range. To overcome those issues, preliminary laboratory tests using the one-factor-at-the-time method (keeping the other variables constant) were performed. Once these preliminary analyses were completed (data not shown), the factors selected for the RSM application were t, T, and S for the HAE and MAE systems, and t, P, and S for the UAE system. Similar findings were reported by other authors when performing optimization studies with other natural matrices (Albuquerque et al., 2016; Caleja et al., 2017). A detailed description for all tested values for each technique can be found in Table A1 (supplemental material section). Concerning the type of employed solvent, and since anthocyanins are polar pigments, they were extracted with hydroalcoholic solutions (ethanol/water mixtures). In all cases, ethanol content was tested in the range 0 to 100%, and confirmed as impacting significantly the achieved anthocyanin extraction yield. In order to maintain anthocyanin stability, citric acid was added to the extraction solvent in order to obtain a pH value around 3. For the RSM study, the S/L variable was kept at 50 g/L (constant value).

In conclusion, the efficiency of the HAE, UAE, and MAE processes for extracting cyanidin 3-rutinoside from fig peel was performed by applying a RSM using three variables in a CCCD (five values for each factor). The coded values, and respective natural values, are presented in Table A1. Once the optimal conditions (t, T, and S for HAE and MAE, and t, P, and S for UAE) were optimized, the study was further advanced towards the study of the S/L effects.

Fig. A2 (presented in the supplemental material section) shows a diagram summary of the work achieved and the steps carried out to optimize the conditions that maximize the extraction of the detected anthocyanin compound in the fig peel (cyanidin 3-rutinoside).

3.1.2. Developed mathematical models after the RSM application

Table 1 shows the results of the responses considered. The Eq. (1) was employed to fit the responses in Table 1 using nonlinear least-squares estimations. The parametric values with higher confidence interval values than the parameter value, were considered as non-significant (ns), and were not used for the model development (Ranic et al., 2014). Table 2 part A shows the significant parametric values of Eq. (1) obtained and the confidence interval values ($\alpha = 0.05$). The ns parameters of RSM approaches (Table 2A) do not improve the reached solutions, but rise the uncertainties of all significant coefficients, and in addition, the ns parameters will alter the solutions in untested conditions. Based on the results of Table 2A, the final significant models for each assessed extraction technique are described below:

For the response format Y_1 (mg C/g R):
for HAE:

$for HAE$: $Y_{HAE}^{Y_1} = 3.71 - 0.22t + 0.22T + 1.30S - 1.17t^2 - 0.05T^2$
$$+ 0.17tT - 0.08TS \qquad (3)$$

for UAE

$$Y_{UAE}^{Y_1} = 5.51 + 0.21t + 0.61P + 2.05S - 0.63P^2 + 0.27S^2 + 0.19tS \qquad (4)$$

for MAE

$$Y_{MAE}^{Y_1} = 6.17 - 0.35t - 0.52T + 1.58S - 0.49T^2 - 0.35tT - 0.31tT$$
$$- 0.36TS \qquad (5)$$

For the response format Y_2 (mg C/g P dw):
for HAE

$$Y_{HAE}^{Y_2} = 14.74 - 0.86t - 1.36T + 3.89S - 0.98T^2 - 0.91S^2 - 0.74tT$$
$$- 0.9TS \qquad (6)$$

for UAE

$$Y_{UAE}^{Y_2} = 4.24 + 0.11t + 0.42P + 0.88S - 0.067t^2 - 0.39P^2 - 0.26S^2$$
$$+ 0.09tS - 0.07PS \qquad (7)$$

for MAE

$$Y_{MAE}^{Y_2} = 4.46 - 0.28t - 0.36T + 1.09S - 0.39T^2 - 0.23S^2 - 0.24tT$$
$$- 0.24TS \qquad (8)$$

For the response format Y_2/Y_1 (g R/g P dw):
for HAE

$$Y_{HAE}^{Y_2/Y_1} = 0.69 + 0.02t + 0.02T - 0.01tT + 0.01tS + 0.01TS \qquad (9)$$

for UAE

$$Y_{UAE}^{Y_2/Y_1} = 0.78 + 0.01t + 0.01P - 0.09S - 0.01t^2 - 0.05S^2 \qquad (10)$$

for MAE

$$Y_{MAE}^{Y_2/Y_1} = 0.72 - 0.01S - 0.01T^2 - 0.01S^2 - 0.01tS \qquad (11)$$

The variables of models (3) to (11) derived from Eq. (1) where X_1 (t, min), X_2 (T, °C or P, W), and X_3 (S, %), whereas Y is the response, sub-indices indicate the applied technique, and the super-indices the three used response criteria (Y_1 in mg C/g R, Y_2 in mg C/g P dw, and Y_2/Y_1 in g R/g P dw). Therefore, eqs. (3) to (11) translate the response patterns, showing a relatively high complexity (higher than 6 parameters) of the possible sceneries for Y_1 and Y_2 value formats and relatively simple solutions for the Y_2/Y_1 response value format (lesser than 6 parameters).

Because the experimental plan is based on coded values of the variables, the obtained model coefficients are empirical and cannot be associated with physical or chemical significance. However, their numerical values can be used for direct comparisons. In fact, the higher is the absolute value of the coefficient, the more important will be the weight of the corresponding variable. Correspondingly, when a factor has a positive effect, the response increases as the values of the involved variable rises, and when the factor has a negative effect, the response decreases.

Eqs. (3) to (11) provide a comprehensive summary of the effects produced by each of the variables defined for the assessed extraction techniques. Several statistical tests were employed to evaluate the ability of the obtained Eqs. (3) to (11) and the results are presented in Table 2B. Overall, the statistical tests are conclusive providing the same findings: Eqs. (3) to (11) are efficient in the subsequent prediction stages. In this regard, and comparatively to the most common statistical criteria presented in Table 2B, the coefficients R^2 and R_{adj}^2, almost in all cases, displayed results higher than 0.9, which indicates a good agreement between the experimental and predicted values. This implies that the variation of the experimental results can be explained by the independent processing variables by using the specific parametric values presented in Table 2A, which validates the models of Eqs. (3) to

Table 1

Experimental RSM results of the CCCD for the optimization of the three main variables involved (X_1, X_2, and X_3) in the HAE, UAE, and MAE for the three response value formats assessed (Y_1, mg C/g R; Y_2, C/g P dw; and Y_2/Y_1 g R/g P dw). Variables, natural values and ranges in Table A1. Three replicates were performed for each condition for each technique.

Variable coded values			Experimental responses			UAE			MAE		
			HAE								
X_1	X_2	X_3	Y_1	Y_2	Y_2/Y_1	Y_1	Y_2	Y_2/Y_1	Y_1	Y_2	Y_2/Y_1
−1	−1	−1	1.031	0.709	0.688	1.783	1.304	0.731	2.997	2.376	0.793
−1	−1	1	6.731	5.137	0.763	8.272	5.820	0.704	7.993	5.623	0.704
−1	1	−1	1.753	1.072	0.612	3.537	2.591	0.732	3.738	2.908	0.778
−1	1	1	5.944	4.660	0.784	6.932	5.002	0.722	7.602	5.413	0.712
1	−1	−1	1.016	0.682	0.671	2.265	1.635	0.722	3.213	2.384	0.742
1	−1	1	5.042	3.792	0.752	9.915	7.333	0.740	7.702	5.357	0.695
1	1	−1	2.622	1.869	0.713	2.091	1.606	0.768	3.159	2.477	0.784
1	1	1	6.163	4.738	0.769	8.585	6.112	0.712	6.267	4.393	0.701
−1.68	0	0	3.702	1.782	0.661	4.865	3.604	0.741	5.994	4.501	0.751
1.68	0	0	2.326	1.570	0.675	5.574	3.880	0.696	6.324	4.522	0.715
0	−1.68	0	3.489	2.325	0.666	2.647	1.885	0.712	6.351	4.576	0.720
0	1.68	0	3.206	2.133	0.665	5.096	3.767	0.739	2.498	1.706	0.683
0	0	−1.68	0.999	0.688	0.689	2.299	1.749	0.760	2.531	1.982	0.761
0	0	1.68	6.051	4.345	0.718	10.307	4.576	0.444	7.209	5.324	0.739
−1.68	−1.68	−1.68	1.098	0.765	0.696	0.576	0.406	0.705	1.449	0.948	0.655
−1.68	−1.68	1.68	6.777	2.405	0.355	4.875	1.936	0.397	7.834	5.546	0.708
−1.68	1.68	−1.68	2.665	1.864	0.699	3.140	2.417	0.770	2.775	1.930	0.696
−1.68	1.68	1.68	4.975	3.716	0.747	7.648	3.273	0.428	6.757	5.142	0.761
1.68	−1.68	−1.68	0.773	0.518	0.670	0.421	0.348	0.827	1.066	0.841	0.788
1.68	−1.68	1.68	3.553	2.636	0.742	6.213	2.443	0.393	8.641	5.958	0.689
1.68	1.68	−1.68	2.128	1.551	0.729	2.623	2.302	0.878	0.488	0.360	0.739
1.68	1.68	1.68	5.747	4.234	0.737	9.145	4.324	0.473	1.973	1.505	0.762
0	0	0	2.428	1.639	0.675	4.734	3.496	0.738	6.720	4.882	0.726
0	0	0	2.558	1.669	0.652	5.751	4.654	0.809	6.251	4.591	0.734
0	0	0	2.510	1.657	0.660	5.256	4.165	0.792	6.065	4.212	0.695
0	0	0	3.049	2.090	0.686	5.340	4.449	0.833	6.063	4.244	0.700
0	0	0	2.558	1.733	0.678	5.177	4.020	0.776	5.863	4.233	0.722
0	0	0	2.555	1.725	0.675	5.907	4.652	0.788	6.747	2.376	0.684

(11) and allows to move to the interpretation of the independent variable effects and the determination of the optimal conditions that maximize the responses.

3.1.3. Effect of the independent variables on the target responses and optimal extraction conditions

The second-order polynomial model of Eq. (1), which has proved its suitability in the previous section, describe two types of effects (linear and non-linear) for each variable and one interactive effect between two pairs of variables. The patterns of the extraction can be explained by means of the parametric values of the second-order polynomial models shown in Table 2A or Eqs. (3) to (11), as described above, or can be illustrated by graphical representations. In this regard, Fig. 1, Fig. A3, and Fig. A4 (supplementary material) show the extraction results for the three response criteria formats for each assessed technique, respectively. The figures are divided in three columns, each one showing the response results (Y_1, Y_2, and Y_2/Y_1) for each of the tested techniques. Additionally, each column is divided into two sections (A and B):

- Section A shows the three-dimensional surface figures for the three possible variable combinations produced by the developed Eqs. (3) to (11). The studied responses (dependent variables) are visualized as a function of the corresponding independent variables by drawing the responses generated by the models. The plots were built by fluctuating two variables within the experimental range and holding the excluded variable constant at the centre of their experimental domain (Table A1). It can be observed that the obtained amount of cyanidin 3-rutinoside is highly dependent on the S variable, for all the tested extraction methods. For the UAE, the effect of the P variable is also considerable, although not so significant as the effect of S. The analysis of the 3D graphs presented in Fig. 1 shows the low influence of t and T on the response of the HAE and MAE methods.

The quadratic effect of the variables observed in HAE was found important, whereas for UAE and MAE the detected relevant effects were the interactive ones.

- Section B illustrates the capability to predict the obtained results and the residual distribution as a function of each one of the considered variables. The statistical information is displayed using two basic graphical criteria, depicting the capacity to predict the obtained results. As previously described in Table 2B, in all cases, the coefficient R^2 displays values higher than 0.9 and the graphical distribution shows the experimental data versus the ones predicted by the model with a linear arrangement, proving the consistency of the RSM models. In addition, the distribution of the residuals as function of each variable are graphically represented and no grouped data or autocorrelations were observed.

3.1.4. Optimal conditions that favours the extraction of anthocyanins and its experimental verification

Once models are statistically and graphically validated, the optimization of the variable conditions to maximize the response values (or minimize, depending on the requirements) was performed by numerical analysis using the simplex procedure. Table 3A shows the variable conditions that optimize the three assessed responses (Y_1, Y_2, and Y_2/Y_1), individually, while Table 3B presents the results of an overall optimization of these responses.

Once the numerical values of the optimal conditions and the maximum responses are achieved, the tendencies of each response were represented in Fig. 2. The graphical illustration allows the visual selection of the most favourable conditions, taking into account simultaneously all responses when the excluded variable is positioned at the individual optimal values of the others (Table 3A). Fig. 2 shows the isolines projections for the combination of the three main involved variables ($\times_1$, $\times_2$, and $\times_3$) in the HAE, MAE, and UAE, for the three

Table 2
Parametric values, symmetric confidence intervals and statistical results of the second-order polynomial model of Eq. (1) after fitting the three response format values (Y_1, mg C/g R; Y_2, C/g P dw; and Y_2/Y_1 g R/g P dw) for the HAE, UAE, and MAE extracting techniques. The parametric subscript 1, 2, and 3 stands for the variables involved t (X_1), T or P (X_2), and S (X_3), respectively. The parameters are presented in coded values according to the CCCD with 5 range levels (Table A1).

Coefficients	Parametric responses to the central composite designs for each technique								
	HAE			UAE			MAE		
	Y_1	Y_2	Y_2/Y_1	Y_1	Y_2	Y_2/Y_1	Y_1	Y_2	Y_2/Y_1
Fitting coefficients obtained									
Intercept									
b_0	3.706 ± 0.333	14.744 ± 0.837	0.687 ± 0.009	5.509 ± 0.442	4.244 ± 0.478	0.775 ± 0.029	6.173 ± 0.322	4.461 ± 0.222	0.724 ± 0.005
Linear effect									
b_1	−0.224 ± 0.188	−0.859 ± 0.471	0.020 ± 0.006	0.206 ± 0.162	0.114 ± 0.262	0.012 ± 0.010	−0.355 ± 0.181	−0.278 ± 0.125	ns
b_2	0.216 ± 0.188	−1.361 ± 0.471	0.021 ± 0.006	0.613 ± 0.162	0.421 ± 0.262	0.013 ± 0.010	−0.518 ± 0.181	−0.361 ± 0.125	ns
b_3	1.297 ± 0.187	3.894 ± 0.470	ns	2.047 ± 0.162	0.884 ± 0.262	−0.086 ± 0.010	1.580 ± 0.181	1.094 ± 0.181	−0.007 ± 0.005
Quadratic effect									
b_{11}	−0.171 ± 0.102	ns	ns	ns	−0.067 ± 0.345	−0.009 ± 0.007	ns	ns	ns
b_{22}	−0.057 ± 0.030	−0.980 ± 0.573	ns	−0.626 ± 0.162	−0.393 ± 0.345	ns	−0.485 ± 0.152	−0.386 ± 0.220	−0.008 ± 0.005
b_{33}	ns	−0.908 ± 0.573	ns	0.274 ± 0.162	−0.261 ± 0.345	−0.050 ± 0.010	−0.348 ± 0.152	−0.226 ± 0.220	0.010 ± 0.005
Interactive effect									
b_{12}	0.171 ± 0.135	−0.738 ± 0.339	−0.012 ± 0.002	ns	ns	ns	−0.310 ± 0.130	−0.241 ± 0.130	ns
b_{13}	ns	ns	0.013 ± 0.002	0.189 ± 0.162	0.092 ± 0.189	ns	ns	ns	ns
b_{23}	−0.084 ± 0.049	−0.904 ± 0.338	0.014 ± 0.001	ns	−0.066 ± 0.188	ns	−0.360 ± 0.130	−0.235 ± 0.130	−0.007 ± 0.005
Statistical information of the fitting analysis									
Obs	28	28	28	28	28	28	28	28	28
R^2	0.9478	0.9129	0.8155	0.9359	0.9206	0.9194	0.9263	0.9352	0.9135
R^2adj	0.9056	0.8933	0.8022	0.9005	0.8954	0.8924	0.9016	0.8974	0.9036

ns: non-significant coefficient; *Obs*: number of observations; R^2: coefficient of determination; R^2adj: adjusted determination coefficient for the model.
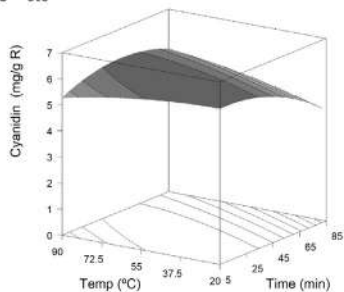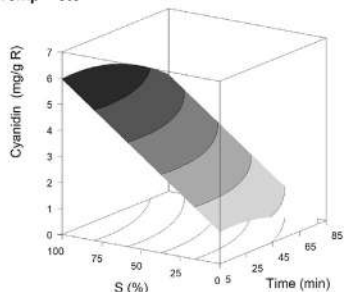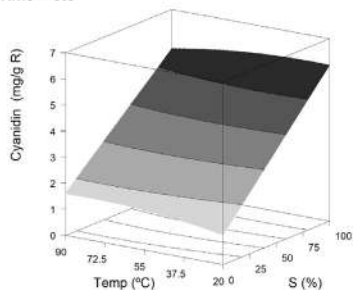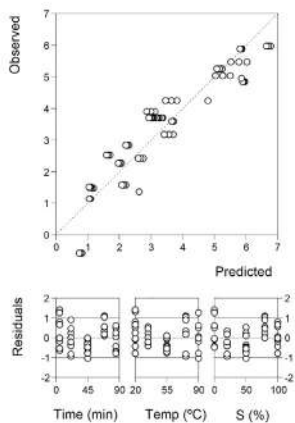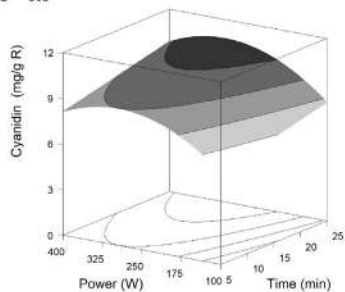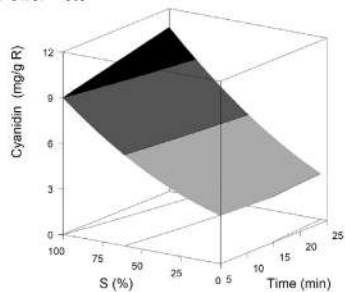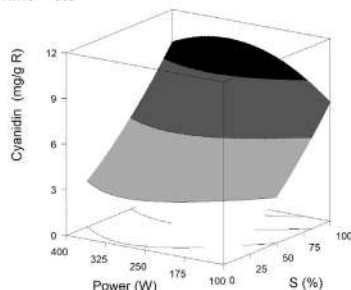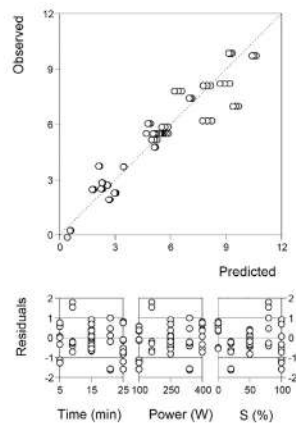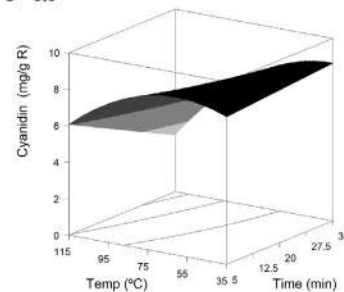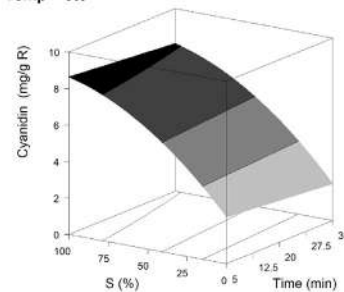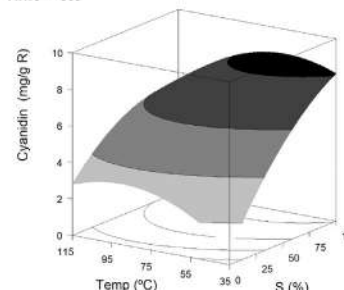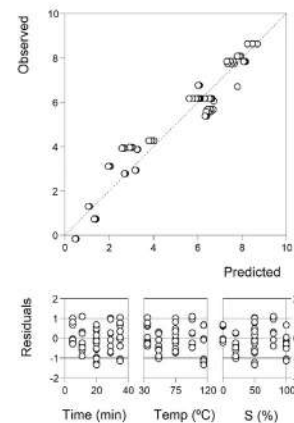
Fig. 1. *Part A*: Illustrates the three-dimensional analysis in terms of the extraction behaviour for the Y_1 (mg C/g R) responses for the optimization of the three main variables involved ($\times_1$, $\times_2$, and $\times_3$) in the HAE, UAE, and MAE. Each net surface shows the predicted response performed by the second order polynomial of Eq. (1). The interactions between each pair of variables in each graph are built when the factor excluded is constantly positioned at the centre of the experimental domain (Table A1, supplementary material). Experimental results are displayed in Table 1 and parametric values used in Eq. (1) are shown in Table 2. *Part B*: Shows a statistical illustration of the goodness of fit by presenting the differences between predicted and observed results and the residual distribution as a function of each of the variables.

response value formats (Y_1, mg C/g R; Y_2, mg C/g P dw; and Y_2/Y_1 g R/ g P dw). The isolines presented in the XY plane are derived from the three-dimensional responses obtained from the second-order polynomial equation of Eqs. (3) to (11). Their analysis is important for decision making when choosing the best conditions to perform the extractions.

Table 3

Optimal individual and global variable conditions (in natural values) that lead to maximal response values for each of the response value formats (Y_1, mg C/g R; Y_2, C/g P dw; and Y_2/Y_1 g R/g P dw) for each extracting technique assessed (HAE, UAE, and MAE).

Criteria		Optimal Variable Conditions			Optimum Response	
		X_1: t (min)	X_2: T (°C) or P (W)	X_3: S (%)		
A) Individual optimal variable conditions:						
HAE	Y_1	14.24 ± 0.16	28.26 ± 2.83	100.00 ± 2.12	5.99 ± 0.60	mg C/g R
	Y_2	49.25 ± 2.48	90.00 ± 8.10	100.00 ± 2.83	4.50 ± 0.27	mg C/g P dw
	Y_2/Y_1	85.00 ± 8.50	90.00 ± 3.60	100.00 ± 1.43	0.80 ± 0.08	g R/g P dw
UAE	Y_1	21.00 ± 1.89	309.53 ± 3.10	100.00 ± 1.45	9.56 ± 0.48	mg C/g R
	Y_2	25.00 ± 1.75	285.07 ± 19.95	100.00 ± 2.04	5.32 ± 0.37	mg C/g P dw
	Y_2/Y_1	23.61 ± 1.18	394.76 ± 3.95	19.96 ± 1.42	0.84 ± 0.08	g R/g P dw
MAE	Y_1	5.00 ± 0.10	60.27 ± 4.22	100.00 ± 3.19	8.63 ± 0.69	mg C/g R
	Y_2	5.00 ± 0.05	64.21 ± 1.28	100.00 ± 2.48	6.21 ± 0.56	mg C/g P dw
	Y_2/Y_1	35.00 ± 1.05	75.00 ± 6.75	0.00 ± 1.63	0.78 ± 0.02	g R/g P dw
B) Global optimal variable conditions:						
HAE	Y_1	13.74 ± 1.91	35.64 ± 7.98	100.00 ± 1.36	5.78 ± 0.12	mg C/g R
	Y_2				4.03 ± 0.22	mg C/g P dw
	Y_2/Y_1				0.56 ± 0.02	g R/g P dw
UAE	Y_1	21.34 ± 0.55	310.58 ± 25.89	100.00 ± 1.23	9.01 ± 0.76	mg C/g R
	Y_2				4.32 ± 0.14	mg C/g P dw
	Y_2/Y_1				0.51 ± 0.21	g R/g P dw
MAE	Y_1	5.00 ± 0.30	62.41 ± 0.57	100.00 ± 3.73	7.43 ± 0.78	mg C/g R
	Y_2				4.11 ± 0.37	mg C/g P dw
	Y_2/Y_1				0.76 ± 0.04	g R/g P dw

Finally, Fig. 3A shows a 2D graphical representation, in which the lines show the response predicted by the models described in Eqs. (3) to (11), when the other studied variables are fixed at their optimal values. The response axes (Y) were maintained on the same scale to facilitate the comparison among the used extraction techniques. The dots (⊙) presented alongside the line highlight the location of the optimal value (Table 3A).

When combining the information produced by the three response criteria (Y_1, Y_2, and Y_2/Y_1), the complete behaviour of each relevant variable influencing the responses is defined in global terms. The global optimizing results are presented in Table 3B and summarized below:

- For the HAE system: the optimal global conditions were at 13.74 ± 1.91 min, 35.64 ± 7.98 °C, and 100.00 ± 1.36% of ethanol, producing 5.78 ± 0.12 mg C/g R (Y_1), 4.03 ± 0.22 mg C/g P dw (Y_2), and 0.56 ± 0.02 g R/g P dw (Y_2/Y_1).

- For the UAE system: the optimal global conditions were at 21.34 ± 0.55 min, 310.58 ± 25.89 W, and 100.00 ± 1.36% of ethanol, producing 9.01 ± 0.76 mg C/g R (Y_1), 4.32 ± 0.14 mg C/g P dw (Y_2), and 0.51 ± 0.21 g R/g P dw (Y_2/Y_1).

- For the MAE system: the optimal global conditions were at 5.00 ± 0.30 min, 62.41 ± 0.57 °C, and 100.00 ± 9.00% of ethanol, producing 7.43 ± 0.78 mg C/g R (Y_1), 4.11 ± 0.37 mg C/g P dw (Y_2), and 0.76 ± 0.04 g R/g P dw (Y_2/Y_1).

For all techniques, the conditions that led to the optimal values were experimentally tested in order to ensure the accuracy of the presented results. Consequently, for the response Y_1, the UAE technique produced the best results, as the increase of t and S led to a residue with greater purity in cyanidin 3-rutinoside. Regarding the response Y_2, the MAE produced the higher values, but the increase of the t and T variables led to the degradation of the anthocyanin compound. The UAE gives rise to
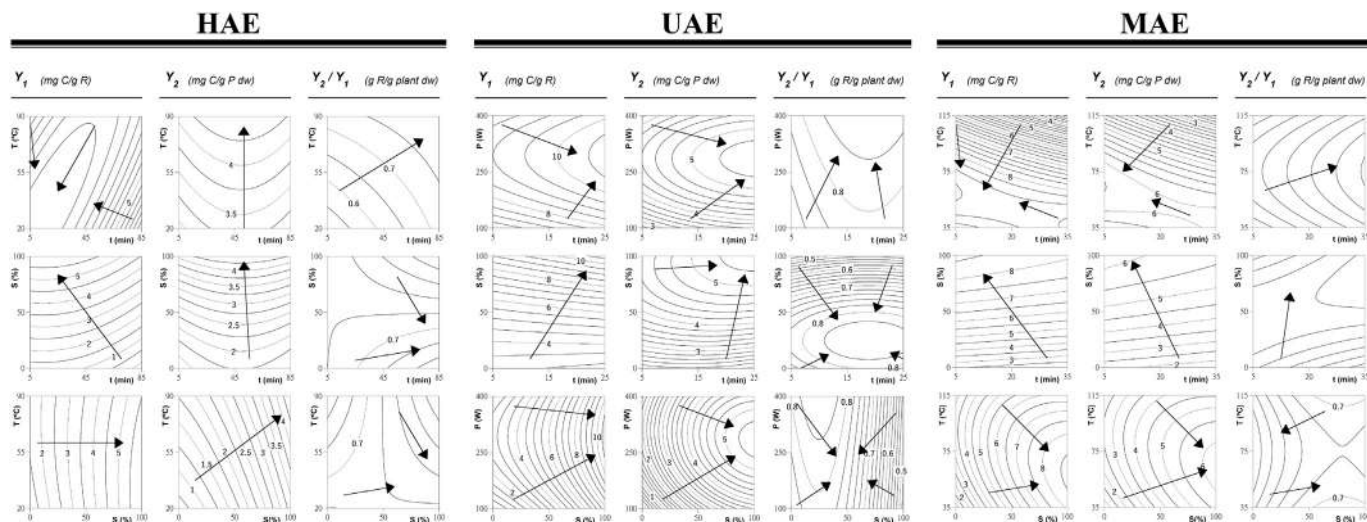

Fig. 2. Shows the contour graphs in terms of the three response value formats assessed (Y_1, mg C/g R; Y_2, mg C/g P dw; and Y_2/Y_1 g R/g P dw) as a function of two pair of variables of the three variables involved (X_1, X_2, and X_3) in the HAE, MAE and UAE. This analysis allows to describe visually the tendencies of each response and guide the selection of the most favourable conditions. Each of the contour graphs represents the isoline projection predicted with the second order polynomial of Eq. (1). The interactions between each pair of variables in each contour graphs are built when the factor excluded is constantly positioned at the individual optimal values of the others (Table 3A). The statistical design and experimental results are described in Table 1. Estimated parametric values are shown in Table 2.
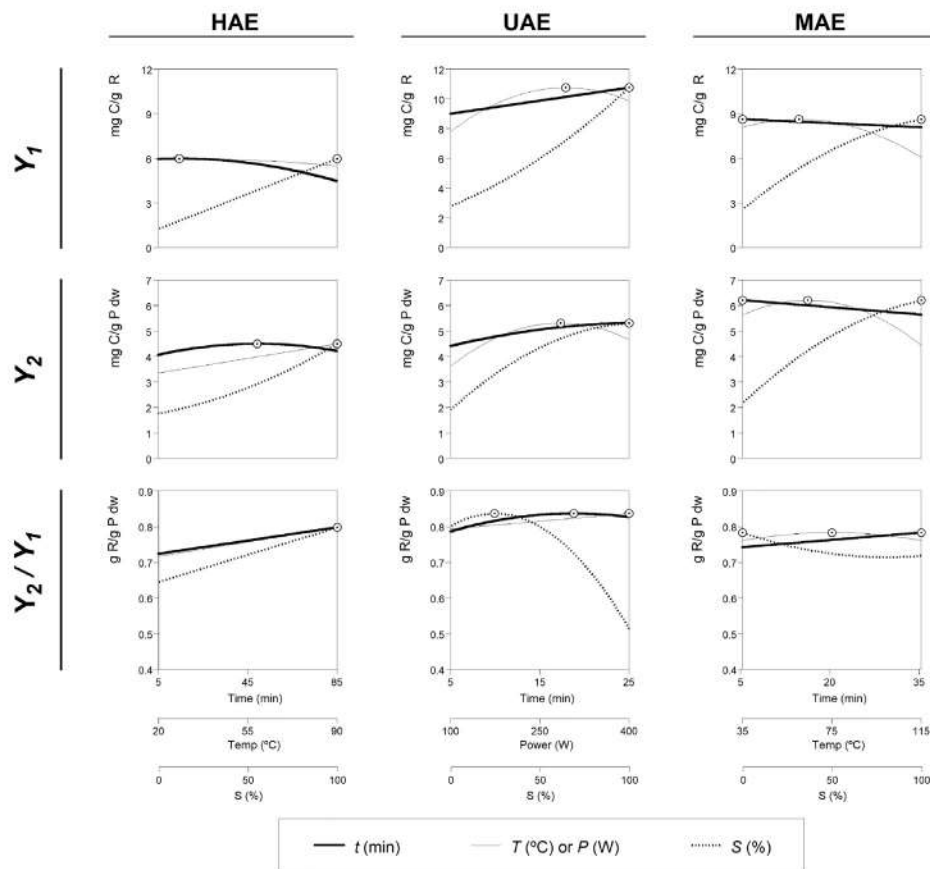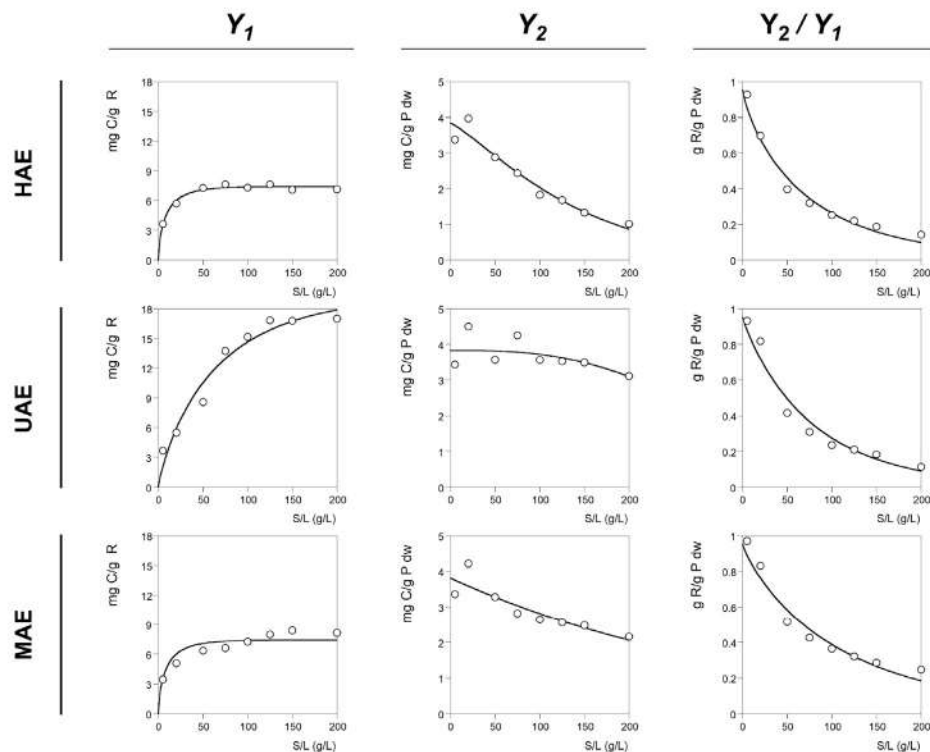
A: Illustration of the interaction between variables

B: Solid-to-liquid ratio patterns

lower Y_2 values, but the extraction was favoured if longer t and S were used. The HAE extraction system ensures a significant yield value as the variables S and T increases, but when the variable t increases the anthocyanin content decrease. However, the conditions optimized in global terms, the value of the variable S that maximized the cyanidin 3-rutinoside extraction is always 100%.

In conclusion, UAE is the best extraction technique, closely followed by MAE, and HAE, which showed to be less effective solutions. These results prove that alternative solid-liquid extraction methods (UAE and MAE) are more suitable than the conventional HAE for the extraction of cyanidin 3-rutinoside from fig peel.

3.2. Dose-response analysis of the solid-to-liquid effect at the optimum conditions

As already described in the bibliography, the ideal solid-to-liquid ratio should be the one that allows the solvent to properly penetrate into the structure of the solid matrix (Pinela et al., 2017), but also the one that allows the solvent to dissolve the target compounds (Albuquerque et al., 2016). Therefore, a study aiming to evaluate the S/L effect was conducted at the global optimal conditions predicted by the polynomial models obtained for HAE, UAE, and MAE techniques.

Primary tests were performed to find the limit value of S/L. The results showed that over 200 g/L the reaction system could not be homogenized properly, thus the dose-response analysis process was designed to analyse the S/L from 5 to 200 g/L.

The dose-response results to S/L effects of the three response value formats (Y_1, Y_2, and Y_2/Y_1) and for the three assessed extraction techniques were evaluated by fitting the Eq. (2) (increasing or decreasing form) to the experimental responses. The obtained parametric values are presented in Table A2 (supplementary material). The effects caused by the S/L on the response value formats are graphically shown in Fig. 3B for the three studied techniques. Fig. 3B shows the experimental results (points◯) and their respective predictions made by the mathematical model of Eq. (2) (lines). In general, a non-linear effect can be observed for all responses as the S/L dose-response increases, causing a saturation-increasing effect (↑) for the Y_1 (mg C/g R) value format and saturation-decreasing effects (↓) for Y_2 (mg C/g P dw) and Y_2/Y_1 (g R/g P dw) value formats. The analysis of the results can be interpreted by means of the two main parameters K and m_n (at 50% or 99% of the response). The parameter K shows the maximum extraction value that can be obtained as a function of the S/L dose-response. Thus, the lower the m_n values are, the higher are the reached extraction levels at a shorter dose-response value, which would limit the possibility of reducing the amount of needed solvent, for industrial purposes. Given these considerations, both values are important to understand the trends of the S/L dose-response effect.

In a more detailed analysis, the following aspects can be observed:

- For Y_1 values, response that gives the purity in C in the extracted residue: a saturation-increasing dose-response pattern was observed, which means that Y_1 initially increases as the S/L increases, but when a certain S/L level is reached, the anthocyanin purity remains constant. For HAE, the response rises until S/L reaches values close to 43.58 ± 0.11 g/L (parametric value $m_{99\%}$ from Eq. (2), Table A2), allowing a concentration of 7.41 ± 0.59 mg C/g R (parametric value K from Eq. (2), Table A2) that remains constant at high S/L values. For UAE, the $m_{99\%}$ value was 302.48 ± 3.48 g/L, with a K value of 19.40 ± 0.78 mg C/g R, and for MAE, 53.26 ± 8.91 g/L were obtained for $m_{99\%}$, with a K of 9.71 ± 1.38 mg C/g R. In the performed HAE and MAE, the increased levels of anthocyanin purity achieved by increasing the S/L were not as pronounced as those observed with UAE, fact that may be related to instrumental limitations.
- For Y_2 values, the response that reflects the C content in the peels: a saturation-decreasing dose-response pattern was observed, which

means that Y_2 initially decreases to zero as S/L increase. For HAE, UAE, and MAE the obtained $m_{50\%}$ values were 107.39 ± 9.67, 302.46 ± 27.22, and 225.07 ± 2.25 g/L, respectively, presenting K values of ~3.8 mg C/g P dw for the three tested techniques. These results may probably reflect the total available anthocyanin content in the fig peels, once a maximum concentration was achieved for all the tested extraction methods. Besides, when the S/L increased, a saturation of the solvent was observed, with a decrease of cyanidin 3-rutinoside levels. However, for the modern extraction techniques (UAE and MAE) this decreasing effect is less noted comparatively with the conventional extraction method (HAE). In fact, for UAE and MAE the S/L effect remains almost constant until ~120 g/L.
- For Y_2/Y_1 values, response that represents the extraction yield of the residue: a saturation-decreasing dose-response pattern was found, which means that Y_2 initially decreases as S/L increases. For HAE, UAE, and MAE the obtained $m_{50\%}$ values were 47.32 ± 1.89, 53.32 ± 0.53, and 74.41 ± 1.49 g/L, respectively, with a maximum residue levels of ~0.95 g R/g P dw (K), for all the assessed techniques.

Given the widespread interest for anthocyanins, there has been an effort to modernize the extraction protocols, reducing the amount of organic solvents (ecological point of view) and improving the extraction yield (economic point of view) (Jiménez et al., 2018). The lack of optimization approaches, specifically in what concerns anthocyanins extraction contributed to detract the use of these natural solutions in food industry. The study concludes that UAE and MAE, reduce both economic and ecological impacts in comparison with the typically HAE process, in the extraction of cyanidin 3-rutinoside from fig peel in an industrial level (Sicaire et al., 2016).

3.3. Comparison with other studies involving the extraction of anthocyanins

To recover anthocyanins from *Ficus carica* L. infructescences peel to be used as natural food colorant, the optimization of the extraction process is one of the crucial stages towards the industrial implementation. Nevertheless, along with the scarcity of studies on the evaluation of anthocyanin content in *F. carica* (entire infructescence, pulp, or peel), to the best of our knowledge none of these studies has previously optimized their extraction from these matrices, which hinders results comparison for this particular matrix. Consequently, the reported total anthocyanin values in the fig peel will be compared with bibliographic results in which the entire infructescence was used, as well as with those that have been reported as the major natural sources of anthocyanins (Khadhraoui et al., 2018).

Previous studies have shown that figs contain greater anthocyanin levels than other atypical natural sources (Harzallah et al., 2016; Vallejo et al., 2012). In a recent study conducted by Wojdyło, Nowicka, Carbonell-Barrachina, and Hernández (2016), dealing with the assess of different fig varieties, it was possible to recover 0.01 to 1.2 mg of anthocyanins per g of entire infructescence dw, using UAE with methanol as the extraction solvent. These values are lower than those obtained in this study for fig peel at the optimal conditions (~3.8 mg/g P dw). The higher concentration obtained with the fig peel could be partly attributed to the performed optimization procedure, which led to an increased extraction efficiency, and thus anthocyanin yield, when compared with results reported for the entire infructescence (Wojdyło et al., 2016). Moreover, further differences could be explained by the use of different extraction solvents (water-ethanol mixtures vs. methanol). It is a fact that methanol presents a high extraction power, especially for polar molecules such as phenolic compounds. Nevertheless, its use for the extraction of anthocyanin compounds seems to be unrealistic. On the other hand, the hydroalcoholic mixture water-ethanol can be considered a bio-solvent alternative for food industry, if properly removed, leading to higher anthocyanin recovery (Bosiljkov et al., 2017).

However, the differences found between anthocyanin levels in the entire infructescence and in the peel could by mainly explained by the fact that these compounds tend to be accumulated in the outer parts of the infructescence, such as peels, in the maturity stages chosen for harvest. This fact is well known and has been investigated with other bio-residues rich in anthocyanins, such as mango and sugarcane peels, which present ~0.1 mg/g P dw (Lopes et al., 2016; Zhao et al., 2018). Even so, the anthocyanin concentration detected in these matrices are far below those found in the fig peels assessed in the present study. Given the fact that in almost all industrial processes involving fig infructescence's they are used in very mature stages, the discarded parts of the fig, including the peels, can become relevant by-products if recovered for extraction of anthocyanins, compounds with natural colouring properties that could be applied as natural additives.

Generally, the most common rich sources of anthocyanins are those derived from *Oryza sativa* L. (var. Glutinosa), presenting 42 mg/g dw (Chen, McClung, & Bergman, 2017), *Phaseolus vulgaris* L. (common beans), with 32 mg/g dw (Mojica, Berhow, & Gonzalez de Mejia, 2017), and *Rubus fruticosus* L. fruits (blackberries), with 17.10 mg/g dw (Elisia, Hu, Popovich, & Kitts, 2006). Although these values are considerably higher than those presented by fig peels, these sources have an already recognized commercial value for other purposes, contrarily to fig peels. Considering that other matrices, such as eggplant peel (0.6 mg/g dw) (Todaro et al., 2009) or grape bark (1 mg/g dw) (Chen et al., 2015), are currently used as common sources of anthocyanins, even presenting a lower concentration than the one found in fig peels, this matrix arises as a promising by-product to be explored for colorant industrial application purposes.

4. Conclusions

Due to the great interest of using natural pigments, such as anthocyanins, in food, pharmaceutical, and cosmetic industries, in the present work different solid-liquid extraction methods were studied and optimized by RSM. The selected techniques were HAE, UAE, and MAE, using three independent variables (*t*, *T*, and *S* for HAE and MAE, and *t*, *P*, and *S* for UAE) to maximize the defined responses: mg C/g R (Y_1); mg C/g P dw (Y_2); and g R/g P dw (Y_2/Y_1). The UAE was the most effective method of this study, capable of producing 3.8 mg C/g P dw and 0.95 g R/g P dw, with an anthocyanin content of 19.4 mg C/g R. These values were obtained at the optimum conditions (21.34 ± 0.55 min, 310.58 ± 25.89 W, 100% ethanol, and 183.01 ± 22.82 g/L). The HAE and MAE techniques revealed similar performances, but slightly lower than the one obtained for UAE. When *S/L* variable was tested, a significant effect was noticed with UAE, resulting in an extract with an increased purity as the *S/L* increased.

The analysis presented provides important data that allows the comparison between different extraction methods, in terms of efficiency, and consequent related decision making. In an industrial level, these methodologies reduce costs related to energy, solvent consumption, equipment investment, etc. Achieving the optimal conditions and maximum the responses is an important step to guide the choice of a suitable and sustainable process.

Acknowledgements

Abbreviations

General abbreviations

HPLC-DAD-ESI/MS	High-performance liquid chromatography coupled to photodiode array detector and mass spectrometer
Eq. or Eqs.	Equation or equations
C	Cyanidin 3-rutinoside
P	Fig peel
R	Extracted dried weight residue
dw	Dry weight
RSM	Response surface methodology
CCCD	*Circumscribed central composite design*
MAE	Microwave assisted extraction
UAE	Ultrasound assisted extraction
HAE	Heat assisted extractionResponse surface methodology experimental design and model equations:

Variables

t	Time or X_1 (min)
T	Temperature or X_2 (°C)
S	Solvent proportion or X_2 (% v/v of ethanol in hydroalcoholic mixtures)
P	Ultrasonic power or X_2 (W)
S/L	Solid-to-liquid ratio or X_2 (g/L)
Responses	
Y_1	mg of cyanidin 3-rutinoside obtained in the extracted dried weight residue (R; mg C/g R)
Y_2	mg of cyanidin 3-rutinoside per g of peel dry matter (mg C/g P dw)
Y_2/Y_1	obtained by dividing the responses Y_2 and Y_1, which provides information regarding the extraction yield of the dried weight residue (g of R/g P dw)Equation
Eq. (1)	Second-order polynomial equation
Y	Dependent variable to be modelled
X_i and X_j	Independent variables to be assessed
b_0	Constant coefficient.
b_i	Coefficients of linear effect.
b_{ij}	Coefficients of interaction effect
b_{ii}	Coefficient of quadratic effect
n	Number of variables
Eqs. (3) to (11)	Second-order polynomial equation derived from Eq. (1) that describe all response formats for all techniques testedDose-response description of the solid-to-liquid ratio effect
W	Weibull equation
W (↑)	Increasing Weibull equation
W (↓)	Decreasing Weibull equation
Eq. (2)	Number of the Weibull equation in its increasing and decreasing form
K	Maximum extraction value. Units would depend in the response format (Y_1, Y_2, and Y_2/Y_1) assessed (i.e., if Y_2 the units would be in mg C/g P dw)
a	Shape parameter related to the maximum slope of the response
n	Any desired level between 0 and 100% of the response (Y_1, Y_2, and Y_2/Y_1)

m_n	The S/L parametric value for the selected n response level (m_{10}, m_{25}, m_{75}, m_{95}, etc.)Statistical evaluation
ns	Non-significant coefficient
Obs	Number of observations
R^2	Coefficient of determination
$R^2 adj$	Adjusted determination coefficient

Appendix A. Supplementary data

Supplementary data to this article can be found online at https://doi.org/10.1016/j.foodres.2018.07.016.

References

Albuquerque, B. R., Prieto, M. A., Barreiro, M. F., Rodrigues, A., Curran, T. P., Barros, L., & Ferreira, I. C. F. R. (2016). Catechin-based extract optimization obtained from *Arbutus unedo* L. fruits using maceration/microwave/ultrasound extraction techniques. *Industrial Crops and Products, 95*, 404–415.

Azmir, J., Zaidul, I. S. M., Rahman, M. M., Sharif, K. M., Mohamed, A., Sahena, F., ... M, A. K. (2013). Techniques for extraction of bioactive compounds from plant materials: A review. *Journal of Food Engineering, 117*(4), 426–436.

Bezerra, M. A., Santelli, R. E., Oliveira, E. P., Villar, L. S., Escaleira, E. A., & Escaleira, L. A. (2008). Response surface methodology (RSM) as a tool for optimization in analytical chemistry. *Talanta, 76*(5), 965–977.

Bonfigli, M., Godoy, E., Reinheimer, M. A., & Scenna, N. J. (2017). Comparison between conventional and ultrasound-assisted techniques for extraction of anthocyanins from grape pomace. Experimental results and mathematical modeling. *Journal of Food Engineering, 207*, 56–72.

Bosiljkov, T., Dujmić, F., Cvjetko Bubalo, M., Hribar, J., Vidrih, R., Brnčić, M., ... Jokić, S. (2017). Natural deep eutectic solvents and ultrasound-assisted extraction: Green approaches for extraction of wine lees anthocyanins. *Food and Bioproducts Processing, 102*, 195–203.

Caleja, C., Barros, L., Prieto, M. A., Barreiro, F. M. F., Oliveira, M. B. P., & Ferreira, I. C. F. R. (2017). Extraction of rosmarinic acid from *Melissa officinalis* L. by heat-, micro-wave- and ultrasound-assisted extraction techniques: A comparative study through response surface analysis. *Separation and Purification Technology, 186*, 297–308.

Chan, C. H., Yusoff, R., & Ngoh, G. C. (2013). Modeling and prediction of extraction profile for microwave-assisted extraction based on absorbed microwave energy. *Food Chemistry, 140*(1–2), 147–153.

Chemat, F., Rombaut, N., Meullemiestre, A., Turk, M., Perino, S., Fabiano-Tixier, A. S., & Abert-Vian, M. (2017). Review of green food processing techniques. Preservation, transformation, and extraction. *Innovative Food Science and Emerging Technologies, 41*, 357–377.

Chemat, F., Rombaut, N., Sicaire, A. G., Meullemiestre, A., Fabiano-Tixier, A. S., & Abert-Vian, M. (2017). Ultrasound assisted extraction of food and natural products. Mechanisms, techniques, combinations, protocols and applications. A review. *Ultrasonics Sonochemistry, 34*, 540–560.

Chen, M. H., McClung, A. M., & Bergman, C. J. (2017). Phenolic content, anthocyanins and antiradical capacity of diverse purple bran rice genotypes as compared to other bran colors. *Journal of Cereal Science, 77*, 110–119.

Chen, S., Zhang, F., Ning, J., Liu, X., Zhang, Z., & Yang, S. (2015). Predicting the an-thocyanin content of wine grapes by NIR hyperspectral imaging. *Food Chemistry, 172*, 788–793.

Dai, J., & Mumper, R. J. (2010). Plant phenolics: Extraction, analysis and their anti-oxidant and anticancer properties. *Molecules, 15*(10), 7313–7352.

Elisia, I., Hu, C., Popovich, D. G., & Kitts, D. D. (2006). Antioxidant assessment of an anthocyanin-enriched blackberry extract. *Food Chemistry, 101*(3), 1052–1058.

Estupiñan, D. C., Schwartz, S. J., & Garzón, G. A. (2011). Antioxidant activity, Total Phenolics content, anthocyanin, and color stability of isotonic model beverages co-lored with Andes berry (*Rubus glaucus* Benth) anthocyanin powder. *Journal of Food Science, 76*(1), S26–S34.

Fattore, M., Montesano, D., Pagano, E., Teta, R., Borrelli, F., Mangoni, A., ... Albrizio, S. (2016). Carotenoid and flavonoid profile and antioxidant activity in "Pomodorino Vesuviano" tomatoes. *Journal of Food Composition and Analysis, 53*(1238), 61–68.

Ferreira, S. L. C., Bruns, R. E., Ferreira, H. S., Matos, G. D., David, J. M., Brandão, G. C., ... dos Santos, L, W. N. (2007). Box-Behnken design: An alternative for the optimization of analytical methods. *Analytica Chimica Acta, 597*(2), 179–186.

García-Moreno, P. J., Batista, I., Pires, C., Bandarra, N. M., Espejo-Carpio, F. J., Guadix, A., & Guadix, E. M. (2014). Antioxidant activity of protein hydrolysates obtained from discarded Mediterranean fish species. *Food Research International, 65*(PC), 469–476.

Gonçalves, G. A., Soares, A. A., Correa, R. C. G., Barros, L., Haminiuk, C. W. I., Peralta, R. M., ... Bracht, A. (2017). Merlot grape pomace hydroalcoholic extract improves the oxidative and inflammatory states of rats with adjuvant-induced arthritis. *Journal of Functional Foods, 33*, 408–418.

Gowd, V., Jia, Z., & Chen, W. (2017). Anthocyanins as promising molecules and dietary bioactive components against diabetes – A review of recent advances. *Trends in Food Science and Technology, 68*, 1–13.

Harzallah, A., Bhouri, A. M., Amri, Z., Soltana, H., & Hammami, M. (2016). Phytochemical content and antioxidant activity of different fruit parts juices of three figs (*Ficus carica* L.) varieties grown in Tunisia. *Industrial Crops and Products, 83*, 255–267.

Jacotet-Navarro, M., Rombaut, N., Deslis, S., Fabiano-Tixier, A.-S., Pierre, F.-X., Bily, A., & Chemat, F. (2016). Towards a "dry" bio-refinery without solvents or added water using microwaves and ultrasound for total valorization of fruit and vegetable by-products. *Green Chemistry, 18*(10), 3106–3115.

Jiménez, L. C., Caleja, C., Prieto, M. A., Barreiro, M. F., Barros, L., & Ferreira, I. C. F. R. (2018). Optimization and comparison of heat and ultrasound assisted extraction techniques to obtain anthocyanin compounds from *Arbutus unedo* L. fruits. *Food Chemistry, 264*, 81–91.

Kalil, S., & Maugeri, F. (2000). Response surface analysis and simulation as a tool for bioprocess design and optimization. *Process Biochemistry, 35*, 539–550.

Khadhraoui, B., Turk, M., Fabiano-Tixier, A. S., Petitcolas, E., Robinet, P., Imbert, R., & Chemat, F. (2018). Histo-cytochemistry and scanning electron microscopy for studying spatial and temporal extraction of metabolites induced by ultrasound. Towards chain detexturation mechanism. *Ultrasonics Sonochemistry, 42*(November 2017), 482–492.

Lopes, M. M. A., Silva, E. O., Canuto, K. M., Silva, L. M. A., Gallão, M. I., Urban, L., ... Miranda, M. R. A. (2016). Low fluence pulsed light enhanced phytochemical content and antioxidant potential of "Tommy Atkins" mango peel and pulp. *Innovative Food Science and Emerging Technologies, 33*, 216–224.

Meullemiestre, A., Breil, C., Abert-Vian, M., & Chemat, F. (2016). Microwave, ultrasound, thermal treatments, and bead milling as intensification techniques for extraction of lipids from oleaginous Yarrowia lipolytica yeast for a biojetfuel application. *Bioresource Technology, 211*, 190–199.

Mojica, L., Berhow, M., & Gonzalez De Mejia, E. (2017). Black bean anthocyanin-rich extracts as food colorants: Physicochemical stability and antidiabetes potential. *Food Chemistry, 229*, 628–639.

Montesano, D., Fallarino, F., Cossignani, L., Bosi, A., Simonetti, M. S., Puccetti, P., & Damiani, P. (2008). Innovative extraction procedure for obtaining high pure lyco-pene from tomato. *European Food Research and Technology, 226*(3), 327–335.

Murado, M. A., & Prieto, M. A. (2013). Dose-response analysis in the joint action of two effectors. A new approach to simulation, identification and modelling of some basic interactions. *PLoS One, 8*(4), e61391.

Ongkowijoyo, P., Luna-Vital, D. A., & Gonzalez De Mejia, E. (2018). Extraction techniques and analysis of anthocyanins from food sources by mass spectrometry: An update. *Food Chemistry, 250*(July 2017), 113–126.

Palassarou, M., Melliou, E., Liouni, M., Michaelakis, A., Balayiannis, G., & Magiatis, P. (2017). Volatile profile of Greek dried white figs (*Ficus carica* L.) and investigation of the role of β-damascenone in aroma formation in fig liquors. *Journal of the Science of Food and Agriculture, 97*(15), 5254–5270.

Pinela, J., Prieto, M. A., Barreiro, M. F., Carvalho, A. M., Oliveira, M. B. P. P., Curran, T. P., & Ferreira, I. C. F. R. (2017). Valorisation of tomato wastes for development of nutrient-rich antioxidant ingredients: A sustainable approach towards the needs of the today's society. *Innovative Food Science and Emerging Technologies, 41*, 160–171.

Prieto, M. A., Curran, T. P., Gowen, A., & Vázquez, J. A. (2015). An efficient methodology for quantification of synergy and antagonism in single electron transfer antioxidant assays. *Food Research International, 67*, 284–298.

Prieto, M. A., & Vázquez, J. A. (2014). In vitro determination of the lipophilic and hy-drophilic antioxidant capacity of unroasted coffee bean extracts and their synergistic and antagonistic effects. *Food Research International, 62*(10), 1183–1196.

Ranic, M., Nikolic, M., Pavlovic, M., Buntic, A., Siler-Marinkovic, S., & Dimitrijevic-Brankovic, S. (2014). Optimization of microwave-assisted extraction of natural an-tioxidants from spent espresso coffee grounds by response surface methodology. *Journal of Cleaner Production, 80*, 69–79.

Rodriguez-Amaya, D. B. (2016). Natural food pigments and colorants. *Current opinion in food science. Vol. 7. Current opinion in food science* (pp. 20–26). Elsevier Ltd.

Rustioni, L., Di Meo, F., Guillaume, M., Failla, O., & Trouillas, P. (2013). Tuning color variation in grape anthocyanins at the molecular scale. *Food Chemistry, 141*(4), 4349–4357.

Salem, N., Msaada, K., Elkahoui, S., Mangano, G., Azaeiz, S., Ben Slimen, I., ... Marzouk, B. (2014). Evaluation of antibacterial, antifungal, and antioxidant activities of saf-flower natural dyes during flowering. *BioMed Research International, 2014*, 1–10.

Sang, J. J., Sang, J. J., Ma, Q., Hou, X.f., & Li, C.q. (2017). Extraction optimization and identification of anthocyanins from *Nitraria tangutorun* Bobr. Seed meal and estab-lishment of a green analytical method of anthocyanins. *Food Chemistry, 218*, 386–395.

Sicaire, A. G., Vian, M. A., Fine, F., Carré, P., Tostain, S., & Chemat, F. (2016). Ultrasound induced green solvent extraction of oil from oleaginous seeds. *Ultrasonics Sonochemistry, 31*, 319–329.

Todaro, A., Cimino, F., Rapisarda, P., Catalano, A. E., Barbagallo, R. N., & Spagna, G. (2009). Recovery of anthocyanins from eggplant peel. *Food Chemistry, 114*(2), 434–439.

Tsatsop, R. K. T., Djiobie, G. T., Kenmogne, B. S., Regonne, K. R., & Ngassoum, M. B. (2016). Optimization of microwave-assisted extraction of bioactive compounds from *Anogeissus Leiocarpus* Guill. & Perr. Stem bark using response surface methodology. *International Journal of Scientific & Technology Research, 5*(05), 1–8.

Vallejo, F., Marín, J. G., & Tomás-Barberán, F. A. (2012). Phenolic compound content of fresh and dried figs (*Ficus carica* L.). *Food Chemistry, 130*(3), 485–492.

Vieira, V., Prieto, M. A., Barros, L., Coutinho, J. A. P., Ferreira, O., & Ferreira, I. C. F. R. (2017). Optimization and comparison of maceration and microwave extraction sys-tems for the production of phenolic compounds from *Juglans regia* L. for the valor-ization of walnut leaves. *Industrial Crops and Products, 107*, 341–352.

Wang, Z., Cui, Y., Vainstein, A., Chen, S., & Ma, H. (2017). Regulation of fig (*Ficus carica* L.) fruit color: Metabolomic and Transcriptomic analyses of the flavonoid biosyn-thetic pathway. *Frontiers in Plant Science, 8*(November), 1–15.

Wojdyło, A., Nowicka, P., Carbonell-Barrachina, Á. A., & Hernández, F. (2016). Phenolic

compounds, antioxidant and antidiabetic activity of different cultivars of *Ficus carica* L. fruits. *Journal of Functional Foods, 25*, 421–432.

Zhao, Z., Yan, H., Zheng, R., Khan, M. S., Fu, X., Tao, Z., & Zhang, Z. (2018). Anthocyanins characterization and antioxidant activities of sugarcane (*Saccharum officinarum* L.) rind extracts. *Industrial Crops and Products, 113*(January), 38–45.

Zhu, Z., He, J., Liu, G., Barba, F. J., Koubaa, M., Ding, L., ... Vorobiev, E. (2016). Recent insights for the green recovery of inulin from plant food materials using non-conventional extraction technologies: A review. *Innovative Food Science and Emerging Technologies, 33*, 1–9.

Zhu, Z., Wu, Q., Di, X., Li, S., Barba, F. J., Koubaa, M., & He, J. (2017). Multistage recovery process of seaweed pigments: Investigation of ultrasound assisted extraction and ultra-filtration performances. *Food and Bioproducts Processing, 104*, 40–47.

Ultrasound as a Rapid and Low-Cost Extraction Procedure to Obtain Anthocyanin-Based Colorants from *Prunus spinosa* L. Fruit Epicarp: Comparative Study with Conventional Heat-Based Extraction

Maria G. Leichtweis [1], Carla Pereira [1], M.A. Prieto [1,2], Maria Filomena Barreiro [1,3], Ilton José Baraldi [4], Lillian Barros [1,*], and Isabel C.F.R. Ferreira [1,*]

[1] Centro de Investigação de Montanha (CIMO), Instituto Politécnico de Bragança, Campus de Santa Apolónia, 5300-253 Bragança, Portugal; mg.leichtweis@hotmail.com (M.G.L.); carlap@ipb.pt (C.P.); michaelumangelum@gmail.com (M.A.P.); barreiro@ipb.pt (M.F.B.)

[2] Nutrition and Food Science Group, Dept. of Analytical and Food Chemistry, CITACA, CACTI, University of Vigo-Vigo Campus, Vigo, Spain

[3] Laboratory of Separation and Reaction Engineering – Laboratory of Catalysis and Materials (LSRE-LCM), Polytechnic Institute of Bragança, Campus Santa Apolónia, 5300-253 Bragança, Portugal

[4] Departamento Acadêmico de Alimentos (DAALM), Universidade Tecnológica Federal do Paraná, Campus Medianeira, 85884-000, Paraná, Brasil; ijbaraldi@gmail.com

* Correspondence: lillian@ipb.pt (L.B.); iferreira@ipb.pt (I.C.F.R.F); Tel.: +351-273-303285 (L.B.); +351-273-303219 (I.C.F.R.F); Fax: +351-273-325405 (L.B.);+351-273-325405 (I.C.F.R.F)

Abstract: An ultrasound rapid and low-cost procedure for anthocyanin-based colorants from *Prunus spinosa* L. fruit epicarp was developed, and the advantages were compared with conventional heat-based extraction. To obtain the conditions that maximize anthocyanins' extraction, a response surface methodology was applied using the variables of time, temperature, and ethanol content, in the case of heat extraction, whereas for ultrasound assisted extraction, temperature was replaced by ultrasound power. Two anthocyanin compounds were identified by HPLC-DAD-ESI/MS—namely, cyanidin 3-rutinoside and peonidin 3-rutinoside. The responses used were the extraction yield and the content of the identified anthocyanins. Ultrasound extraction was the most effective method at 5.00 ± 0.15 min, 400.00 ± 32.00 W, and 47.98% ± 2.88% of ethanol obtaining 68.60% ± 2.06% of extracted residue, with an anthocyanin content of 18.17 mg/g (extract-basis) and 11.76 mg/g (epicarp-basis). Overall, a viable green process was achieved that could be used to support pilot-scale studies for industrial production of anthocyanin-based colorants from *P. spinosa* fruit epicarp.

1. Introduction

Prunus spinosa L. (blackthorn) is a spontaneous wild shrub found in Portugal, Spain, and other European countries. Its fruits are commonly used for liqueur and jam preparations, as well as for medicinal purposes [1]. Nevertheless, no reports were found regarding the industrial, or large scale, use of these fruits, probably because of their bitter and astringent taste.

The valorization of agricultural products has gained much attention in the late years as a mean for a sustainable management, which can concomitantly increase the profit of local economies. In this regard, *P. spinosa* constitutes an underexploited source and can serve as a raw material for the

recovery/production of compounds for food applications [2]. As with other *Prunus* species, anthocyanin compounds can be found in blackthorn fruits at high levels, being responsible for their typical coloration [3,4]. In fact, a complex profile of anthocyanins was previously identified in *P. spinosa* fruits, among which cyanidin 3-rutinoside and peonidin 3-rutinoside were found to be predominant [5,6].

Anthocyanins are natural pigments belonging to the phenolic compounds group and, within that, to the flavonoids class, presenting a range of colors between red, blue, and violet that are characteristic of various fruits and vegetables [7]. Beyond their various physiological benefits, which include effects against cardiovascular diseases, atherosclerosis, and cancer, recently, an increasing interest in these compounds began to arise because of their colorant properties [8,9].

The industrial production of natural-based colorants has been established for years and consists mainly of obtaining colorant-rich extracts through conventional heat assisted extraction (HAE, or maceration) using water as a solvent followed by several isolation/drying steps. This type of conventional process, although used at large-scale, is known for requiring high-energy consumption and long extraction times [10–12]. Alternative extraction processes, able to replace traditional ones, have been established to shorten the needed time, decrease energy requirements, and reduce solvent consumption. Among the non-conventional procedures applied to anthocyanins' extraction, ultrasound, microwave, and supercritical fluid assisted extraction techniques have attracted, in the recent years, the attention of industrials and researchers [10,13]. Regarding ultrasound assisted extraction (UAE), it is considered an inexpensive, simple, and efficient alternative to conventional techniques [14]. The extraction capability of UAE is attributed to mechanical and cavitation phenomena, which lead to cells' disruption, particle size reduction, and enhanced mass transfer across the cell membrane [11,13].

To obtain anthocyanin-rich extracts, it is crucial to consider the factors affecting the stability of these compounds, including structure and concentration, pH, temperature, light exposure, oxygen levels, and used extraction solvents [15]. Thus, the choice of the extraction method, along with the optimization of relevant extraction variables, are essential to guarantee a maximum recovery efficiency [16]. Additionally, the efficiency is also strongly affected by the variability observed among different matrices [17]. Through response surface methodology (RSM), it is possible to optimize the relevant variables simultaneously, obtaining polynomial models capable of describing, within the tested experimental interval, the ideal conditions that maximize the used response criteria [13].

In the present study, the goal was to explore blackthorn anthocyanin composition and promote a higher commercial value of these wild fruits through the development of an anthocyanin-based coloring extract. For that purpose, the fruit epicarp was used because it has a much more intense color than the pulp, and thus a higher concentration of anthocyanins and less interfering compounds in the extraction process (e.g., sugars). To the best of our knowledge, and according to a thorough literature survey, no reference or report on the optimization of anthocyanin compounds extraction from fruit epicarps of *P. spinose* was found. Therefore, the present study aimed to optimize the extraction of these compounds from *P. spinosa* fruit epicarps through HAE and UAE techniques, evaluating the following variables: i) type of solvent (water and green organic solvents); ii) extraction time; iii) solid-to-liquid ratio; and iv) temperature (for HAE) or pressure (for UAE). The most efficient parameters were obtained by response surface methodology (RSM). The identification and quantification of the anthocyanin compounds present in the extracts was assessed by HPLC-DAD-ESI/MS.

2. Results

2.1. Development of RSM Models to Optimize Responses and Conditions

The RSM is a valuable instrument to assess the impact of the main extraction factors and their interactions on one or more responses. The technique uses fixed experimental designs with the major goals of minimizing the experimental labor and finding optimal solutions. In this regard, the work presented here uses the *circumscribed central composite design (CCCD)* design plan, which is a popular

design among researchers when trying to optimize food processing methods [18], such as the extraction of anthocyanin compounds.

In a previous study [5], authors identified, using HPLC-DAD-ESI/MS, the anthocyanin compounds of cyanidin 3-rutinoside ($[M + H]^+$ at m/z 595) and peonidin 3-rutinoside ($[M + H]^+$ at m/z 609) in *P. spinosa* fruits, and highlighted that the colorant capacity of these fruits is mainly attributed to these compounds. Although authors quantify the content of those anthocyanin compounds in *P. spinosa* fruits, the conditions of extraction were not optimized. Therefore, based on those preliminary findings, it seems logical to continue to explore the potential of *P. spinosa* fruits as a source of anthocyanin compounds. In this regard, the study applies a RSM technique under a *CCCD* to optimize the operating conditions of the extraction of two common techniques in the industrial environment (HAE and UAE) with the intention of maximizing their extraction. However, because the major quantity of anthocyanin compounds in *P. spinosa* fruits is located in the fruit epicarp, in this study, we ignored the inside parts of the fruit and focused the attention on the fruit epicarps. Additionally, by focusing on the epicarps, we are avoiding a high content of interfering compounds in the extraction process (e.g., sugars) that would require further purification steps. Figure A1 (supplemental material) shows a complete summary of all the steps used for the optimization procedure in order to recover the anthocyanin compounds from the epicarps of *P. spinosa* fruits. Figure A2 (supplementary material) shows a chromatographic example of HPLC-DAD-ESI/MS results for the quantification of anthocyanin compounds in the epicarps of *P. spinosa* fruits.

Table 1 shows the experimental results derived from the *CCCD* used to optimize the extraction of anthocyanins from the fruits epicarps (Y_1, mg C/g R; Y_2, mg C/g E dw; and *Yield*, %) for each one of the computed extraction techniques (HAE and UAE). As described, the *CCCD* experimental results are subjected to the mathematical analysis of Equation (1), by applying a fitting procedure coupled with non-linear least-squares estimations. The parametric values of Equation (1) derived from this analytical procedure, the corresponding confidence interval of the parameters (α = 0.05) found after modelling the extraction response values, and basic statistical information of the mathematical procedure are presented in Table 2. The parametric values considered non-significant (*ns*) values were excluded from model construction and the final equations for describing the responses assessed using significant terms are presented in Table A1 (supplementary material).

The significant parametric values in Table 2 are presented as a function of the codification criteria of the *CCCD*. Although they could be presented as the real numerical ranges of the variables assessed (X_1 to X_3), such information would not provide any additional insights of the regression analysis performed or the possible effects that may occur. The key information is the weight of the numerical values of the significant parameters; therefore, it seems logical to present them under a codification mode that allows us to compare the values between them effortlessly. Therefore, based on the numerical values derived, some global conclusions can be deduced as follows:

- For the HAE technique: In global terms, the significant parametric values within the linear effect (LE) group have a far more relevant contribution to the description of the responses than the interactive effect (IE), with the quadratic effect (QE) group being the less representative one (LE > IE >> QE). In the extraction *Yield* response, the three variables assessed (*t*, *T*, and *S*) showed similar contributions to its description. Regarding the response values of Y_1 (mg CT/g R) and Y_2 (mg CT/g E dw), the contribution of the variables is *S* >> *T* > *t*.
- For the UAE technique: The contribution to the description of effects of the responses by the significant parametric values is distributed as LE > QE >> IE. In all the responses assessed (extraction *yield*, Y_1 and Y_2 values), the contribution of the variables is *S* >> *P* > *t*.

Table 1. Experimental results of the *CCCD* used for the response surface methodology (RSM) optimization of the three main variables involved (X_1, X_2, and X_3) in the heat assisted extraction (HAE) and ultrasound assisted extraction (UAE). Responses comprised three format values assessed (Y_1, mg C/g R; Y_2, mg C/g E dw; and *Yield*, %).

	Experimental Design									HAE							UAE						
	Coded Values			HAE			UAE			Residue	Individual Content				Total Content		Residue	Individual Content				Total Content	
	X_1	X_2	X_3	X_1: t	X_2: T	X_3: S	X_1: t	X_2: P	X_3: S	*Yield*	Y_1C1	Y_1C2	Y_2C1	Y_2C2	Y_1CT	Y_2CT	*Yield*	Y_1C1	Y_1C2	Y_2C1	Y_2C2	Y_1CT	Y_2CT
				min	°C	%	min	W	%	%	mg/g R	mg/g R	mg/g E	mg/g E	mg/g R	mg/g E	%	mg/g R	mg/g R	mg/g E	mg/g E	mg/g R	mg/g E
1	−1	−1	−1	21.2	34.2	20.3	9.1	160.8	20.3	53.75	6.65	3.04	3.58	1.64	9.73	5.21	61.24	9.26	3.65	5.67	2.24	12.91	7.91
2	−1	−1	1	21.2	34.2	79.7	9.1	160.8	79.7	45.43	7.54	4.65	3.42	2.11	12.22	5.54	52.87	9.45	4.44	5.00	2.35	13.89	7.34
3	−1	1	−1	21.2	75.8	20.3	9.1	339.2	20.3	57.26	6.08	2.81	3.48	1.61	8.78	5.09	70.17	8.96	3.44	6.29	2.41	12.40	8.70
4	−1	1	1	21.2	75.8	79.7	9.1	339.2	79.7	48.85	8.35	4.44	4.08	2.17	12.74	6.25	58.80	9.36	4.51	5.50	2.65	13.87	8.15
5	1	−1	−1	68.8	34.2	20.3	20.9	160.8	20.3	55.45	6.88	2.90	3.82	1.61	9.66	5.42	59.12	10.66	3.69	6.30	2.18	14.35	8.48
6	1	−1	1	68.8	34.2	79.7	20.9	160.8	79.7	50.00	10.05	4.05	5.03	2.02	14.03	7.05	55.22	8.99	4.14	4.97	2.29	13.14	7.25
7	1	1	−1	68.8	75.8	20.3	20.9	339.2	20.3	60.18	6.72	2.81	4.04	1.69	9.37	5.73	67.05	8.79	2.86	5.90	1.92	11.65	7.82
8	1	1	1	68.8	75.8	79.7	20.9	339.2	79.7	53.09	11.01	4.39	5.84	2.33	15.26	8.17	57.19	8.69	4.24	4.97	2.42	12.92	7.39
9	−1.68	0	0	5	55	50	5	250	50	53.88	8.15	3.80	4.39	2.05	12.01	6.44	68.58	10.53	4.77	7.22	3.27	15.30	10.49
10	1.68	0	0	85	55	50	25	250	50	56.51	9.09	3.70	5.14	2.09	12.74	7.23	56.13	10.14	4.56	5.69	2.56	14.71	8.25
11	0	−1.68	0	45	20	50	15	100	50	49.49	11.09	4.70	5.49	2.33	15.59	7.82	55.99	12.41	5.45	6.95	3.05	17.86	10.00
12	0	1.68	0	45	90	50	15	400	50	60.78	8.68	3.42	5.27	2.08	11.96	7.36	76.95	10.60	4.40	8.16	3.38	15.00	11.54
13	0	0	−1.68	45	55	0	15	250	0	54.73	3.81	1.63	2.09	0.89	5.46	2.98	50.18	8.22	1.92	4.12	1.19	10.14	5.31
14	0	0	1.68	45	55	100	15	250	100	47.62	5.68	2.69	2.70	1.28	8.23	3.99	34.40	11.06	1.15	3.81	0.39	12.21	4.20
15	−1.68	−1.68	−1.68	5	20	0	5	100	0	54.39	4.24	1.85	2.30	1.01	6.01	3.31	47.94	8.15	3.73	3.91	1.79	11.88	5.69
16	−1.68	−1.68	1.68	5	20	100	5	100	100	36.34	2.45	1.65	0.89	0.60	4.12	1.49	33.12	6.25	1.50	2.07	0.50	7.75	2.57
17	−1.68	1.68	−1.68	5	90	0	5	400	0	56.79	3.53	1.59	2.00	0.90	5.13	2.90	61.16	10.89	4.46	6.66	2.73	15.36	9.39
18	−1.68	1.68	1.68	5	90	100	5	400	100	47.24	4.51	2.39	2.13	1.13	6.88	3.26	28.92	11.57	4.64	3.34	1.34	16.21	4.69
19	1.68	−1.68	−1.68	85	20	0	25	100	0	51.72	4.45	2.00	2.30	1.03	6.40	3.33	45.30	9.99	4.55	4.53	2.06	14.54	6.59
20	1.68	−1.68	1.68	85	20	100	25	100	100	39.88	4.46	1.75	1.78	0.70	6.21	2.48	28.91	9.60	1.71	2.78	0.50	11.31	3.27
21	1.68	1.68	−1.68	85	90	0	25	400	0	64.04	2.14	0.78	1.37	0.50	2.95	1.87	51.96	9.85	3.88	5.12	2.02	13.73	7.13
22	1.68	1.68	1.68	85	90	100	25	400	100	61.84	6.75	2.82	4.17	1.74	9.54	5.91	23.34	10.08	3.72	2.35	0.87	13.80	3.22
23	0	0	0	45	55	50	15	250	50	56.07	8.65	3.78	4.85	2.12	12.53	6.97	65.72	10.85	4.50	7.13	2.96	15.35	10.08
24	0	0	0	45	55	50	15	250	50	56.55	8.79	4.13	4.97	2.34	13.00	7.31	65.90	10.93	4.34	7.20	2.86	15.27	10.06
25	0	0	0	45	55	50	15	250	50	54.57	8.99	4.09	4.91	2.23	13.22	7.14	66.06	10.44	4.04	6.89	2.67	14.47	9.56
26	0	0	0	45	55	50	15	250	50	54.35	8.65	3.78	4.70	2.05	12.36	6.76	67.94	11.08	4.35	7.53	2.96	15.43	10.48
27	0	0	0	45	55	50	15	250	50	54.57	9.26	4.20	5.02	2.27	13.33	7.14	67.80	10.27	4.09	6.96	2.77	14.36	9.74
28	0	0	0	45	55	50	15	250	50	54.35	9.12	4.18	5.02	2.30	13.37	6.76	68.10	10.26	3.92	6.99	2.67	14.18	9.66

In general, positive and highly significant effects of LE, QE, and IE are found to moderately affect the studied responses. In both techniques assessed (HAE and UAE), the variable S is the most relevant one. Initial increases of S cause an increase of the extraction efficiency until it reaches a maximum, in which case the increase will cause a decrease in the extraction, but its interactive effect with the variable t and T or P causes a more favorable influence.

Additionally, using the significant parametric values of Table 2 coupled with a simplex methodology, it is possible to determine the absolute/relative optimal values of conditions to maximize the responses individually or globally, in order to obtain the most efficient extraction process. Table 3 shows the individual and global optimal response values and the corresponding conditions that produced them. In consequence, the extracting techniques (HAE and UAE) according to the three response value formats (Y_1, mg C/g R; Y_2, mg C/g E dw; and *Yield*, %) for each assessed anthocyanin (C1 and C2), as well as for the total anthocyanin content (CT = C1 + C2), are depicted.

Table 2. Parametric results of the second-order polynomial equation of Equation (1) for the HAE and UAE techniques assessed and for the three response value formats (Y_1, mg C/g R; Y_2, mg C/g E dw; and *Yield*, %). The parametric subscript 1, 2, and 3 stands for the variables involving t (X_1), T or P (X_2), and S (X_3), respectively. Analyses of significance of the parameters ($\alpha = 0.05$) are presented in coded values. Additionally, the statistical information of the fitting procedure to the model is presented.

| PARAMETERS		RESIDUE	INDIVIDUAL CONTENT				TOTAL CONTENT	
		Yield	Y_1C1	Y_1C2	Y_2C1	Y_2C2	Y_1CT	Y_2CT
HAE								
Intercept	b_0	54.86±0.72	9.35±0.38	4.15±0.19	5.07±0.17	2.26±0.08	13.48±0.55	7.29±0.23
Linear effect	b_1	1.54±0.43	0.33±0.21	ns	0.25±0.09	ns	0.28±0.21	0.26±0.13
	b_2	3.12±0.43	ns	ns	0.15±0.09	0.05±0.02	ns	0.19±0.13
	b_3	-3.07±0.43	0.56±0.21	0.33±0.11	0.17±0.09	0.11±0.05	0.88±0.31	0.27±0.13
Quadratic effect	b_{11}	ns	-0.26±0.21	-0.09±0.07	-0.10±0.05	-0.05±0.03	-0.35±0.26	-0.16±0.15
	b_{22}	ns	ns	ns	ns	ns	ns	ns
	b_{33}	-1.24±0.42	-1.60±0.26	-0.69±0.13	-0.94±0.11	-0.40±0.06	-2.26±0.37	-1.33±0.15
Interactive effect	b_{12}	0.78±0.31	0.00±0.00	ns	ns	ns	ns	ns
	b_{13}	0.54±0.31	0.26±0.15	0.04±0.02	0.18±0.07	0.04±0.03	0.31±0.22	0.22±0.09
	b_{23}	0.69±0.31	0.31±0.15	0.14±0.08	0.21±0.07	0.09±0.03	0.45±0.22	0.29±0.09
Statistics (R^2)		0.9375	0.9100	0.8755	0.9443	0.9272	0.9046	0.9489
UAE								
Intercept	b_0	68.11±1.70	10.42±0.47	4.10±0.28	6.98±0.22	2.83±0.13	14.46±0.62	9.75±0.31
Linear effect	b_1	-1.70±0.96	ns	ns	-0.13±0.12	-0.10±0.07	ns	-0.22±0.17
	b_2	2.12±0.96	0.23±0.21	0.18±0.15	0.25±0.12	0.14±0.07	0.37±0.35	0.36±0.17
	b_3	-6.46±0.96	ns	-0.16±0.15	-0.55±0.12	-0.26±0.07	ns	-0.82±0.17
Quadratic effect	b_{11}	-2.29±1.16	ns	0.26±0.20	-0.13±0.11	ns	ns	ns
	b_{22}	ns	ns	0.35±0.20	ns	0.19±0.09	0.66±0.42	0.27±0.21
	b_{33}	-7.33±1.16	-0.36±0.27	-0.84±0.20	-1.02±0.15	-0.68±0.09	-1.22±0.42	-1.84±0.21
Interactive effect	b_{12}	ns	-0.34±0.20	-0.11±0.11	-0.18±0.09	-0.07±0.05	-0.46±0.25	-0.23±0.12
	b_{13}	ns	ns	ns	ns	ns	ns	ns
	b_{23}	-1.29±0.69	0.17±0.10	0.22±0.11	-0.08±0.05	ns	0.41±0.25	ns
Statistics (R^2)		0.9431	0.7825	0.9032	0.9316	0.9035	0.8986	0.9380

Table 3. Variable conditions in natural values that lead to optimal global and individual response values for RSM for each of the extracting techniques assessed (HAE and UAE), for the three response value formats (Y_1, mg C/g R; Y_2, mg C/g E dw; and *Yield*, %), for each compound assessed (C1 and C2), and for the total compounds (CT=C1+C2).

| CRITERIA			OPTIMAL VARIABLE CONDITIONS			OPTIMUM RESPONSE	
			X_1: t (min)	X_2: T (ºC) or P(W)	X_3: S (%)		
A) Individual optimal variable conditions							
		Yield	85.00±8.50	90.00±4.50	38.01±3.04	65.10±3.91	%
HAE	Y_1	C1	64.89±5.19	90.00±8.10	62.01±3.10	9.71±0.49	mg C1/g R
		C2	47.18±3.30	90.00±7.20	62.22±6.22	4.27±0.34	mg C2/g R
		CT	58.85±5.89	90.00±9.00	61.97±6.20	13.89±0.14	mg CT/g R
	Y_2	C1	84.27±0.84	90.00±3.60	63.11±3.79	5.64±0.51	mg C1/g E dw
		C2	48.06±1.92	90.00±0.90	59.98±3.60	2.38±0.21	mg C2/g E dw
		CT	70.76±5.66	90.00±4.50	60.82±3.04	7.89±0.55	mg CT/g E dw
UAE		*Yield*	12.79±0.51	400.00±32.00	32.51±1.95	74.53±2.24	%
	Y_1	C1	5.00±0.10	400.00±28.00	61.80±1.85	11.82±0.71	mg C1/g R
		C2	5.00±0.10	400.00±28.00	53.58±1.07	6.45±0.45	mg C2/g R
		CT	5.00±0.10	400.00±20.00	58.39±4.09	18.32±1.47	mg CT/g R
	Y_2	C1	5.00±0.50	400.00±4.00	40.11±2.81	7.88±0.16	mg C1/g E dw
		C2	5.00±0.40	400.00±28.00	44.35±4.43	3.96±0.28	mg C2/g E dw
		CT	5.00±0.35	400.00±20.00	43.37±4.34	12.23±0.86	mg CT/g E dw
B) Global optimal variable conditions							
		Yield				50.89±3.05	%
HAE	Y_1	C1				9.71±0.29	mg C1/g R
		C2				4.22±0.13	mg C2/g R
		CT	49.02±2.94	90.00±7.20	50.00±0.50	13.93±0.42	mg CT/g R
	Y_2	C1				5.57±0.11	mg C1/g E dw
		C2				2.36±0.05	mg C2/g E dw
		CT				7.93±0.08	mg CT/g E dw
UAE		*Yield*				68.60±2.06	%
	Y_1	C1				11.74±0.23	mg C1/g R
		C2				6.43±0.32	mg C2/g R
		CT	5.00±0.15	400.00±32.00	47.98±2.88	18.17±1.82	mg CT/g R
	Y_2	C1				7.81±0.47	mg C1/g E dw
		C2				3.95±0.24	mg C2/g E dw
		CT				11.76±0.82	mg CT/g E dw

2.2. Alternative Visual Illustration of the Effects of the Extraction Variables on the Target Responses Used

Although the parametric values show the behavior of the responses, and could be used to understand their patterns, a more visual way to express the effects of variables on the extraction of any type of response is to generate 3D surface and/or contour plots, by varying two variables in the experimental range under investigation and holding the other one at a fixed level. In this regard, Figure 1 and Figure 2 show the 3D surface and 2D contour plots, respectively, representing the influence of the investigated effects of HAE and UAE parameters on the extraction behavior. The plots enable one to visualize the influence and interaction between the variables. Visual analyses of 3D surface and 2D contour plots are in accordance with parametric values derived from the multiple regression analysis, as described in Table 2 (parametric values) and Table A1 (full mathematical models, supplementary material).

Yield		*Residue (Y₁)*		*Epicarp (Y₂)*	
HAE	*UAE*	*HAE*	*UAE*	*HAE*	*UAE*
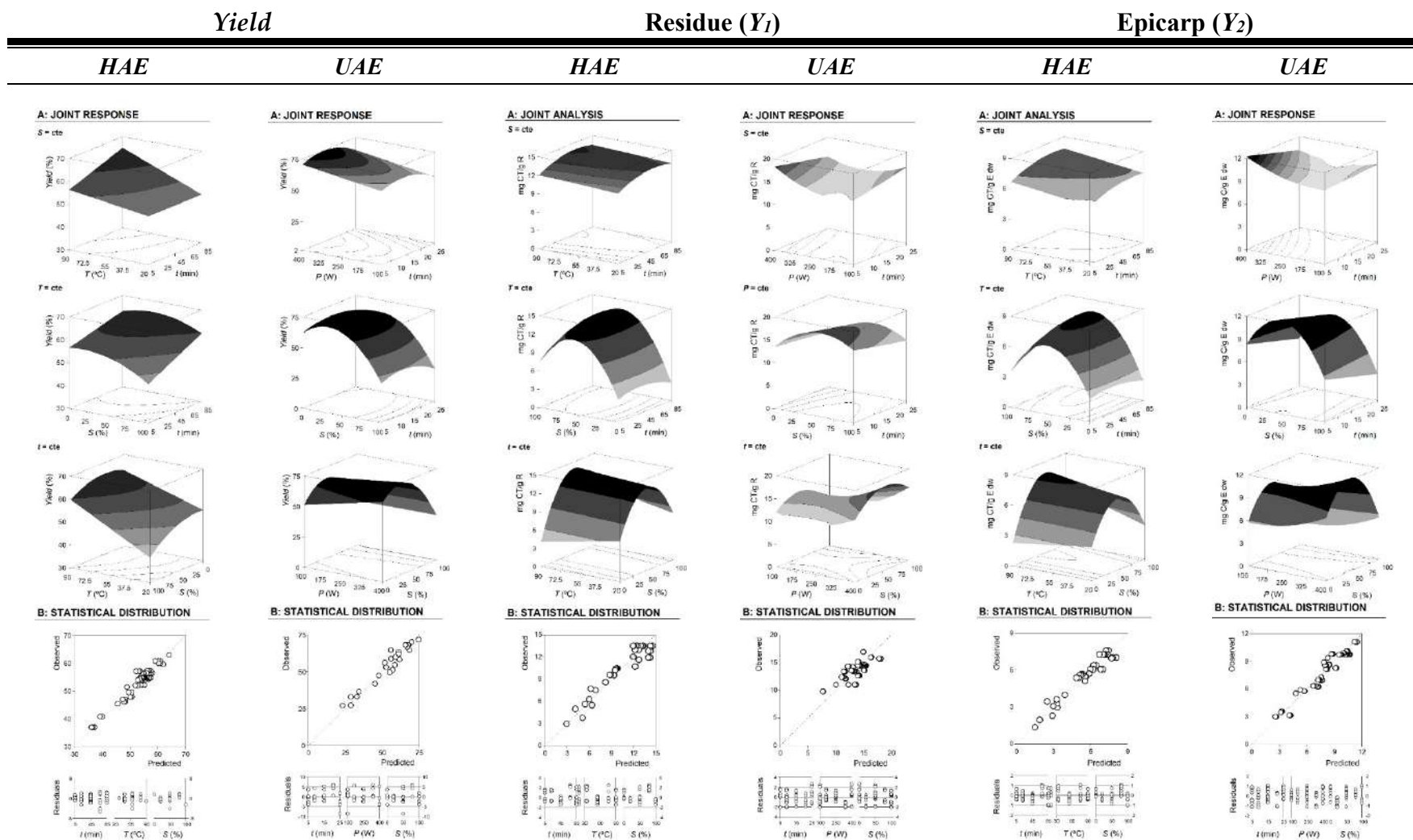
Figure 1. Illustration of the graphical results obtained by heat assisted extraction (HAE) and ultrasound assisted extraction (UAE) for the extraction *yield* of the residual content material (R) and the total detected anthocyanin compounds (cyanidin 3-rutinoside and peonidin 3-rutinoside, CT = C1 + C2) in terms of two response formats (Y_1, mg C/g R and Y_2, mg C/g E dw). Full results are described in Table 1. Every figure is presented in two parts. Part A shows the 3D net surfaces predicted by Equation (1) when the excluded variable is positioned at the individual optimum (Table 3). Part B describes the statistical analysis in a graphical form to show the goodness of fit of the models applied.

YIELD	**C1**	**C2**
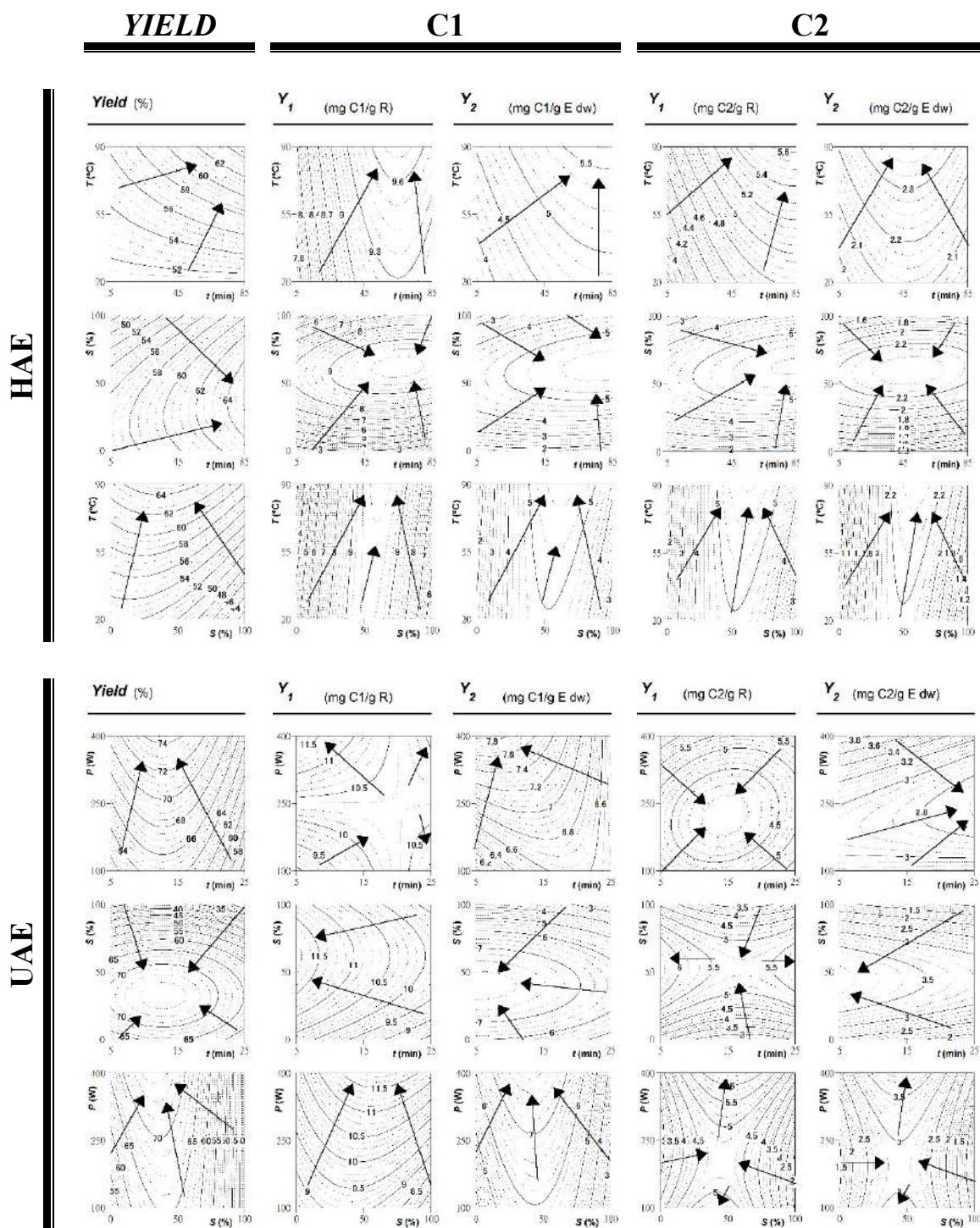
Figure 2. The optimized isolines projections for the extraction of C1 (cyanidin 3-rutinoside) and C2 (peonidin 3-rutinoside) as a function of the combination of the three main variables involved (X_1, X_2, and X_3) in the HAE and UAE. For each compound, the two response value formats (Y_1, mg C/g R and Y_2, mg C/g E dw) are presented to describe the most favorable conditions. Furthermore, the response projections of the *yield* of the extracted residual material are presented. All the contour graphs were built by the second order polynomial models generated by Equation (1) (Table A1) when the excluded variable is positioned at the individual optimum (Table 3).

The extraction results for HAE and UAE, as function of the combination of the three main involved variables (X_{1-3}: t, T or P, and S), can be observed in Figure 1 and Figure 2. In this regard, Figure 1 shows the 3D surface plots of the extracted R (*Yield*, %), and CT, in two response formats (Y_1, mg CT/g R and Y_2, mg CT/g E dw). On the other hand, Figure 2 shows the optimized isolines projections for C1 (cyanidin 3-rutinoside) and C2 (peonidin 3-rutinoside) extraction, in the two response value formats (Y_1, mg C/g R and Y_2, mg C/g E dw). These figures show, respectively, optimized 3D graphical and 2D isolines projection results for the extracted anthocyanins (C1 or C2) as function of the three combined variables (t, T or P, and S) in HAE and UAE. The total anthocyanins (C1+C2) are accounted together (CT) in Figure 1, and individually in Figure 2. They are helpful to visualize the tendencies of each response and lead to define of the maximum favorable conditions, considering all together all responses.

Additionally, Figure 1B exemplifies the competence to predict the obtained results. In statistical terms, the distribution of residues (Figure 1) presents, for the majority of the cases, more than 90% of reliability, showing a good agreement between experimental and predicted values. This is also verified by the achieved high R^2 values (Table 2), which indicates the percentage of variability explained by the model.

In HAE, small differences between the extraction behavior of the two considered anthocyanins (when comparing C1 and C2, or Y_1 and Y_2) were clearly distinguished. The opposite occurred in UAE, the effects were distinct for each one of the detected anthocyanins, as well as according to the response format. However, for both extraction techniques, the S variable was the most significant one, producing a relevant impact on the level of extraction of all anthocyanins assessed. As described above, the LE and the QE of the significant parametric values of the variable S can be perceived in all figures. In almost all cases, the variable S indicates a maximum level at ~50% of hydroalcoholic mixture (water/ethanol, *v/v*). The negative impact of quadratic term of the variable S can be explained through the increase of water in the process, which expands the yield of extraction. Other negative effects such as those between T or P and S may suggest that the further use of lower P, in combination with higher S, will avoid the anthocyanin degradation. The results are in accordance with others recently reported by other authors [19–21], in which inclined surfaces to the side of T or P may increase the solubility of target compounds by using stronger energies, and consequently improve their release from the sample matrix, while destroying the integrity of connective and structural tissues.

2.3. Conditions That Maximize the Anthocyanins Extraction and Experimental Verification

The aim of this study was to maximize the extraction yield of targeted anthocyanin compounds from epicarps of *P. spinosa* fruits, in the applied HAE and UAE techniques, within pre-set variable conditions and ranges. The values of the variable conditions that lead to optimal response values for RSM using a *CCCD*, obtained with the aid of *simplex* procedure, for each of the assessed extracting techniques are shown in Table 3. Figure 3 part A shows the individual summary of the effects of all variables assessed for HAE and UAE systems in 2D illustrations, where the variables are positioned at the individual optimal values of the others (Table 3). The dots (⊙) presented alongside each line highlight the location of the optimum value, meanwhile lines are the predicted behavior found by the mathematical analysis of Equation (1) generated by the theoretical second-order polynomial models described in Table A1. Next, some relevant details of the results produced are highlighted:

- For the HAE: the global optimal variable conditions were found at 49.02 ± 2.94 min, 90.00 ± 7.20 °C, and 50.00% ± 0.50% of ethanol, producing maximum response values of 13.93 ± 0.42 mg CT/g R (Y_1), 7.93 ± 0.08 mg CT/g E dw (Y_2), and 50.89% ± 3.05% (*yield* of the extracted residue).
- For the UAE: the global optimal variable conditions were found at 5.00 ± 0.15 min, 400.00 ± 32.00 W, and 47.98% ± 2.88% of ethanol, producing maximum response values of 18.17 ± 1.82 mg CT/g R (Y_1), 11.76 ± 0.82 mg CT/g E dw (Y_2), and 68.60% ± 2.06 % (*yield* of the extracted residue).

Considering both the individual and global values, the higher amount of extracted compounds was obtained for the UAE technique. The ideal solvent composition was almost the same, and the two techniques required high energy values, where the highest values of T and P proposed by the

experimental design were the optimal, but the UAE needed less *t* than HAE (~90% less). The obtained results are in accordance with similar conclusions found previously [10,17,22], in which UAE proved to consume less energy because of the lower *t* needed, and provide higher extraction values while increasing the purity and, additionally, aiding to meet the requirements of a green extraction concept.
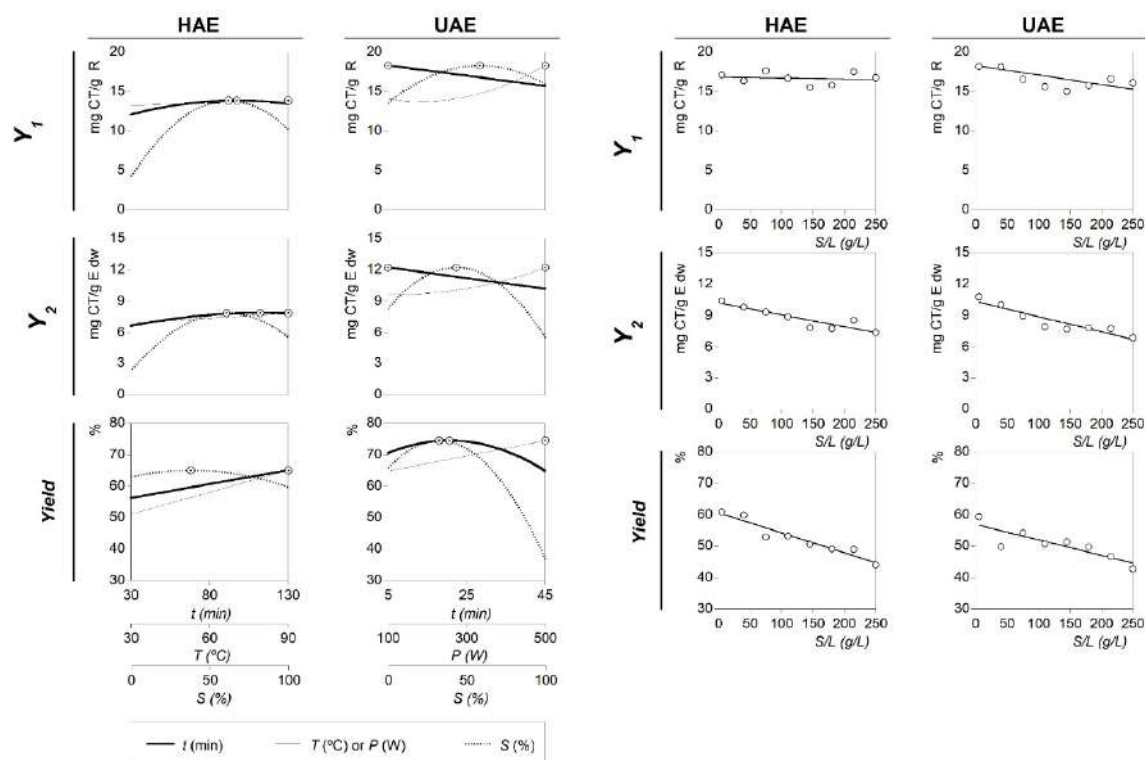
Figure 3. Final graphical effects of all variables assessed for HAE and UAE systems. Part A shows the individual 2D responses as a function of all the variables assessed that were positioned at the individual optimal values of the others (Table 2). The points (⊙) presented alongside each line highlight the location of the optimum value. Lines and dots are generated by the theoretical second order polynomial models generated by Equation (1) (Table A1). Part B shows the dose response of *S/L* at the global optimal values of the other three variables (Table 3). The limit value (~150 g/L) shows the maximum achievable experimental concentration until the sample cannot be physically stirred at laboratory scale. RSM—response surface methodology.

2.4. Dose-Response Analysis of the Solid-to-Liquid Ratio Effect at the Optimal Conditions

The study of *S/L* effect was performed at the optimal conditions (Table 3) predicted by the polynomial models obtained for each extraction technique (HAE and UAE) using the total anthocyanin content (CT), as quantified by HPLC analysis, as the response factor. The individual *S/L* study for each individual anthocyanin (C1 or C2) was not presented because the behavior was similar to the pattern of the total amount. In both processes, the *S/L* was designed to verify the behavior between 5 and 250 g/L. The maximum value of 250 g/L was used as a limit condition because of the impossibility of producing a homogenized extraction when higher values were used.

The obtained dose responses of the *S/L* were consistent for both HAE and UAE systems, and could be described by a simple linear relationship (shown in Part B of Figure 3). All experimental points are distributed around the linear equation; consequently, the dose response is explained by the slope (*m*) of the linear relationship. None of the cases showed positive *m* values (the extraction efficiency increases as the *S/L* rate increases), and two cases showed non-significant values or a zero value of *m* (the efficiency doesn't change as the *S/L* increases). In all the other cases, the *m* showed negative values (the efficiency decreases as the *S/L* increases). The responses from the Y_1 value format, for HAE and UAE, were the ones that showed non-significant *m* values, whereas all other responses

showed significant negative values of *m* (Y_1 and *Yield* for HAE and UAE). The conclusions derived from this analysis are described below:

- For the Y_1 value format, the response of the parametric *m* value in HAE and UAE presents a non-significant interval of confidence, which means that the changes in the response are not statistically supported and, therefore, the parameter must be considered equal to zero. In other words, the amount of anthocyanins in the extracted residue does not vary as a function of the *S/L* increase. The extraction values were defined numerically by the intercept parametric value (*b*) of the linear equation as 14.85 ± 2.29 and 18.25 ± 3.95 mg CT/g R for HAE (R^2 = 0.9920) and UAE (R^2 = 0.9817), respectively.

- For the Y_2 value format, the parametric values for HAE were *b* = 9.21 ± 1.37 mg CT/g E dw and *m* = −0.0113 ± 0.0051, with R^2 = 0.9566; while for UAE, *b* = 10.32 ± 1.48 mg CT/g E dw and *m* = −0.0143 ± 0.0038, with R^2 = 0.9244. Negative *m* values show that the *S/L* increase leads to a decrease in the extraction ability, obtaining a maximum value of extraction at 5 g/L and a minimum at 250 g/L. However, the observed decrease is slight (less than −0.02), which means that the increase of 1 g/L implies the loss of 0.0113 ± 0.0051 mg CT/g E dw for the HAE process and 0.0143 ± 0.0038 mg CT/g E dw for UAE. Such values produce losses at the maximum tested experimental value (250 g/L) of ~15%, comparative with the one extracted at 5 g/L. Nevertheless, the economic advantages of working at 250 g/L are far more superior than the possible benefits of extracting at the optimal *S/L* value.

- For the *Yield* value format, the parametric values for HAE were *b* = 54.62% ± 4.87% and *m* = −0.0636 ± 0.0123, with R^2 = 0.9516; whereas for UAE, *b* = 58.90% ± 7.77% and *m* = −0.0491 ± 0.0116, with R^2 = 0.9618. Although, at the initial *S/L* values, the results obtained for HAE and UAE conducted to similar extraction yields, these values decreased as the *S/L* increased. The *m* parametric value is significantly lower for the UAE process, resulting in higher extraction yield values at 250 g/L. These results are in accordance with the conclusions highlighted in the literature, where UAE is reported as enhancing the extraction process by increasing the mass transfer between the plant material and the solvent [23]. The UAE leads to better cell disruption, facilitating the release of the extractable compounds by increasing the contact surface area between the solid and liquid phases [22,23].

2.5. Comparison with Other Studies Involving the Extraction of Anthocyanins

There are few works in the literature dealing with anthocyanins in *P. spinosa* fruits. In one of these studies with *P. spinosa* fruits, Guimarães et al. [5] performed the extraction using methanol with 0.5% TFA added as solvent, and identified eight different anthocyanins, predominantly peonidin 3-rutinoside and cyanidin 3-rutinoside, with 34.47 ± 0.03 μg/100 g fruits dw and 31.12 ± 0.11 μg/100 g fruits dw, respectively. Other authors [6], found 3.5 ± 0.5 mg of anthocyanins/100 g dw of *P. spinosa* fruits. Both authors used the whole fruit, while in this study, only the epicarp was used as the extraction material, a fact that may justify the significant differences between the encountered results, when compared with the present study. Compared with the pulp, the fruit epicarp presents a greater intensity of color and, therefore, a higher concentration of anthocyanins, in addition to less interfering compounds, is obtained. Moreover, another fact that aided the production of large amounts of anthocyanins from the extracted material was the optimization of the extraction process, which led to increased extraction efficiency and yield. In another study that used *P. spinosa* fruits as a source of anthocyanins [6], the total content was quantified by spectrophotometric methods, presenting values that cannot be compared with those found in the present study.

Some examples of other plant-based sources of anthocyanins are *Oryza sativa* L. (var. Glutinosa) bran, which shows 42.00 mg/g [24]; *Phaseolus vulgaris* L. (common beans) fruit coat, presenting 32.00 mg/g [25]; and *Rubus fruticosus* L. (blackberries) fruit, which possess 17.10 mg/g [26]. Although these values are slightly higher than those presented by *P. spinosa* fruits, in general, the referred fruits and vegetables already have a high commercial value and other industrial purposes, unlike *P. spinosa* fruits. On the other hand, residues such as grape vine (*Vitis vinifera* L.) pomace, and mango (*Mangifera indica*) skin presented lower anthocyanin amounts, that is, 6.33 mg/g [27] and 2.03 to 3.60 mg/g [28],

respectively. Thus, these wild fruits revealed to be an excellent source of anthocyanins, serving as a base raw-material for the production of natural colorant additives for commercial purposes.

3. Discussion

The minimalism of using conventional methods (HAE or maceration) versus the compensations of new non-conventional technologies (microwave, ultrasound, cold pressing, squeezing, etc.) to recover compounds from plant materials, as well as by-products, is a principal topic in the list of many industries in order to increase profitability by decreasing energy costs and reducing greenhouse gas emissions to meet legal requirements. Additionally, non-conventional technologies favor the safety of processes and the quality of products, as well as the functionality and product standardization.

Scientific literature shows clear evidence that extraction procedures of target compounds from plant-based products must be assessed individually. Therefore, a nonstop effort needs to be performed, as agro-industrial and food sectors are looking for by-products' valorization into added-value products. However, in order to take full advantage of the technological advances, the extraction conditions need to be optimized. Mathematical solutions, such as RSM tools, could increase the efficiency and profitability of the process and help to change conventional extraction approaches.

Colorants are one of the most important additives in terms of marketing because their presence in food products is considered to influence customers' perceptions, choices, and preferences. *P. spinosa* fruit epicarps have been scarcely explored and, to the best of the authors knowledge, the potential industrial use of their anthocyanin compounds has not been previously investigated. In such a context, the present work presents a new rapid method to extract anthocyanin compounds from *P. spinosa* fruit epicarps. RSM and other mathematical strategies were successfully employed to optimize the extraction conditions that maximize the anthocyanin compounds' recovery to produce a rich extract with potential industrial application as a natural coloring additive.

4. Materials and Methods

4.1. Plant Material

Ripe *P. spinosa* fruits were harvested in Bragança (Trás-os-Montes, Northeast Portugal) in September 2017, the epicarp was separated from the rest of the fruit body, frozen, and lyophilized. They were then triturated, to be reduced to a fine powder (~ 20 mesh), and stored under refrigeration, protected from light until further use.

4.2. Extraction Procedures for P. Spinosa *Fruit Epicarps*

4.2.1. Heat Assisted Extraction (HAE)

HAE was performed in a water reactor agitated internally with a Cimarec™ Magnetic Stirrer at a constant speed (~500 rpm, Thermo Scientific, San Jose, CA, USA), following a procedure previously performed [13]. The powdered epicarp samples of *P. spinosa* (1.0 g) were extracted with 20 mL of solvent (ethanol/water) acidified with citric acid (pH = 3), under diverse conditions, as previously defined by the established RSM plan (Table 1). The ranges of the experimental design were as follows: time (t or X_1, 5 to 85 min), temperature (T or X_2, 20 to 90 °C), and ethanol content (S or X_3, 0% to 100%). The solid-to-liquid ratio (S/L or X_4) was kept at 50 g/L for all conditions.

4.2.2. Ultrasound-Assisted Extraction (UAE)

An ultrasonic device (QSonica sonicators, model CL-334, Newtown, CT, USA) equipped with a water reactor (EUP540A, Euinstruments, France) at a fixed frequency (40 kHz) was used for UAE procedure. The variables considered were as follows: ultrasonic power (P, in watts), S, and t, which were programmed according to the defined RSM plan (Table 1), following a procedure previously performed [29]. The powdered epicarp samples (2.5 g) were placed in a reactor with 50 mL of solvent (ethanol/water) acidified with citric acid (pH = 3), and extracted under diverse conditions,

maintaining the *S/L* constant at 50 g/L. The ranges of the experimental design were as follows: *t* (X_1, 5 to 25 min), *P* (or X_2, 100 to 400 W), and *S* (or X_3, 0% to 100%).

4.2.3. Post-Extraction Sample Processing

When all the individual extraction conditions were carried out (for HAE and UAE), the samples were immediately centrifuged (6000 rpm during 20 min at 10 °C) and filtered (paper filter Whatman nº 4) to eliminate the non-dissolved material. The supernatant was collected and divided into two portions for HPLC and extraction yield analysis. The portion separated for HPLC analysis (3 mL) was dried at 35 °C, re-dissolved in acidified water (citric acid solution with pH 3), and filtered through an LC filter disk (0.22 μm), whereas the portion for the extraction yield determination (5 mL) was dried at 105 °C during 48 h and thereafter weighted.

4.3. Identification and Quantification of Anthocyanins by HPLC

The extract was analyzed using an HPLC-DAD-ESI/MSn (Dionex Ultimate 3000 UPLC, Thermo Scientific, San Jose, CA, USA) system, previously described [30]. The detection was carried out using a DAD (520 nm as the preferred wavelength) and mass spectrometer (Linear Ion Trap LTQ XL mass spectrometer, Thermo Finnigan, San Jose, CA, USA) equipped with an ESI source. The anthocyanins present in the samples were characterized according to their UV and mass spectra. The anthocyanins cyanidin 3-rutinoside (C1) and peonidin 3-rutinoside (C2) were the most relevant compounds found, and were, therefore, quantified using a five-level calibration curve of known concentrations (200–20 μg/mL) of cyanidin 3-glucoside ($y = 243287\,x - 1000000$; $R^2 = 0.9953$, Polyphenols, Sandnes, Norway) and peonidin 3-glucoside ($y = 122417\,x - 447974$; $R^2 = 0.9965$, Polyphenols, Sandnes, Norway).

4.4. Response Value Formats for Results Presentation

The two anthocyanin compounds (C, either C1 or C2) and their sum (C total, CT) were used as responses in each applied technique. The results were presented according to two response formats (*Y*): Y_1, in mg of C per gram of extracted residue (mg C/g R), which was specifically used to evaluate the C purity in the extracts; and Y_2, in mg of C per g of fruit epicarp dry weight (mg C/g E dw), which was specifically used to analyses the C extraction yield. Both responses were equally analyzed, but additional considerations regarding the last one (Y_2, mg C/g E dw) were taken in the results presentation, becuse it is considered as an important guiding response when dealing in terms of optimization for industrial transference. Note that by dividing those responses, Y_2/Y_1, the extracted residue quantity (g R/g E dw) is obtained, which provides information regarding the third response criterion expressed (*Yield*, %).

4.5. Experimental Design, Model Analysis, and Statistical Evaluation

4.5.1. RSM Experimental Design

Trials based on one-at-the-time analysis (analysis of each of the variables for each one of the selected techniques) were conducted, the ranges originating significant changes were selected (Table 1). The joint effects of the three defined variables were studied using a *circumscribed central composite design* (*CCCD*), using five levels for each one with twenty eight response combinations, as described previously [31].

4.5.2. Mathematical Model

The experimental data produced by the RSM design were analyzed mathematically by means of least-squares calculation, using the following second-order polynomial equation with interactive terms [32]:

$$Y = b_0 + \sum_{i=1}^{n} b_i X_i + \sum_{\substack{i=1 \\ j>i}}^{n-1} \sum_{j=2}^{n} b_{ij} X_i X_j + \sum_{i=1}^{n} b_{ii} X_i^2 \tag{1}$$

where *Y* is the dependent variable (response variable) modelled, X_i and X_j define the independent variables, b_0 is the constant coefficient, b_i is the coefficient of linear effect, b_{ij} is the coefficient of interaction effect, b_{ii} the coefficient of quadratic effect, and *n* is the number of variables. As responses, the following three value formats were used: Y_1 (mg C/g R), Y_2 (C/g E dw), and *Yield* (%).

4.5.3. Procedure to Optimize the Variables to a Maximum Response

A simplex algorithm method was used to find the optimum values by solving nonlinear problems in order to maximize the extraction yield and the recovery of anthocyanin compounds, as explained previously [33]. Certain limitations were imposed (i.e., times cannot be lower than 0) to avoid variables with unnatural and unrealistic physical conditions.

4.5.4. Dose-Response Analysis of the Solid-to-Liquid Ratio

Once the optimal conditions (X_1, X_2, and X_3) were found, the following natural optimization step was used to describe the pattern of the *S/L* (or X_4, expressed in g/L). The objective was to achieve more productive conditions as required by industrial applications. In all cases, experimental points are distributed following linear patterns as the *S/L* increases, consequently, linear models with intercepts were used to evaluate the responses. The parametric value of the slope (*m*) was used to assess the dose response. Positive values will indicate an increase in the extraction responses, whereas negative values will designate a decrease in the extraction efficiency, as the *S/L* increases.

4.6. Mathematical Procedures

The analytical procedures to model the data, to determine the parametric values, confidence intervals, and statistical calculations, were obtained following the descriptions of other authors [34]. In brief, (a) the parametric values were obtained using the quasi-Newton algorithm (least-square) by running the integrated macro '*Solver*' in Microsoft Excel; (b) the coefficient significance of the parameters produced ($\alpha = 0.05$) was assessed using the '*SolverAid*' macro to conclude their confidence intervals; and c) the model consistency was proven by means of several statistical criteria, such as (i) the Fisher *F*-test ($\alpha = 0.05$); (ii) the '*SolverStat*' macro; and (iii) the R^2 coefficient.

5. Conclusions

The efficiency of the UAE was higher than that obtained with HAE. The main anthocyanins identified were cyanidin 3-rutinoside and peonidin 3-rutinoside, being the ones quantified. Through the optimization of the extraction process, it was possible to reach by UAE 18.17 ± 1.82 mg CT/g R (Y_1), 11.76 ± 0.82 mg CT/g E dw (Y_2), and 68.60% ± 2.06% (yield of the extracted residue), with the optimal parameters of extraction being 5.00 ± 0.15 min, 400.00 ± 32.00 W, and 47.98% ± 2.88% of ethanol. The used mathematical models (RSM and dose-response models) were statistically significant and allowed the optimization of the anthocyanins extraction. For the *S/L* effects, inspected at the optimum conditions, the responses for all assessed criteria followed a decreasing linear relation until 250 g/L.

In conclusion, the present study contributed to the valorization of the wild fruits of *P. spinosa* by exploring anthocyanin-rich extracts that can find potential application as natural colorants in different industrial fields. For that purpose, an optimized extraction method was obtained using advanced and efficient extraction systems.

Conflicts of Interest: The authors declare no conflict of interest.

References

1. Morales, P.; Ferreira, I.C.F.R.; Carvalho, A.M.; Fernández-Ruiz, V.; Sánchez-Mata, M.S.O.S.C.C.; Cámara, M.; Morales, R.; Tardío, J. Wild edible fruits as a potential source of phytochemicals with capacity to inhibit lipid peroxidation. *Eur. J. Lipid Sci. Technol.* **2013**, *115*, 176–185.
2. Naziri, E.; Nenadis, N.; Mantzouridou, F.T.; Tsimidou, M.Z. Valorization of the major agrifood industrial by-products and waste from Central Macedonia (Greece) for the recovery of compounds for food applications. *Food Res. Int.* **2014**, *65*, 350–358.
3. Usenik, V.; Fabčič, J.; Štampar, F. Sugars, organic acids, phenolic composition and antioxidant activity of sweet cherry (*Prunus avium* L.). *Food Chem.* **2008**, *107*, 185–192.
4. Ieri, F.; Pinelli, P.; Romani, A. Simultaneous determination of anthocyanins, coumarins and phenolic acids in fruits, kernels and liqueur of *Prunus mahaleb* L. *Food Chem.* **2012**, *135*, 2157–2162.
5. Guimarães, R.; Barros, L.; Dueñas, M.; Carvalho, A.M.; Queiroz, M.J.R.P.; Santos-Buelga, C.; Ferreira, I.C.F.R. Characterisation of phenolic compounds in wild fruits from Northeastern Portugal. *Food Chem.* **2013**, *141*, 3721–3730.
6. Pinacho, R.; Cavero, R.Y.; Astiasarán, I.; Ansorena, D.; Calvo, M.I. Phenolic compounds of blackthorn (*Prunus spinosa* L.) and influence of in vitro digestion on their antioxidant capacity. *J. Funct. Foods* **2015**, *19*, 49–62.
7. Hernández-Herrero, J.A.; Frutos, M.J. Degradation kinetics of pigment, colour and stability of the antioxidant capacity in juice model systems from six anthocyanin sources. *Int. J. Food Sci. Technol.* **2011**, *46*, 2550–2557.
8. Olivas-Aguirre, F.J.; Rodrigo-García, J.; Martínez-Ruiz, N.D.R.; Cárdenas-Robles, A.I.; Mendoza-Dïaz, S.O.; Álvarez-Parrilla, E.; González-Aguilar, G.A.; De La Rosa, L.A.; Ramos-Jimï¿½nez, A.; Wall-Medrano, A. Cyanidin-3-O-glucoside: Physical-chemistry, foodomics and health effects. *Molecules* **2016**, *21*.
9. Dahmoune, F.; Nayak, B.; Moussi, K.; Remini, H.; Madani, K. Optimization of microwave-assisted extraction of polyphenols from *Myrtus communis* L. leaves. *Food Chem.* **2015**, *166*, 585–595.
10. Zhu, Z.; He, J.; Liu, G.; Barba, F.J.; Koubaa, M.; Ding, L.; Bals, O.; Grimi, N.; Vorobiev, E. Recent insights for the green recovery of inulin from plant food materials using non-conventional extraction technologies: A review. *Innov. Food Sci. Emerg. Technol.* **2016**, *33*, 1–9.
11. Wang, X.; Wu, Y.; Chen, G.; Yue, W.; Liang, Q.; Wu, Q. Optimisation of ultrasound assisted extraction of phenolic compounds from *Sparganii rhizoma* with response surface methodology. *Ultrason. Sonochem.* **2013**, *20*, 846–54.
12. Wang, W.; Jung, J.; Tomasino, E.; Zhao, Y. Optimization of solvent and ultrasound-assisted extraction for different anthocyanin rich fruit and their effects on anthocyanin compositions. *LWT - Food Sci. Technol.* **2016**, *72*, 229–238.
13. Roriz, C.L.; Barros, L.; Prieto, M.A.; Morales, P.; Ferreira, I.C.F.R. Floral parts of *Gomphrena globosa* L. as a novel alternative source of betacyanins: Optimization of the extraction using response surface methodology. *Food Chem.* **2017**, *229*, 223–234.
14. Agcam, E.; Akyıldız, A.; Balasubramaniam, V.M. Optimization of anthocyanins extraction from black carrot pomace with thermosonication. *Food Chem.* **2017**, *237*, 461–470.
15. Rodriguez-Amaya, D.B. Natural food pigments and colorants. In *Current Opinion in Food Science*; Elsevier Ltd, 2016; Vol. 7, pp. 20–26 ISBN 2214-7993.
16. Jiménez L., C.; Caleja, C.; Prieto, M.A.; Barreiro, M.F.; Barros, L.; Ferreira, I.C.F.R. Optimization and comparison of heat and ultrasound assisted extraction techniques to obtain anthocyanin compounds from *Arbutus unedo* L. fruits. *Food Chem.* **2018**, *264*, 81–91.
17. Montesano, D.; Fallarino, F.; Cossignani, L.;; Simonetti, M.S.; Puccetti, P.; Damiani, P. Innovative extraction procedure for obtaining high pure lycopene from tomato. *Eur. Food Res. Technol.* **2008**, *226*, 327–335.
18. Bezerra, M.A.; Santelli, R.E.; Oliveira, E.P.; Villar, L.S.; Escaleira, E.A.; Escaleira, L.A. Response surface methodology (RSM) as a tool for optimization in analytical chemistry. *Talanta* **2008**, *76*, 965–977.

19. Pinela, J.; Prieto, M.A.; Carvalho, A.M.; Barreiro, M.F.; Oliveira, M.B.P.; Barros, L.; Ferreira, I.C.F.R. Microwave-assisted extraction of phenolic acids and flavonoids and production of antioxidant ingredients from tomato: A nutraceutical-oriented optimization study. *Sep. Purif. Technol.* **2016**, *164*, 114–124.

20. Roriz, C.L.; Barros, L.; Prieto, M.A.; Barreiro, M.F.; Morales, P.; Ferreira, I.C.F.R. Modern extraction techniques optimized to extract betacyanins from *Gomphrena globosa* L. *Ind. Crops Prod.* **2017**, *105*, 29–40.

21. Oludemi, T.; Barros, L.; Prieto, M.A.; Heleno, S.A.; Barreiro, M.F.; Ferreira, I.C.F.R. Extraction of triterpenoids and phenolic compounds from: Ganoderma lucidum: Optimization study using the response surface methodology. *Food Funct.* **2018**, *9*.

22. Chemat, F.; Rombaut, N.; Sicaire, A.G.; Meullemiestre, A.; Fabiano-Tixier, A.S.; Abert-Vian, M. Ultrasound assisted extraction of food and natural products. Mechanisms, techniques, combinations, protocols and applications. A review. *Ultrason. Sonochem.* **2017**, *34*, 540–560.

23. Tomšik, A.; Pavlić, B.; Vladić, J.; Ramić, M.;; Vidović, S. Optimization of ultrasound-assisted extraction of bioactive compounds from wild garlic (*Allium ursinum* L.). *Ultrason. Sonochem.* **2016**, *29*, 502–11.

24. Chen, M.H.; McClung, A.M.; Bergman, C.J. Phenolic content, anthocyanins and antiradical capacity of diverse purple bran rice genotypes as compared to other bran colors. *J. Cereal Sci.* **2017**, *77*, 110–119.

25. Mojica, L.; Berhow, M.; Gonzalez de Mejia, E. Black bean anthocyanin-rich extracts as food colorants: Physicochemical stability and antidiabetes potential. *Food Chem.* **2017**, *229*, 628–639.

26. Elisia, I.; Hu, C.; Popovich, D.G.; Kitts, D.D. Antioxidant assessment of an anthocyanin-enriched blackberry extract. *Food Chem.* **2006**, *101*, 1052–1058.

27. Bosiljkov, T.; Dujmić, F.; Cvjetko Bubalo, M.; Hribar, J.; Vidrih, R.; Brnčić, M.; Zlatic, E.; Radojčić Redovniković, I.; Jokić, S. Natural deep eutectic solvents and ultrasound-assisted extraction: Green approaches for extraction of wine lees anthocyanins. *Food Bioprod. Process.* **2017**, *102*, 195–203.

28. Ajila, C.M.; Naidu, K.A.; Bhat, S.G.; Rao, U.J.S.P. Bioactive compounds and antioxidant potential of mango peel extract. *Food Chem.* **2007**, *105*, 982–988.

29. Backes, E.; Pereira, C.; Barros, L.; Prieto, M.A.; Kamal, A.; Filomena, M.; Ferreira, I.C.F.R. Recovery of bioactive anthocyanin pigments from *Ficus carica* L . peel by heat , microwave , and ultrasound based extraction techniques. *Food Res. Int.* **2018**, *113*, 197–209.

30. Gonçalves, G.A.; Soares, A.A.; Correa, R.C.G.; Barros, L.; Haminiuk, C.W.I.; Peralta, R.M.; Ferreira, I.C.F.R.; Bracht, A. Merlot grape pomace hydroalcoholic extract improves the oxidative and inflammatory states of rats with adjuvant-induced arthritis. *J. Funct. Foods* **2017**, *33*, 408–418.

31. Heleno, S.A.; Prieto, M.A.; Barros, L.; Rodrigues, A.A.; Barreiro, M.F.; Ferreira, I.C.F.R. Optimization of microwave-assisted extraction of ergosterol from *Agaricus bisporus* L. by-products using response surface methodology. *Food Bioprod. Process.* **2016**, *100*, 25–35.

32. Pinela, J.; Prieto, M.A.; Barros, L.; Carvalho, A.M.; Oliveira, M.B.P.P.; Saraiva, J.A.; Ferreira, I.C.F.R. Cold extraction of phenolic compounds from watercress by high hydrostatic pressure: Process modelling and optimization. *Sep. Purif. Technol.* **2018**, *192*, 501–512.

33. Vieira, V.; Prieto, M.A.; Barros, L.; Coutinho, J.A.P.; Ferreira, O.; Ferreira, I.C.F.R. Optimization and comparison of maceration and microwave extraction systems for the production of phenolic compounds from *Juglans regia* L. for the valorization of walnut leaves. *Ind. Crops Prod.* **2017**, *107*, 341–352.

34. Caleja, C.; Barros, L.; Prieto, M.A.; Barreiro, F.M.F.; Oliveira, M.B.P.; Ferreira, I.C.F.R. Extraction of rosmarinic acid from *Melissa officinalis* L. by heat-, microwave- and ultrasound-assisted extraction techniques: A comparative study through response surface analysis. *Sep. Purif. Technol.* **2017**, *186*, 297–308.

Sample Availability: Samples of the plant and extracts are available from the authors.